GEM TN-93-451

GEM Muon Group Meeting - SSCL

August 3-4, 1993

Abstract:

Agenda, attendees, and presentations of the GEM Muon Group Meeting held at the SSC Laboratory on August 3&4, 1993.

Agenda of the GEM Muon Group Meeting

SSCL, August 3-4, 1993

--------- August 3 ---------

(1) Report of the Chamber Committee - Gena Mitselmakher convenor

G.Mitselmakher - Introduction

C.Wuest - Activities at LLNL

C.Belser - Prototype pannel status

I.Golutvin - CSC activity at Dubna

C.Johnson - Chamber design progress

O.Steger - Muon chamber numerating system

U.Nauenberg - Integration of Readout

O.Prokofiev - Progress with small prototypes

(2) Muon System Optimization Discussion

I.Golutvin - Comments on GEM Muon System Performance

O.Prokofiev - Lorentz angle compensation in the CSC

Yu.Bonushkin - Simulations and Measurements of the Muon System possible gas mixture

S.Timofeev - GEM Magnetic Field

N.Martovetsky - GEM Magnet Field Increase Consequences

(3) Test Beam Program 4:00 PM - 7:00 PM

outline of program - Carl Bromberg, Vladimir Glebov, Gena Mitselmakher

assignment of tasks - group

(4) Chamber Interface and Alignment

C.Belser - Chamber Interface with Support Structure

Yu. Gerstein - Simulations of the GEM muon alignment system

--------- August 4 ----------

(5) Report on simulations - Roger McNeil convenor

SiGEM - Yu. Fisyak

Hit level MC - Torre Wenaus

relaxation of calorimeter depth ? - Roger McNeil

GEM Muon Group Meeting
SSCL, August 3-4, 1993

Name	Institution	Phone	E-mail
1. Vladimir Glebov	SSCL	214-708-6321	GLEBOV@SSCVX1
2. Gena Mitselmakher	SSCL	214-708-6001	MITSELMAKHER@SSCVX
3. CURT BELSER	LLNL	510-423-2472	BELSER1@LLNL.GOV
4. COLEMAN JOHNSON	SSCL	214-708-1188	JOHNCOLE@SSCVX1
5. A. OTTO STEGER	SSCL	214-708-1135	STEGOTTO@SSCVX1
6. A. GORDEEV	SSCL	214-708-1169	GORDEEV@SSCVX1
7. DAN GAIGALAS	SSCL	214-708-3266	GAIGALAS@SSCVX1
8. Frank Taylor	MIT	617-253-7249	FET@MITLNS
9. Cas Milner	SSCL	6216	Milner@SSCVX1
10. Yinzhi Huang	SSCL	214-708-6009	HUANGY2@SSCVX1
11. Jim SHANK	Boston U.	617-353-6028	shank@cbsgi1.bu.edu
12 Mike Marx	SUNY/SB	516 632 8102	sbhep::marx
13 Harvey Newman	Caltech	818 395 6656 011 41 22 7676366	newman@cithex
14 Igor Golutvin	Dubna	(214) 708-3064	IGOLUTVIN@SSCVX1
15 Bill Willis	Nevis	914 591-8100x205	willis@Nevis
16 Maged Atiya	BNL	516 282 3067	atiya@BNLDAG
17 TORRE WENAUS	LLNL	510 423 1813	WENAUS@PDSF.
18 OLEG PROKOFIEV	PNPI	214-708-4486	PROKOFOE@SSCVX1
19. Craig R. Wuest	LLNL	510-423-2909	WUEST@LLNL.GOV

GEM Muon Group Meeting
SSCL, August 3-4, 1993

Name	Institution	Phone	E-mail
21. S. Timofeev	SSCL	x 6292	SSCVXT::Timofeev
21. U. Nauenberg	U. of Colorado	(303) 492-7715	URIEL@RMCHEP.COLORADO.EDU
22. Larry Rosenson	MIT	617-253-7595	ROSENSON@MITLNS
23. Vladik Balagura	SSCL	(214)-708-4478	balagura@sscvx1
24 Carl Bromberg	MSU	517-353-1809	bromberg@msupx
25 Michael Danilov	ITEP	(214) 708 6350	Danilov@SSCVX1
26. Yuri Bonushkin	SSCL	(214) 708 3078	BONUSHKIN@SSCVX
27 Yuri Gerstein	SSCL/ITEP	x 3007	GERSTEIN@sscvx1
28. Gary Sanders	SSC/LANL	6189	SANDERS@SSCVX1
29. Gary Deis	SSC/LANL	6207	DEIS@SSCVX1
30. Ryszard Stroynowski	SMU	(214) 768-4076	RYSZARD@SSCVX1
31. Jacques Pier Amory	SSC.	–	PIERAMORY@SSVX1.
32 MIKE GAMBLE	SSCL	(214)708-6301	gamble@arcvx
33. Barry Barish	SSCC	6326	BARISH@SSCVX1
34. Ken Freeman	SSCL	1113	kfreeman@sscvx1
35. Milind Diwan	SSCL	4477	DIWAN@SSCVX1
36 Mike Harris	SSCL	6143	HARRIS@SSCVX1
37 Nicolai Martovetsky	SSCL	6324	MARTOVETSKY@SSCVX1

GEM Muon Group Meeting
SSCL, August 3-4, 1993

	Name	Institution	Phone	E-mail
38	George Yost	SSCL	X 6028	YOST@SSCUX1
39	Doug Trainer	SSCL	X 6317	DJTRAINER@SSCUX
40	Simon Blumberg	SSCL	X 6269	BLUMBERG@SSCUX1
41	Roger McNeil	LSU	504-388-6857	PHMCNE@LSUVAX
42	Jim Sullivan	MIT/BU	617-253-7537	SULLIVAN@MITLN

LLNL CSC R&D Activities

- Alignment Test Stand:
  - Fabrication of foundation support for granite tables
  - Final design of chamber support system
  - Redesign of alignment system based on hybrid option
  - Procurement of 13 cameras, frame grabber and video card

- Panel prototyping:
  - Small panel prototyping for alternative processes
    - new edge fillers (polymer concrete)
    - strength, creep tests
    - measurement of Cu mylar strips
    - Cu mylar on G10
  - Small panels for intra-chamber alignment tests
  - Large panel prototyping for standard processes

- Wire tests:
  - GTE wire (US) vs LUMA wire (Sweden)
    - surface finish
    - uniformity vs length (0.75 km)
    - tensile strength

LLNL CSC R&D Activities

- CSC Structural Design Bible
  - Benchmarking of structure codes with prototype panels
  - Alternative interface designs
  - Integrated structure/interface modeling for chamber deformation
  - Bolt patterns, shear deformations, etc.

- CSC Process Design Bible
  - Panel fabrication processes
  - Chamber mock-ups for gap frame evaluation
  - Experimentation and evaluation of polymer concretes
  - Alternatives to G10 (e.g., polyimides)

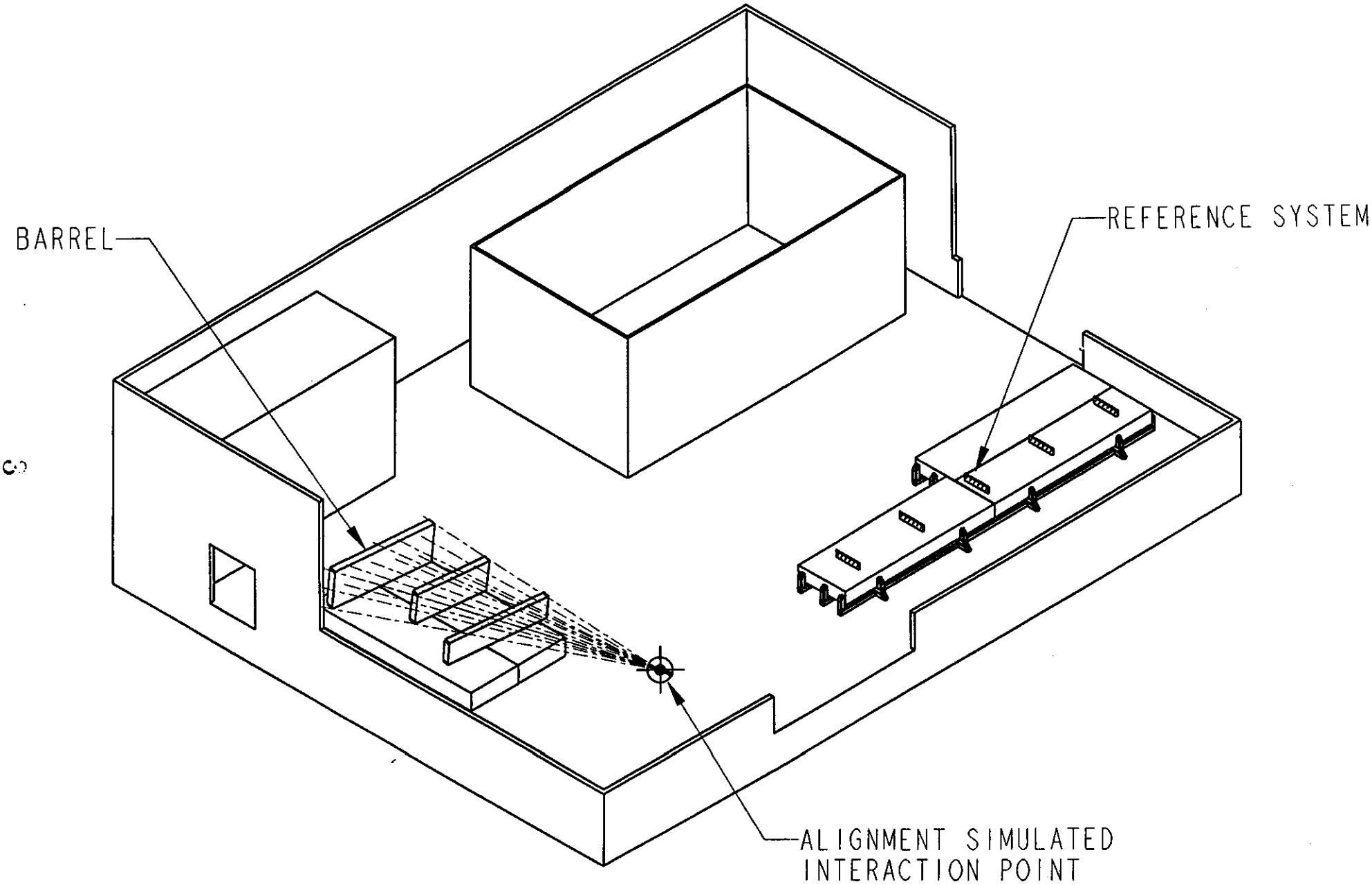
BARREL
REFERENCE SYSTEM
ALIGNMENT SIMULATED
INTERACTION POINT

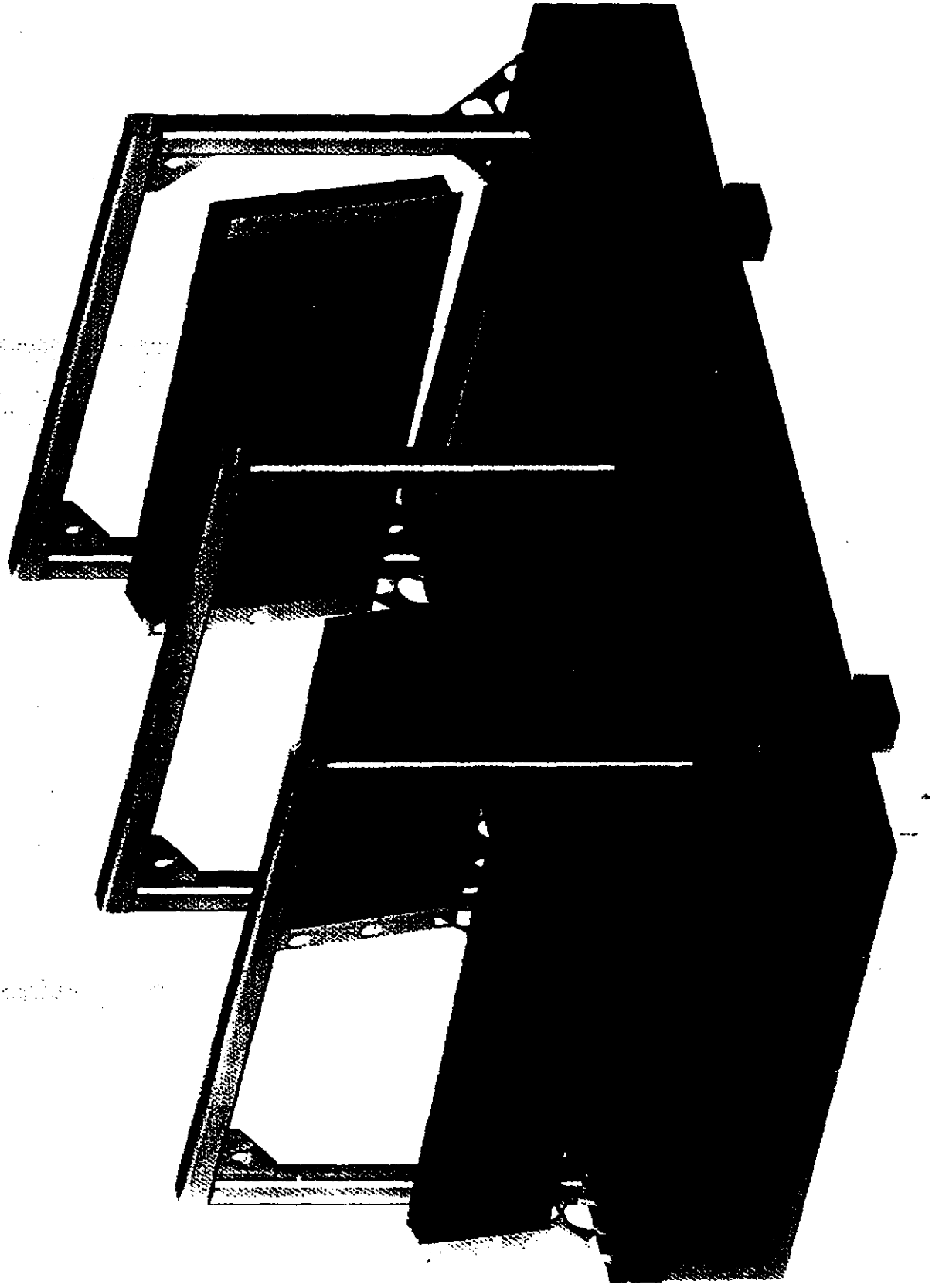

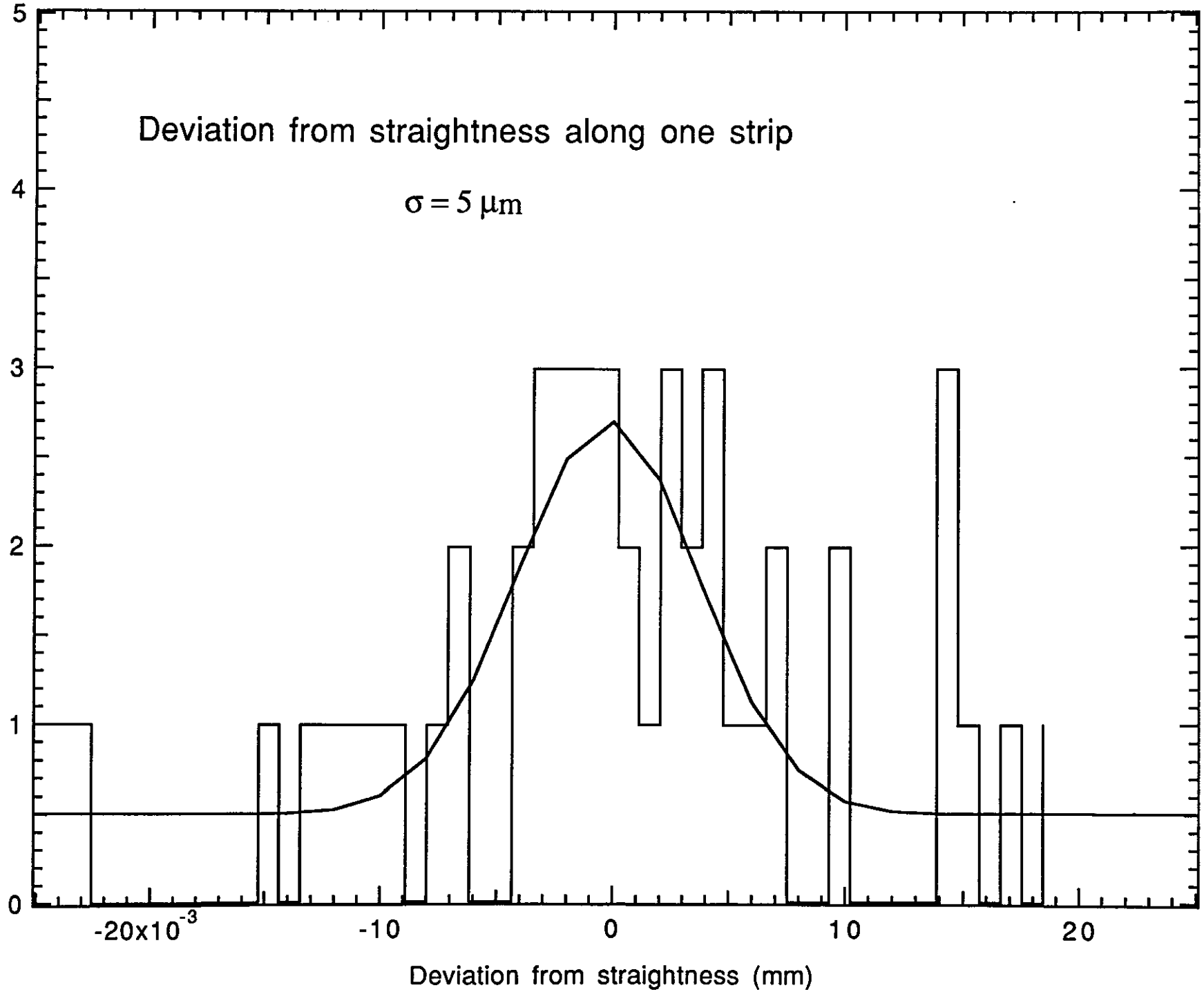
Deviation from straightness along one strip
σ = 5 μm
5
4
3
2
1
0
-20x10^-3
-10
0
10
20
Deviation from straightness (mm)

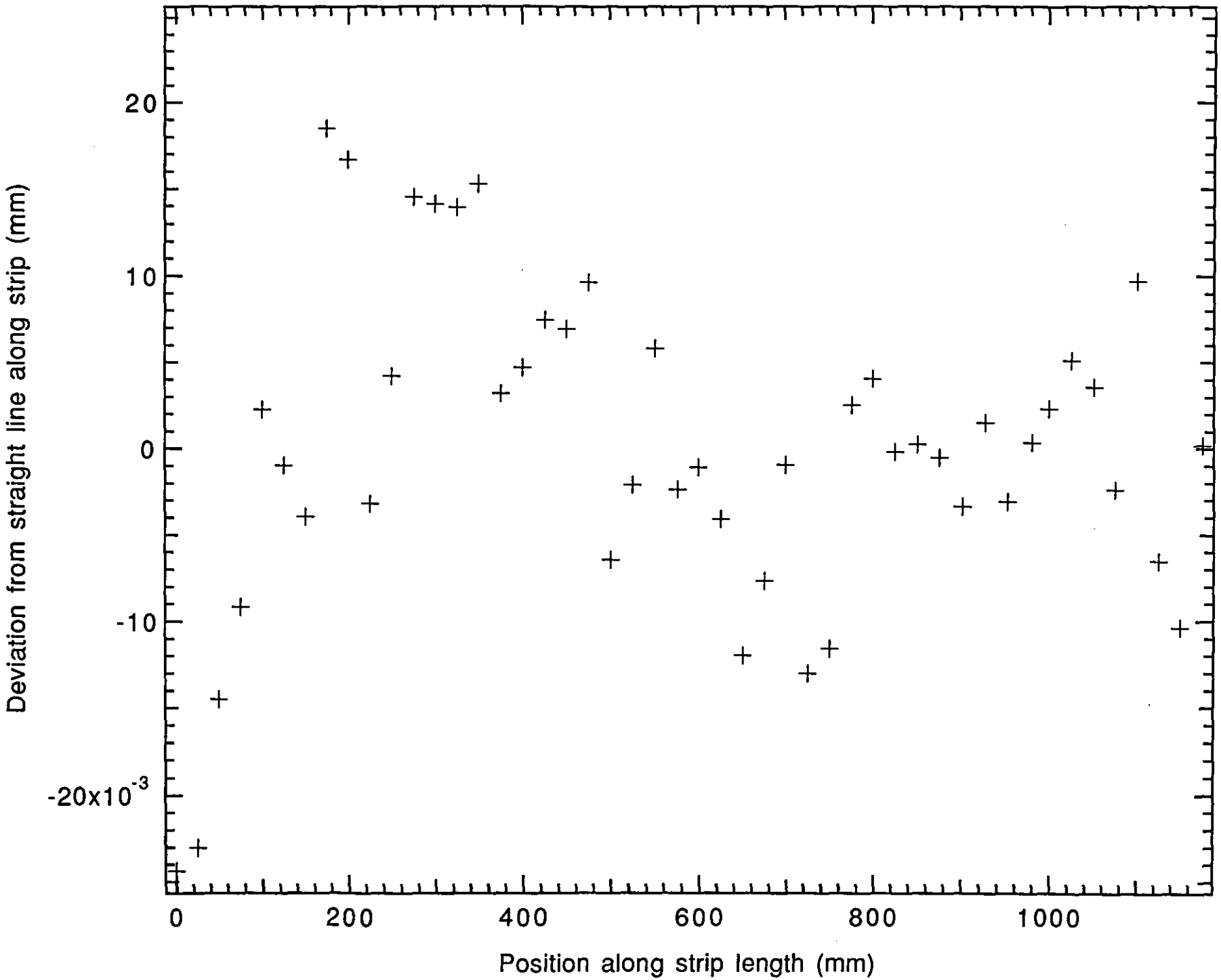
20
10
0
-10
-20x10^-3
Deviation from straight line along strip (mm)
0
200
400
600
800
1000
Position along strip length (mm)

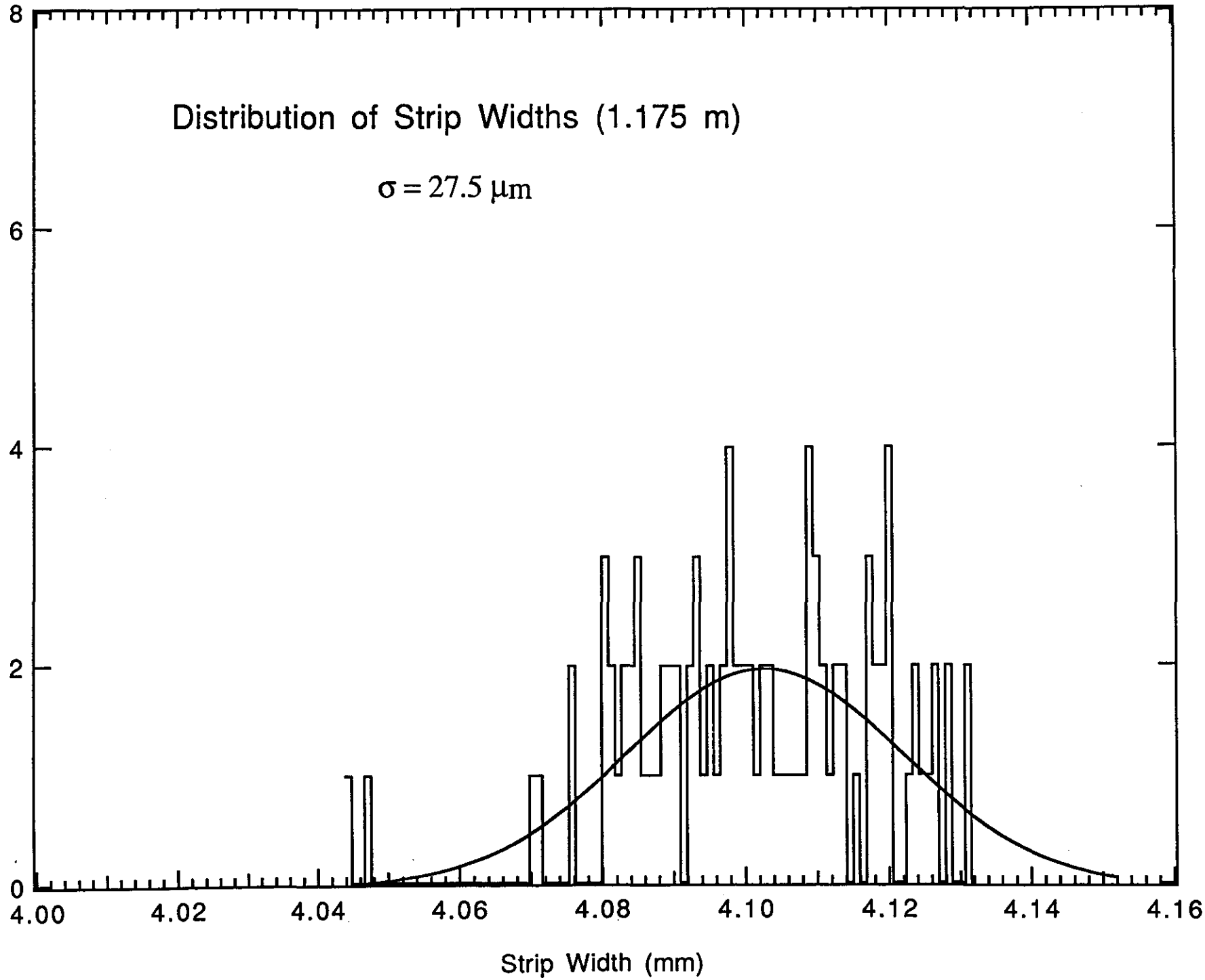
Distribution of Strip Widths (1.175 m)
σ = 27.5 μm
8
6
4
2
0
4.00
4.02
4.04
4.06
4.08
4.10
4.12
4.14
4.16
Strip Width (mm)

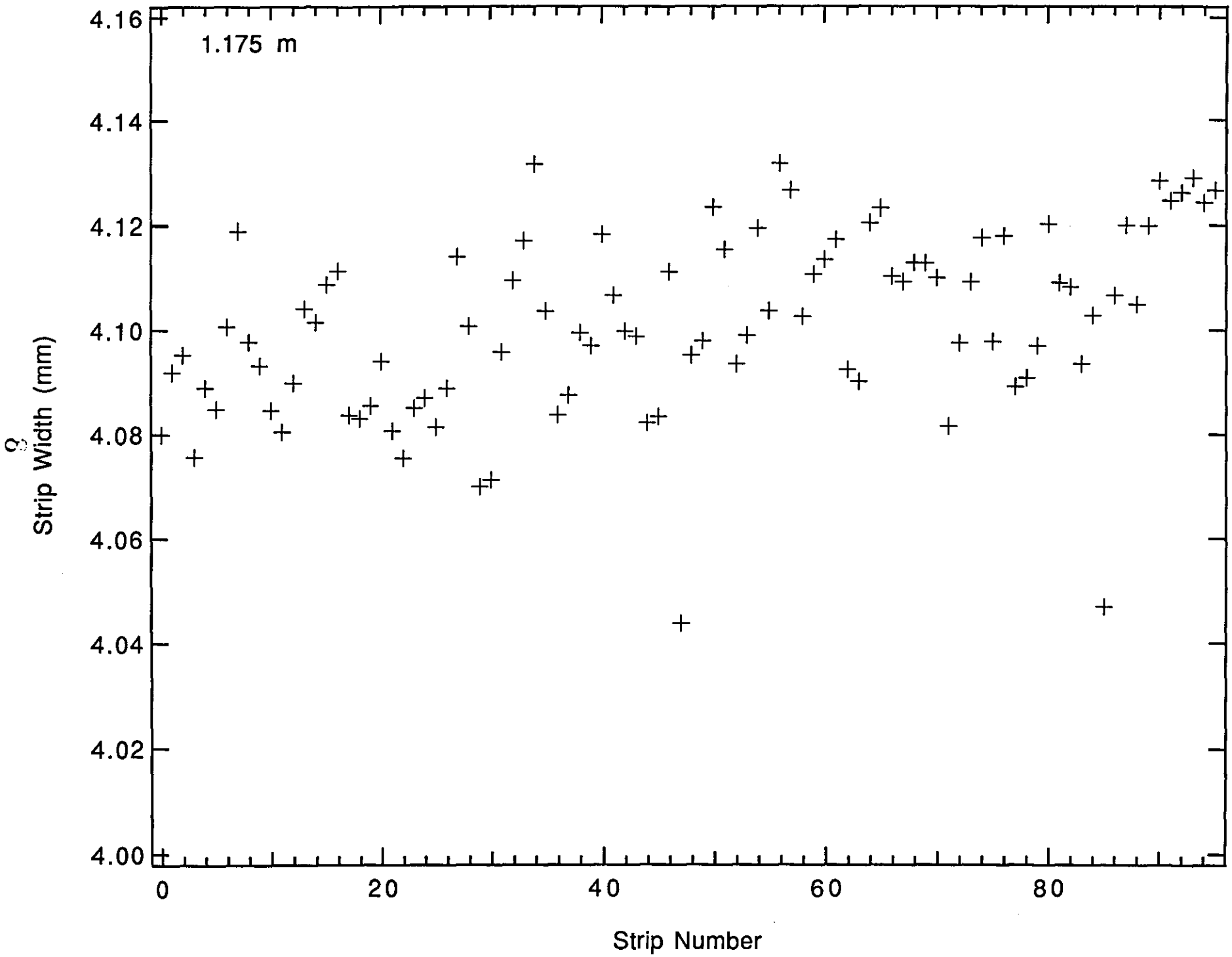
1.175 m
4.16
4.14
4.12
4.10
4.08
4.06
4.04
4.02
4.00
Strip Width (mm)
0
20
40
60
80
Strip Number

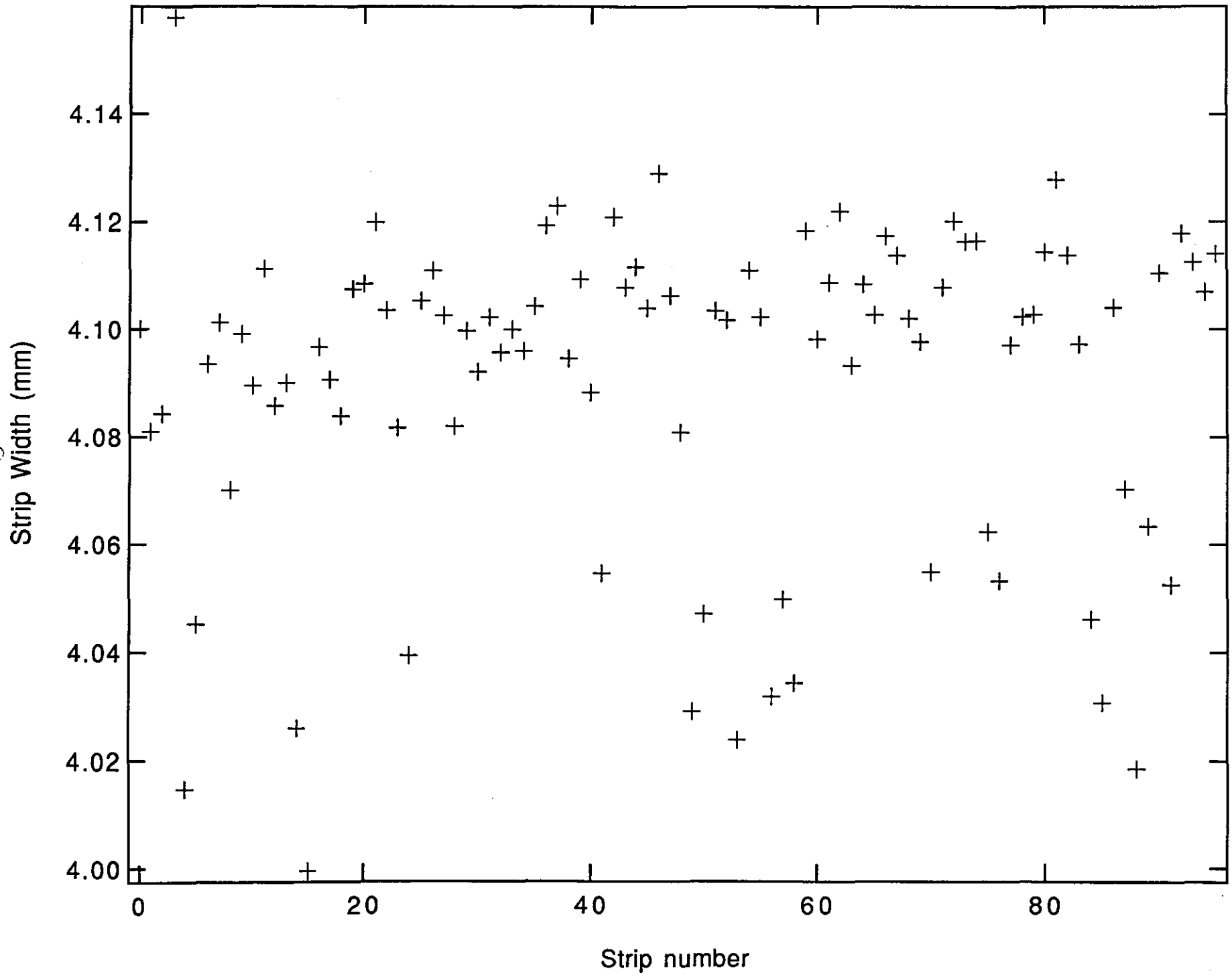
4.14
4.12
4.10
4.08
4.06
4.04
4.02
4.00
Strip Width (mm)
0
20
40
60
80
Strip number

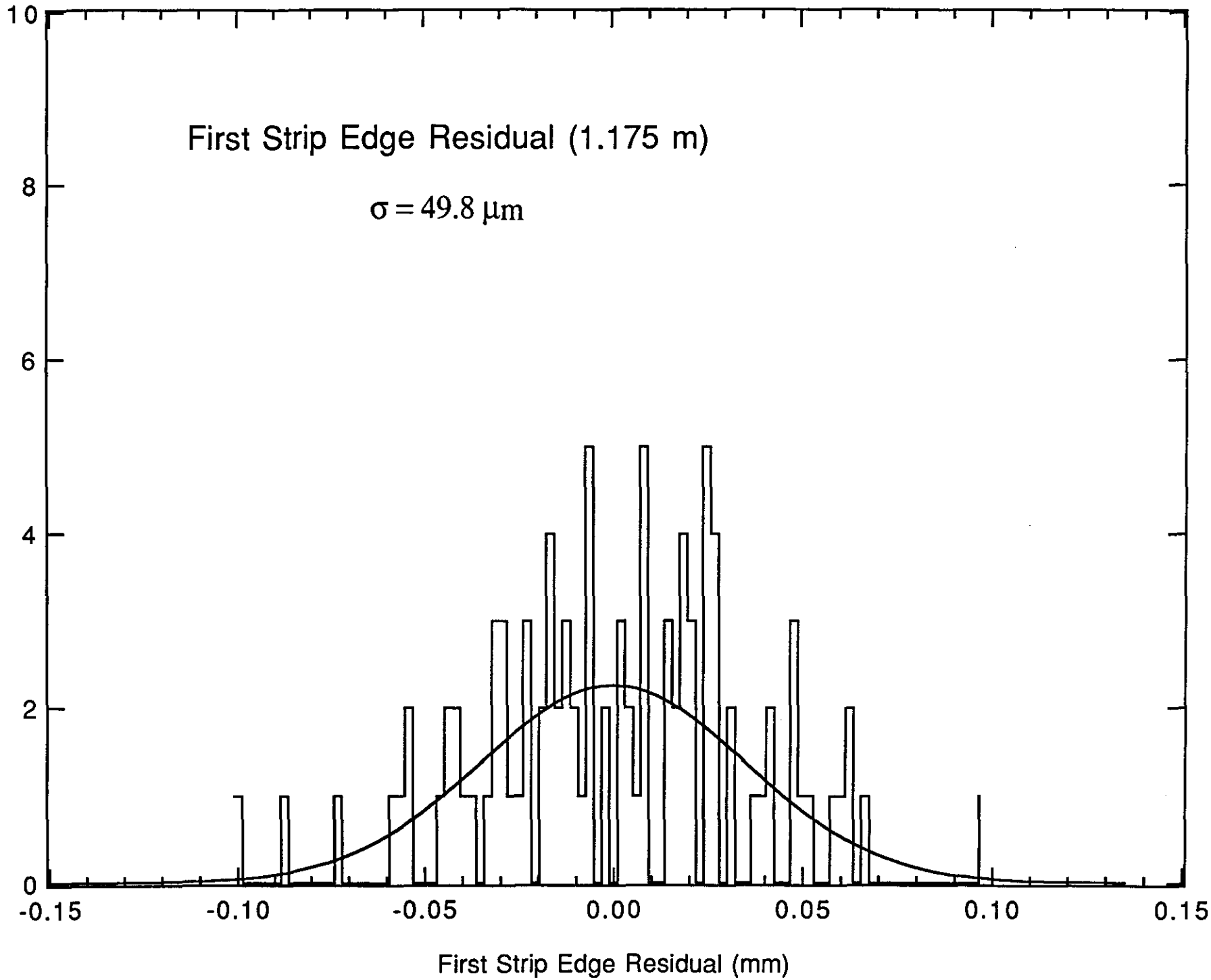
First Strip Edge Residual (1.175 m)
σ = 49.8 μm
10
8
6
4
2
0
-0.15
-0.10
-0.05
0.00
0.05
0.10
0.15
First Strip Edge Residual (mm)

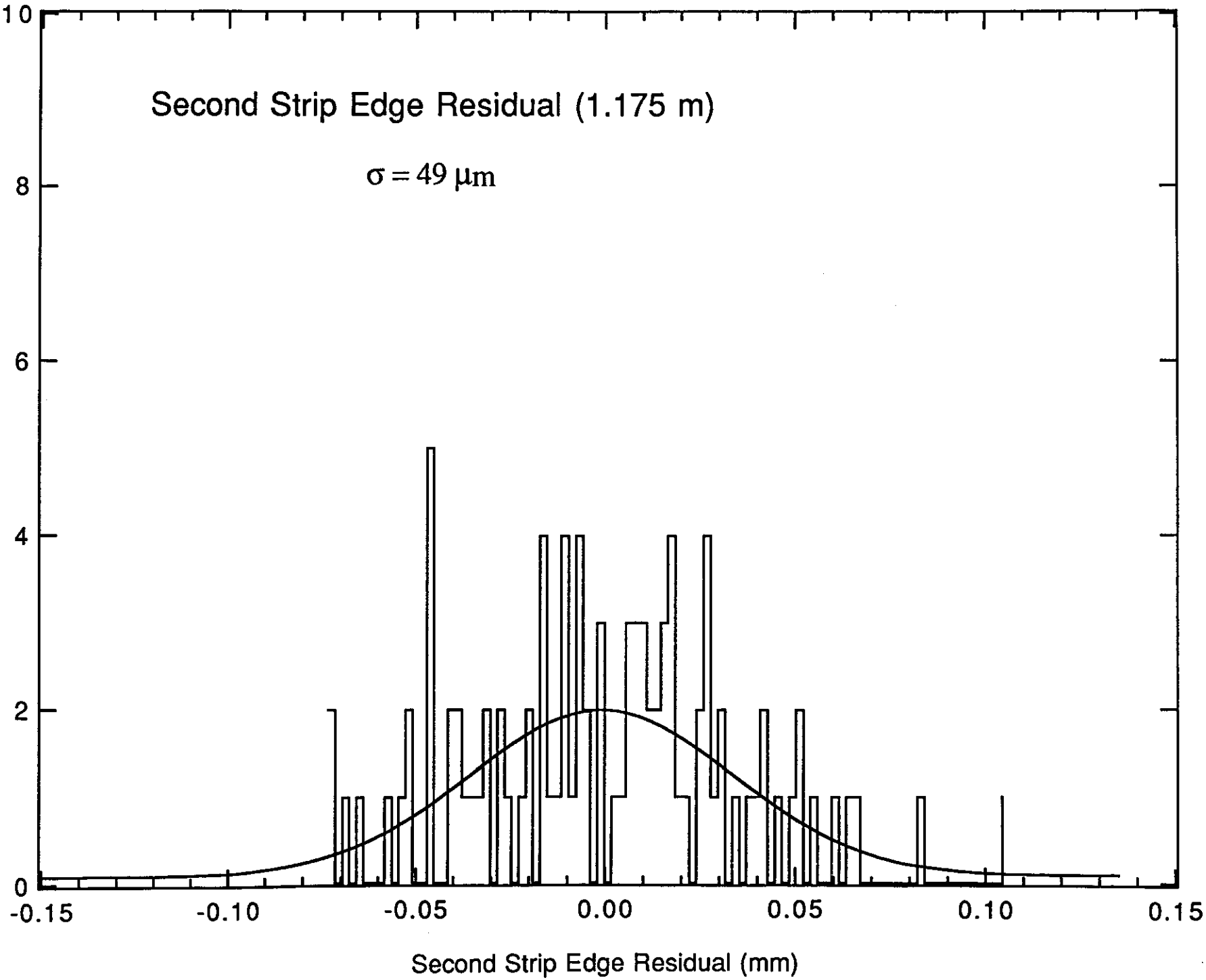
Second Strip Edge Residual (1.175 m)
σ = 49 μm
10
8
6
4
2
0
-0.15
-0.10
-0.05
0.00
0.05
0.10
0.15
Second Strip Edge Residual (mm)

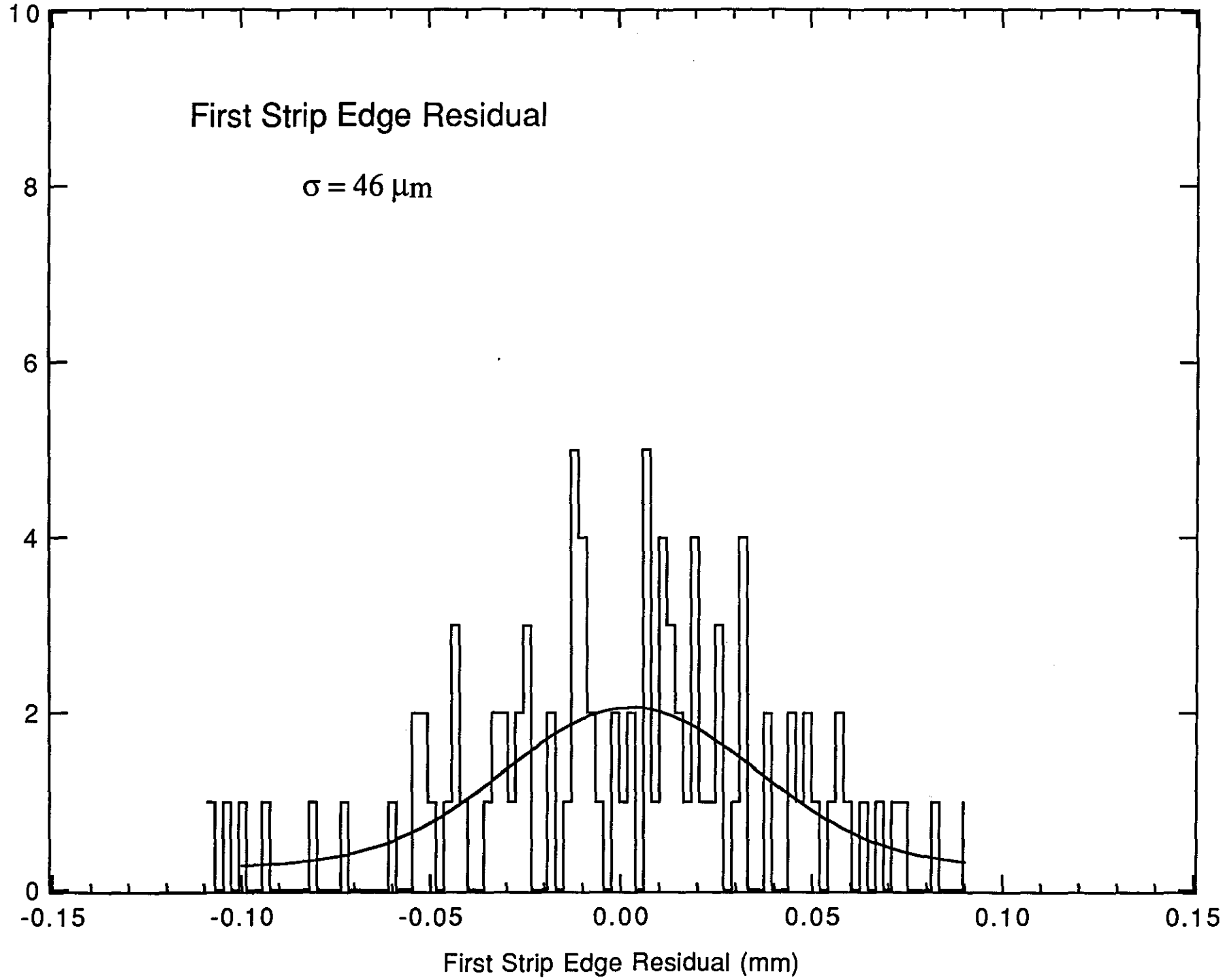
First Strip Edge Residual
σ = 46 μm
10
8
6
4
2
0
-0.15
-0.10
-0.05
0.00
0.05
0.10
0.15
First Strip Edge Residual (mm)

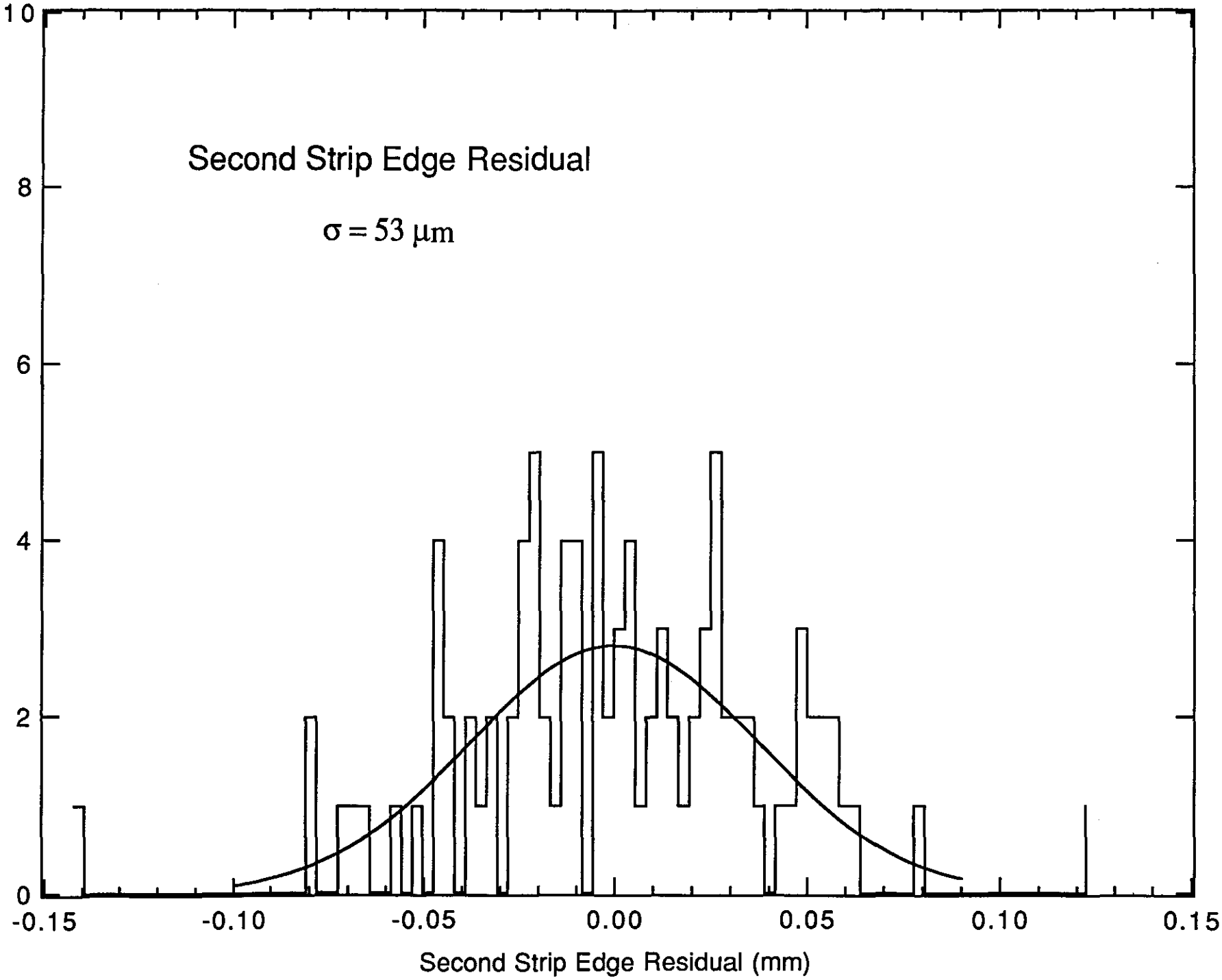
Second Strip Edge Residual
σ = 53 μm
10
8
6
4
2
0
-0.15
-0.10
-0.05
0.00
0.05
0.10
0.15
Second Strip Edge Residual (mm)

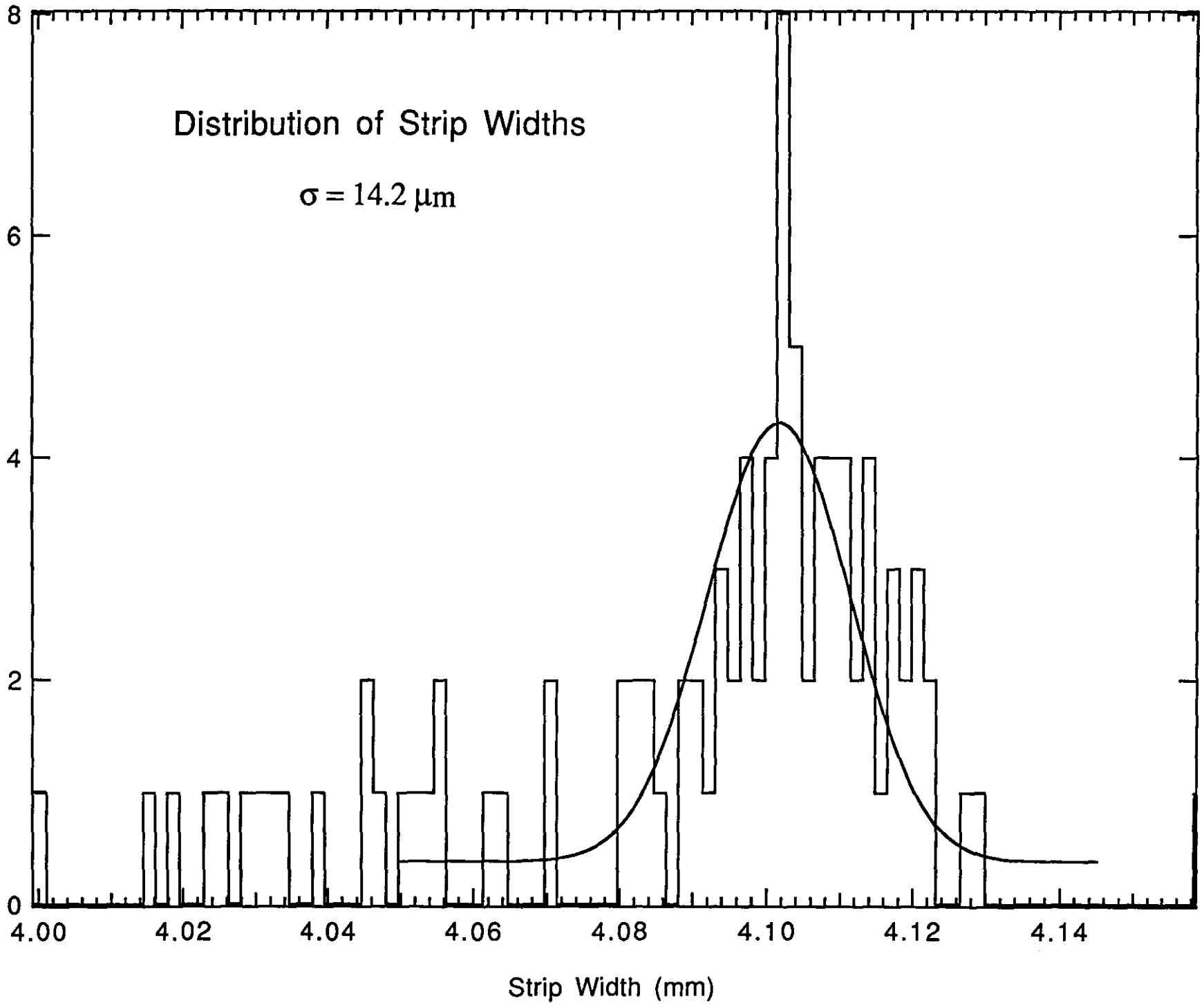
Distribution of Strip Widths
σ = 14.2 μm
8
6
4
2
0
4.00
4.02
4.04
4.06
4.08
4.10
4.12
4.14
Strip Width (mm)

Near-Term Prototyping Efforts

Intra-Chamber Alignment Verification Test ...

- Verify TDR "baseline" alignment concept using on-board fiducials and precision washers for panel-to-panel transfer.
  - Fabricate multiple copies of a "standardized" small (1' x 2') panel incorporating alignment features and simulating etched circuit features as extensively as practical.
  - Demonstrate fiducial transfer "steps" from cathode strips to chamber assembly.
  - Develop statistics for accuracies obtained during each fiducial transfer.

- Add straightness monitor components to verify alignment transfer from panels.

- Evaluate alternative alignment technique and compare to "baseline".
  - Labor required to align and verify
  - Skill levels required

- Experiments (minimum of 2 panels in assembly).
  - "TDR baseline" (circuit board fiducials with precision washers). AUG./SEPT.
  - "Pin-Transfer" alternative. SEPT.
  - "Stretched-Wire" straightness monitor sensor . SEPT. – ?

Near-Term Prototyping Efforts (cont.)

"Standardized", small panel design (developed for the alignment tests) used for prototyping chamber design features and components.

- A progression of small panels can be fabricated and/or modified as needed for inclusion in an increasingly sophisticated chamber assembly.
- An assembly of 7 small panels will duplicate most proposed chamber dimensions ***except*** for full length and width (adequate for simulating "local" features that are simply replicated along the length and width of a chamber assembly).
- Designs features submitted from collaboration members can be prototyped and evaluated as part of an integrated assembly.
- Alternative designs for a specific feature can be evaluated "side-by-side" in the same assembly if desired.
- "Real" materials, components, and assembly techniques will be incorporated as available.
- Prototyping experience will aid the design of a fully engineered, full size chamber as well as providing fabrication and assembly experience necessary for planning factory production.

Specific Prototyping Efforts - Large Panels

Two large honeycomb panels (~4' x 10') to be fabricated ...

- One panel incorporates existing 2-piece etched cathode circuit board at SSCL.
- Unetched Cu-clad boards from GE will be used for all other faces.
- Both panels will incorporate design features for inclusion in Dubna prototype chamber if schedule permits.
- All components will be characterized before assembly for comparison with finished assembly.
- Fabricator is aware of ambitious design specifications (flatness and parallelism) but will utilize existing technology.
  - Room temperature adhesive to be used for large panels.
  - Other fabrication methods will be examined using small panels.
- Cost: $14k not including face sheets and characterization (at LLNL).
- Delivery date expected end of August 1993.

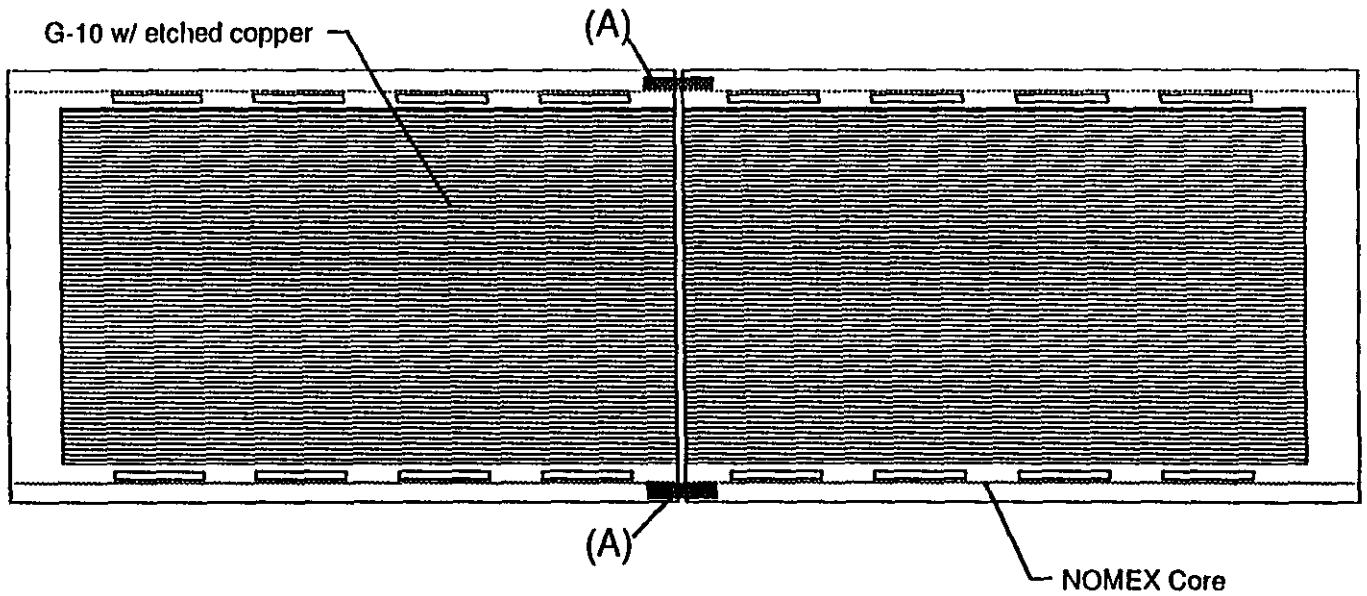

Face sheet assembly:

- Two copper clad (and etched) G-10 sheets are aligned and temporarily attached (A).
- Adhesive and NOMEX core positioned on face sheet.
- Face sheet trimmed to fit Nomex.

CSC Panel Fabrication Specs

Panel Definition: A 19 mm (nominal) honeycomb NOMEX core (1.8 lb/ cu. ft.; 0.25 in. cell) sandwiched between two .5 mm fiberglass (G-10 or FR-4; NEMA specs.) face sheets. The fiberglass face sheets are copper cladded (17 μm thick; 1/2 oz. per sq. ft.) on the outward facing sides. The copper on one of the face sheets is etched to provide a precision cathode plane.

Specifications (prioritized)

1. Flatness
   100 μm over 1.2 m
2. Parallelism
   100 μm over 1.2 m
3. Net thickness (incl. face sheets)
   20 mm ± 250 μm
4. Squareness
   Diagonal measurements ± 250 μm of each other
5. Length and width dimensions
   Not set at this time.

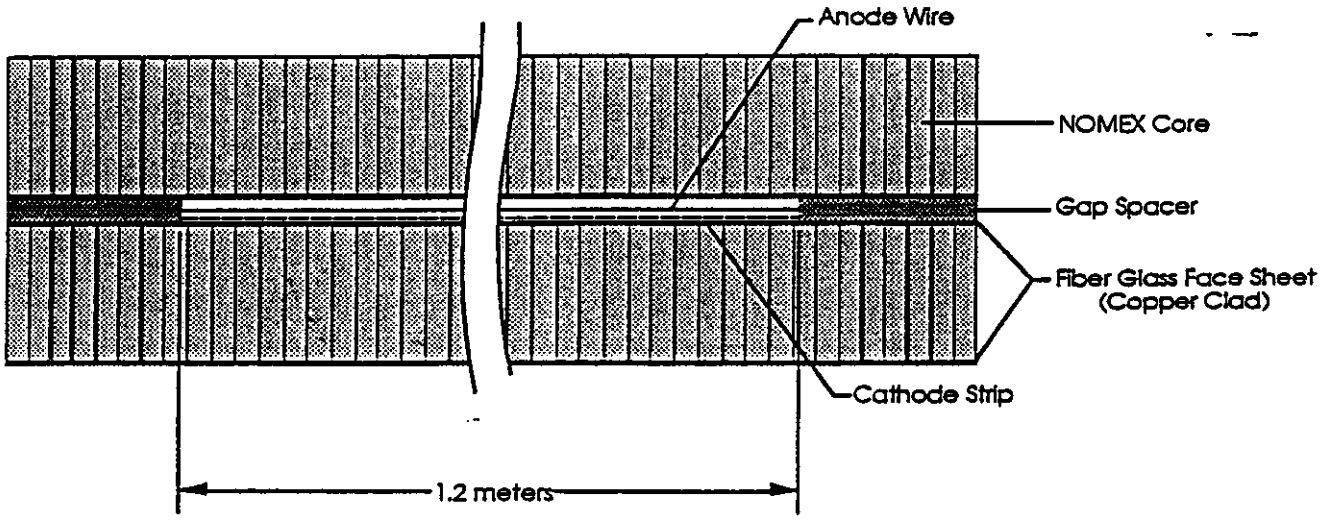

Specific Prototyping Efforts - Small Panels

Panels ...

* • Materials and fabrication techniques AUG. - DEC.
  • Panel internal reinforcements (edges and center spacer posts)
  • Casting techniques for "integrated" panel edge details (a la Polychronakos) } SEPT.-DEC.
  • Layout of etched cathode circuit routing

Chamber assembly, internal ... OCT. — ?

- Cathode spacer posts (at bolts and middle of chamber)
- Anode wire support and wire fixation design
- Internal layout of electronics and circuit routing
- HV distribution

Chamber assembly, external ... OCT. — ?

- Panel-to-panel gas sealing design (bolted and alternative ideas)
- Utility feedthroughs and connections
- Edge connectors (anode and cathode)
- Straightness monitor components (projective and stretched-wire)
- Attachment details (for chamber mounting to support structure)
- Anode and cathode electronics module locations and cable routing

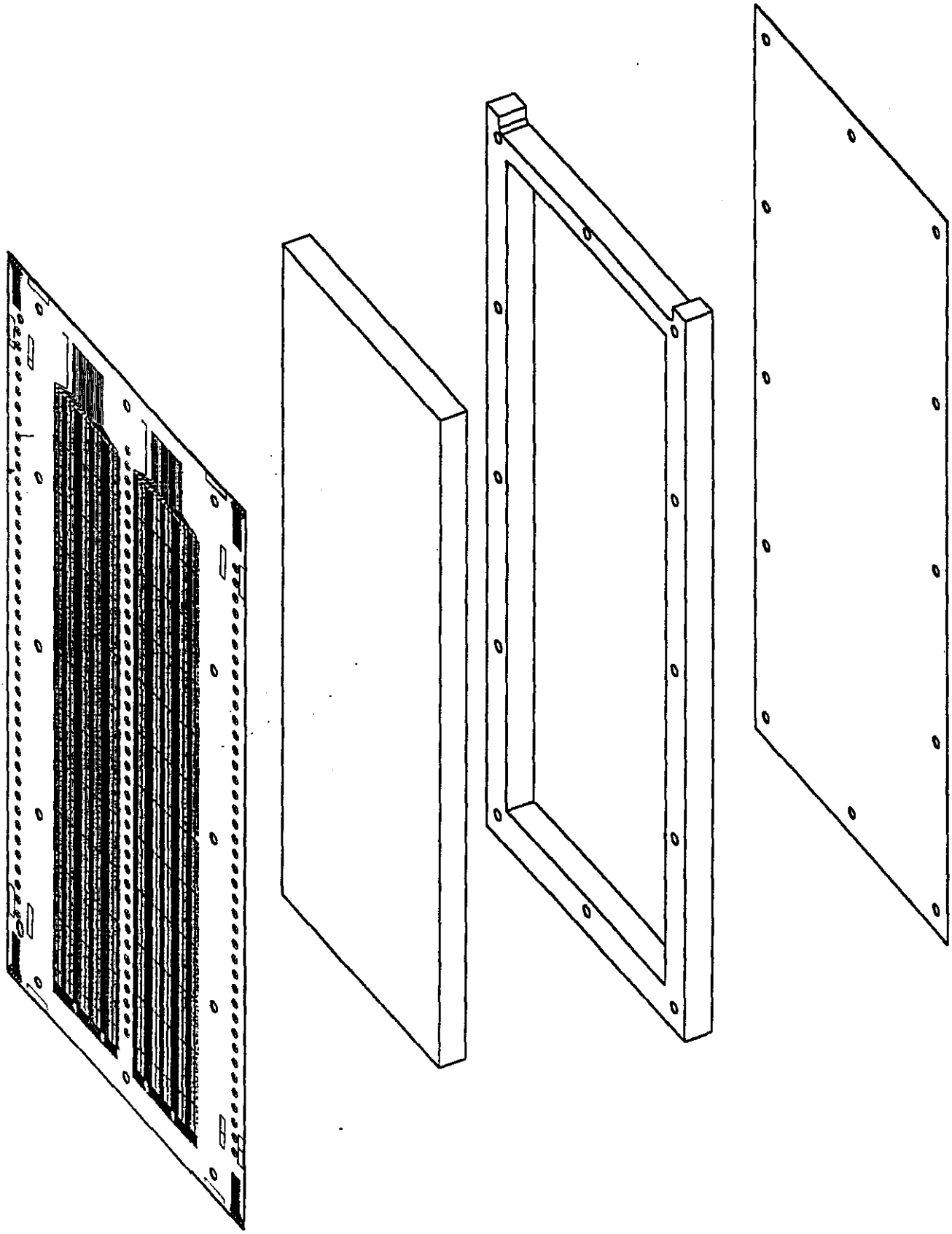

CSC ACTIVITY AT Dubna

I. GOLUTVIN

August 3, 1993

(1) 0,3 M × 3.0 M 4 GAP PROTOTYPE

- CONSTRUCTION WAS COMPLETED (END OF MAY)

- TECHNOLOGICAL ISSUES HAVE BEEN AGRESSIVELY STUDIED

- NOW THIS PROTOTYPE IS BEING TESTED AT DUBNA WITH COSMIC RAYS

CSC 3m x 0.3m

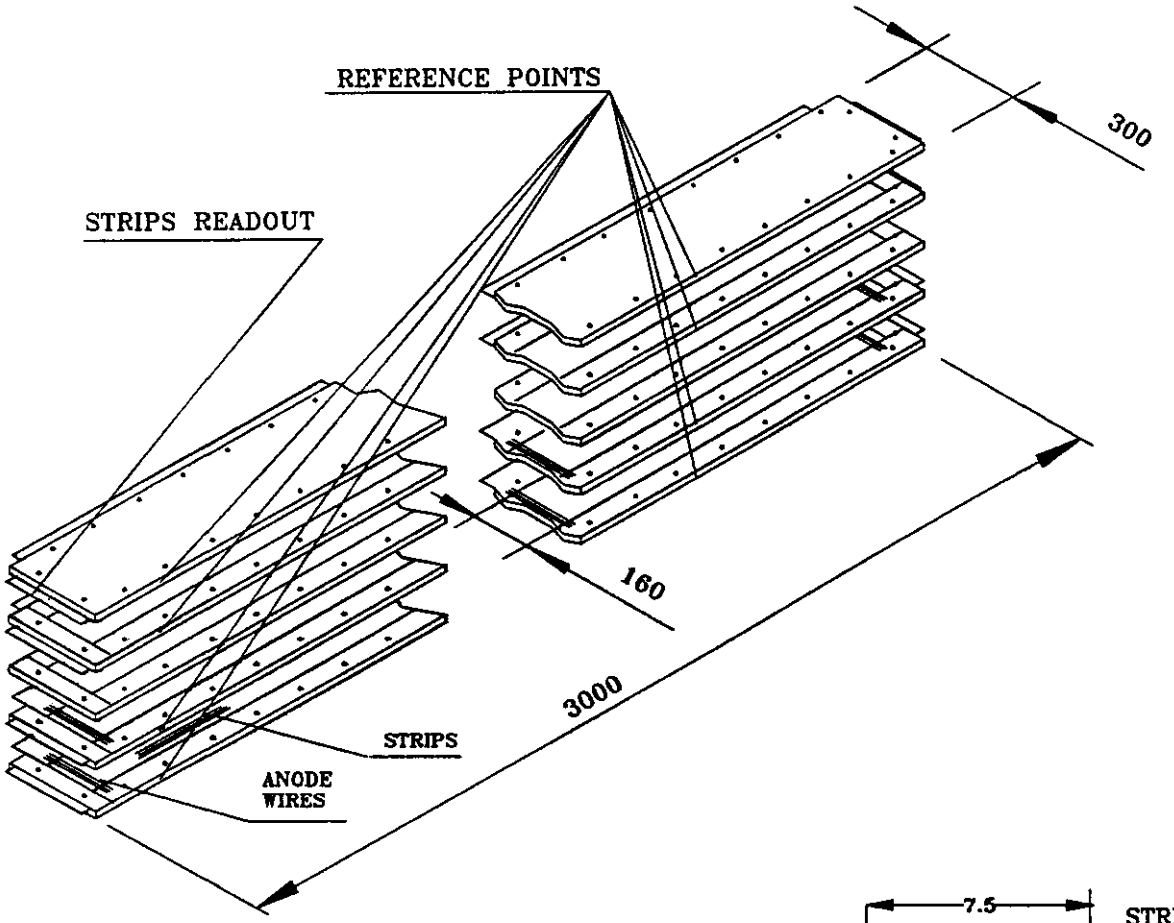

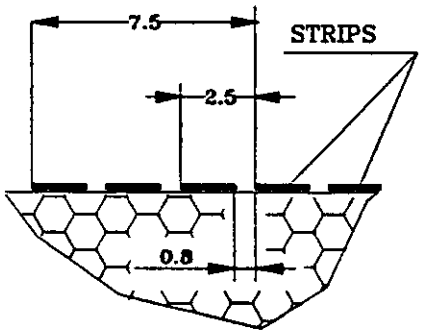

CROSS SECTION
ALONG THE WIRE

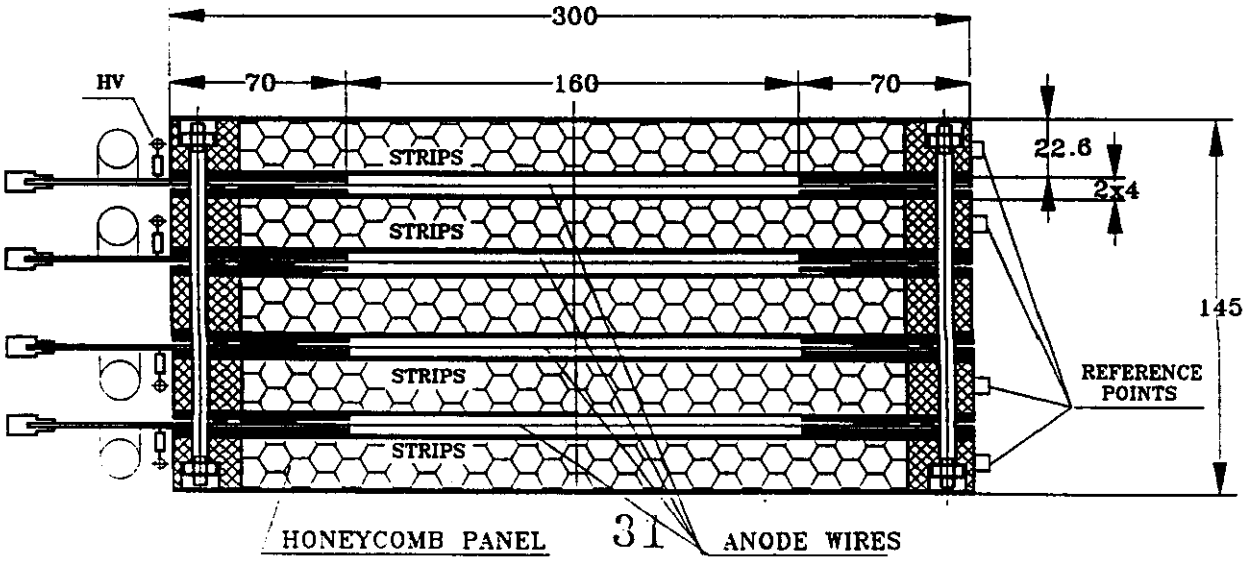

THE MAIN RESULTS OF TECHNOLOGY DEVELOPMENT:

- EXPERIENCE WITH 3M LONG CSC PRODUCTION;
- GAP IS CONTROLLED WITH A PRECISION ± 50 μm
- WIRE TENSION IS CONTROLLED WITH A PRECISION ± 1%.
- INTERSTRIP CAPACITANCES ARE CONTROLLED WITH A PRECISION ± 3%
- CHECK OF STRIPS
- HV TEST PROCEDURE
- WIRE CLEANING TECHNOLOGY
- ASSEMBLING THE CHAMBER WITH THE ELECTRODE TO ELECTRODE ALIGNMENT BETTER THEN ± 25 μm

AS A RESULT OF THIS TECHNOLOGY R&D

- STABLE CSS OPERATION AT $(1 \div 2)\,10^5$
- NO ADDITIONAL NOISE DUE TO DEFECTS
- ALIGNMENT ± 25 μm

EXPERIENCE WITH BNL ELECTRONICS:

AMPLEX:

- CROSSTALK ± 5%;
- NONLINEARITY;
- EXTRA NOISE IN THE 1ST AND THE LAST CHANNELS;

PAMPL:

- LEAKAGE THROUGH THE INPUT CAPACITOR;
- POOR PROTECTION OF THE MAIN TRANSISTOR

PCB:

- CROSSTALK ON TEST STRIPS

② 0,5M × 0,5M 4GAP PROTOTYPE.

- UNDER CONSTRUCTION
- WILL BE READY BY AUGUST 15

MAJOR GOALS:

(*) TECHNOLOGY R&D

(**) TEST OF ALTERNATIVE CONCEPTS OF READOUT ELECTRONICS

(***) PERFORMANCE STUDY

- THIS PROTOTYPE IS MADE OF 100% RUSSIAN MATERIALS
- STRIPED ELECTRODES ARE MADE AT DUBNA

(3) 1.1 m × 3.0 m 6 GAP PROTOTYPE.

GOAL: THE 1ST FULL SCALE GEM MUON SYSTEM PROTOTYPE

CSC 3m x 1.1m

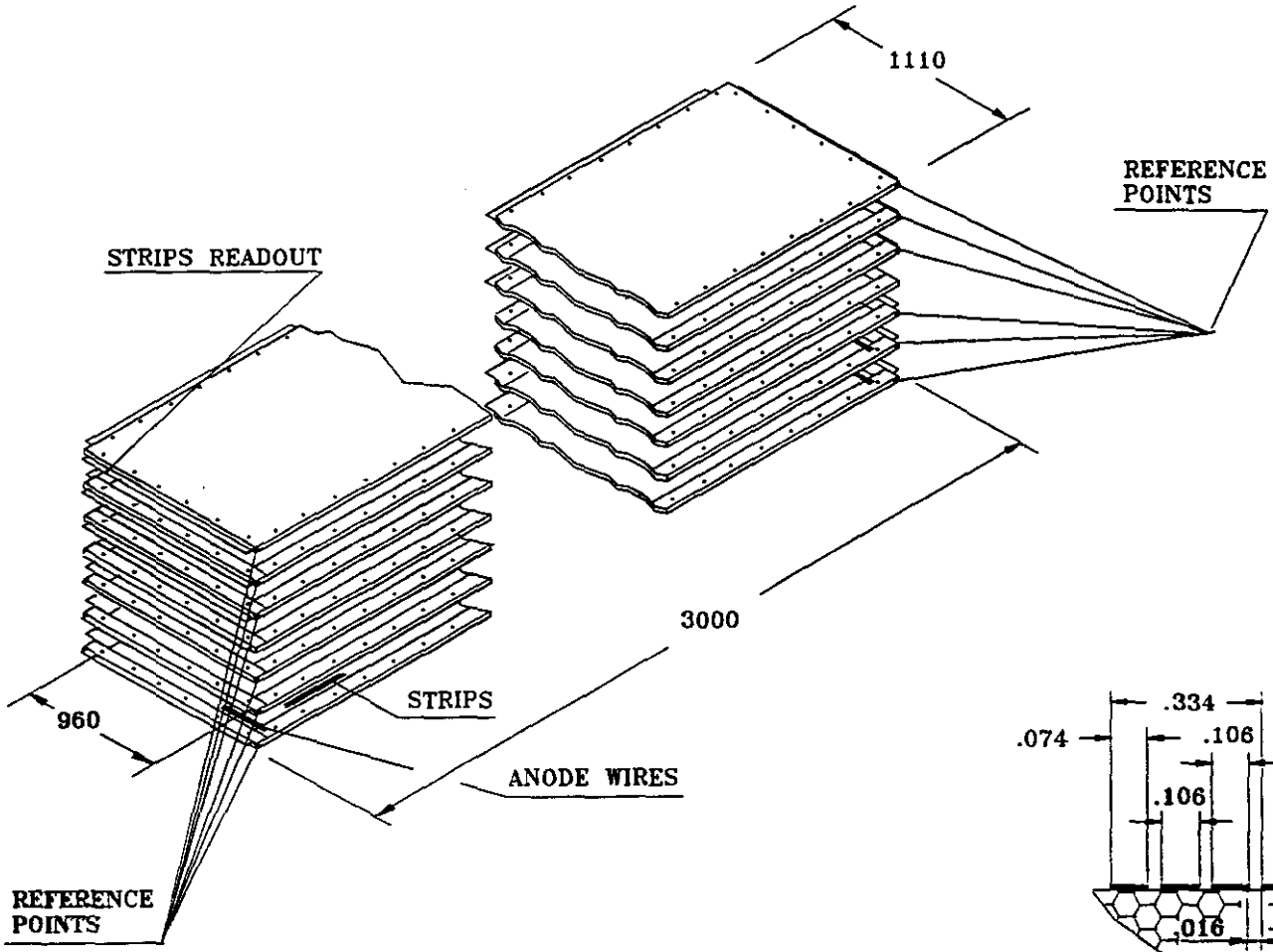

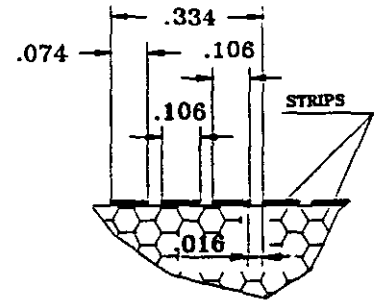

CROSS SECTION
ALONG THE WIRE

(dimensions in in.)

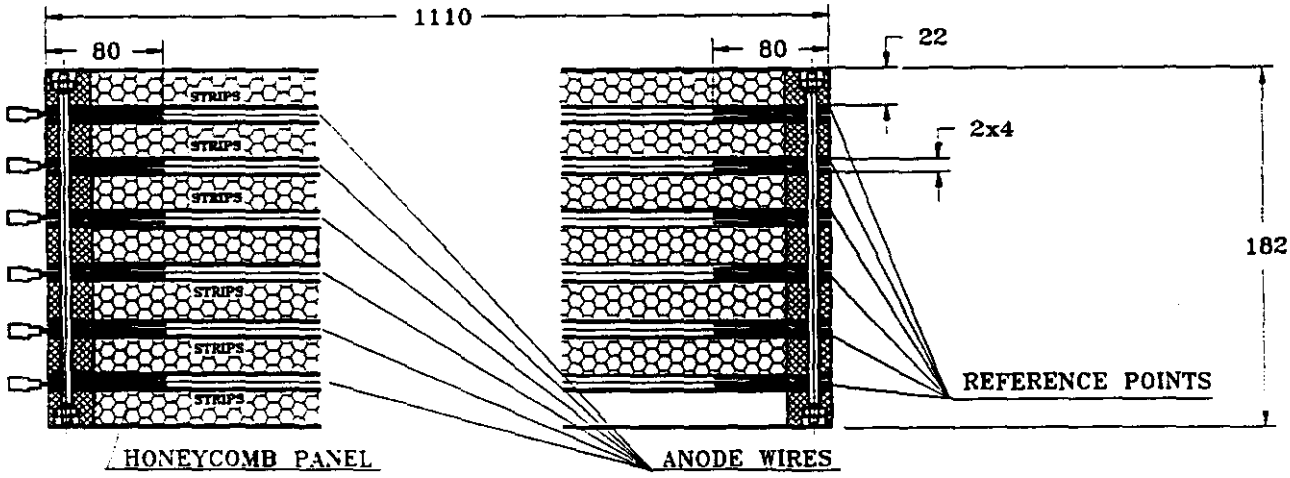

(dimensions in mm)

CSC PROTOTYPES PRODUCTION FACILITY

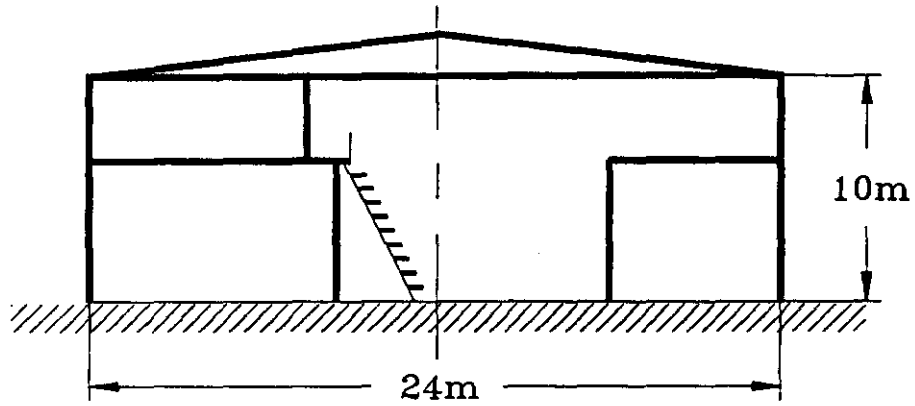

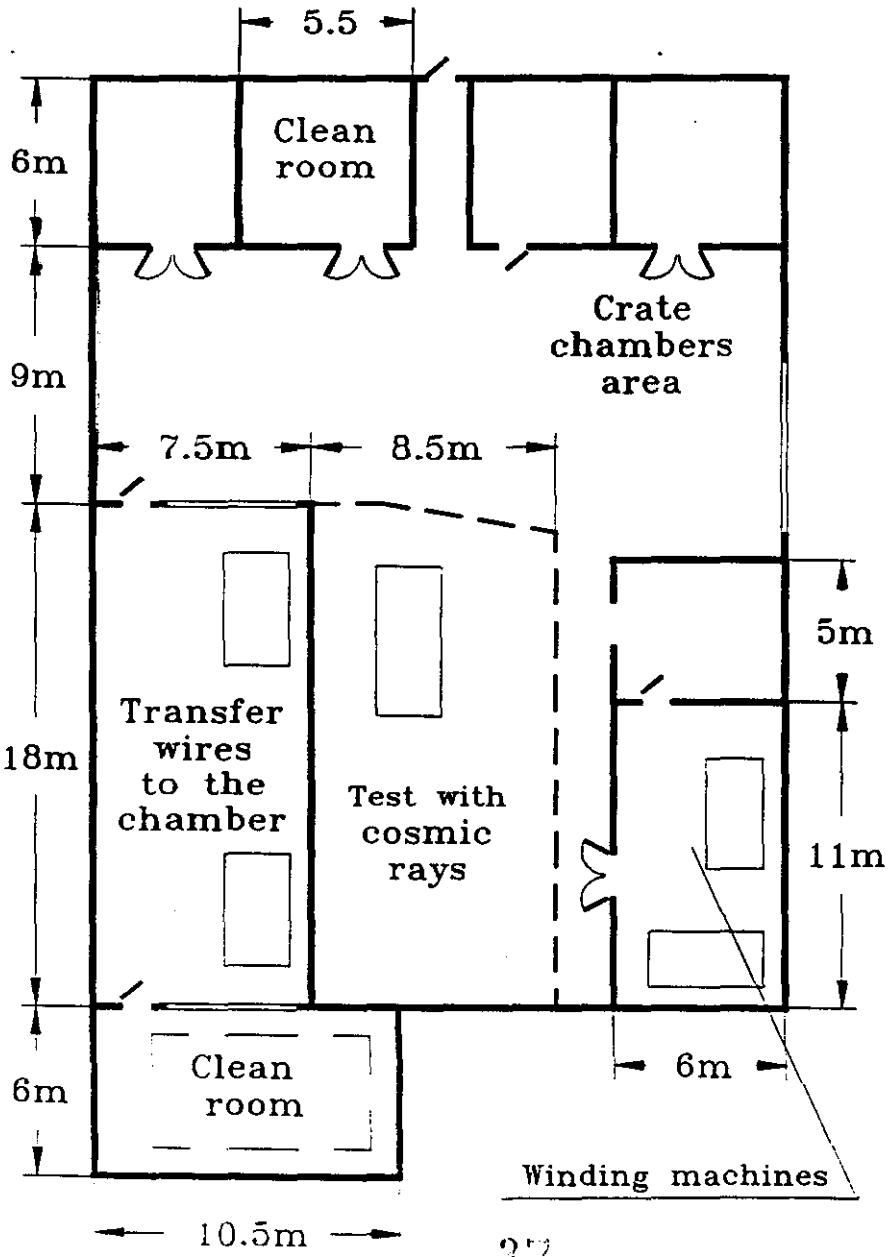

CLEAN ROOM

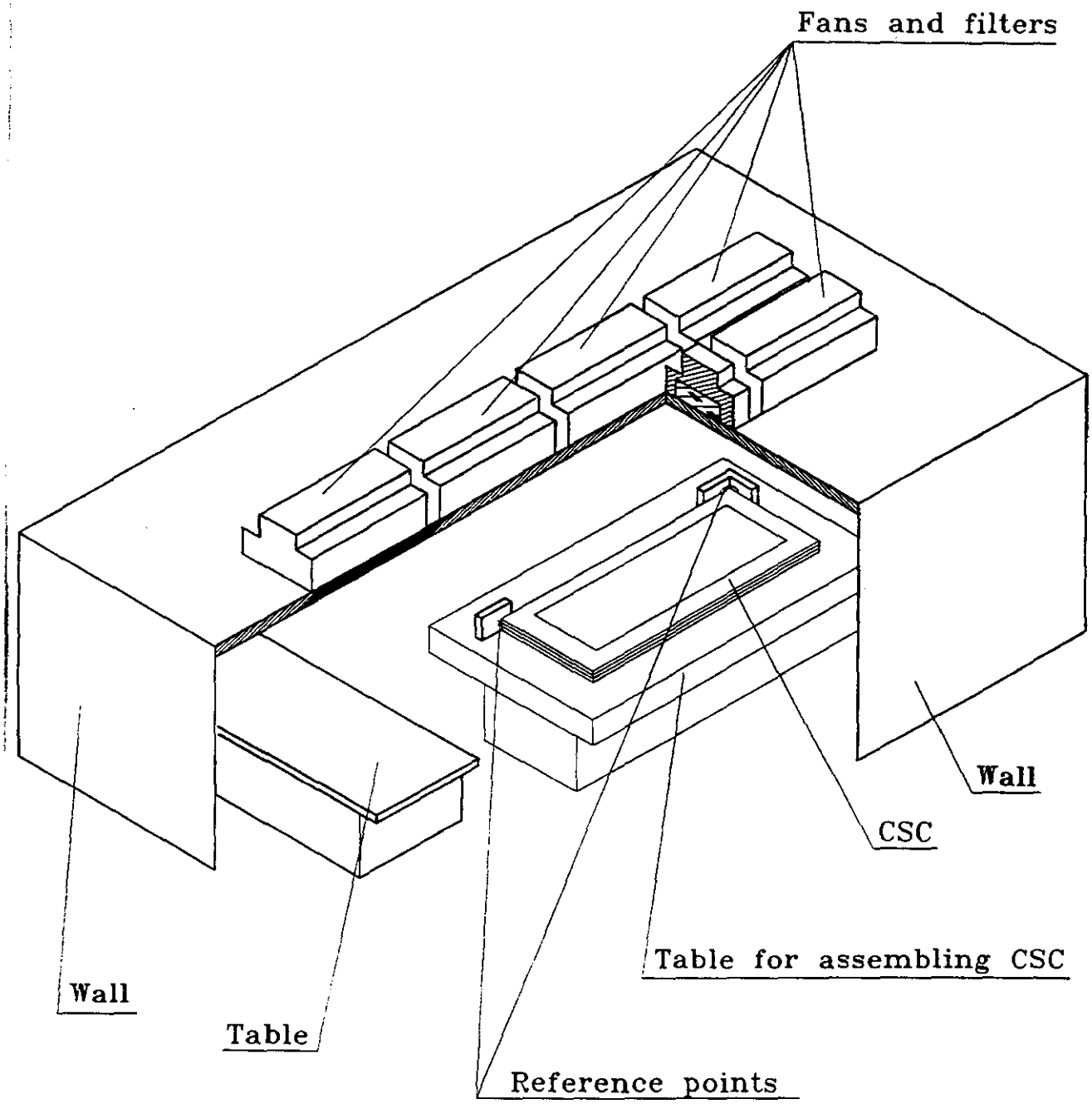

T = 20 C
HUMIDITY = 60%
AIR RATE CLEAN =10 000 dust part./cu.ft

CSC PROTOTYPE MILESTONES

* 1.	Panels preprocessing	June 1993
* 2.	Materials from SSCL received	June 1993
3.	Panels processing, precise gauges mounting, stripped boards gluing	2 August 1993
4.	Getting bars ready for gluing	13 August 1993
5.	Glue bars to panels	15 August 1993
6.	Drill holes	16 August 1993
* 7.	Test assembly of the panels	**17 August 1993**
8.	Assemble spacers and gas outlets	24 August 1993
9.	Cover strips with resistive mater.	25 August 1993
10.	Install anode wires	1 September 1993
11.	Mount Capacitors, resistors, connectors	2 September 1993
*12.	Assembled planes acceptance check	**3 September 1993**
13.	Get planes ready to assemble, clean	4 September 1993
*14.	Assemble chamber	**5 September 1993**
15.	Mount exterior parts	8 September 1993
*16.	Final test	**9-13 September 1993**
*17.	Packing	**14 September 1993**

Steps 4-6, 8-9, 10-13 go in parallel for all planes.
Key operations are shown in bold.

STATUS OF $1.1 \times 3.0\ m^2$ PROTOTYPE

- HONEYCOMB PANELS ARE READY
- MATERIALS FROM SSCL ARE STILL IN U.S.A.

  SCHEDULE WILL MOVE TO END Oct/ BEG. NOV

! THE CRUCIAL ISSUE NOW IS TRAVEL EXPENCIES FOR DUBNA TEAM TO COME AT SSC TO PARTICIPATE IN SETTING UP AND CONDUCTING THE TTR TEST

!! ANOTHER CRUCIAL ISSUE IS READOUT ELECTRONICS

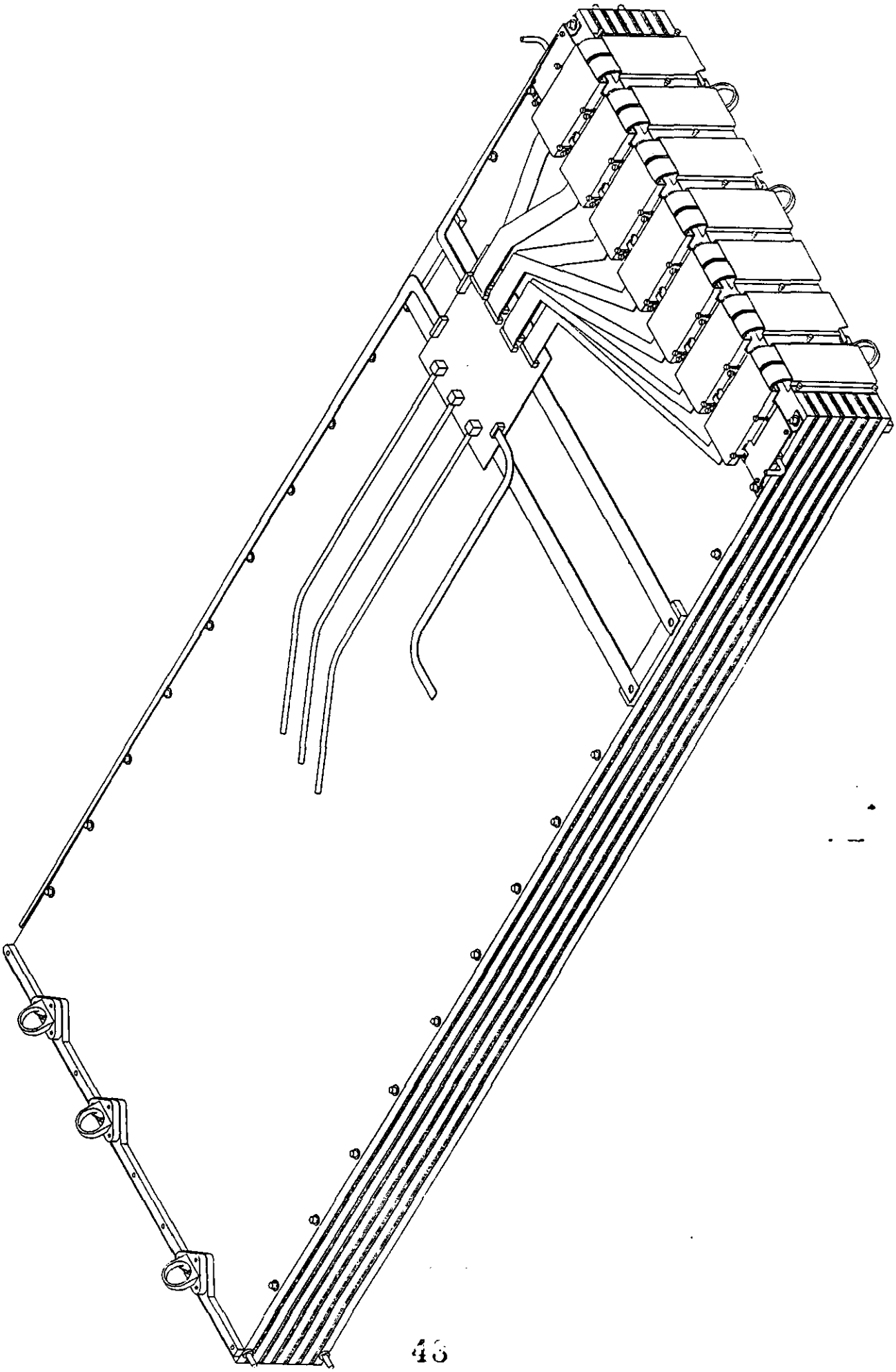

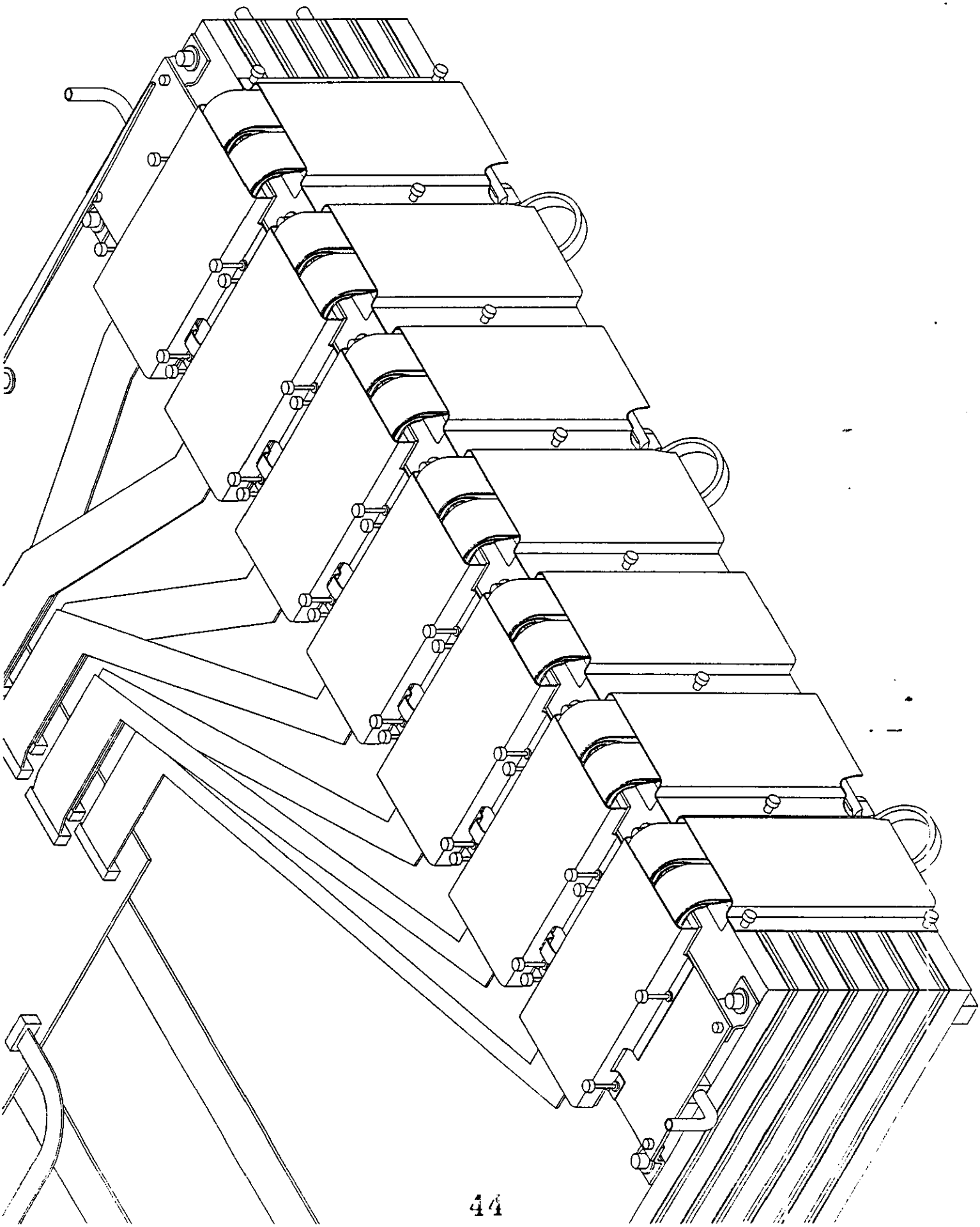

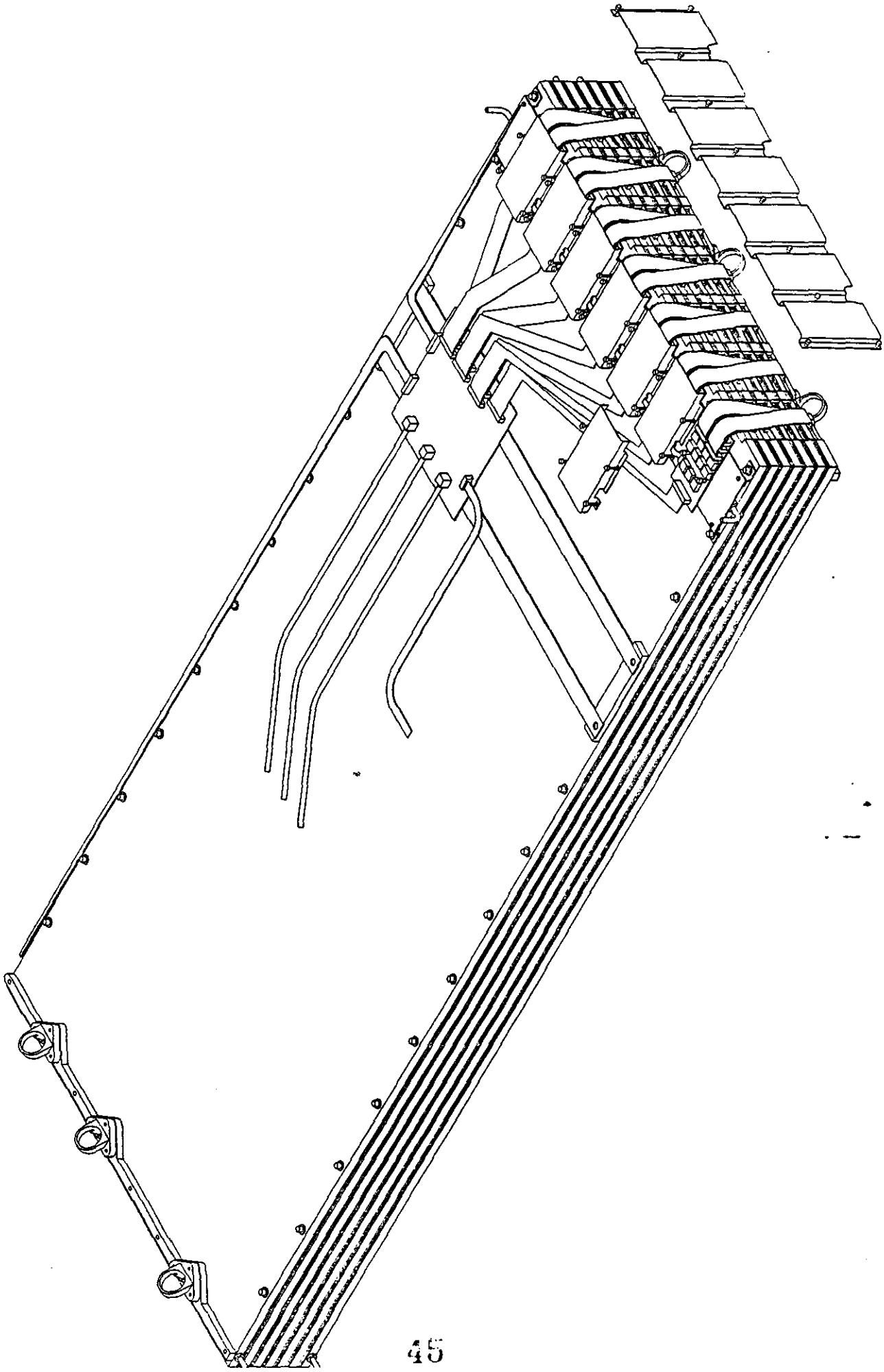

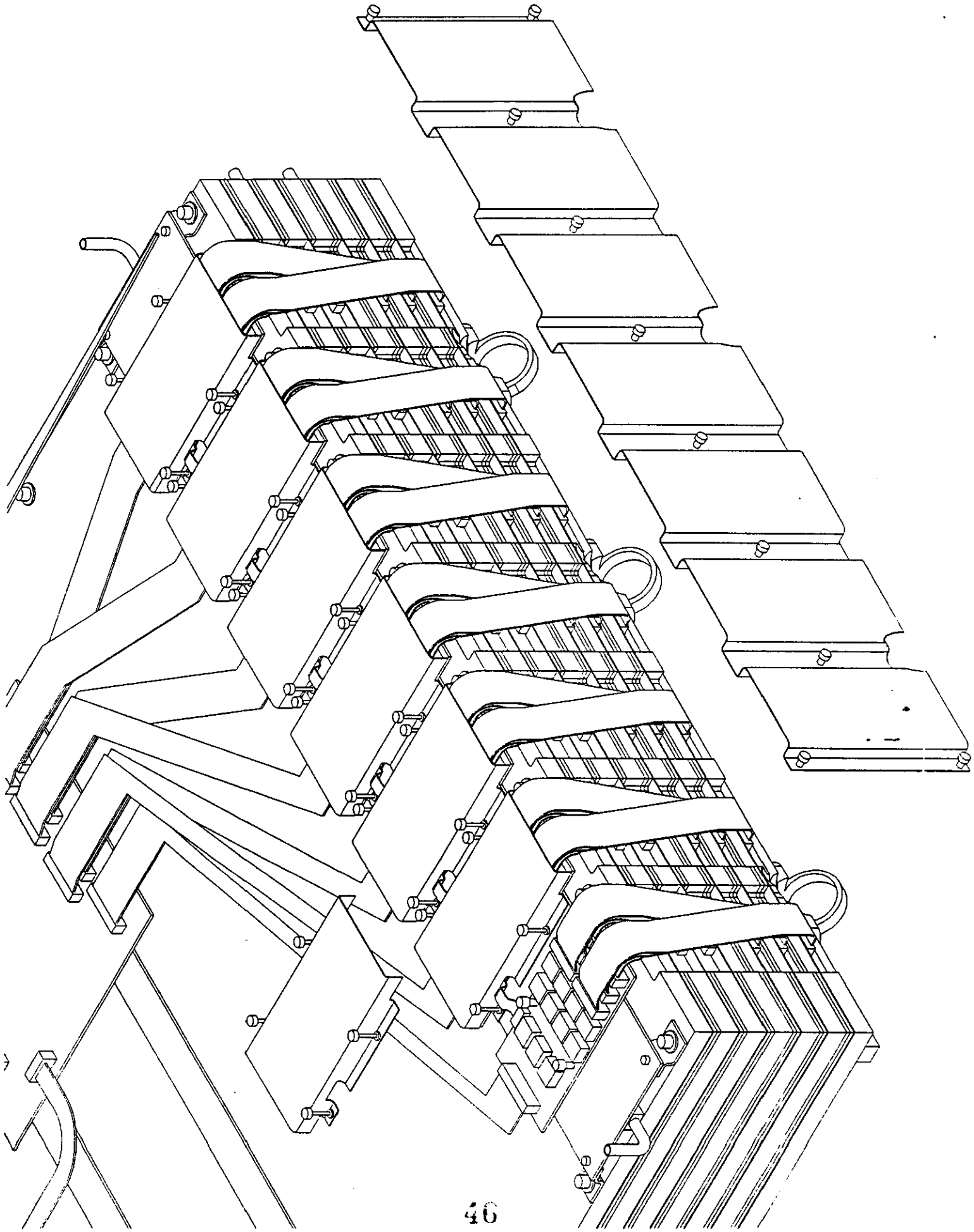

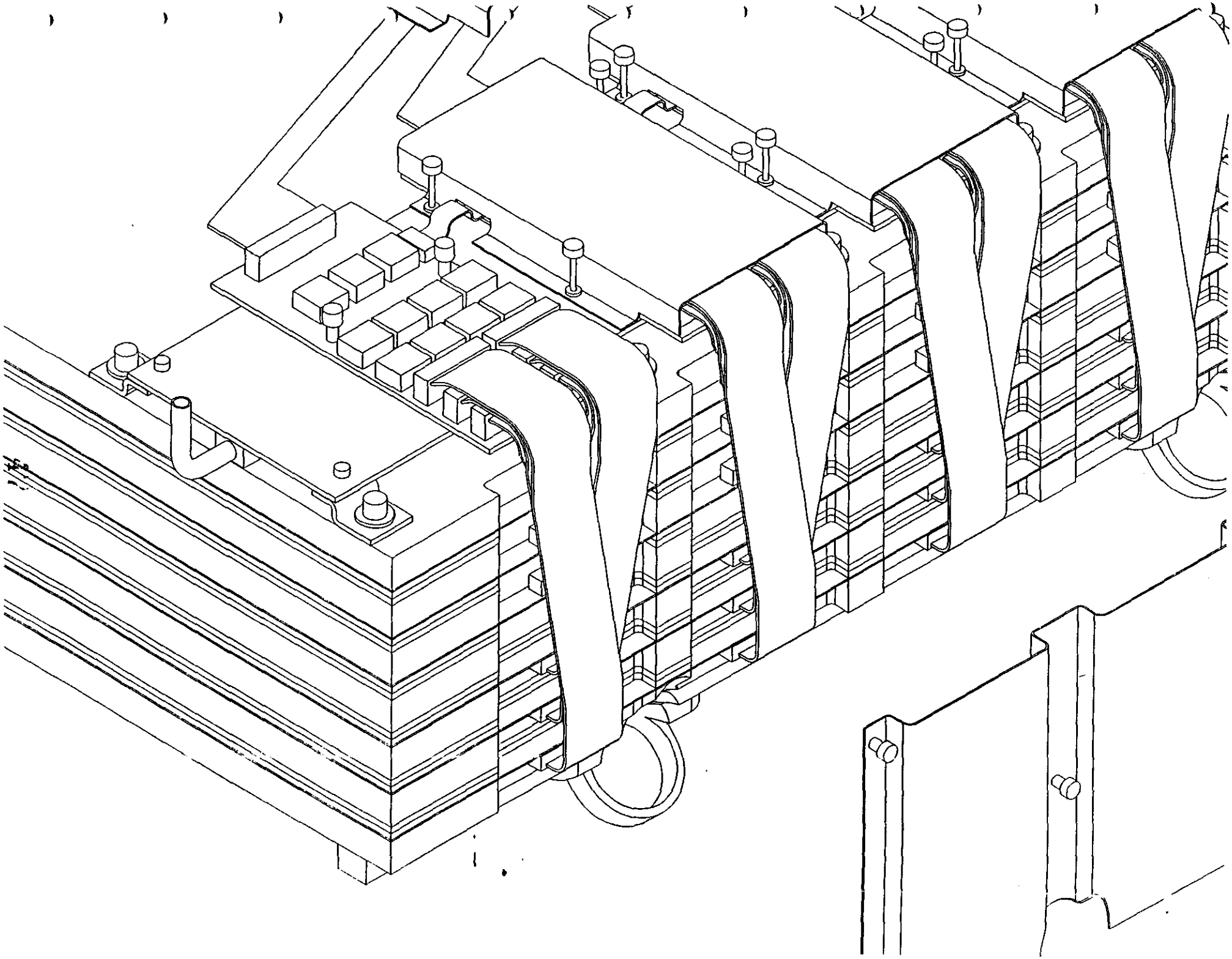

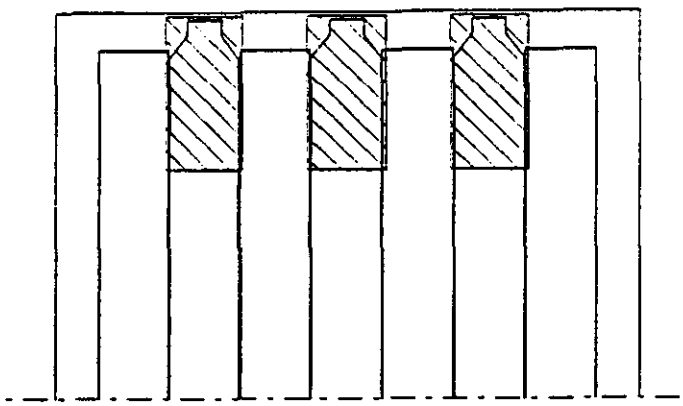

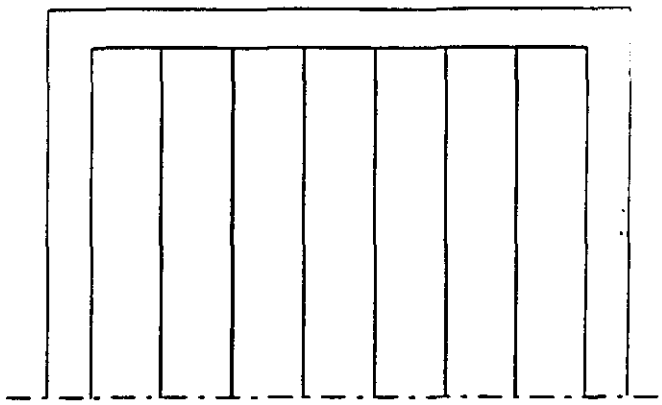

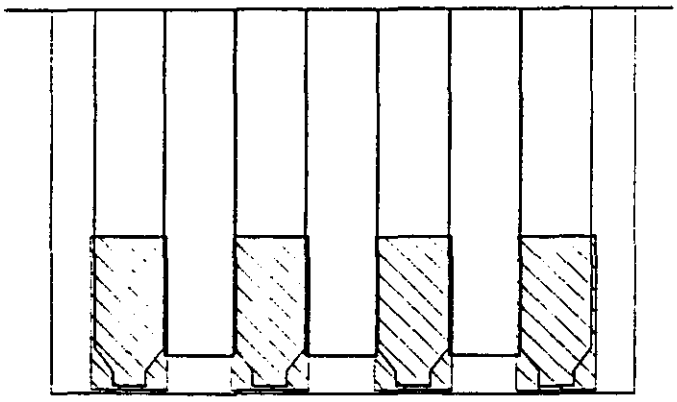

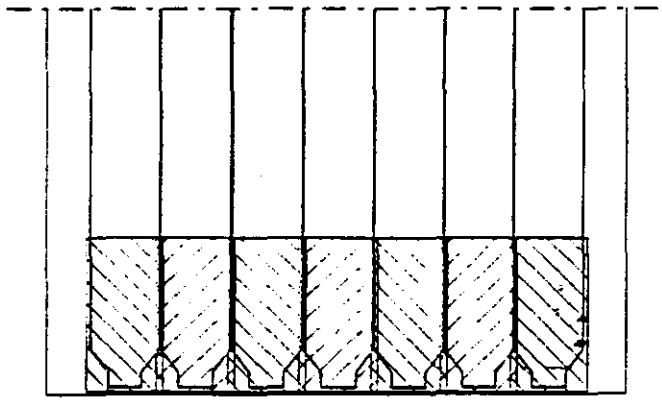

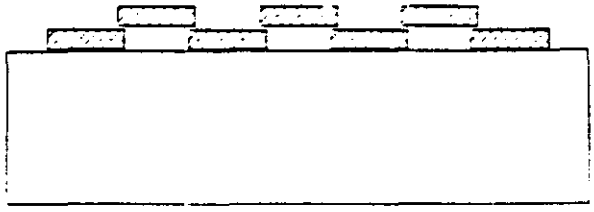

MUON CHAMBER NUMBERING SYSTEM

BARREL SHOWN

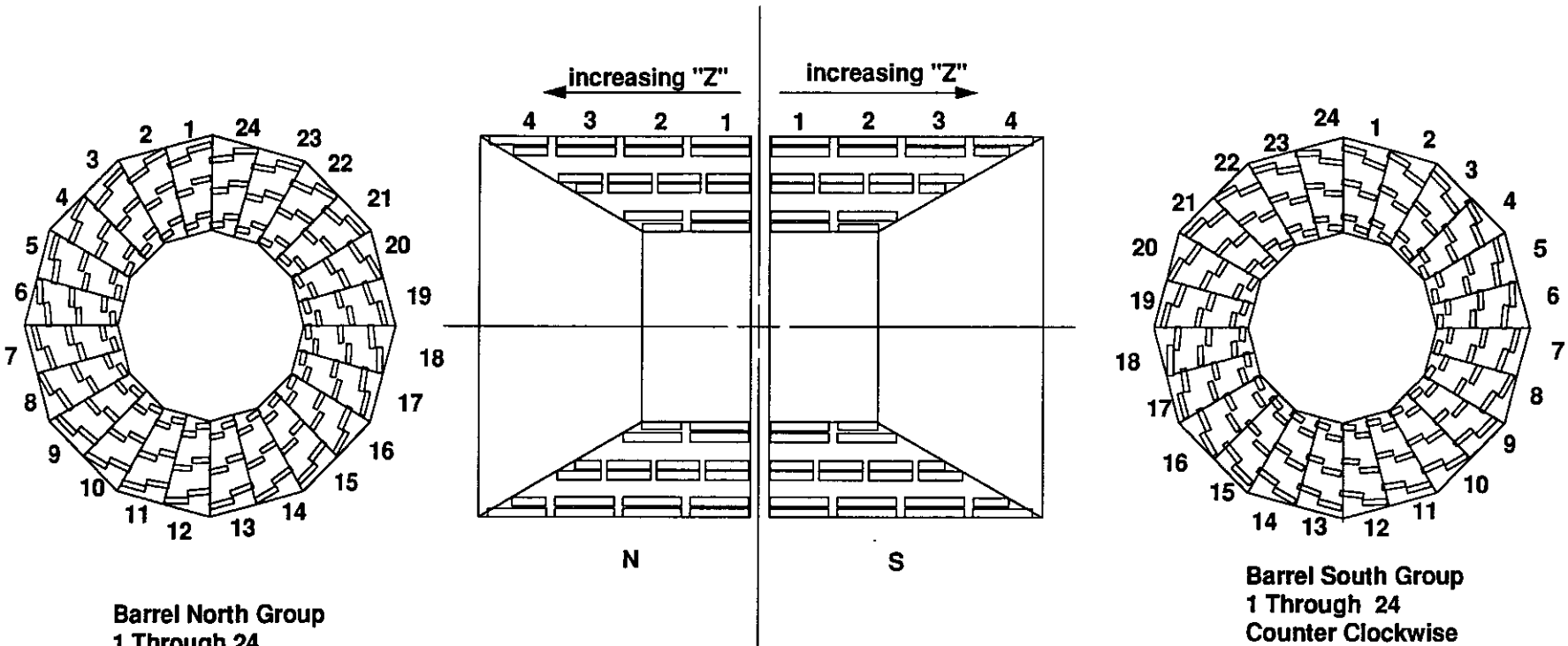

I B N 1 3 A 1

- I = INNER, M = MIDDLE, O = OUTER
- B = BARREL, E = END CAP
- N = NORTH, S = SOUTH
- SEGMENT 1 - 24 N
- ALIGNMENT TOWER 1, 2, 3, 4
- B = TOP, A = BOTTOM
- CHAMBER GEOMETRY ACTIVE AREAS 1 - 8

MUON CHAMBER IDENTIFICATION

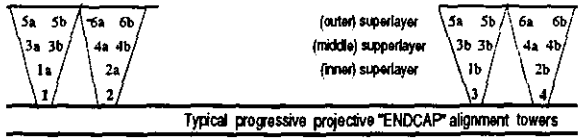

Typical progressive projective "ENDCAP" alignment towers

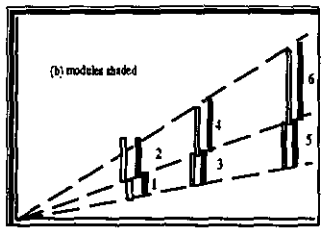

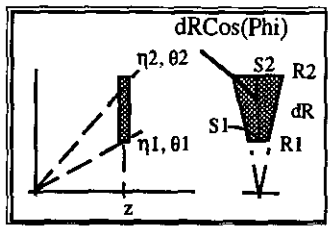

PROPOSED ENDCAP CHAMBER SERIAL / LOCATION	SUPERLAYER	LOCATION	DIRECTION	SEGMENT	ALIGNMT TOWER	A/TOT B/BOTTOM	CHAMBER GEOMETRY	ALIGNMENT PROJECTIVE TOWER	CHAMBER GEOMETRY	GEM endcap active volume m^3	GEM 50%Carbon Dioxide 0.50 m^3	GEM 30%Argon 0.30 m^3	GEM 20%CF4 0.20 m^3
	I	EC	S	1	1	a	1	1	1a)	0.40			
	I	EC	S	1	3	b	1	3	1b)	0.48			
	I	EC	S	1	2	a	2	2	2a)	1.35			
	I	EC	S	1	4	b	2	4	2b)	1.25			
										3.49			
	M	EC	S	2	1	a	3	1	3a)	1.42			
	M	EC	S	2	1	b	3	1	3b)	1.57			
	M	EC	S	2	2	a	4	2	4a)	2.90			
	M	EC	S	2	2	b	4	2	4b)	3.21			
										9.11			
	O	EC	S	1	1	a	5	1	5a)	3.92			
	O	EC	S	1	1	b	5	1	5b)	4.22			
	O	EC	S	1	2	a	6	2	6a)	8.95			
	O	EC	S	1	2	b	6	2	6b)	9.61			
										26.70	19.65	11.79	7.86
	M	EC	S	2	3	a	3	3	3a)	39.30	19.65	11.79	7.86
	M	EC	S	2	3	b	3	3	3b)				
	M	EC	S	2	4	a	4	4	4a)				
	M	EC	S	2	4	b	4	4	4b)				
	O	EC	S	1	3	a	5	3	5a)				
	O	EC	S	1	3	b	5	3	5b)				
	O	EC	S	1	4	a	6	4	6a)				
	O	EC	S	1	4	b	6	4	6b)				

PROPOSED BARREL CHAMBER SERIAL / LOCATION	SUPERLAYER	LOCATION	DIRECTION	SEGMENT	ALIGNMT TOWER	b/TOP a/BOTTOM	CHAMBR GEOMETRY	NORTH 1/2barrel active volume [m^3]	GEM barrel active volume [m^3]	GEM Carbon Dio 0.50 [m^3]	GEM 30%Argon 0.30 [m^3]	GEM 20%CF4 0.20 [m^3]
	I	b	n	1	3	a	1	1.56				
	I	b	n	1	4	a	2	1.30				
	I	b	n	1	1	b	1	1.56				
	I	b	n	1	2	b	1	1.56				
	M	b	n	1	3	a	3	2.65				
	M	b	n	1	3	a	4	2.37				
	M	b	n	1	4	a	5	1.59				
	M	b	n	1	4	a	6	1.59				
	M	b	n	1	1	b	3	2.65				
	M	b	n	1	1	b	4	2.37				
	M	b	n	1	2	b	5	2.24				
	M	b	n	1	2	b	7	2.38				
	O	b	n	1	3	a	8	5.86				
	O	b	n	1	3	a	8	5.86				
	O	b	n	1	4	a	8	5.86				
	O	b	n	1	4	a	8	4.60				
	O	b	n	1	1	b	8	5.86				
	O	b	n	1	1	b	8	5.86				
	O	b	n	1	2	b	8	5.86				
	O	b	n	1	2	b	8	5.86				
								69.44	138.87	69.44	41.66	27.77

A. OTTO STEGER

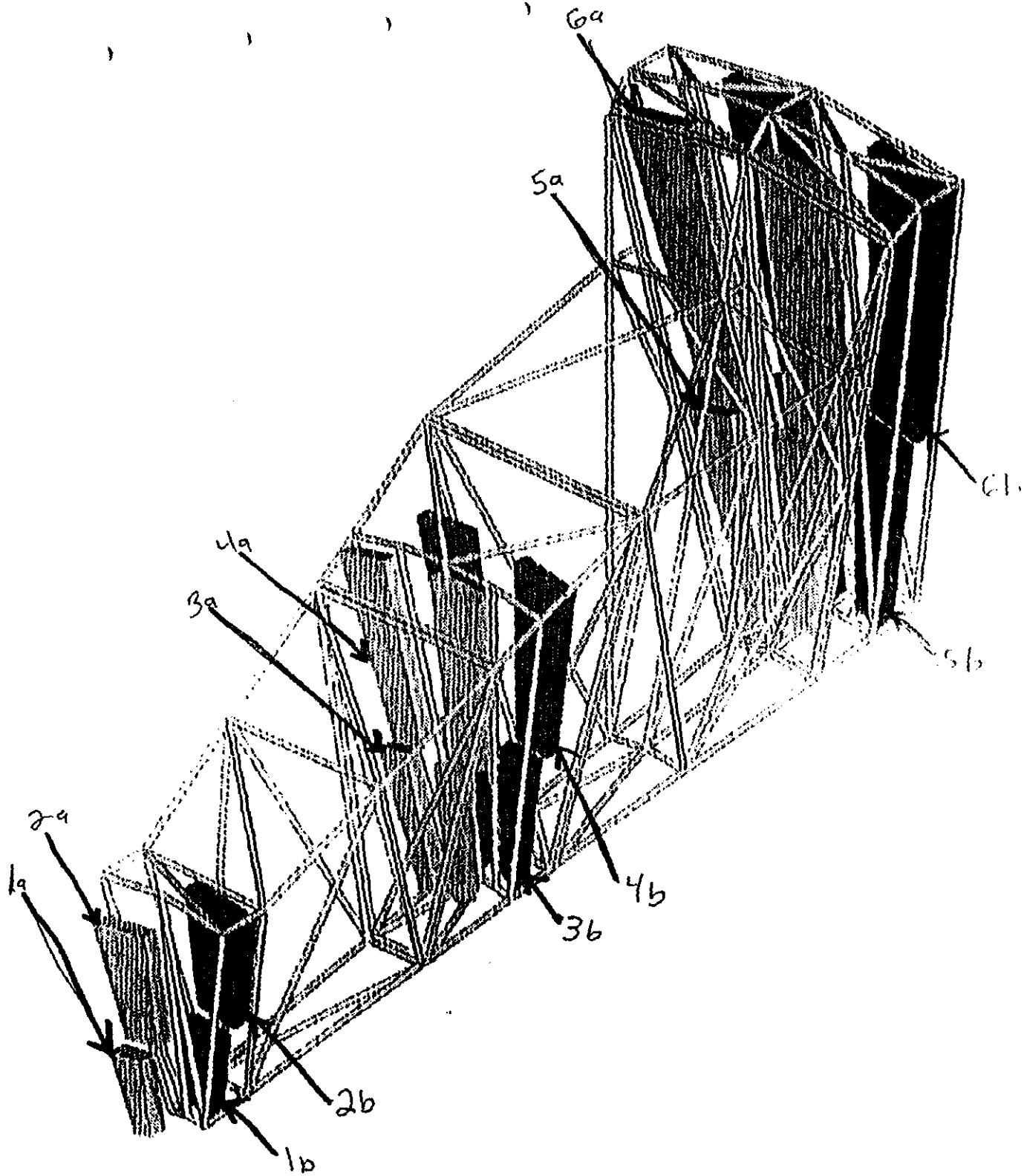
6a
5a
6b
5b
4a
3a
4b
3b
2a
1a
2b
1b

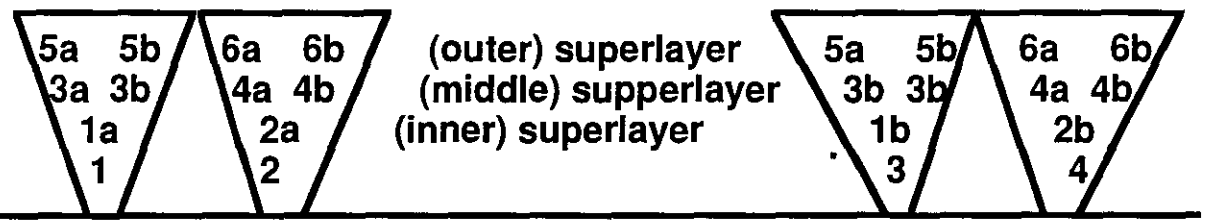

Typical progressive projective alignment towers

TYPICAL ALIGNMENT TOWER

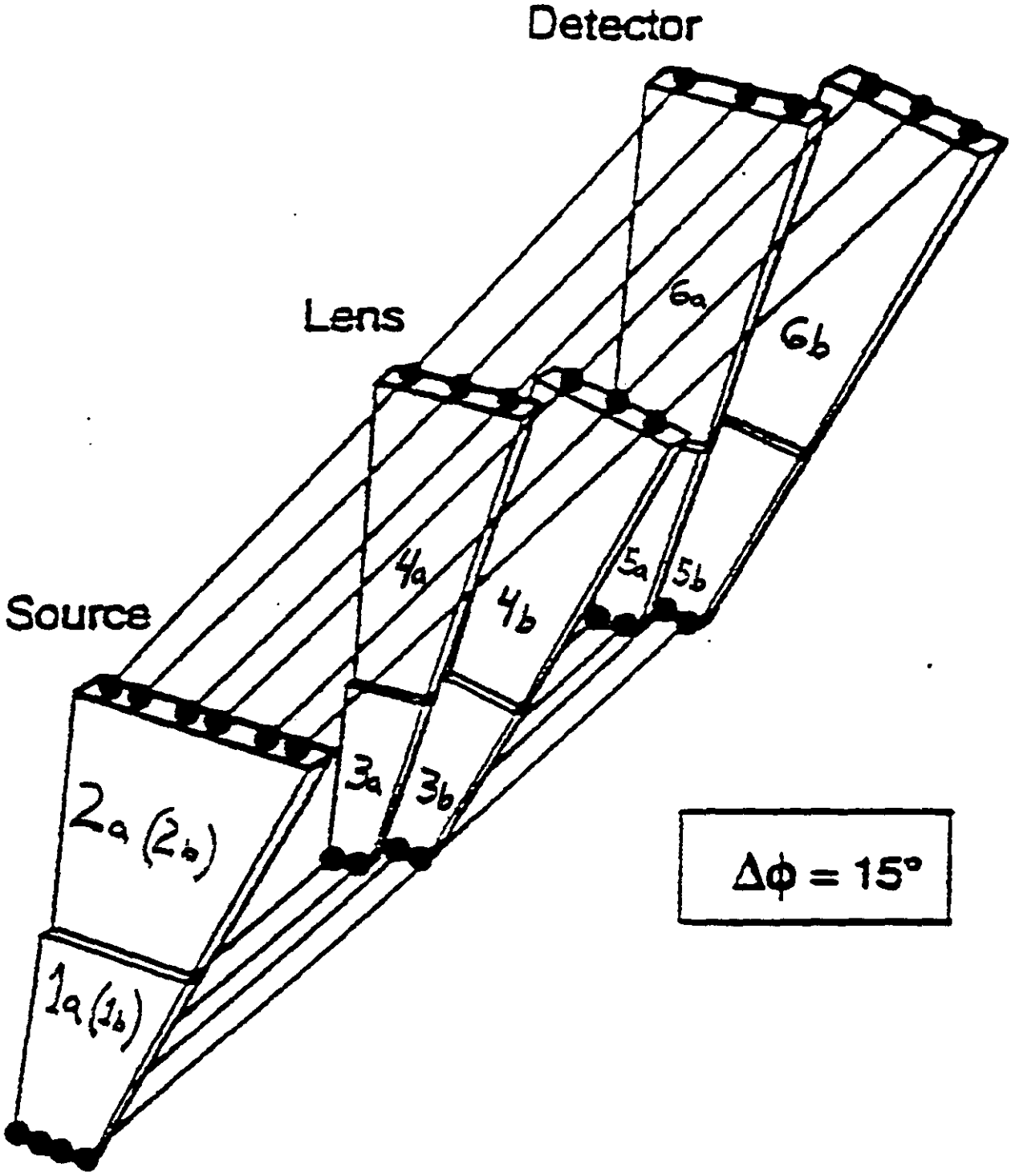

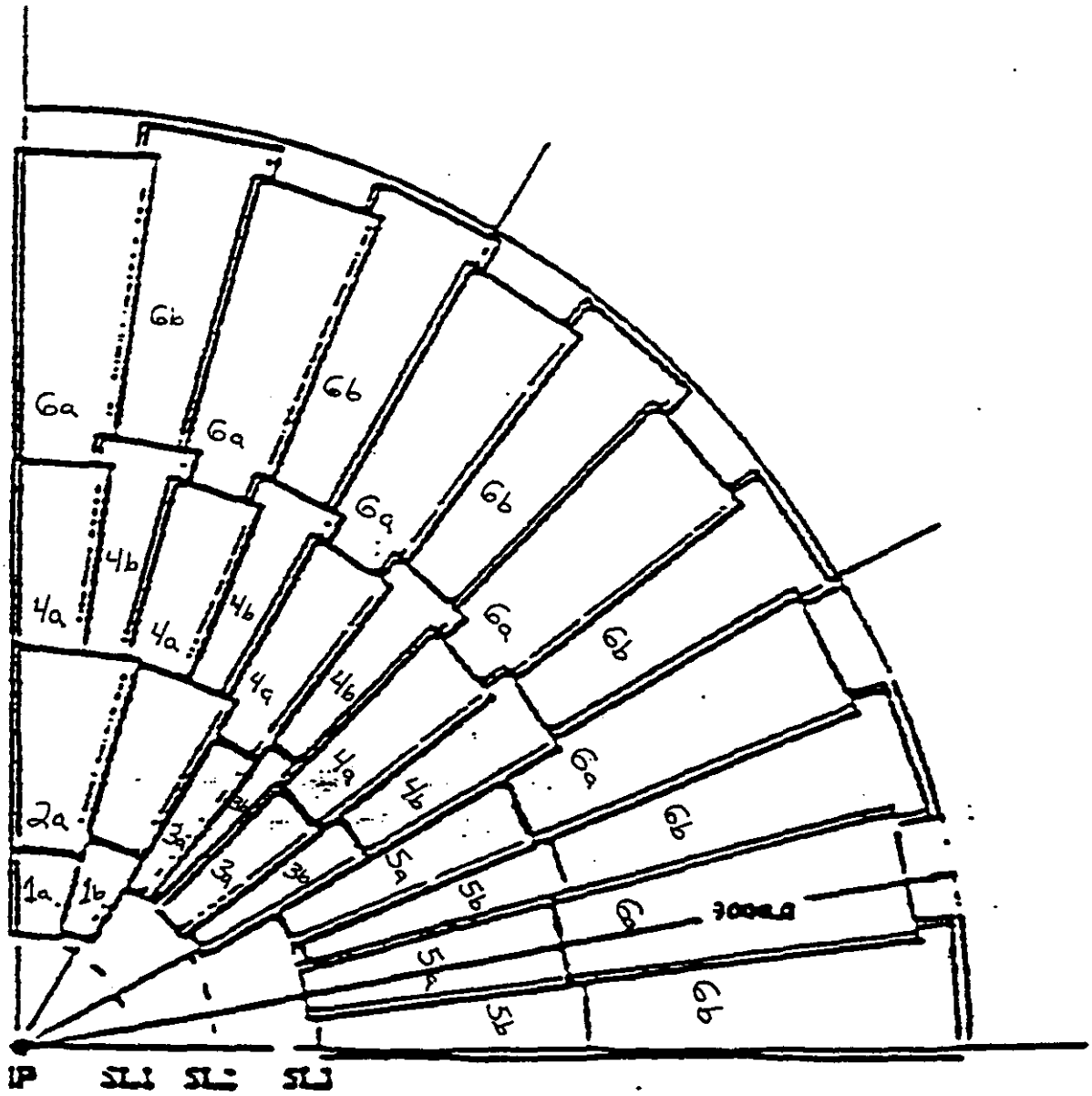

Figure 4.1c Endcap Muon Chamber Layout (1/4 Section) View from IP

TYPICAL ALIGNMENT TOWER

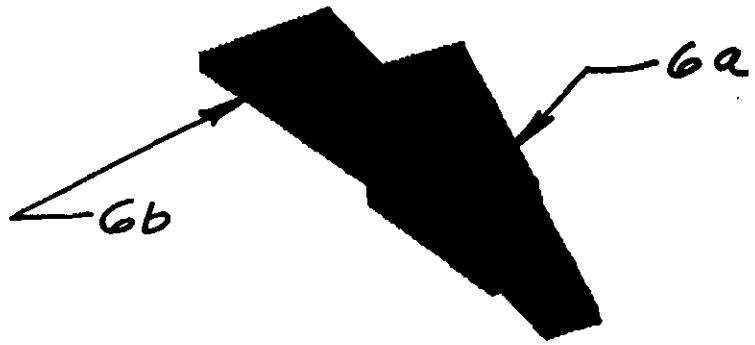

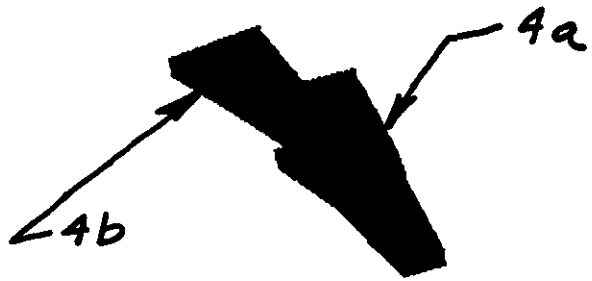

TYPICAL ALIGNMENT TOWER

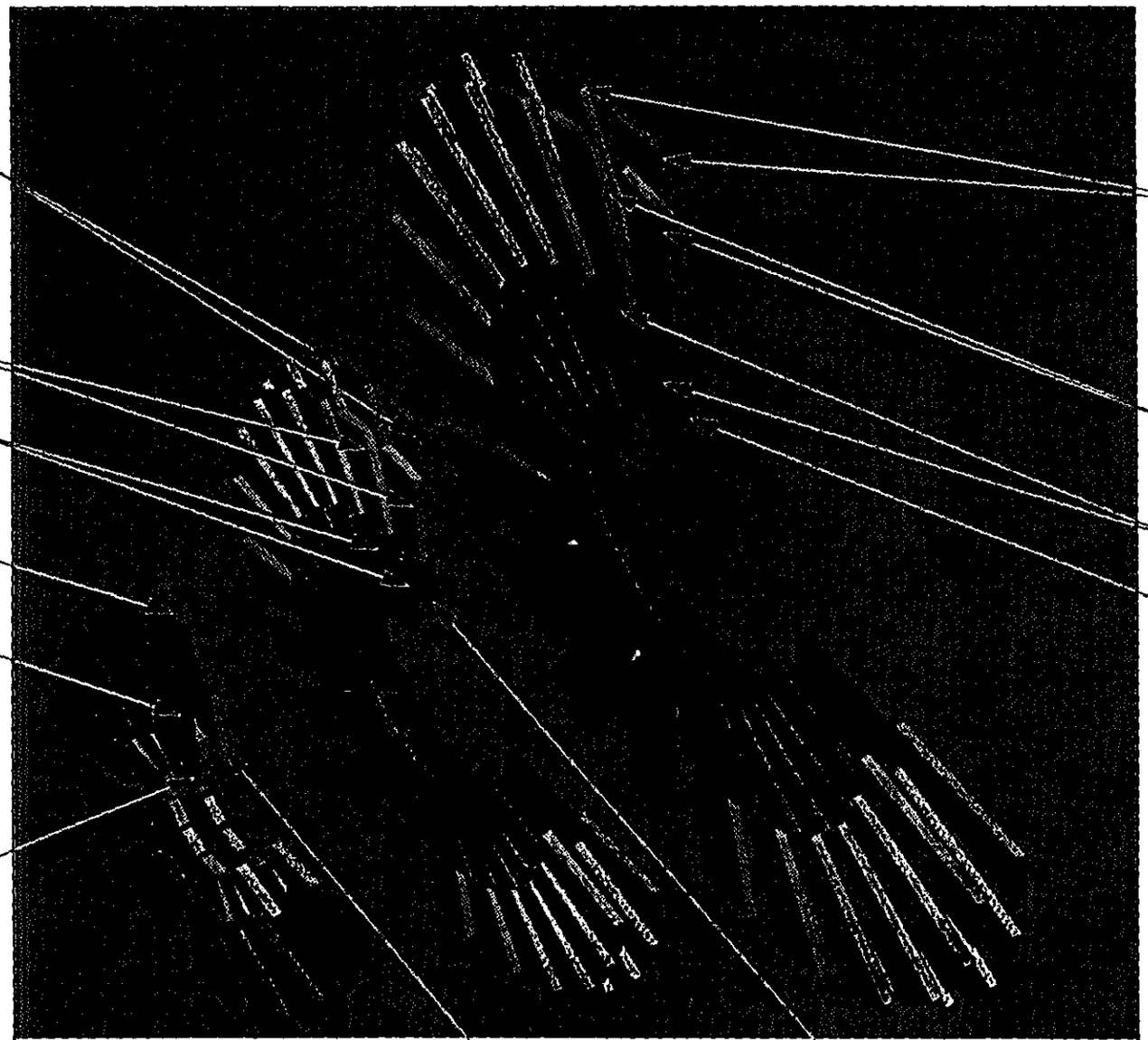

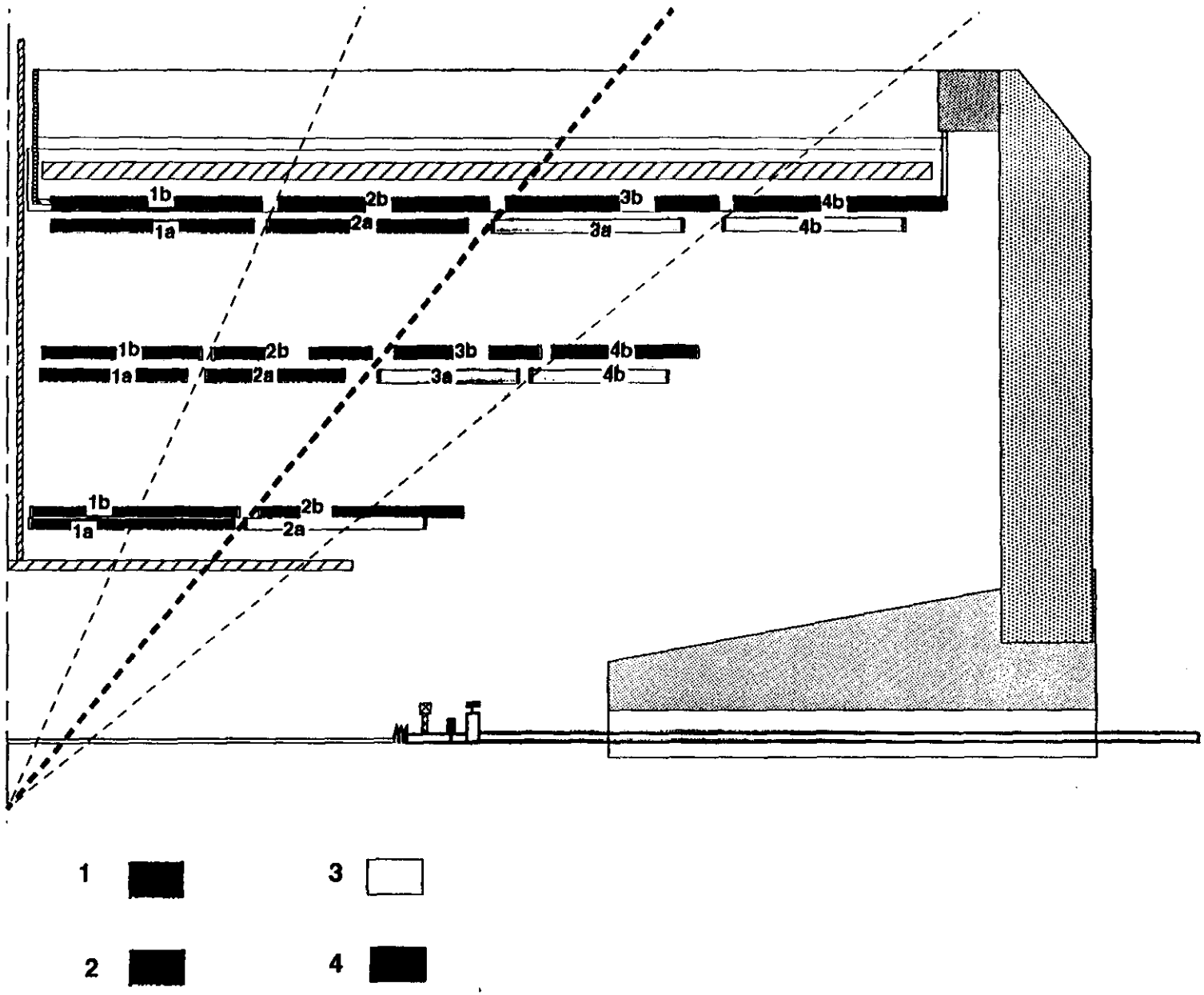

1/2 BARREL

a)

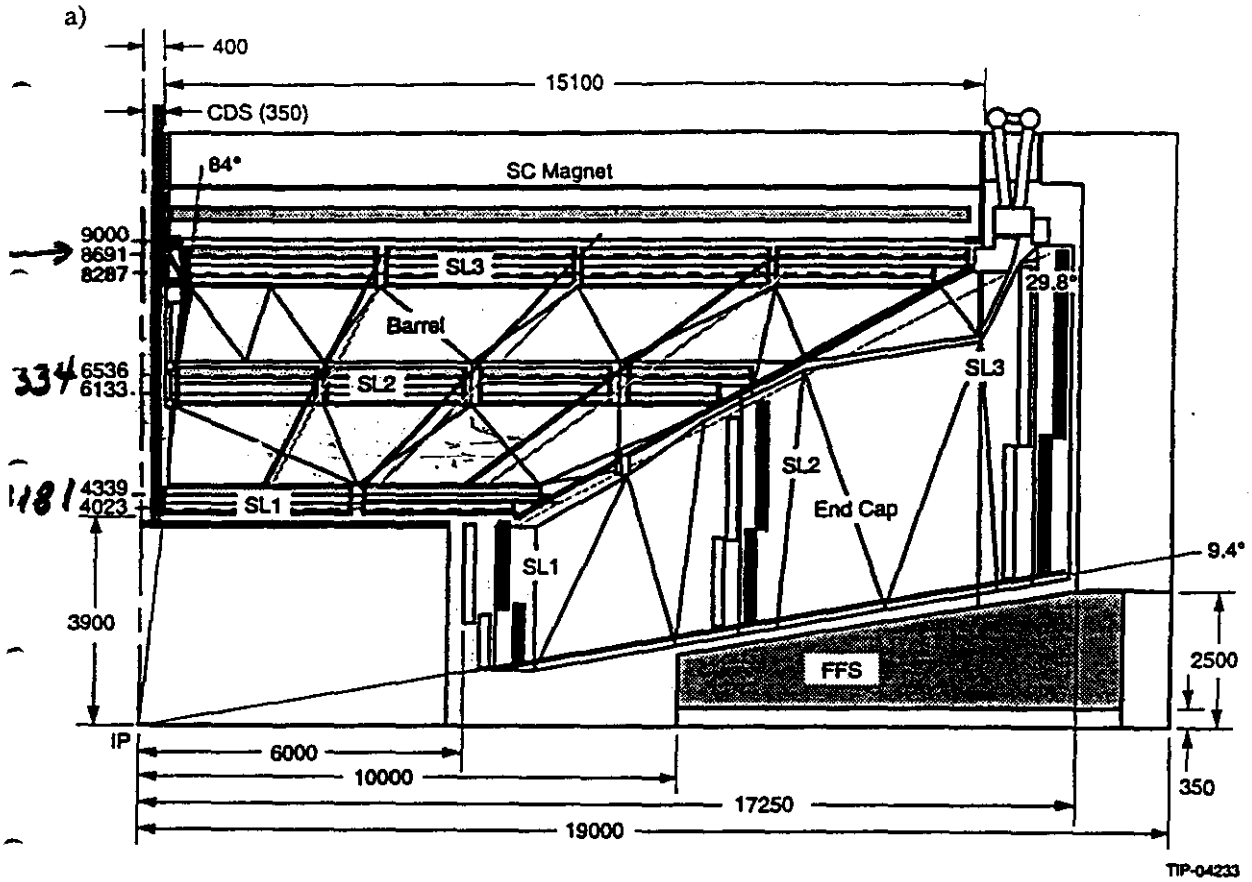

b)

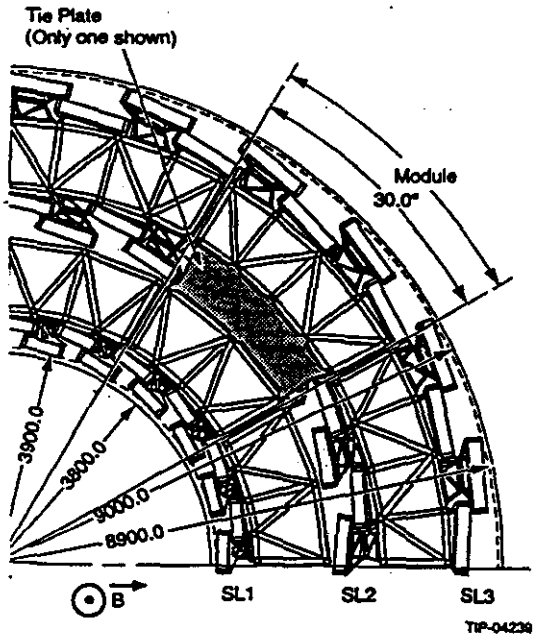

c)

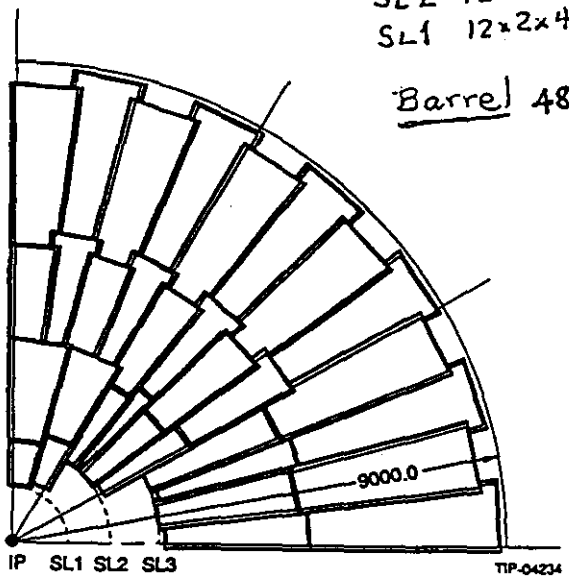

½ Barrel

SL3 12×4×4 = 192
SL2 12×4×4 = 192
SL1 12×2×4 = 96
480

Barrel 480×2 = 960

3. 4-1. Overview of the GEM muon system: (a) shown in quadrant view, and (b) barrel end view, (c) endcap w from IP.

Table 4-3. Barrel region physical parameters.

Barrel Region							
Superlayer	Chamber Width (m)	Chamber Length (m)	Chamber Mass (kg)	Quantity (Per Module)	Quantity (2 Barrels)	Module Mass (kg)	Barrel-Half (kg)
Outer	1.390	3.540	223	14	336	3118	37418
Outer	1.390	2.814	183	2	48	366	4396
Middle	1.139	2.574	145	4	96	578	6938
Middle	1.139	2.320	133	6	144	796	9556
Middle	1.139	2.199	127	4	96	507	6087
Middle	1.139	1.602	99	2	48	197	2367
Inner	0.831	3.540	151	6	144	905	10865
Inner	0.831	2.972	129	2	48	257	3087
TOTALS				40	960	6726	80716

Table 4-4. Endcap—Physical Parameters.

Endcap Region					
Super Layer	Chamber Width (Max/Min) (m)	Chamber Length (m)	Chamber Mass (kg)	Quantity (1 Endcap)	Endcap-each (kg)
Outer	0.870/0.515	2.640	113	48	5433
Outer	1.310/0.840	3.530	186	48	8924
Middle	0.630/0.390	1.820	66	48	3164
Middle	0.900/0.610	2.223	96	48	4604
Inner	0.730/0.435	1.154	58	24	1385
Inner	1.150/0.665	1.875	113	24	2705
TOTALS				240	26215

It is desirable to recalibrate the electronics frequently to check that the required accuracy is being maintained. However, the readout electronics of several of the prototypes tested at the TTR showed acceptable stability over periods at least as long as 36 hours. Our experience with these detectors gives us confidence that we will be able to achieve the 1% calibration precision goal.

A collection of physical and operating parameters for the CSC are given in Table 4-13.

Results from the R&D Program

We have pursued an active program of CSC prototyping and development during the past year. A number of different test chambers have been evaluated in the cosmic ray Texas Test Rig (TTR) at the SSCL, at the RD5 muon test beam at CERN, and at the 1.7 GeV proton beam at the Gatchina Synchrocyclotron.[7,8,35–39] We have also studied sensitivity of a CSC to neutrons, and tests with x-rays have been done to study details of chamber design. The detailed results of R&D on CSCs are presented here.

Table 4-13. Typical characteristics of CSC.

Parameter	Units	Superlayer 1	Superlayer 2	Superlayer 3
Wire spacing, s	mm	2.54	2.54	2.54
Anode/cathode distance, h	mm	2.54	4.0	5.0
Readout pitch, w	mm	5.71	8.48	10.7
Gap between strips, w_g	mm	0.400	0.400	0.400
Width of readout strip, w_r	mm	1.05	1.78	2.38
Width of floating strip, w_f	mm	1.75	2.25	3.56
Capacitance of readout node	pF/m	50	50	50
Capacitance between strips	pF/m	48	48	48
Resistance between strips (typical)	MΩ	20	20	20
diameter = 30μ Anode wire radius, r_a	mm	0.015	0.015	0.015
Equivalent cylindrical cell radius, r_c	mm	9.35	56.9	196.1
Wire capacitance per unit length, C_0	pF/m	8.68	6.79	5.90
Operating Voltage (nominal gain) 5×10^4	V	2600	3400	4000
Electric field at either cathode, E_c	V/cm	5000	5000	5000
Electric field on wire surface, E_r	V/cm	2.7×10^5	2.7×10^5	2.7×10^5
Positive ion mobility, μ^+	$cm^2/s/V$	1.27	1.27	1.27
Time constant, t_0	ns	2.11	2.09	2.10
Fraction of the avalanche charge collected by an anode in 30 ns		0.21	0.17	0.14
Fraction of the avalanche charge collected by an anode in 300 ns		0.39	0.30	0.26
Fraction of the anode charge induced on either cathode		0.39	0.33	0.30
Total ionization (normal track)	ion pairs	90	145	180
Minimum wire tension	gr	50	97	151

DISTANCE BETWEEN CATHODE READOUT STRIPS

INNER SUPERLAYER

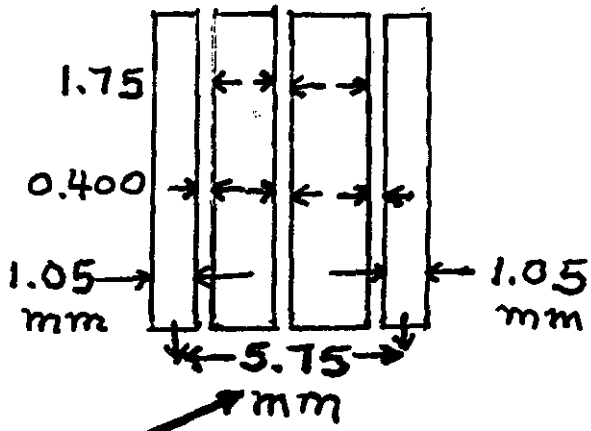

TDR = 5.71 mm

$$d = \frac{1.05}{2} \times 2 + 0.400 \times 3 + 1.75 \times 2 = 5.75$$

MIDDLE SUPERLAYER

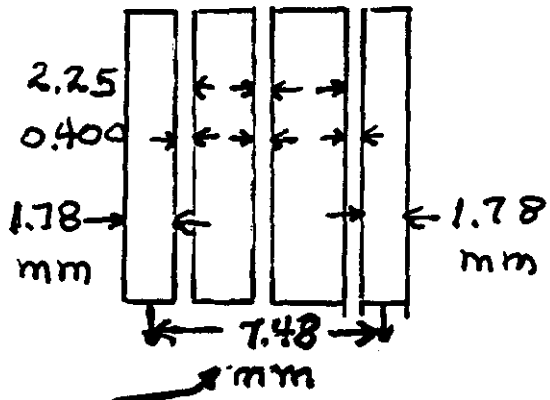

TDR = 8.48 mm

$$d = \frac{1.78}{2} \times 2 + 0.400 \times 3 + 2.25 \times 2 = 7.48$$

OUTER SUPERLAYER

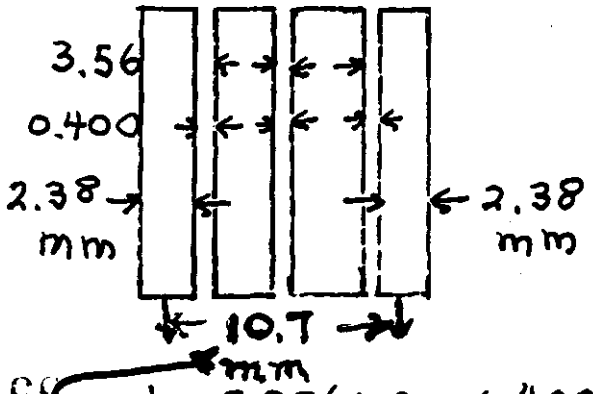

TDR = 10.7 mm

$$d = 2.38 \times 2 + 0.400 \times 3 + 3.56 \times 2 = 10.7$$

ELECTRONICS

OF READOUT CHANNELS

7 Readout Cards; 96 channels/card

6 Layers/Superlayer

$\therefore$ $96/6 = 16$ channels/layer

$16 \times 7 = 112$ channels/layer.

$\mathcal{L}_\varphi$ READOUT

Inner Superlayer	111×5.75 mm =	638.3 mm
Middle Superlayer	111×7.48 mm =	830.3 mm
	111×8.48 mm =	941.3 mm
Outer Superlayer	111×10.70 mm =	1,187.7 mm

NEEDED COVERAGE $(2\pi r)\left(\frac{30^\circ}{360^\circ}\right)\frac{1}{4}$

Inner Superlayer $= \frac{2\pi \times 4339}{48} =$ 568.0 mm

Middle Superlayer $= \frac{2\pi \times 6536}{48} =$ 855.6 mm

Outer Superlayer $= \frac{2\pi \times 9000}{48} =$ 1178.1 mm

'INNER SUPERLAYER'

ELECTRONIC CARD LAYOUT

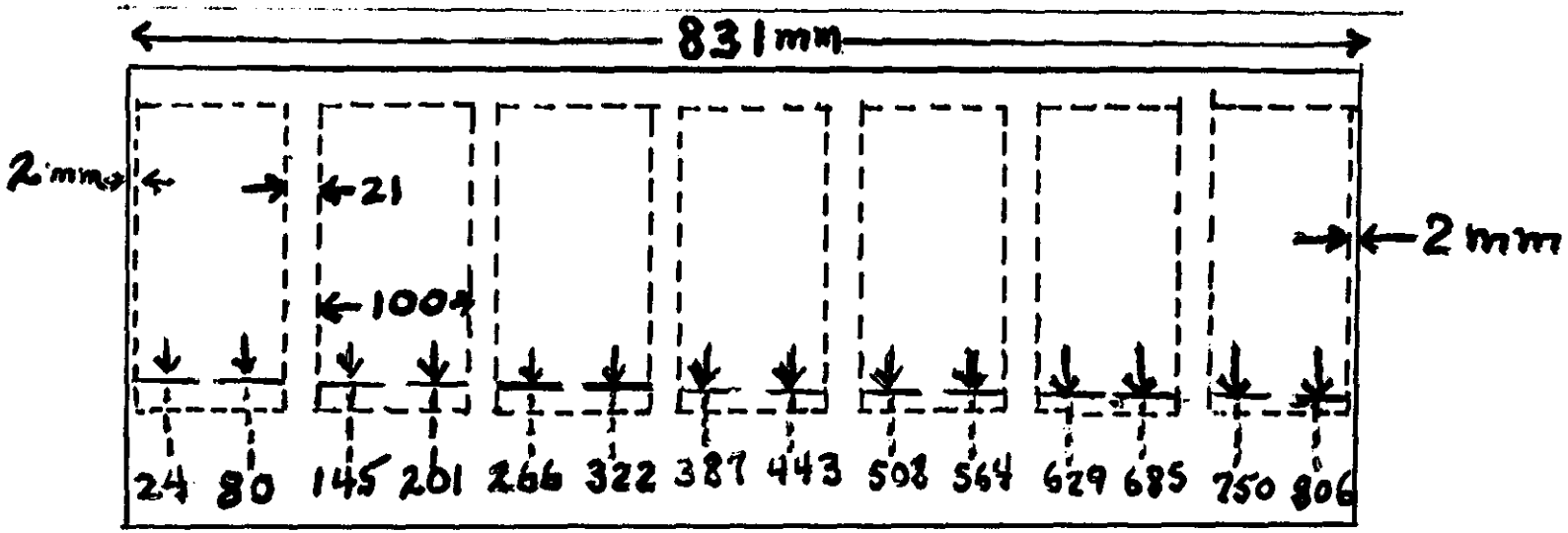

CATHODE STRIPS OUTPUT

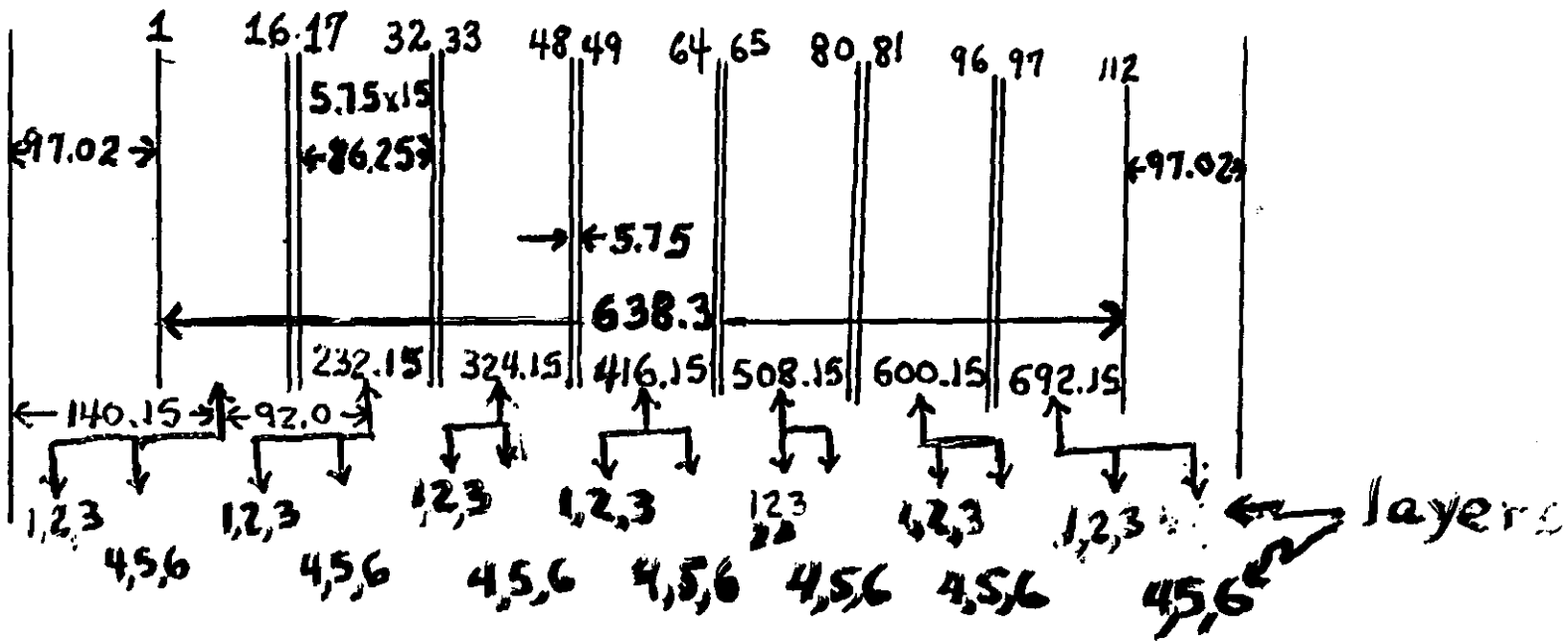

Small CSC prototype production

1 Barrel (ITEP)

- 6 layers CSC ($40\times46cm^2$)
- 4 configuration of the cathode strip
- pitch: 5.5mm, 8.5mm, 10.0mm
- one configuration without floating strips (8.5mm)

Art work has been done

Production (BNL): 6×4 cathode plates + reserve 4 plates

Total: 28 cathode plates

2 Endcap (PNPI)

- 1 layer CSC ($27\times35cm^2$)
- 3 configuration parallel cathode strip
- Radial strip configuration? Don't needed.
- 1 anode wire plate

(wires shifted for compensation of the Lorentz effect)

• CSC with rotatable anode frame.

It's needed to perform R&D program

with Endcap configuration of the magnetic field

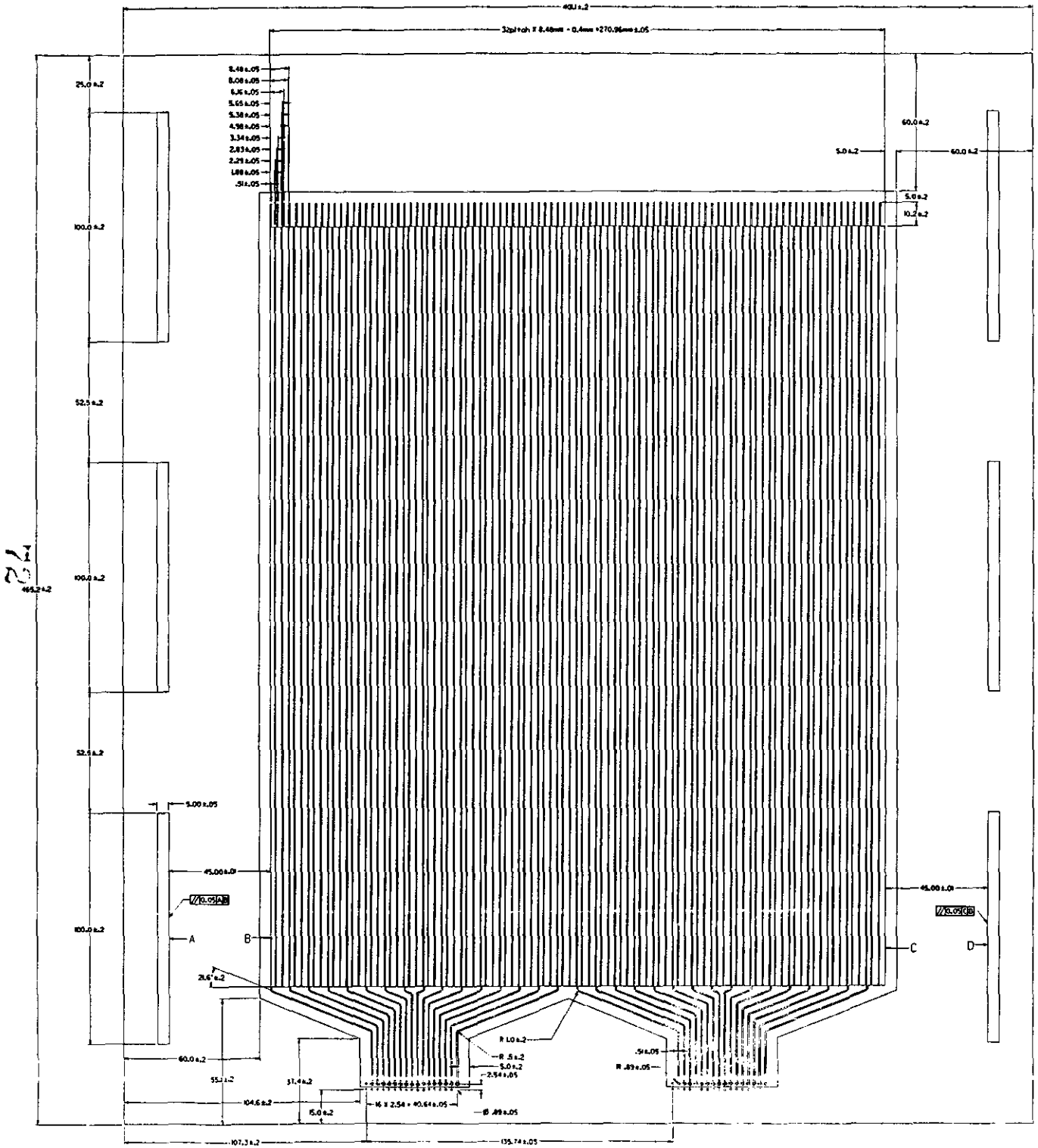

Small CSC prototype
(Barrel)

COMMENT ON GEM MUON SUBSYSTEM PERFORMANCE

(WHERE WE ARE AND WAY TO GO)

I. GOLUTVIN

AUGUST 3, 1993

1. Where we are?

COMPARISON WITH
OTHER SSC/LHC
DETECTORS

- ATLAS (LOI)
- CMS (LOI)
- SDC (TDR)

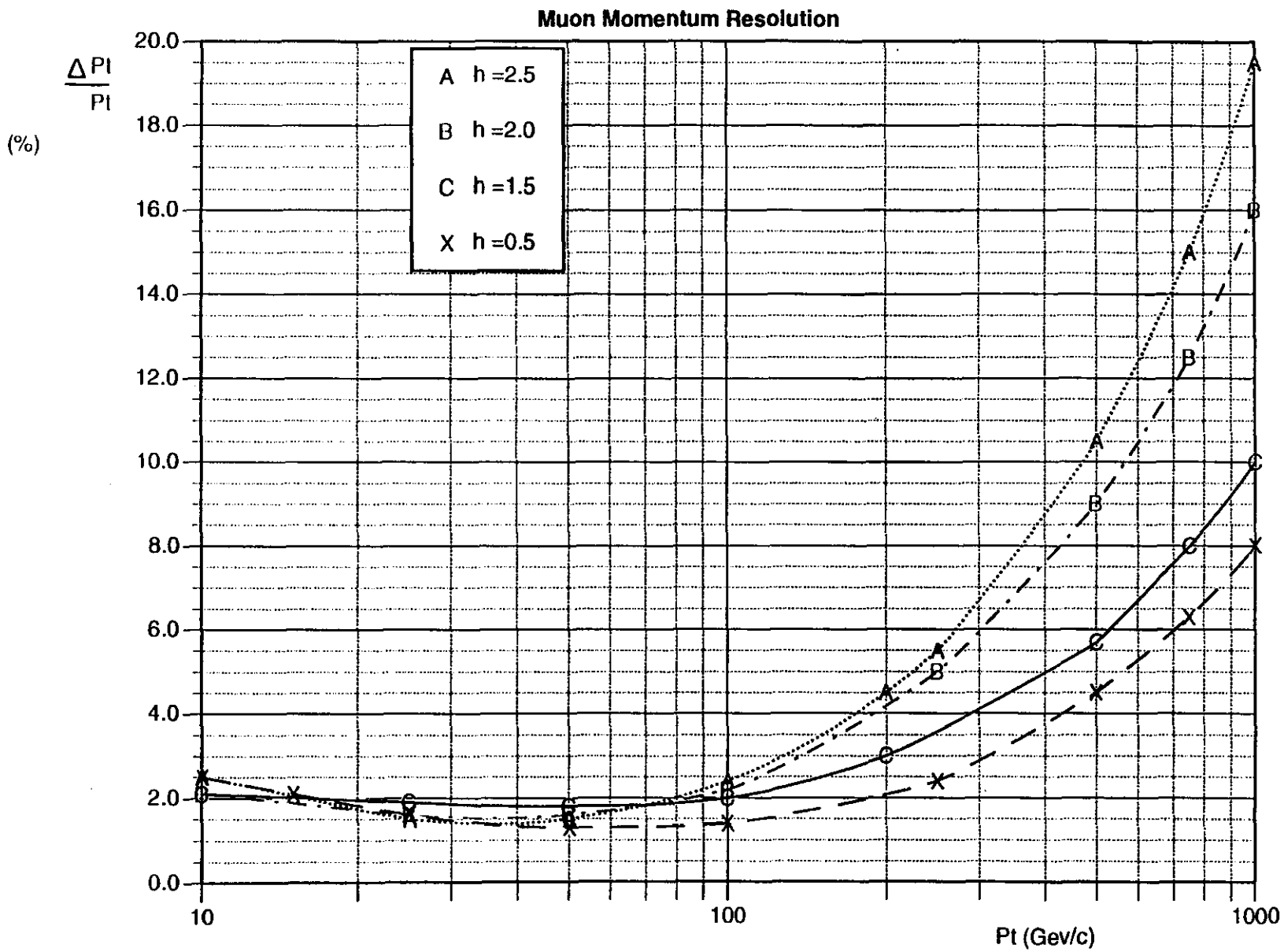
Muon Momentum Resolution
ΔPt / Pt
(%)
A h =2.5
B h =2.0
C h =1.5
X h =0.5
20.0
18.0
16.0
14.0
12.0
10.0
8.0
6.0
4.0
2.0
0.0
10
100
1000
Pt (Gev/c)

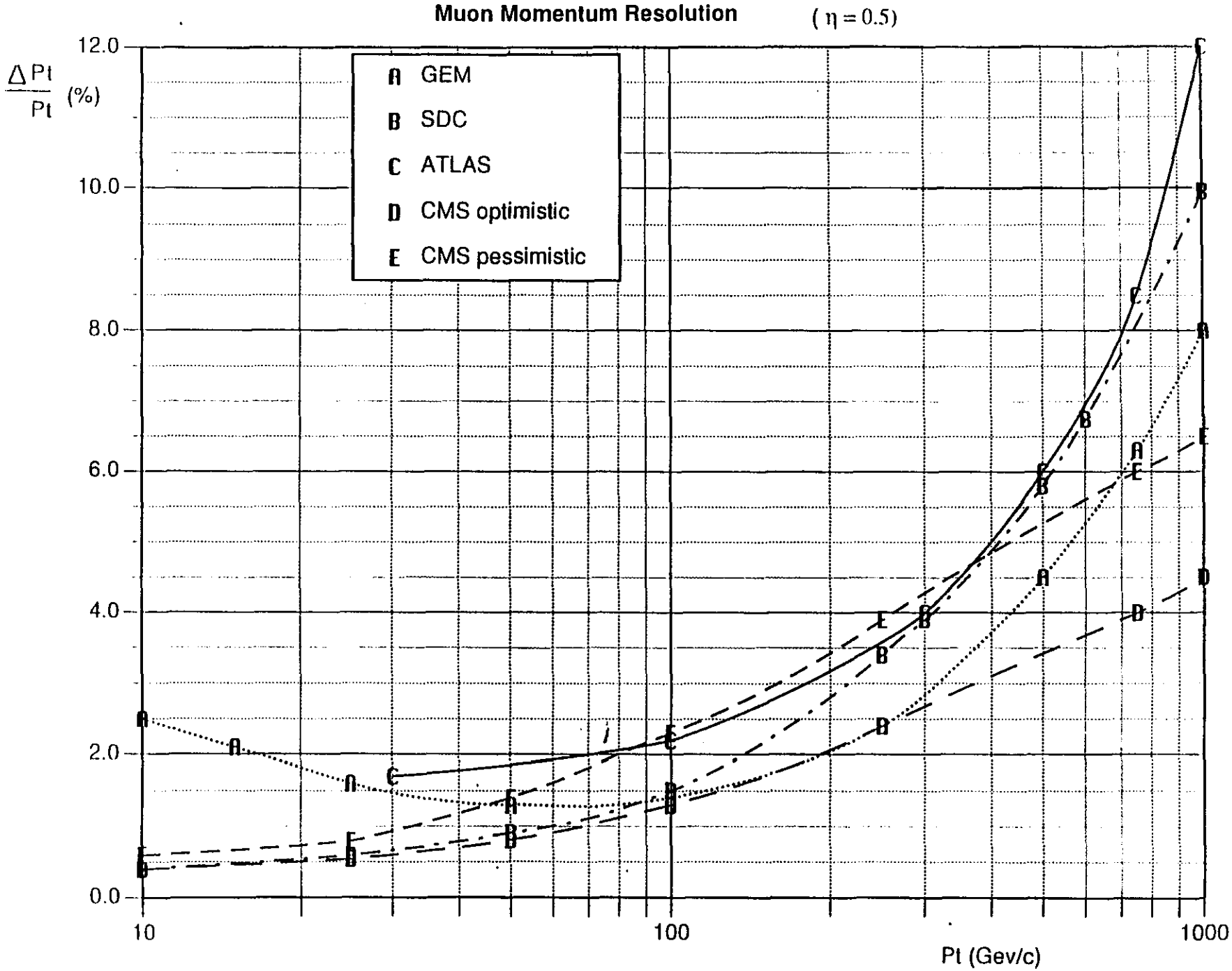
Muon Momentum Resolution
(η = 0.5)
ΔPt / Pt (%)
12.0
10.0
8.0
6.0
4.0
2.0
0.0
10
100
1000
Pt (Gev/c)
A GEM
B SDC
C ATLAS
D CMS optimistic
E CMS pessimistic

CMS RESOLUTIONS

	Optimistic	Pessimistic
VERTEX	20 μm	50 μm
SiTra	15 μm	25 μm
MSGC	60 μm	100 μm
Muon	100 μm	150 μm

In the low energy sector

($P_t = 10 \div 50$ GeV/c)

GEM can not compete with SDC and ATLAS

Low magnetic field

$\Downarrow$

Momenta cannot be measured before the CALORIMETER

$\Downarrow$

Large dE/dx contribution

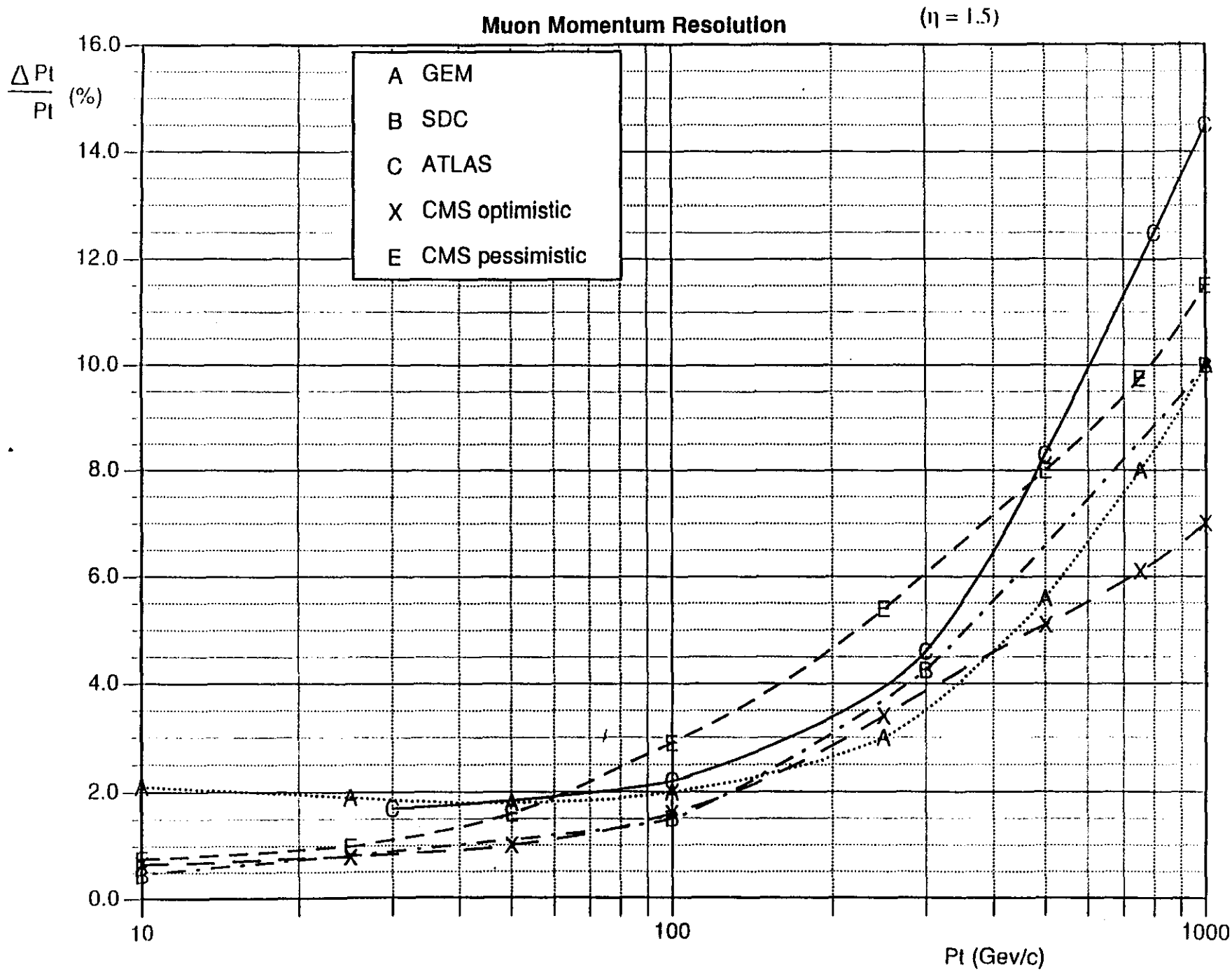
Muon Momentum Resolution
(η = 1.5)
ΔPt/Pt (%)
16.0
14.0
12.0
10.0
8.0
6.0
4.0
2.0
0.0
A GEM
B SDC
C ATLAS
X CMS optimistic
E CMS pessimistic
10
100
1000
Pt (Gev/c)

$\eta = 0.5 - 1.5$

In the most populated sector

($p_t = 100 - 600$ GeV/c)

GEM is the best

In the high energy sector

($p_t > 700$ GeV/c)

GEM is better than ATLAS and SDC but worse than CMS

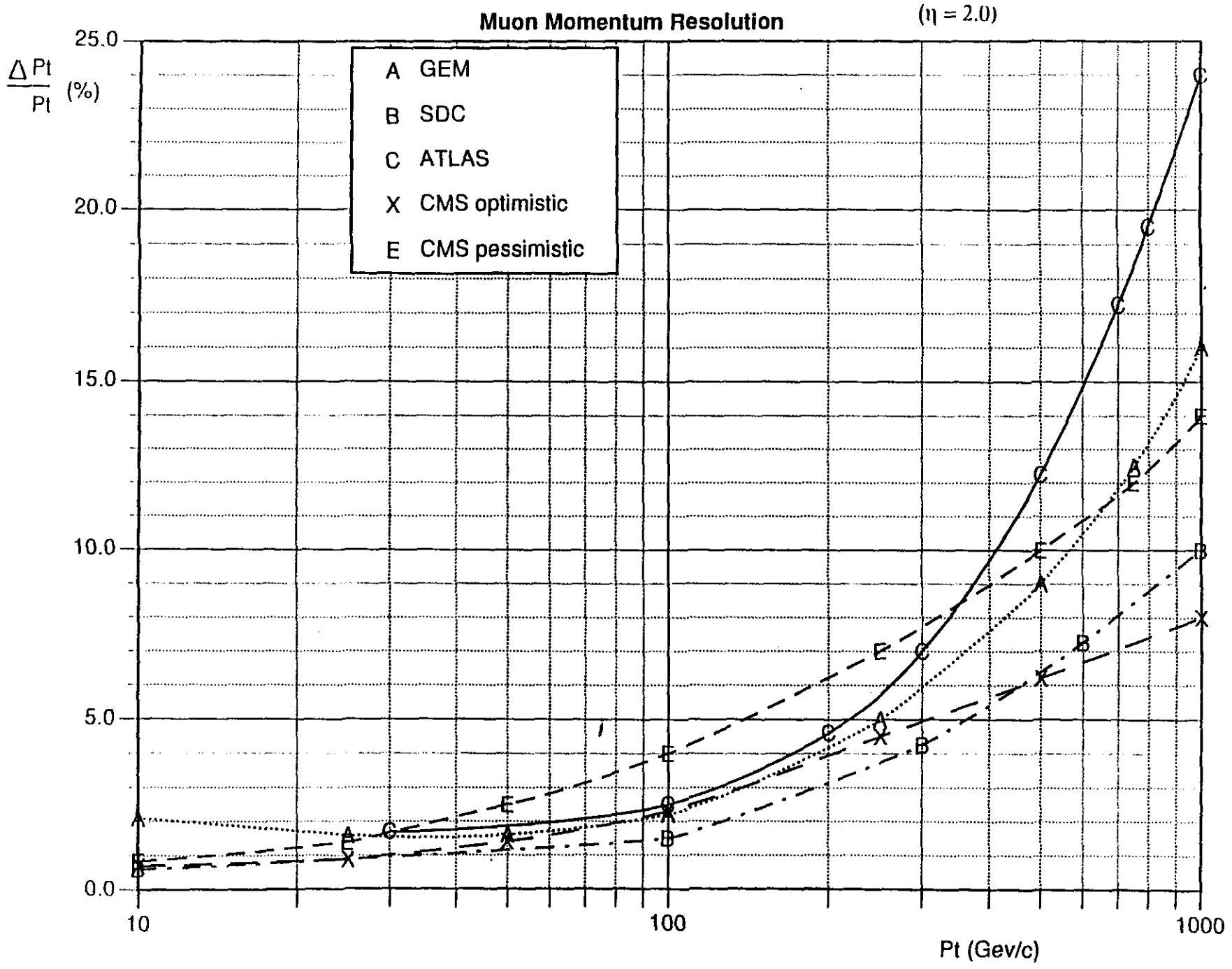
Muon Momentum Resolution
(η = 2.0)
ΔPt/Pt (%)
25.0
20.0
15.0
10.0
5.0
0.0
A GEM
B SDC
C ATLAS
X CMS optimistic
E CMS pessimistic
10
100
1000
Pt (Gev/c)

$\eta = 2.0$

GEM is worse than
CMS AND SDC

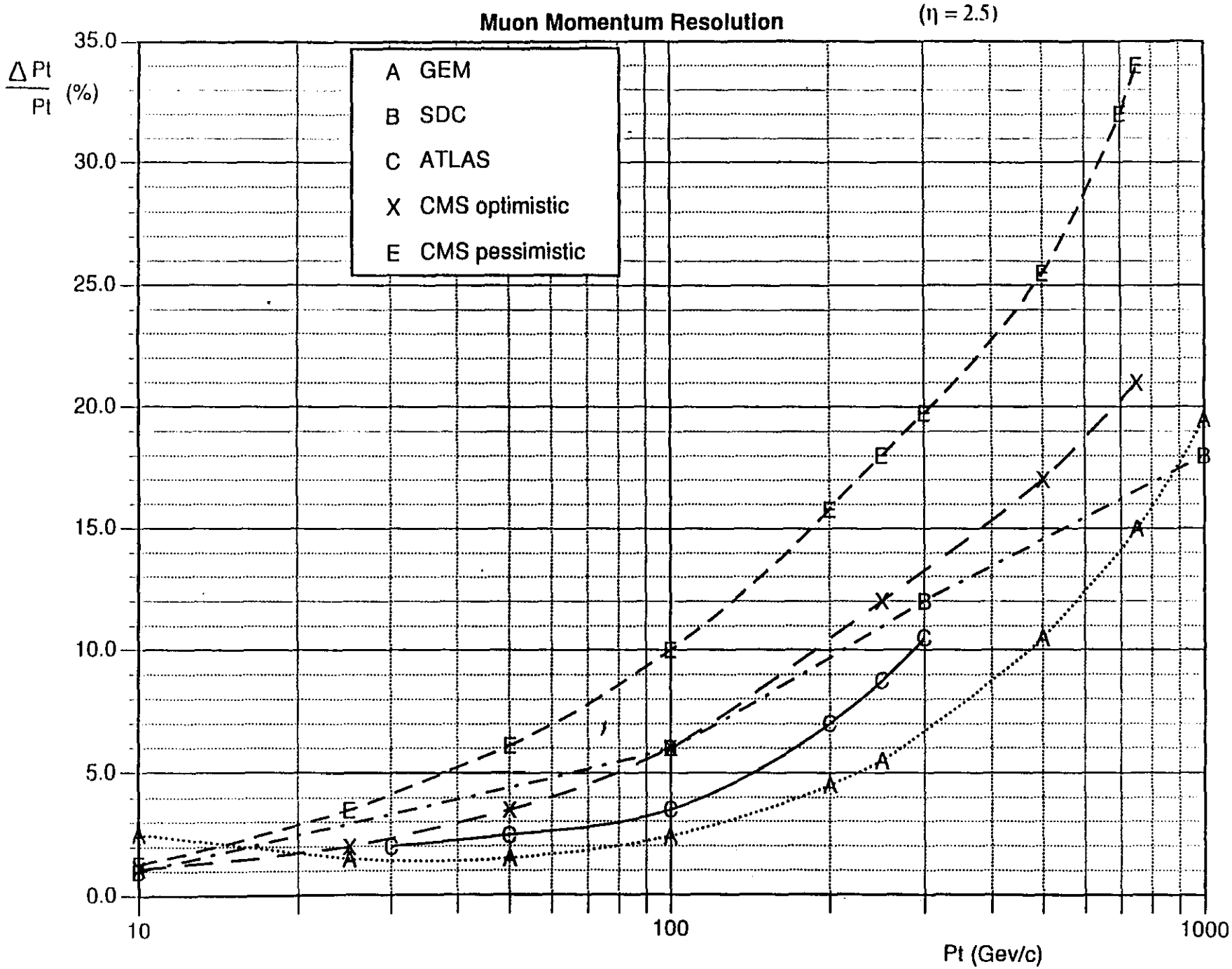
Muon Momentum Resolution
(η = 2.5)
ΔPt/Pt (%)
35.0
30.0
25.0
20.0
15.0
10.0
5.0
0.0
A GEM
B SDC
C ATLAS
X CMS optimistic
E CMS pessimistic
10
100
1000
Pt (Gev/c)

$\eta = 2.5$

GEM is again the best

CONCLUSION:

MUON MOMENTUM RESOLUTION IN HIGH ENERGY SECTOR SHOULD BE IMPROVED

2. WAY TO GO

- MAKE BETTER RESOLUTION IN HIGH ENERGY SECTOR

- IMPROVE COVERAGE

  - ~25% OF EFFICIENCY TO $H \rightarrow 4\mu$ ARE LOST IN CENTRAL SUPPORT (TDR)

MUON MOMENTUM RESOLUTION

★ INCREASE MAGNETIC FIELD

★ INCREASE LEVER ARM

$$\left.\right\} \frac{\Delta p}{p} \sim \frac{1}{BL^2}$$

★ MAKE VERTEX CONSTRAIN WORK BETTER

THERE ARE 3 REASONS WHY VERTEX CONSTRAIN DOES NOT IMPROVE RESOLUTION PROPORTIONALLY L^2:

• PRECISION OF VERTEX MEASUREMENT

• • GLOBAL ALIGNMENT PROBLEM

• • • MULTIPLE SCATTERING IN HADRON CALORIMETER

→ DOMINATING

⇓

$\frac{X_0}{\lambda}$ RATION OF THE ABSORBER SHOULD BE MINIMIZED!

No. of λ and X_0 in Bar/Endcap Cal. vs η Kr/Pb option

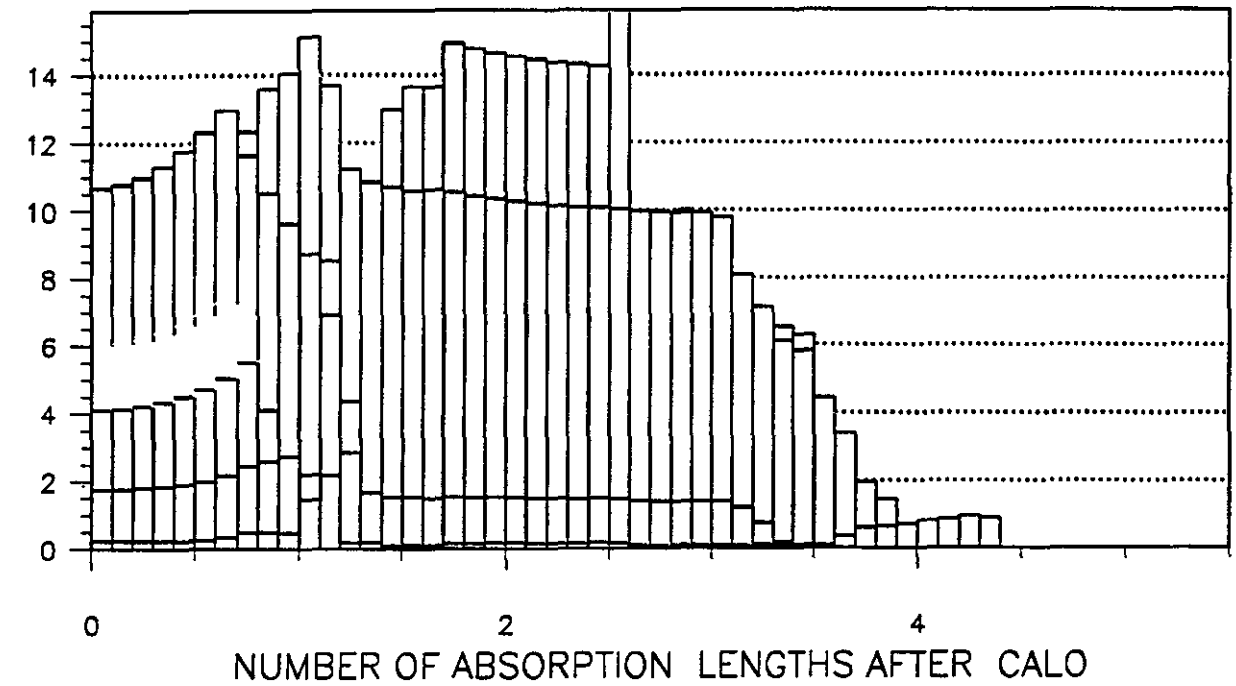

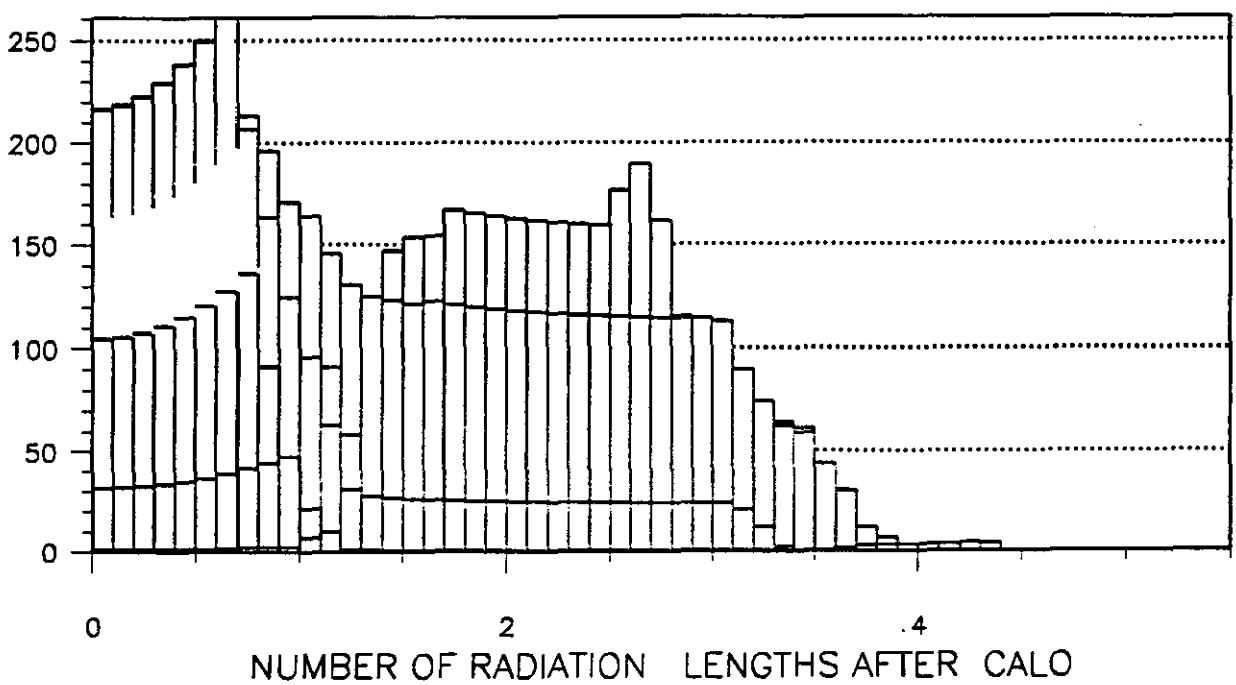

No. of λ and X_0 in Bar/Endcap Cal. vs η Kr/Cu option

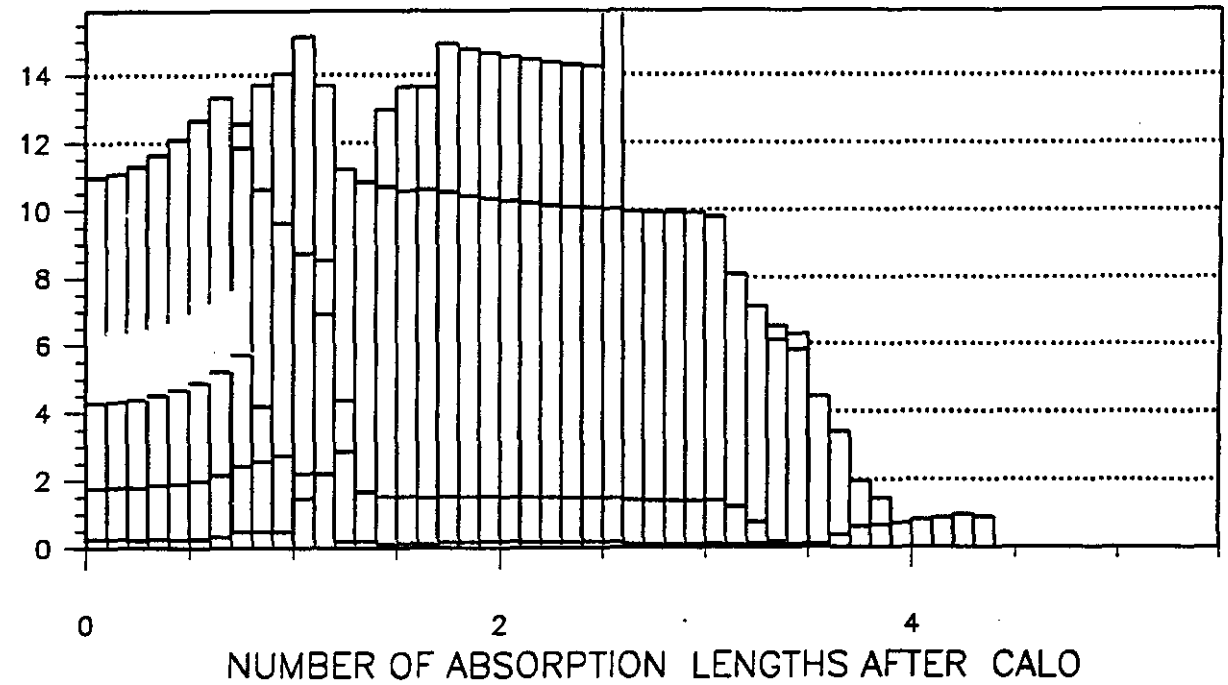

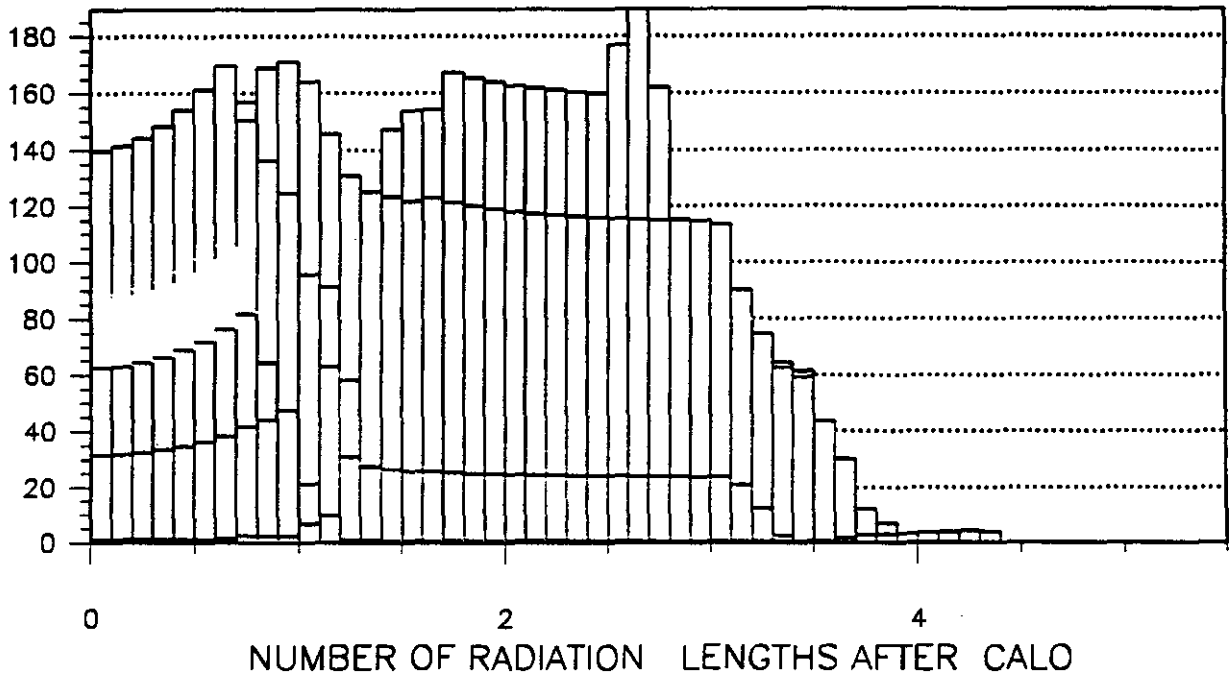

COVERAGE

- PROJECTIVE ALIGNMENT
- CHAMBERS OVERLAPPING

BASIC FORMULA:

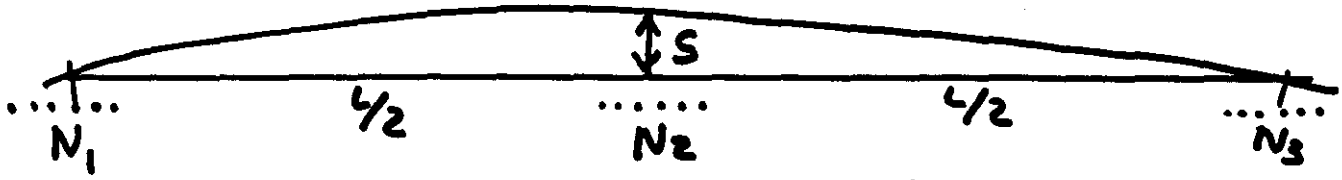

$$\frac{\Delta p}{p} = \frac{\Delta S}{S} = \frac{27\,p\left(\frac{TeV}{c}\right)}{\beta L^2 (Tm)} \sqrt{\frac{\sigma_{S1}^2}{2} + \sigma_{S2}^2 + \frac{\sigma_{S3}^2}{2}} + \frac{0.1}{\beta L (Tm)} \sqrt{\frac{X_2}{X_0}}$$

$\sigma_{S1}, \sigma_{S2}, \sigma_{S3}$ - RESOLUTION OF SUPERLAYERS 1, 2, 3

$$\sigma_{Si}^2 = \frac{\sigma_i^2}{N_i \epsilon_i}$$

σ_i - SINGLE LAYER RESOLUTION IN SUPERLAYER i

N_i - NUMBER OF LAYERS IN SUPERLAYER i $(N_i = 6)$

ϵ_i - SINGLE LAYER EFFICIENCY

$\frac{X_2}{X_0}$ - RAD. LENGTH OF SUPERLAYER 2

(1) RESOLUTION OF SUPERLAYER 2 SHOULD BE OPTIMIZED

$$\text{MIN} \left\{ \frac{\sigma_2^2}{N_2 \epsilon_2} \right\}$$

(2) MULTIPLE SCATTERING IN SUPERLAYER 2 SHOULD BE MINIMIZED

$$\text{MIN} \left\{ \frac{X_2}{X_0} \right\}$$

DOMINATING REQUIREMENTS:

- MINIMUM NUMBER OF CHAMBERS IN THE MIDDLE SUPERLAYER
- MINIMUM NUMBER OF RAD. LENGTH IN THE CHAMBER AND IN THE FRAMES

DRIVING CONSTRAINS:

- MAXIMUM POSSIBLE LENGTH OF ANODE WIRES (L_w)
- ANGULAR RANGE IN THE MIDDLE CHAMBER ($\Delta\varphi$)

$$L_w = 120 \text{ cm}$$
$$\Delta\varphi = \pm 5^\circ$$

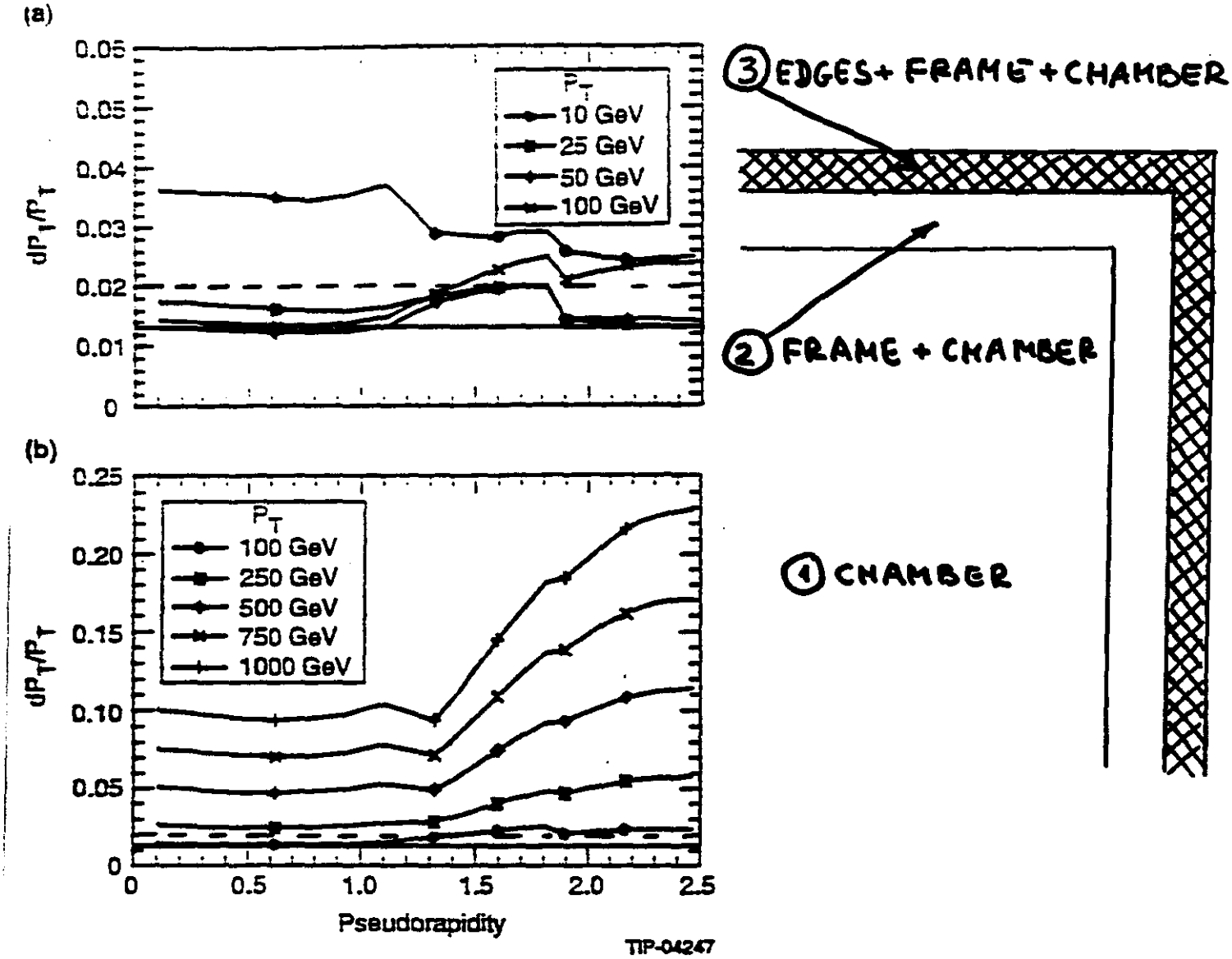

FIG. 4-19. Transverse momentum resolution for standalone three superlayer system:
a) $10 \leq p_T$ 100 GeV and
b) $100 \leq p_T \leq 1000$ GeV.

EDGES AND FRAMES ARE MADE OF EPOXY

① 0.063 X_0 $\left(\frac{\Delta P}{P}\right)_{MS} = 0.6\%$

② 0.21 X_0 $\left(\frac{\Delta P}{P}\right)_{MS} = 1.3\%$ ——

③ 0.66 X_0 $\left(\frac{\Delta P}{P}\right)_{MS} = 2\%$ - - - -

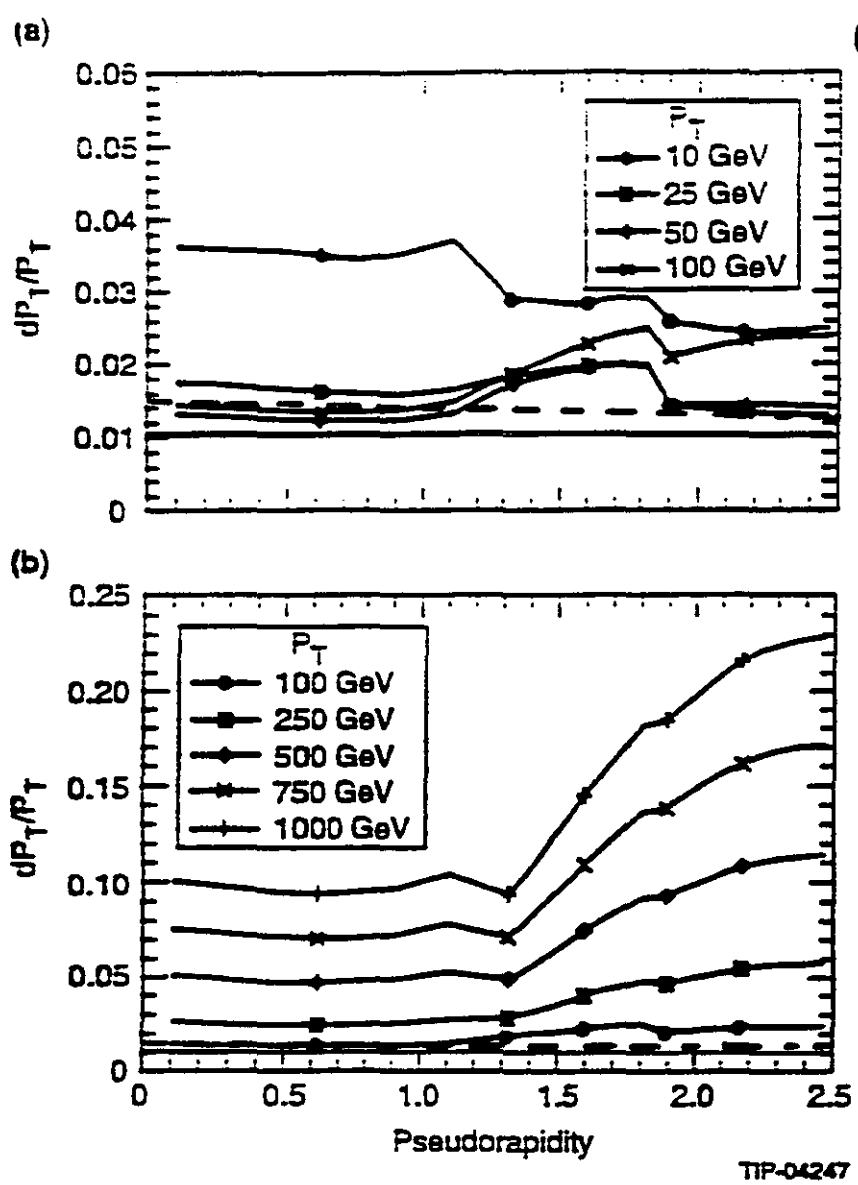

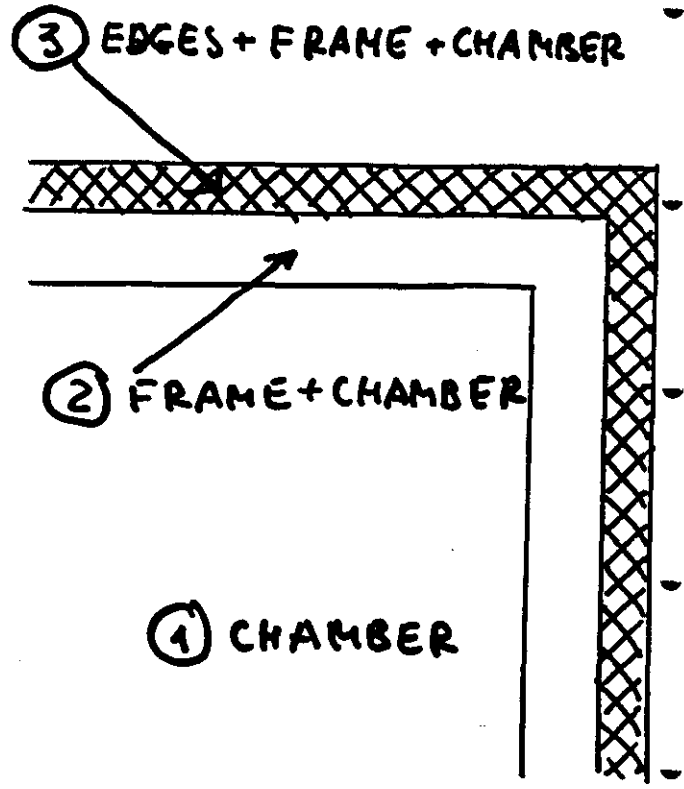

FIG. 4-19. Transverse momentum resolution for standalone three superlayer system:
a) $10 \leq p_T$ 100 GeV and
b) $100 \leq p_T \leq 1000$ GeV.

EDGES AND FRAMES ARE MADE OF POLYMER CONCRETE

1 $0.063\ X_0$ $\left(\frac{\Delta P}{P}\right)_{MS} = 0.6\%$

2 $0.14\ X_0$ $\left(\frac{\Delta P}{P}\right)_{MS} = 1\%$ ———

3 $0.37\ X_0$ $\left(\frac{\Delta P}{P}\right)_{MS} = 1.5\%$ - - - -

CONCLUSIONS:

1. THERE IS NO CRUCIAL EFFECT OF MULTIPLE SCATTERING IN CSC FRAMES AND EDGES ON MUON MOMENTUM RESOLUTION: CHAMBERS OVERLAPPING DOES NOT MAKE A VITAL DETERIORATION

2. THERE IS NO NEED TO MINIMIZE THE WIDTH OF FRAMES AND EDGES

3. INCREASING THE WIRE LENGTH IN THE MIDDLE SUPERLAYER TO THE MAXIMUM POSSIBLE (120 cm) WILL DECREASE THE NUMBER OF FRAMES AND EDGES BY 25%

1. WIDTH OF THE CHAMBERS IN THE MIDDLE SUPERLAYER

2. MATERIAL IN THE CSC

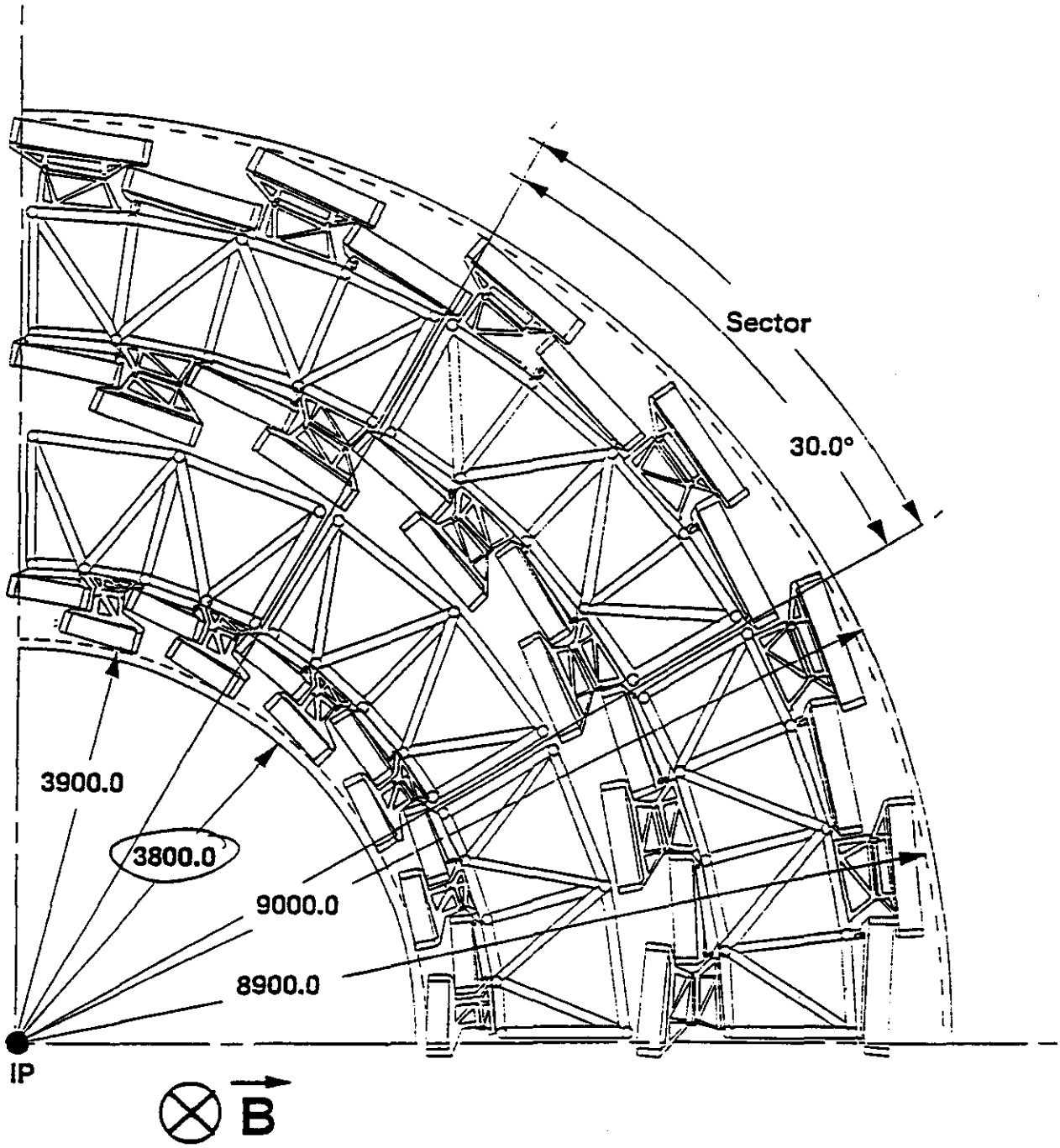

Figure 4.3.3.2: Muon System End View (1/4 Section)
View from South End of UG Hall

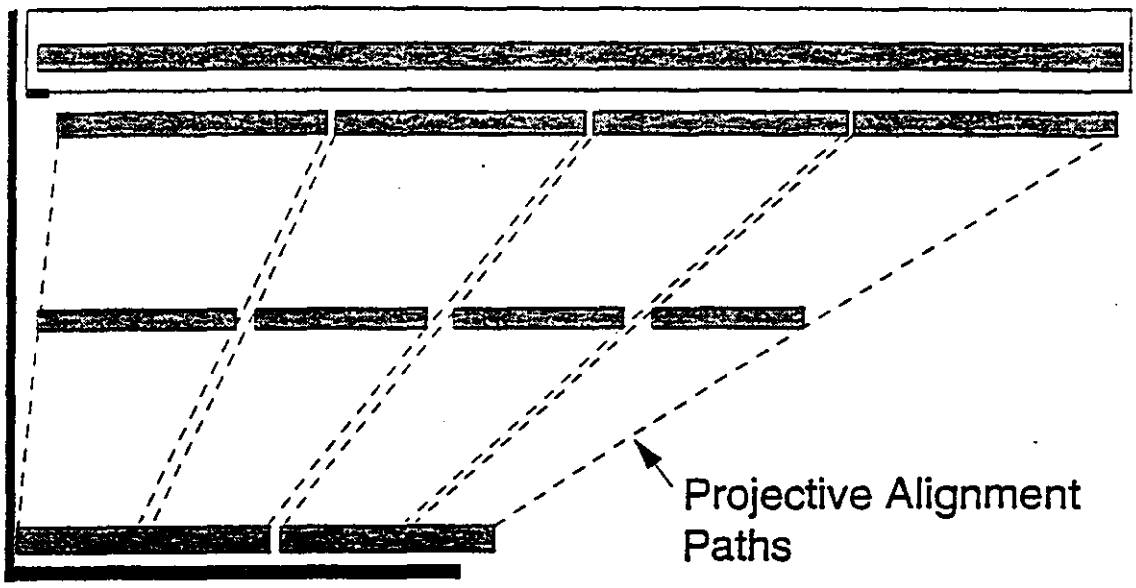

Side View (rθ)

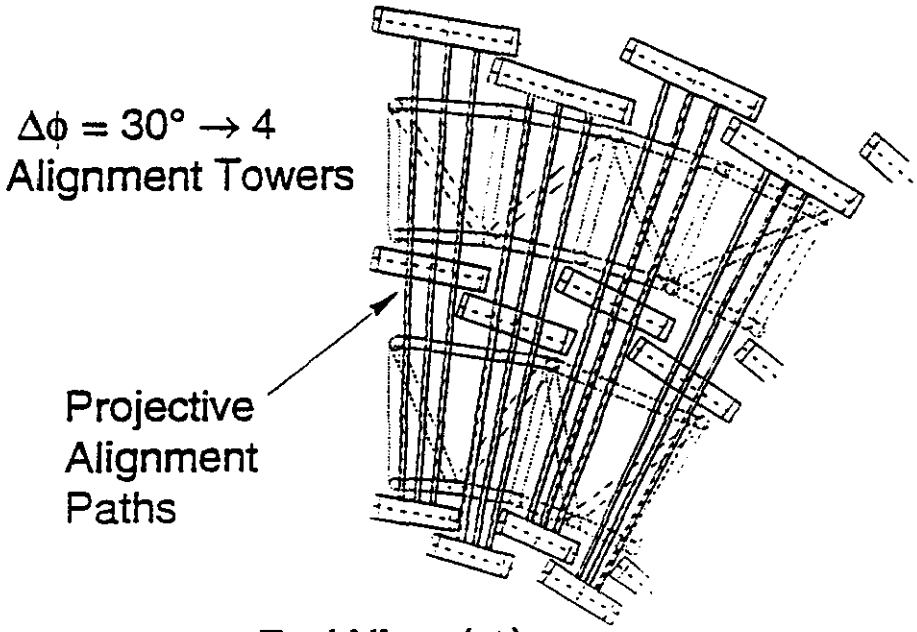

End View (rφ)

TIP-03836

Super-Layer	Layer/SL	Mid-Plane Radii
Outer	Outer	8691 mm
Outer	Inner	8287 mm
Middle	Outer	6536 mm
Middle	Inner	6133 mm
Inner	Outer	4340 mm
Inner	Inner	4023 mm

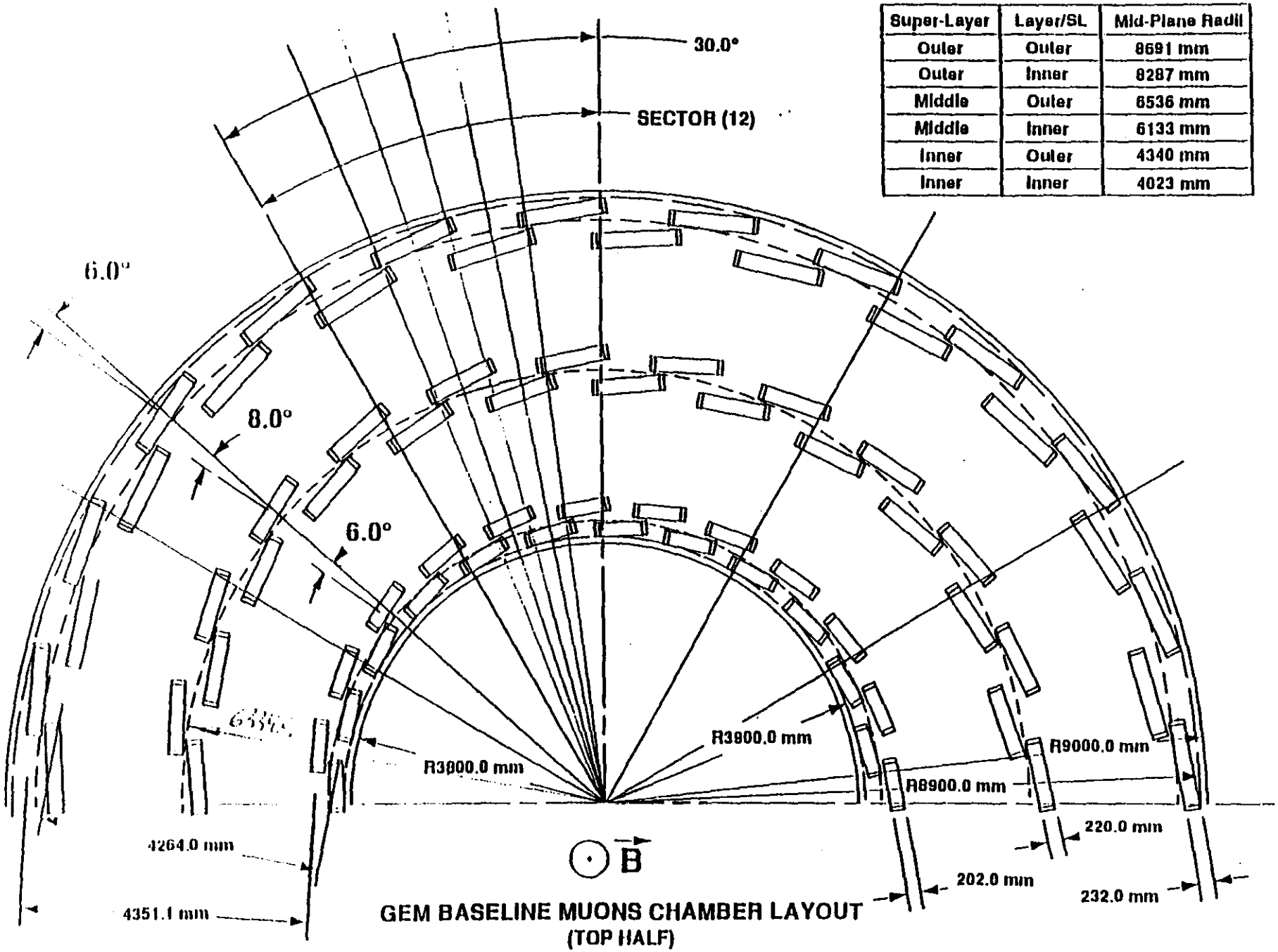

GEM BASELINE MUONS CHAMBER LAYOUT
(TOP HALF)
(CCW TILTED MAGNET END)

F. Nimblett
03 March 1993

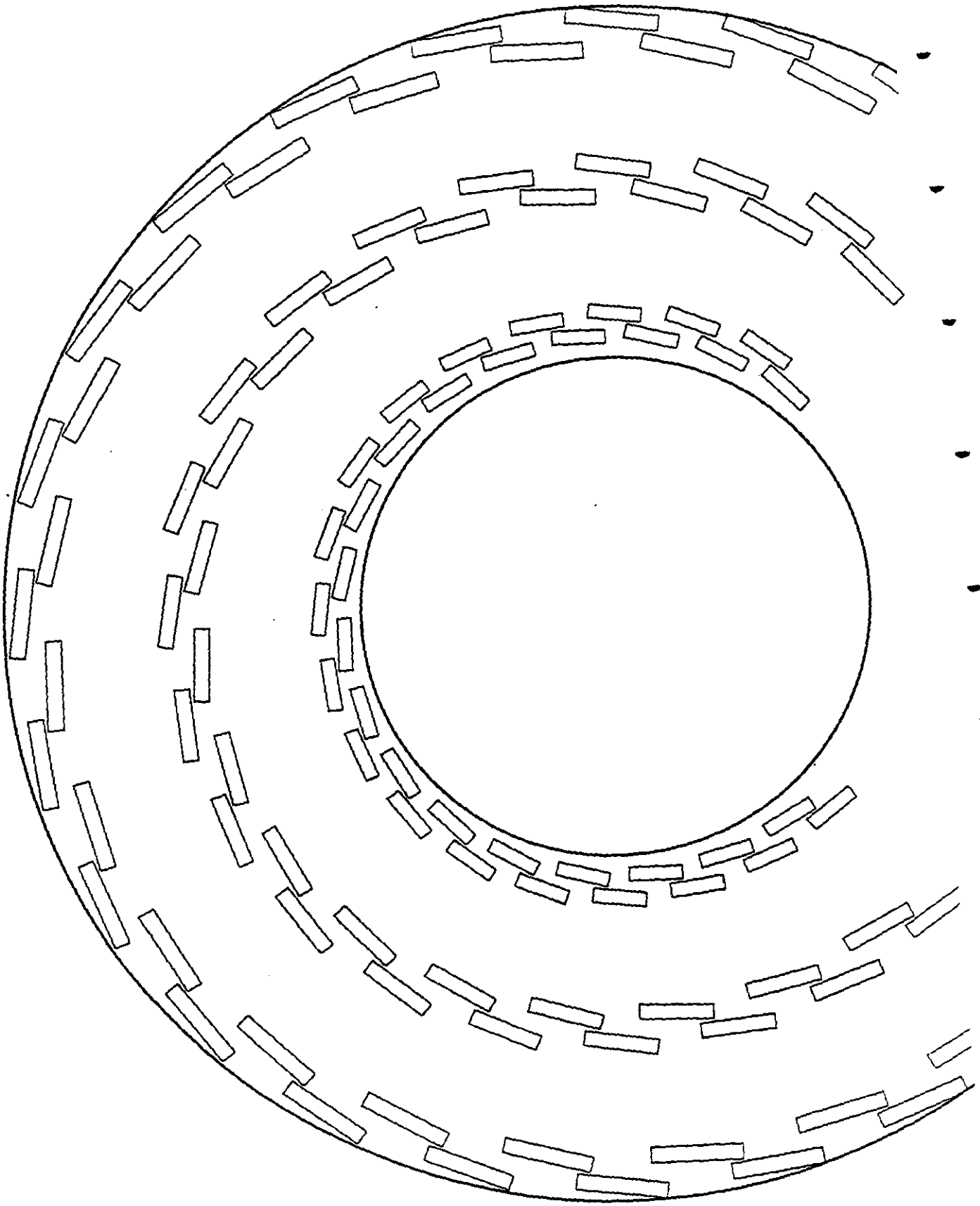

93/07/29 00.26

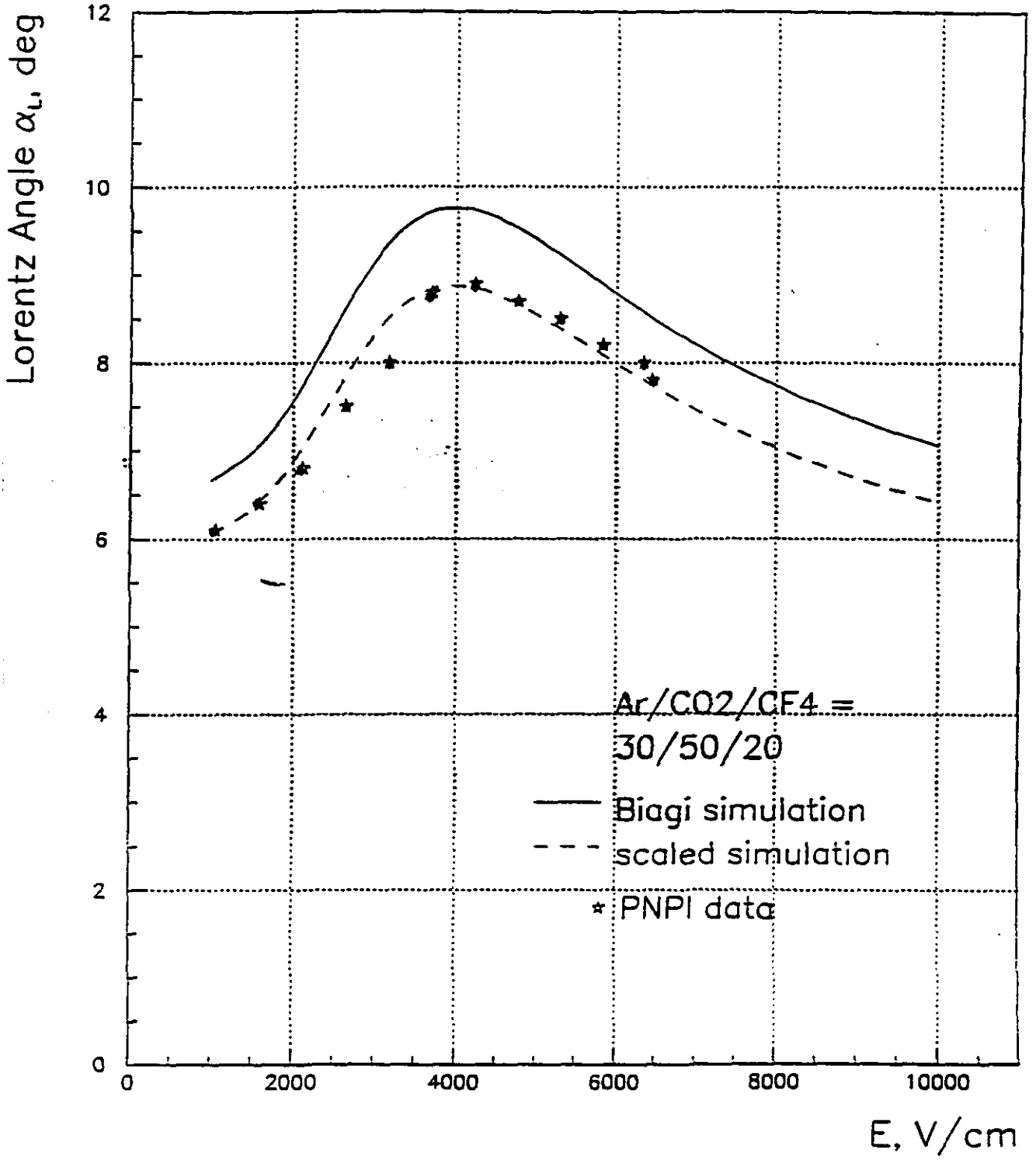

O. PROKOFIEV
Y. BONUSHKIN

93/07/29 01.42

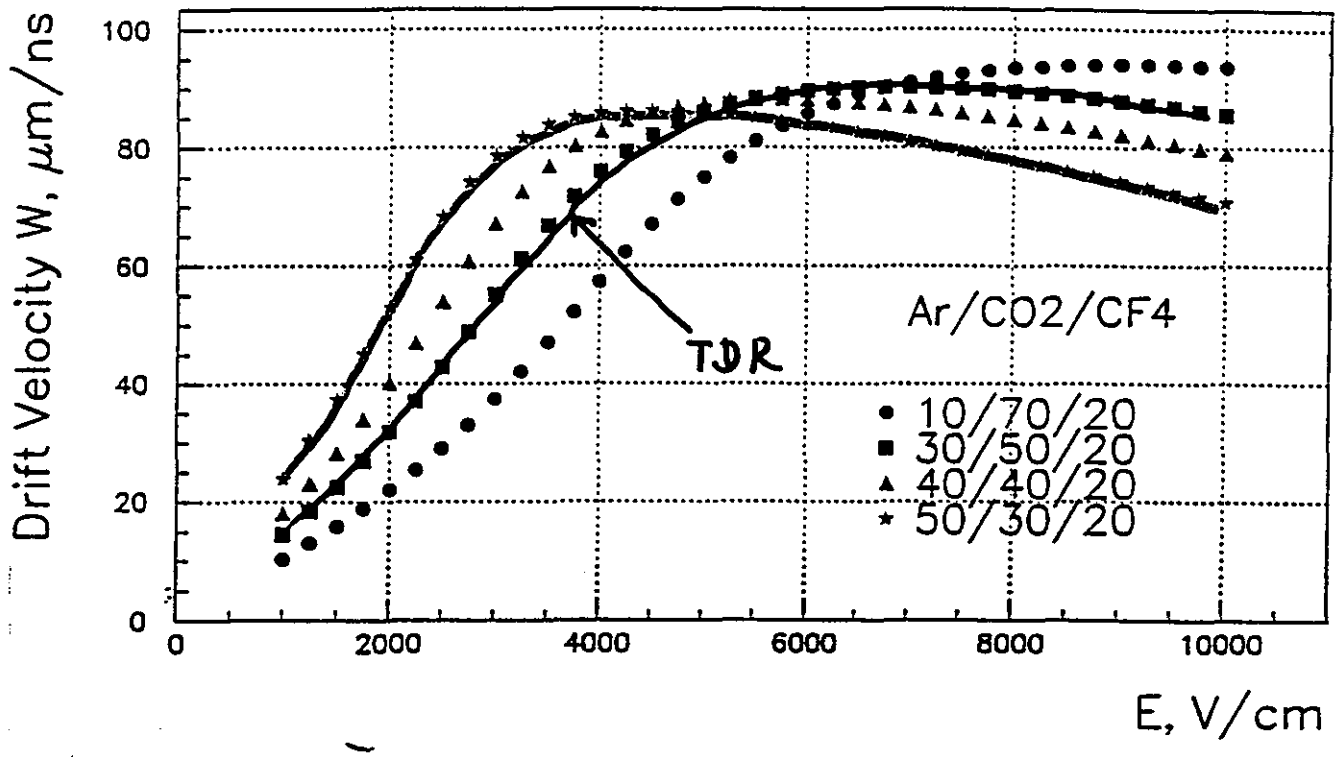

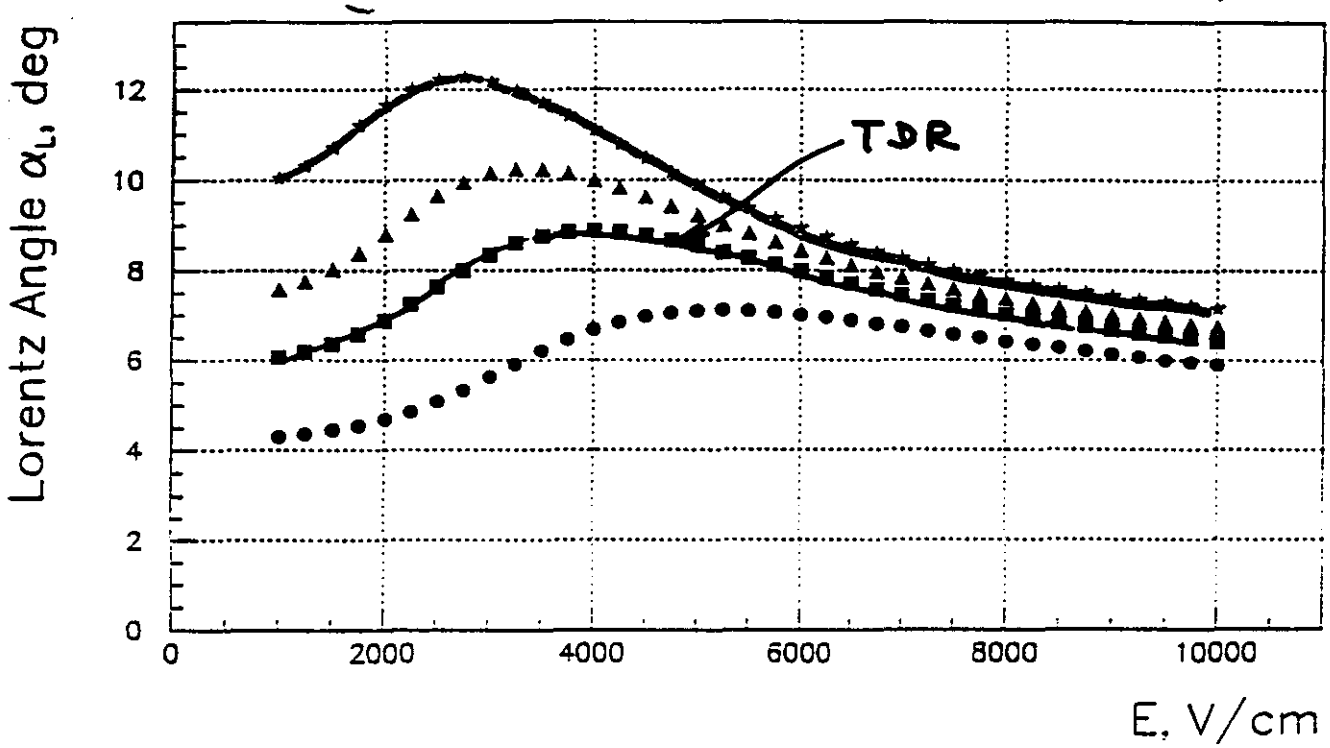

O. PROKOFIEV
Y. BONUSHKIN

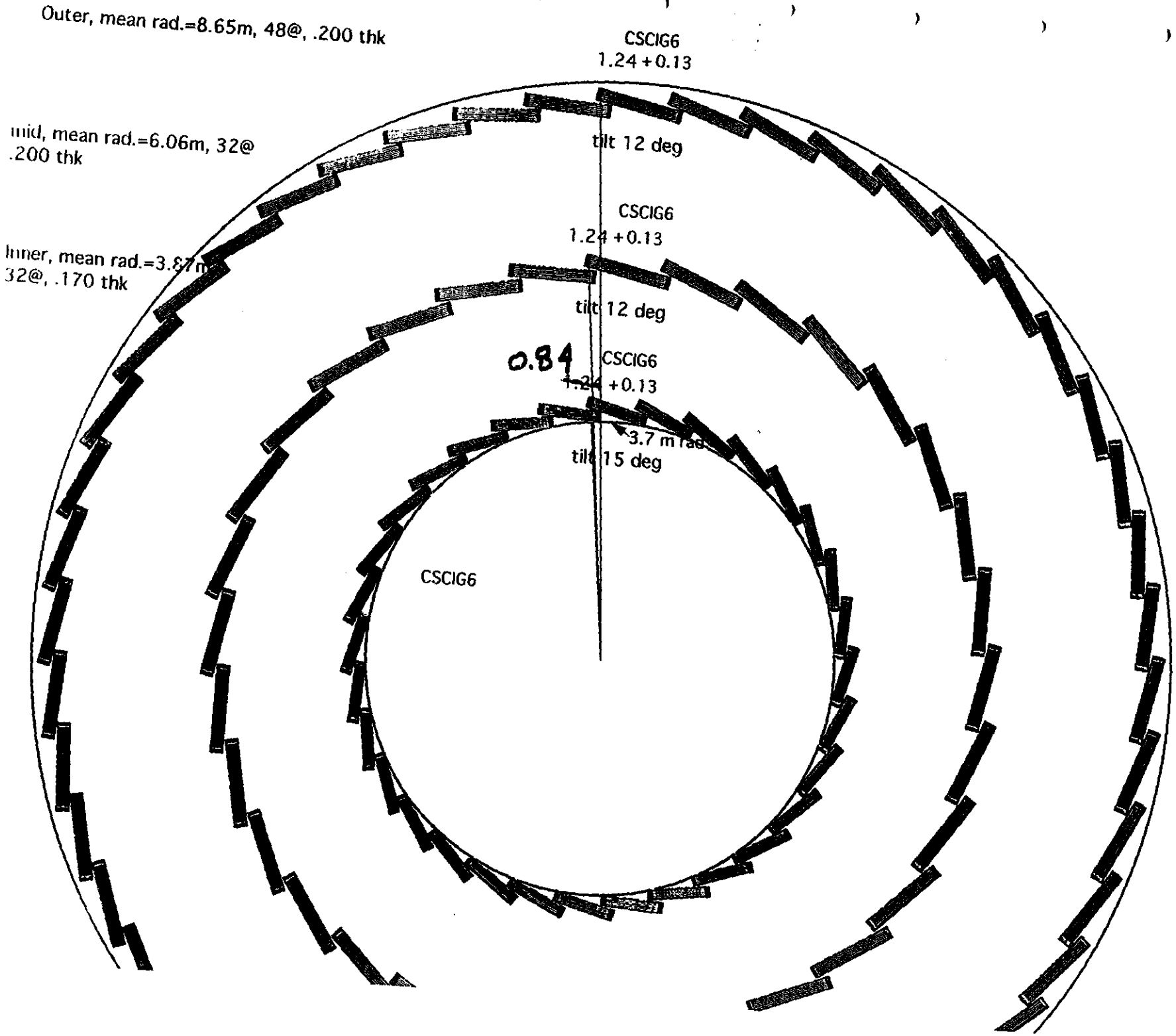
Outer, mean rad.=8.65m, 48@, .200 thk
CSCIG6
1.24 +0.13
tilt 12 deg
mid, mean rad.=6.06m, 32@
.200 thk
CSCIG6
1.24 +0.13
Inner, mean rad.=3.87m
32@, .170 thk
tilt 12 deg
0.84
CSCIG6
1.24 +0.13
3.7 m rad
tilt 15 deg
CSCIG6

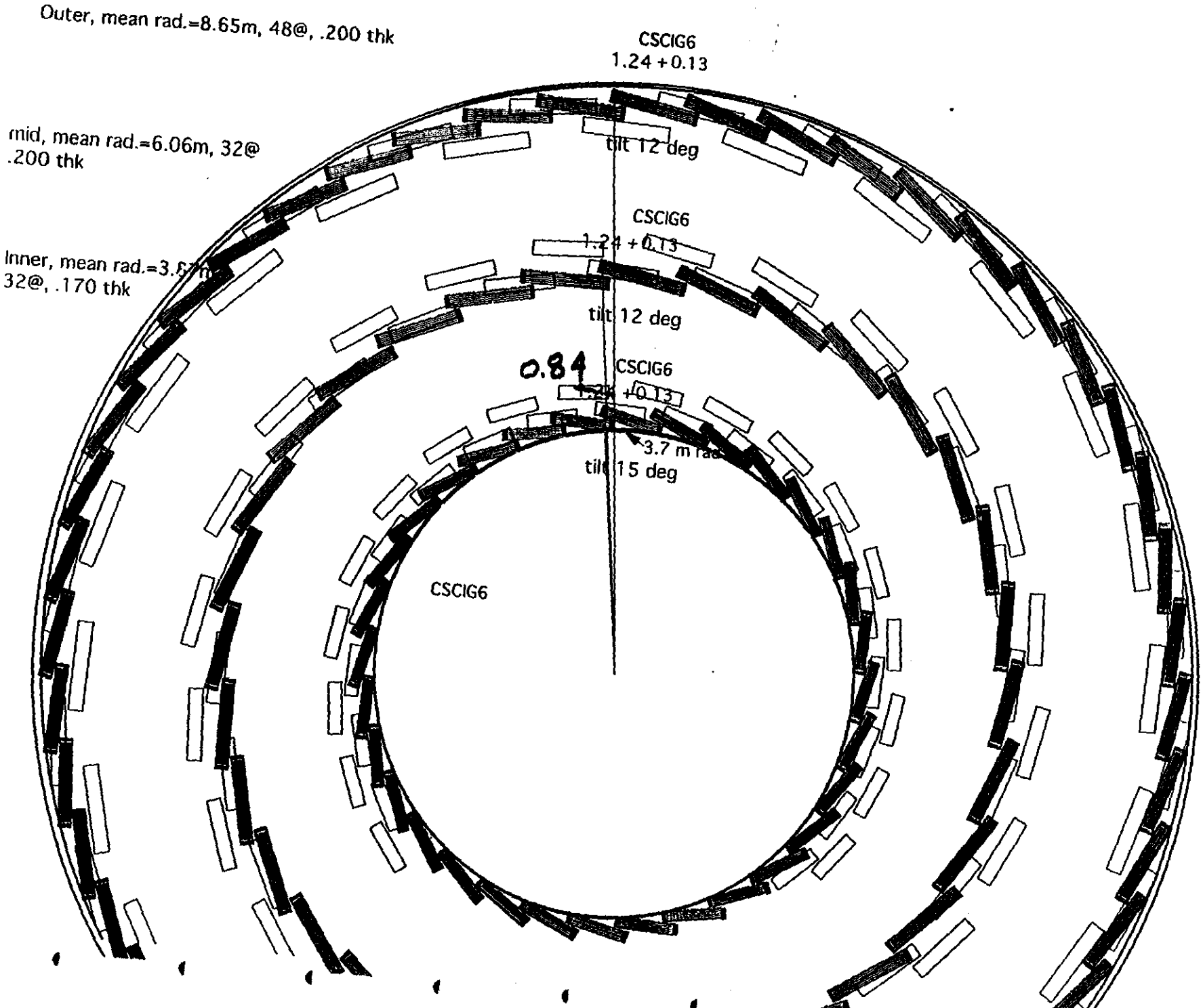
Outer, mean rad.=8.65m, 48@, .200 thk
CSCIG6
1.24 +0.13
tilt 12 deg
mid, mean rad.=6.06m, 32@
.200 thk
CSCIG6
1.24 +0.13
Inner, mean rad.=3.6
32@, .170 thk
tilt 12 deg
0.84
CSCIG6
+0.13
3.7 m
tilt 15 deg
CSCIG6

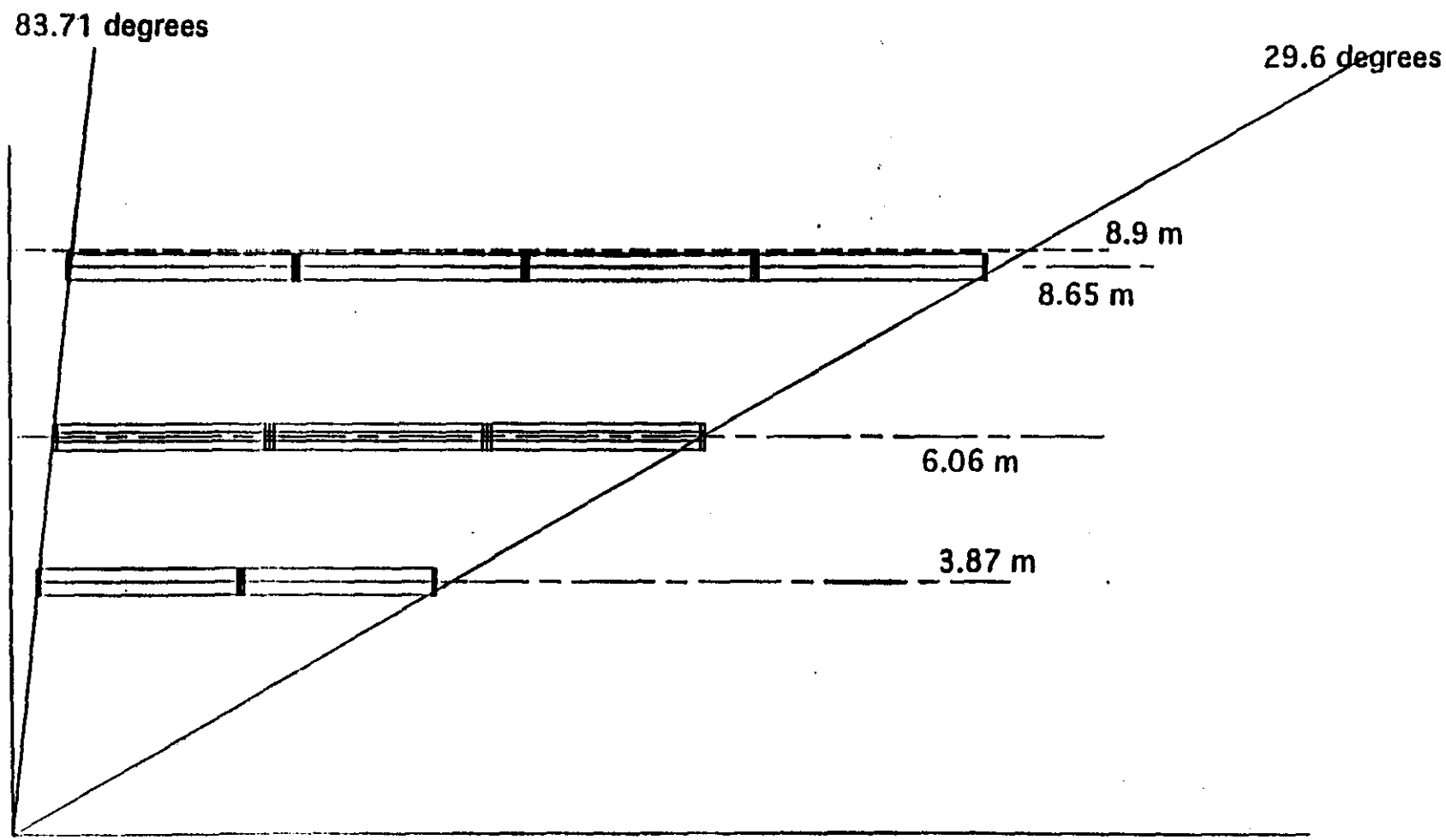
83.71 degrees
29.6 degrees
8.9 m
8.65 m
6.06 m
3.87 m

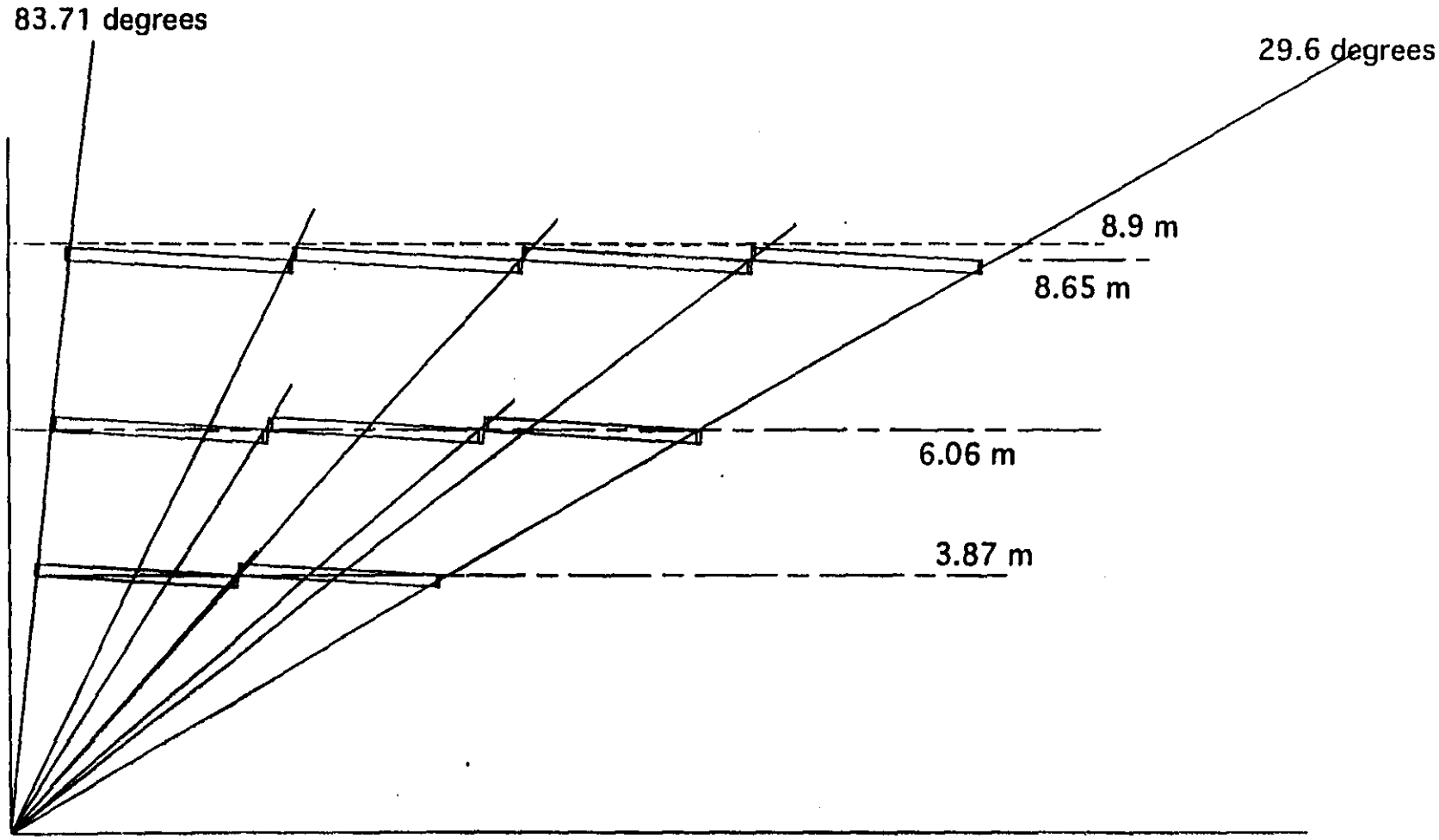
83.71 degrees
29.6 degrees
8.9 m
8.65 m
6.06 m
3.87 m

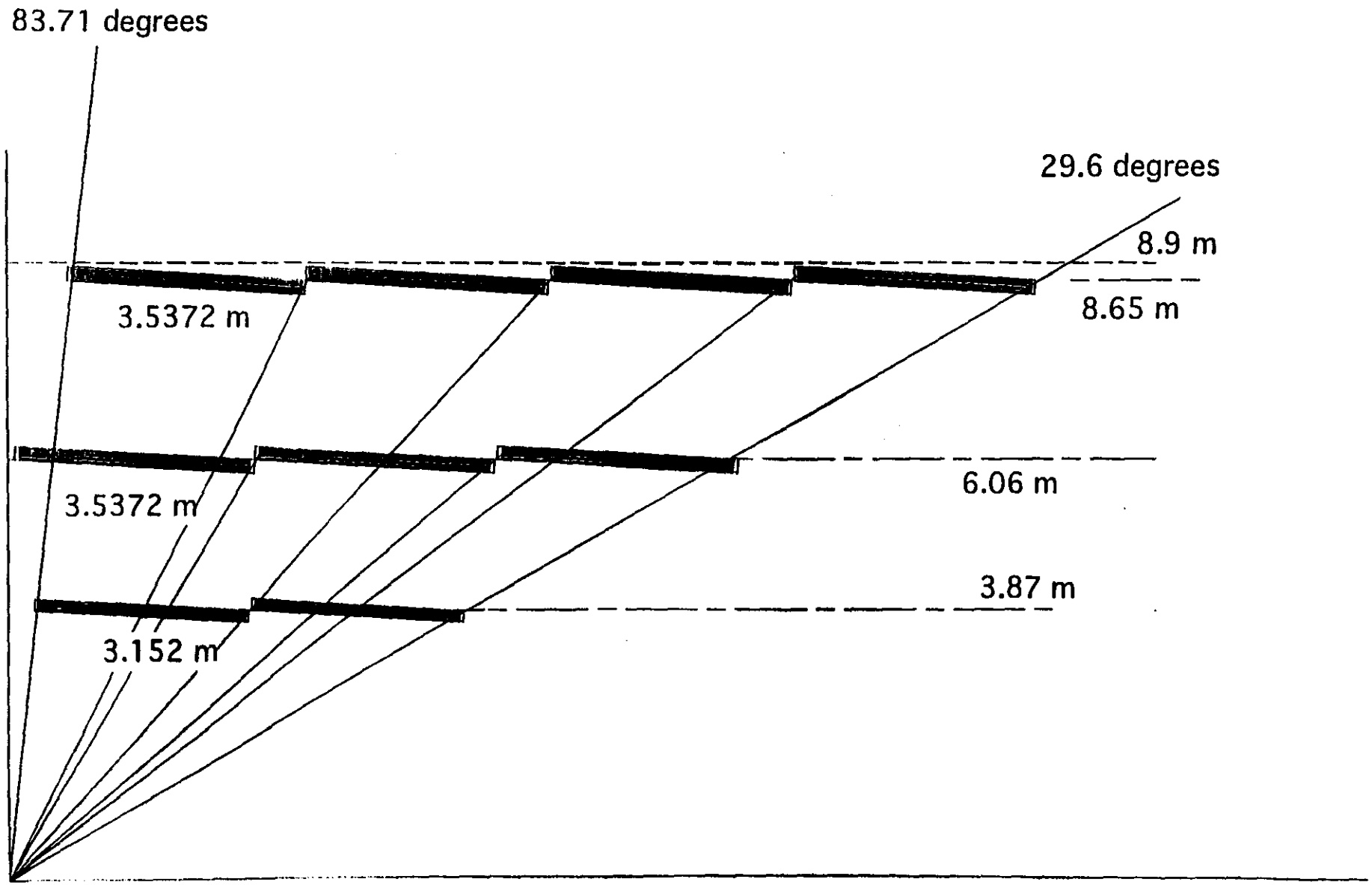
83.71 degrees
29.6 degrees
8.9 m
8.65 m
3.5372 m
3.5372 m
6.06 m
3.87 m
3.152 m

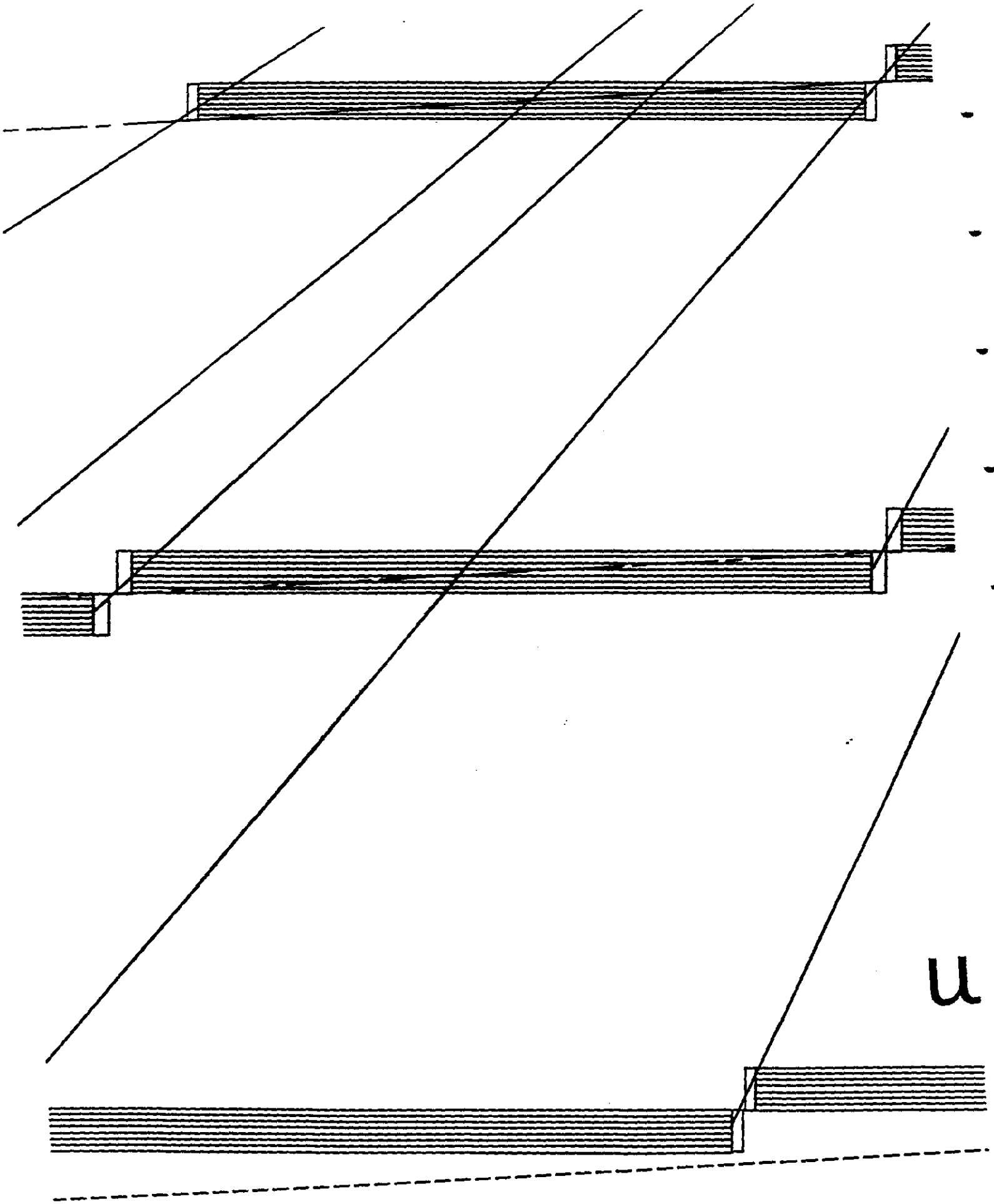
u

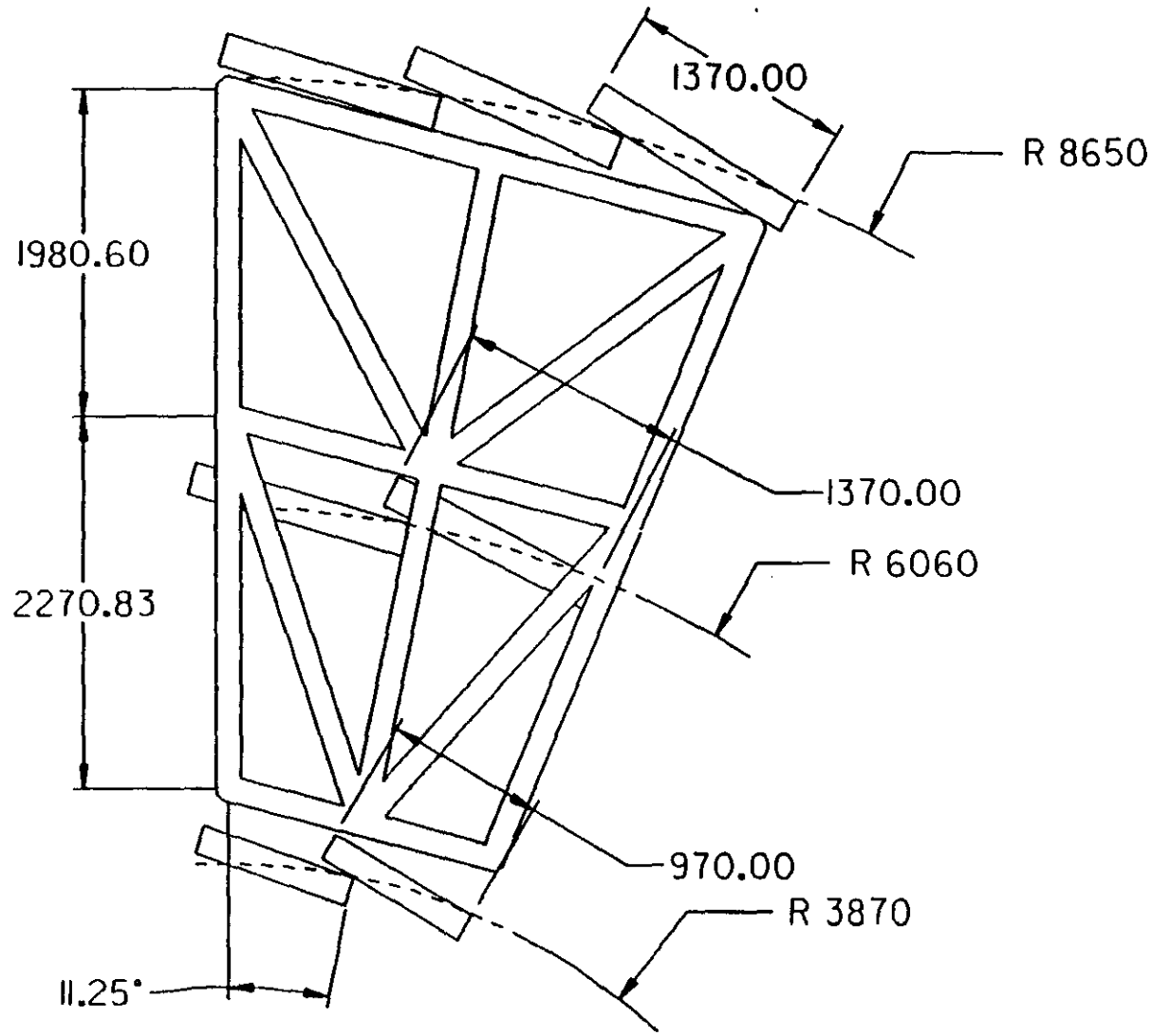
1370.00
R 8650
1980.60
1370.00
R 6060
2270.83
970.00
R 3870
11.25°

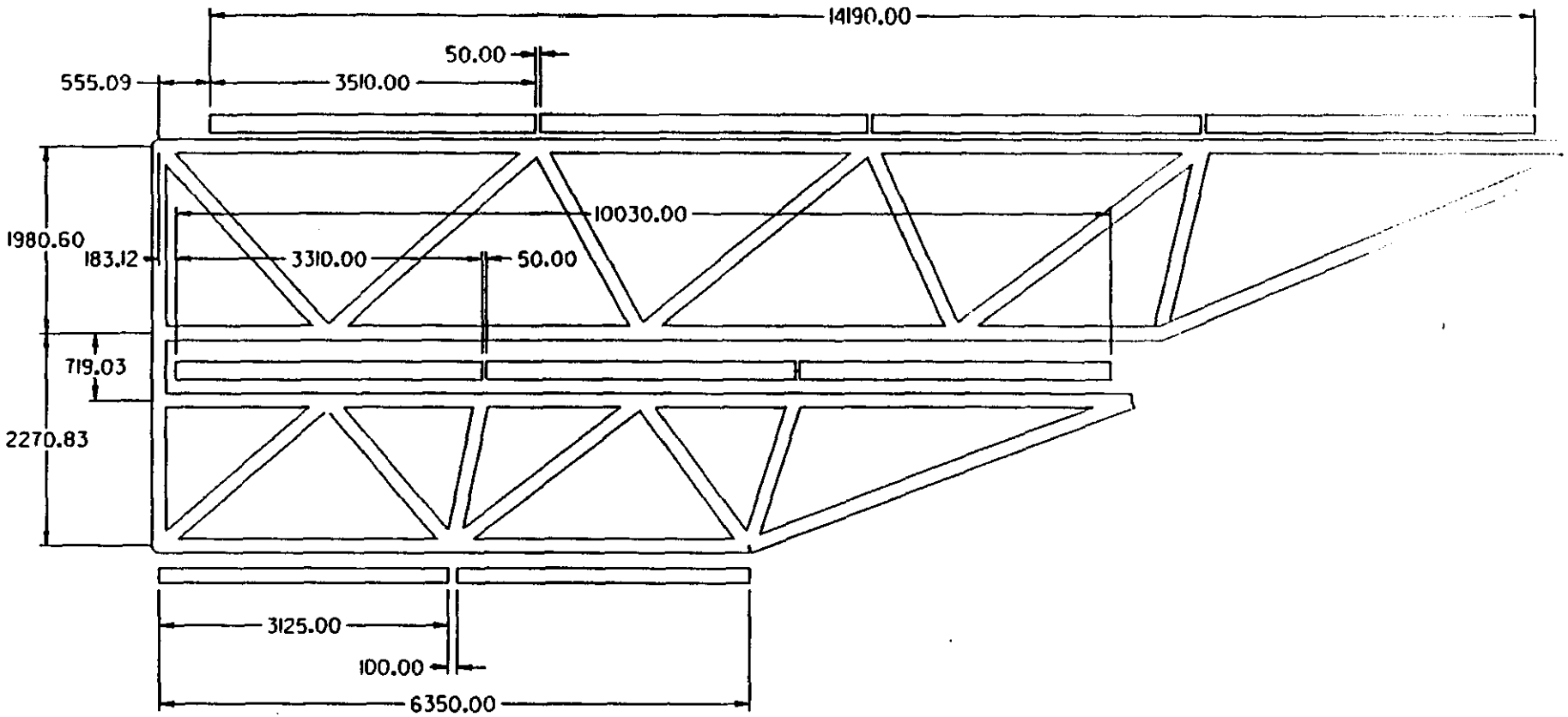
14190.00
50.00
555.09
3510.00
10030.00
1980.60
183.12
3310.00
50.00
719.03
2270.83
3125.00
100.00
6350.00

From: Mehdi Zarghamee (7/30/93)
To: Mike Gamble
CC: Mike Marx, Joe Paradiso
Mail*Link® SMTP Comments on Frank Nimblett'
Received: by qmail.ssc.gov with SMTP;30 Jul 1993 16:16:16 -0600
Received: by ihb.compuserve.com (5.67/5.930129sam)
id AA04523; Fri, 30 Jul 93 17:14:54 -0400
Date: 30 Jul 93 17:10:37 EDT
From: Mehdi Zarghamee <72614.2335@CompuServe.COM>
To: Mike Gamble <Mike_Gamble@qmail.ssc.gov>
Cc: Mike Marx <MARX@SSCVX1.SSC.GOV>, Joe Paradiso <NEUROMANCER@DRAPER.COM>
Subject: Comments on Frank Nimblett's Memo of 7/29/93
Message-Id: <930730211036_72614.2335_CHN55-2@CompuServe.COM>

Hi Frank,

1. Chambers are not staggered in the proposed 48-32-32 phi segmentation system.
Therefore, you do not need two different modules, as you stated. Furthermore, the
replacement of two rows of staggered chambers by a single row saves space.

2. The effect of 48-32-32 phi segmentation on the radial location of the structural joints
and the depth of the truss work can be summarized as follows:

For MIC1 R1= 4.18 m, R2 = 6.43 m, R3 = 8.25 m, changed from R1 = 4.61 m, R2 =
6.85 m, and R3 = 7.97 m. This shows that the depth of the outer bay increases from 1.1
m to 1.8 m and the depth of the inner bay is effectively unchanged at 2.2 m. Therefore,
there is more space altogether.

For MIC2, R1 and R3 are the same as for MIC1, but R2 = 5.69 m as compared to R2
= 5.90 m in the current design. Therefore, the depth of the outer bay increases from
2.07 m to 2.56 m, and the depth of the inner bay increases from 1.29 m to 1.51 m.
Hence, an increases in the depth of both bays.

Regards, Mehdi Zarghamee

SUMMARY (WAY TO GO?)

1. MAXIMIZE $\vec{B}$: 0.8T → 1.0T ? → 0.9T

2. OPTIMIZE CALO THICKNESS (TRIGGER RATE):

   $11\lambda \rightarrow 9.5\lambda$?

3. MAXIMIZE LEVER ARM (L):

   $\theta_L = 9° \rightarrow 12°$

   48/48/48/ → 32/32/48

   3.7 → 3.5m ?

4. MINIMIZE RATIO X_0/λ IN CALO

   Pb → Cu ?

5. MINIMIZE NUMBER OF CHAMBERS IN THE MIDDLE SUPERLAYER:

   $48 \times 4 = 192 \rightarrow 32 \times 3 = 96$ (×2!)

6. OVERLAP CHAMBERS IN φ AND θ:

   100% COVERAGE ; LOW DENSITY FRAMES

7. FIGHT FOR CHAMBER AND ALIGNMENT PRECISION

Reminder!

- THE GEM MAGNET IS NEEDED FOR MUON MOMENTA RECONSTRUCTION ONLY

- $$\frac{\Delta p}{p} \sim \frac{1}{BL^2}$$
- EFFECTIVE LEVER ARM IS 4.8 M

→ THE COST OF 1" CLEARANCE ≥ 1M$

→ 25 CM CORRESPOND 10% IN B

⇓

8. TUBING HAS TO BE COMPLEMENTED BY ABSORBERS (TO INCREASE λ WITHOUT INCREASING THE ENVELOP DIMENSIONS) !!!

Lorentz angle compensation in the Cathode Strip Chambers

1 Magnetic field strenght and orientation for Barrel and Endcap CSC.

2 Lorentz effect in the CSC.

3 Choise of the gas mixtures

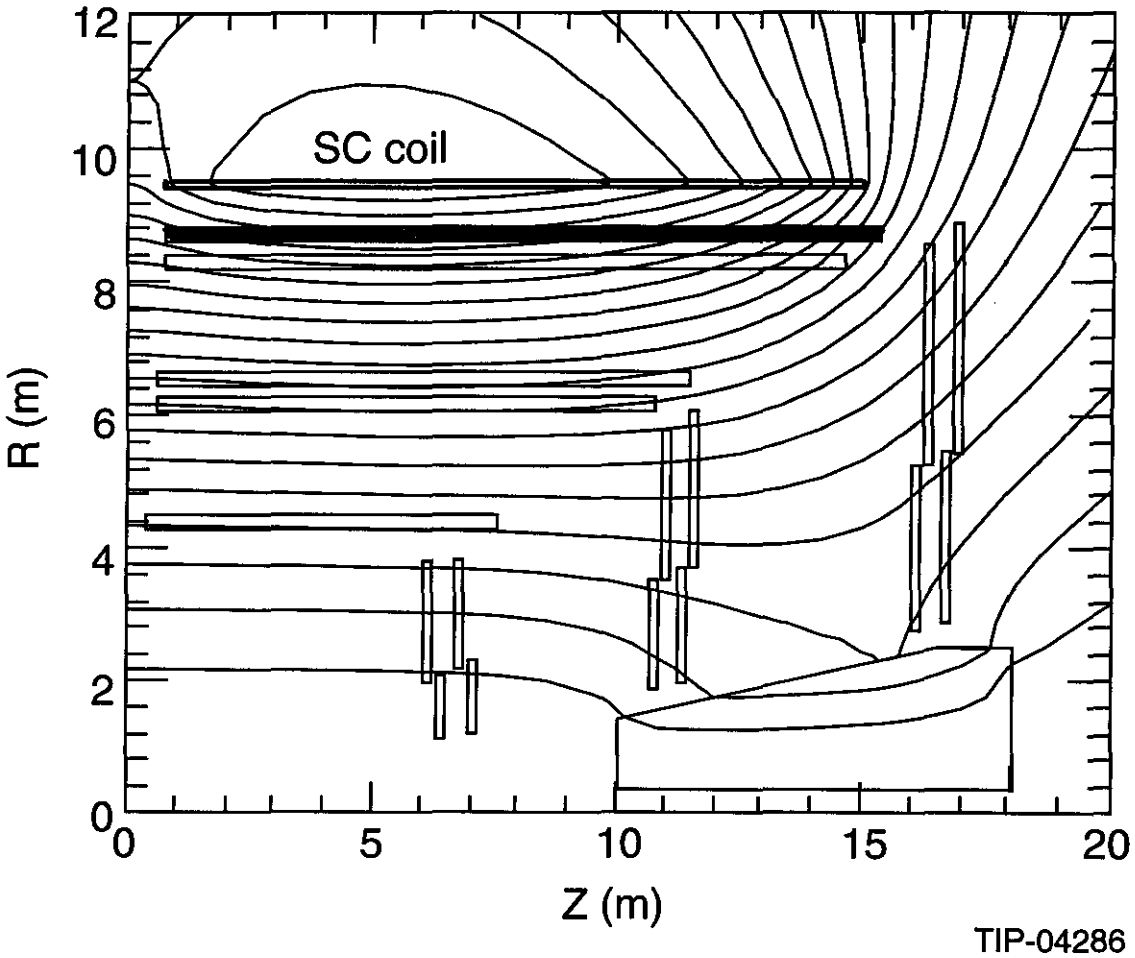
SC coil
R (m)
Z (m)
0
2
4
6
8
10
12
0
5
10
15
20
TIP-04286

r8588.pic
27/Jul/93 11:46:56 Page 29 : plot comp=bz

Timofeev S.

Barrel
R=8588 mm

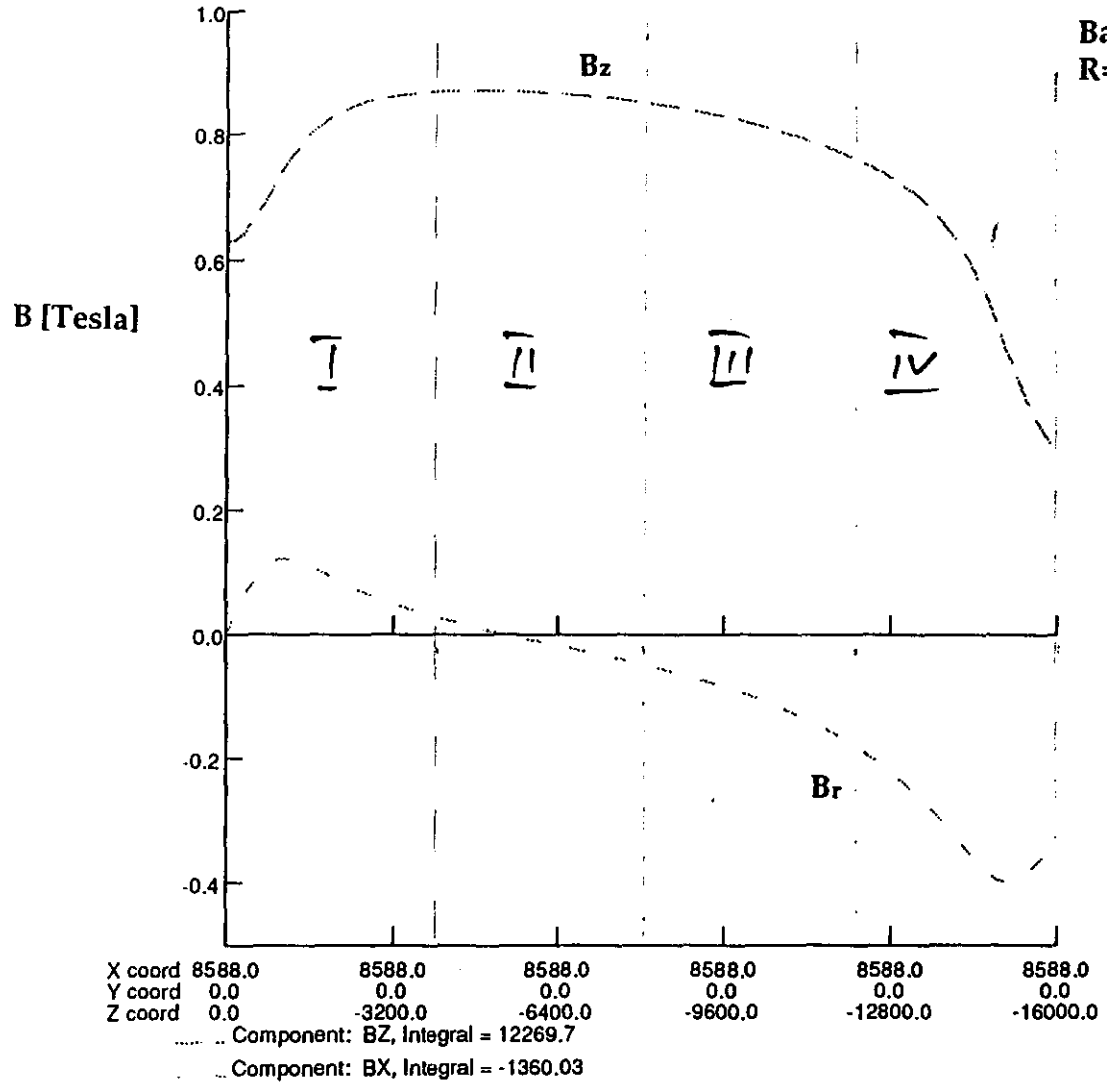

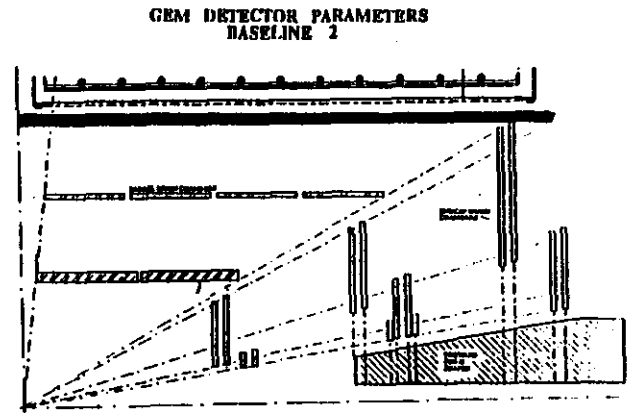

VF/OPERA-3d
(Post-processor)

z16250.pic
27/Jul/93 10:42:58 Page 21 : plot comp=bz

Timofeev S.

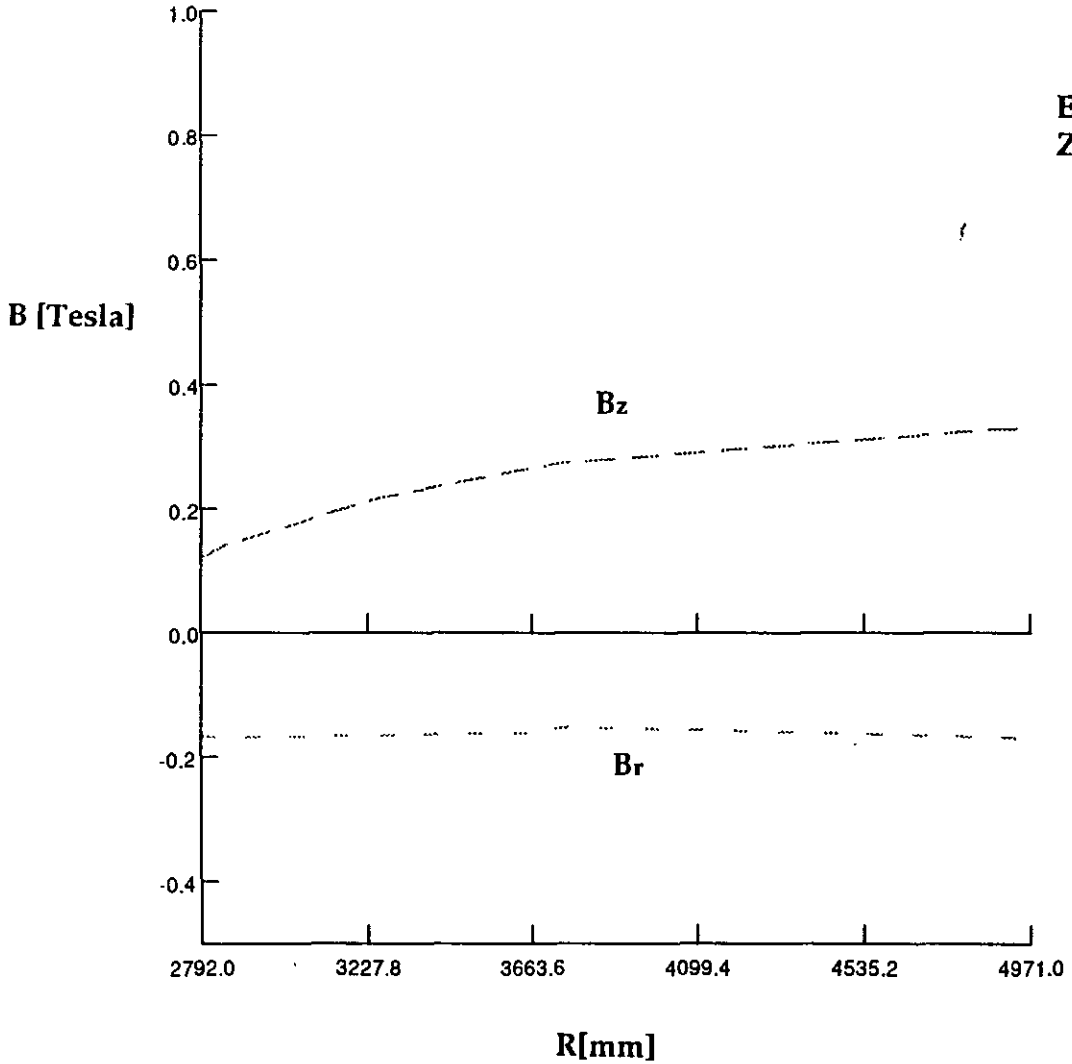

Endcap
Z=-16250 mm

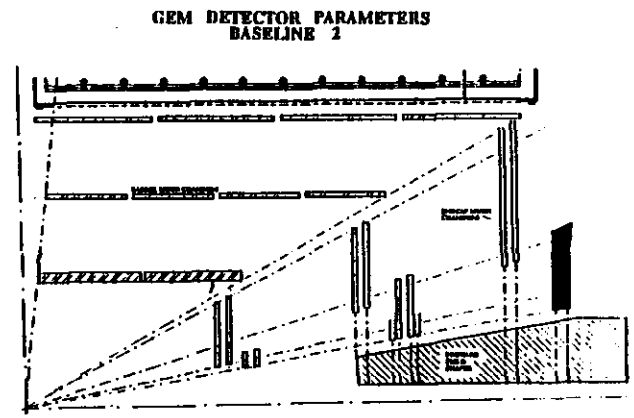

VF/OPERA-3d
(Post-processor)

Magnetic field in the CSC

Barrel

Chamber layers			Bz (T)	Br (T)
Inner	I.P.	1	0.83 ± 0.01	< 0.01
		2	0.83 ± 0.01	< 0.01
Middle	I.P	1	0.80 ± 0.03	< 0.05
		2	0.83 ± 0.02	
		3	0.78 ± 0.10	< 0.10
		4	0.65 ± 0.12	
Outer	I.P	1	0.75 ± 0.10	< 0.05
		2	0.83 ± 0.01	< 0.03
		3	0.80 ± 0.03	0.15 ± 008
		4	0.55 ± 0.25	0.30 ± 0.10

End Cap

Inner	I.P.	1	0.83 ± 0.01	< 0.02
		2	0.83 ± 0.01	< 0.02
Middle	I.P	1	0.64 ± 0.03	0.18 ± 0.08
		2	0.75 ± 0.01	0.06 ± 0.06
Outer	I.P	1	0.25 ± 0.07	− 0.16 ± 0.02
		2	0.46 ± 0.06	− 0.20 ± 0.10

Barrel

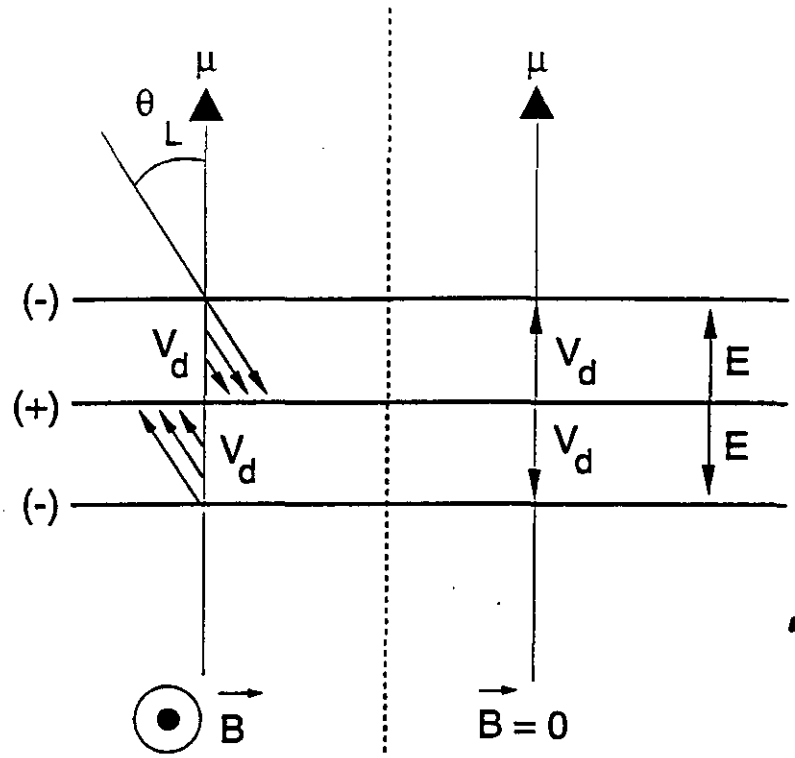

Titling

Lorentz angle compensation

Endcap

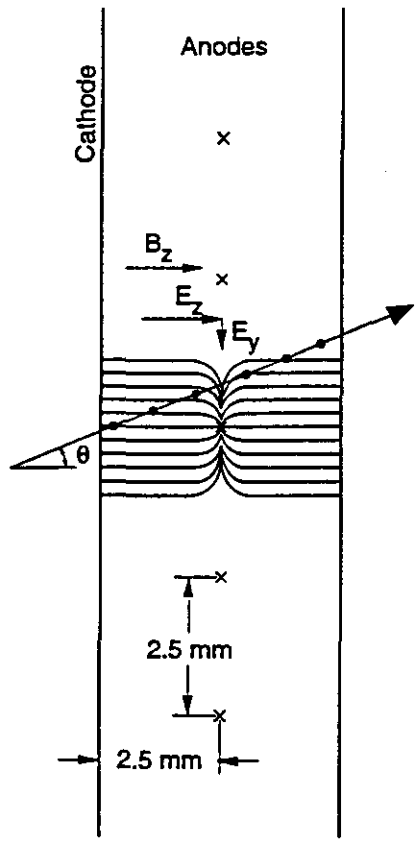

Rotating anode wires

compensation effective magnetic angle

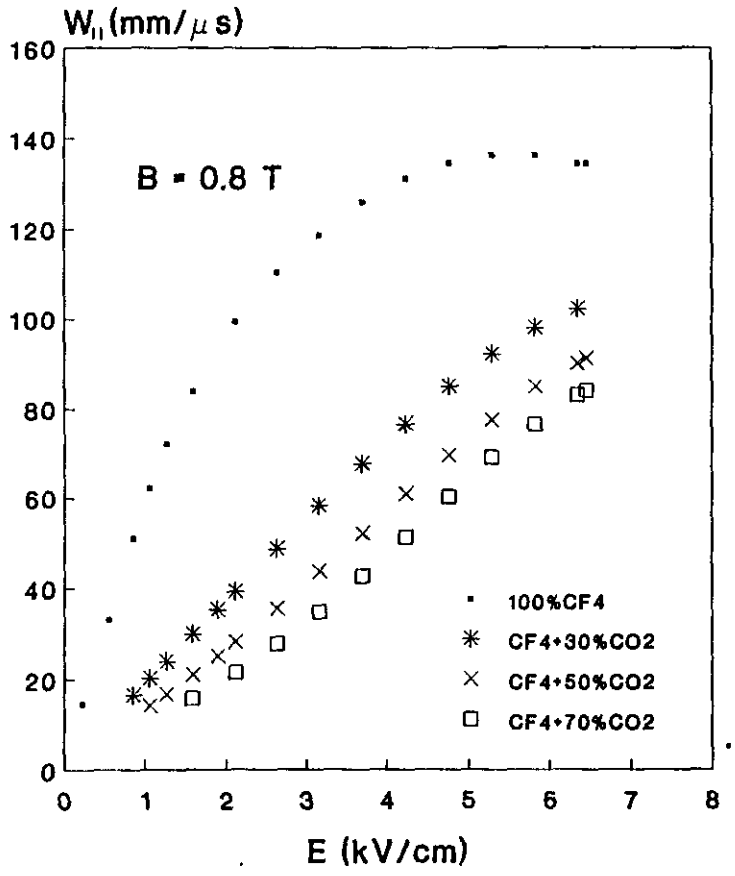

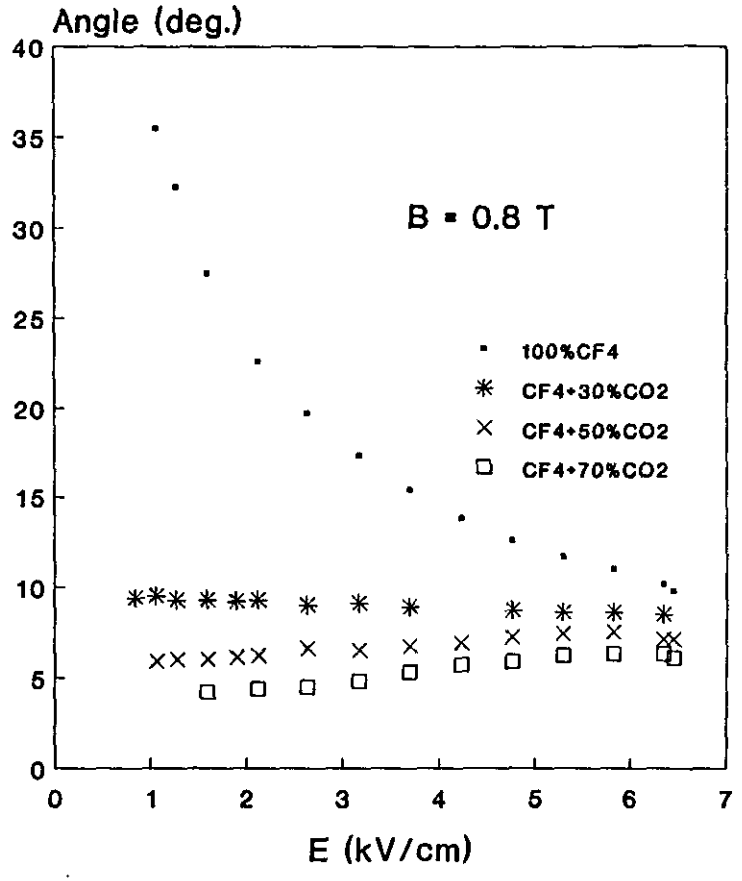

$CO_2 - CF_4$ gas mixtures

TN 93-417

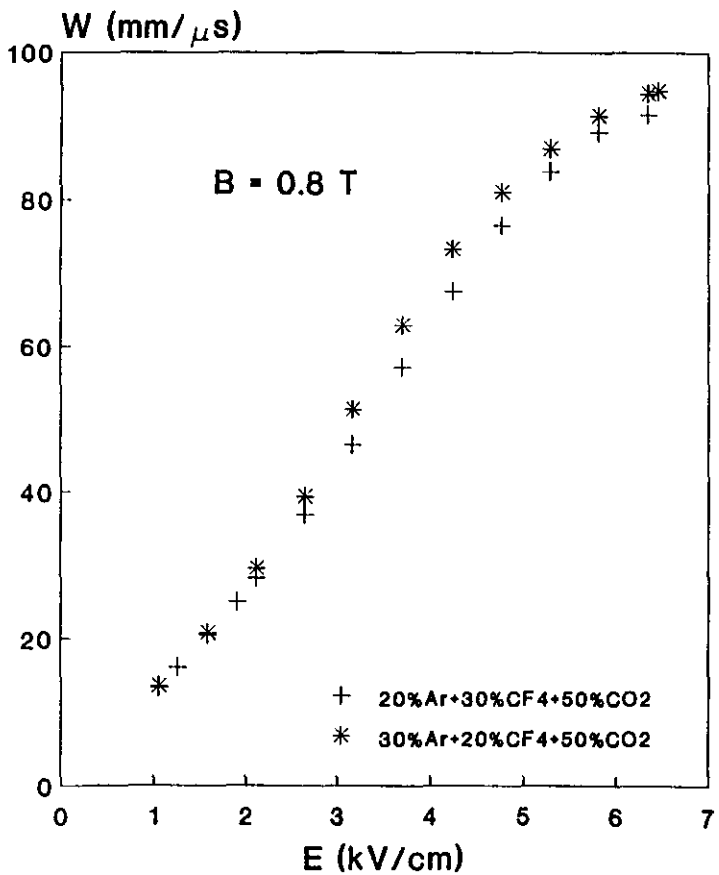

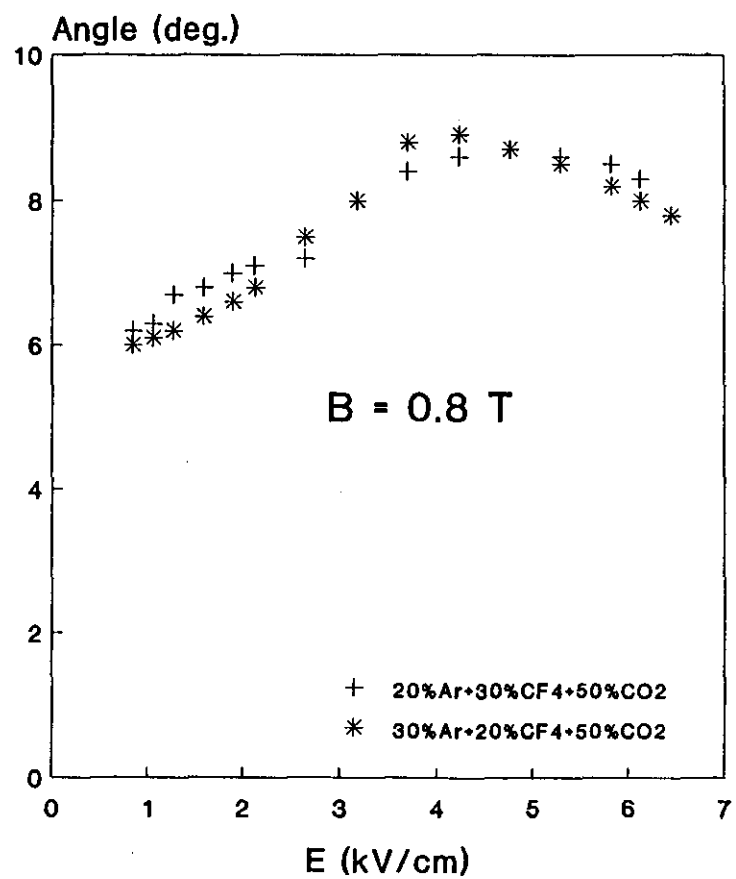

1. High drift velocity (≈ 80 mm/μs)
2. Small Lorentz angle ($\approx 9°$)
3. Adequate gas gain ($\approx 5 \cdot 10^4$)

E x B effect at the anode wires in the Endcap CSC

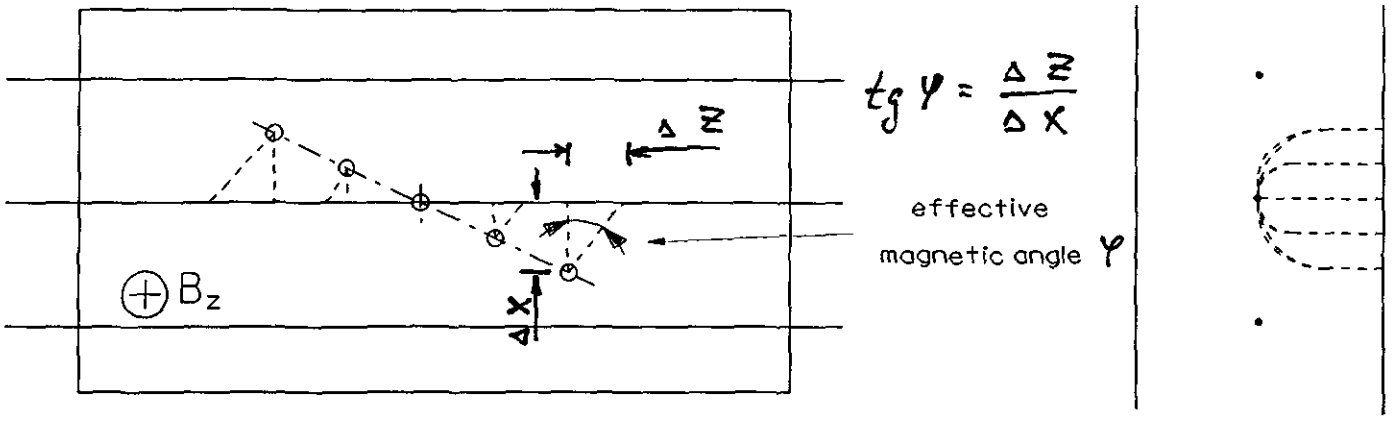

$$tg\,\varphi = \frac{\Delta z}{\Delta x}$$

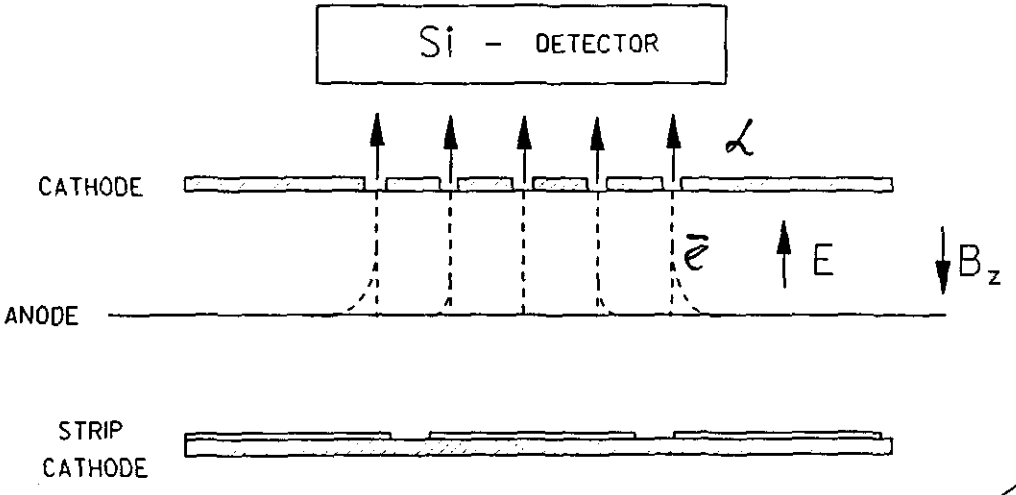

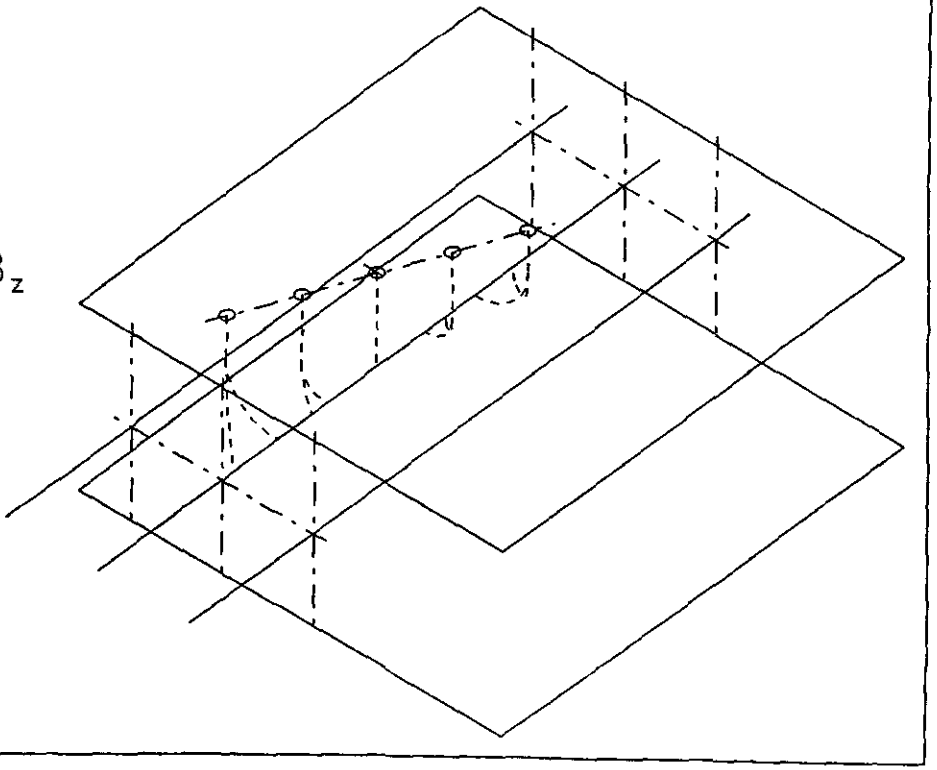

ELECTRON DRIFT $B = 0$

ELECTRON DRIFT $B \neq 0$

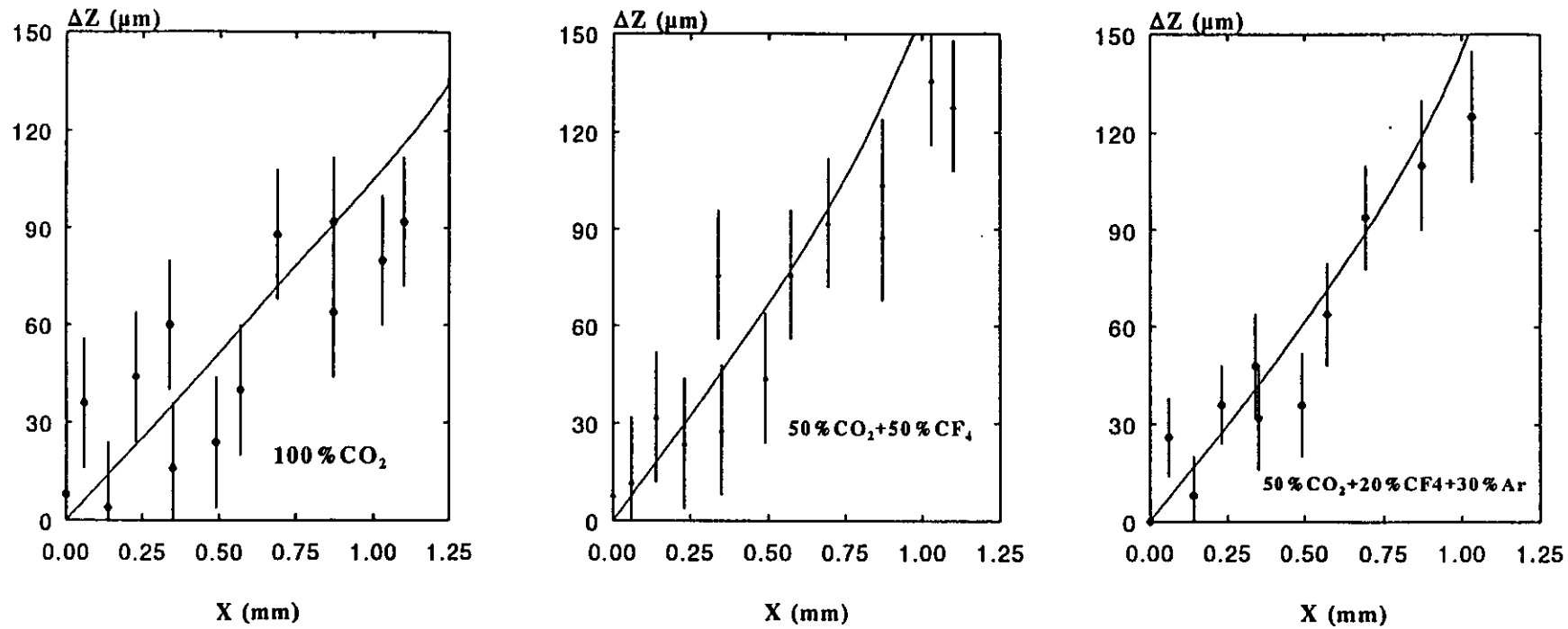
ΔZ (μm)
150
120
90
60
30
0
0.00
0.25
0.50
0.75
1.00
1.25
X (mm)
100 % CO_2
50 % CO_2+50 % CF_4
50 % CO_2+20 % CF4+30 % Ar

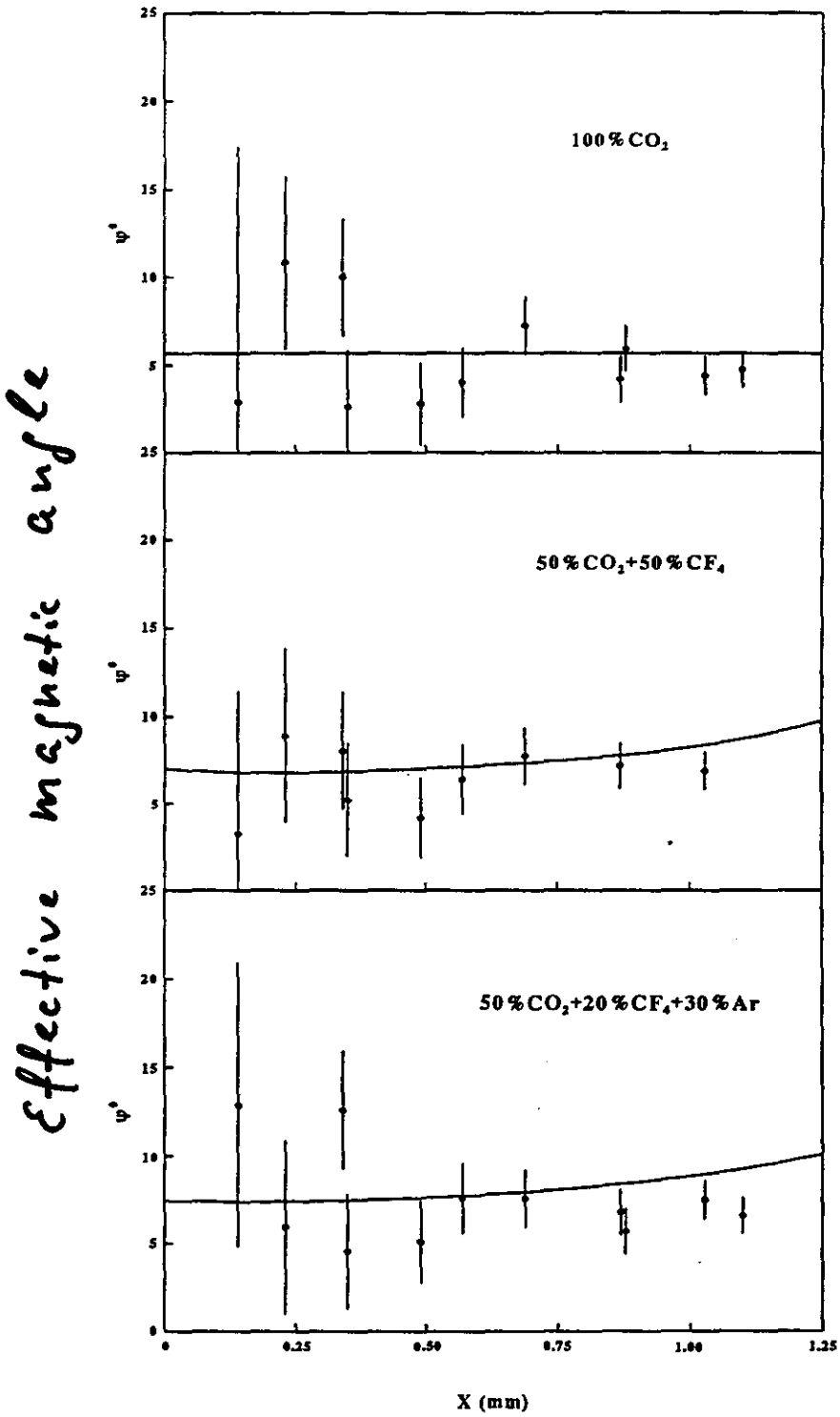

$$\varphi = \operatorname{arctg} \frac{\Delta Z}{\Delta X}$$

presented by Yu. Bonushkin

Simulations and measurements of the Muon System possible gas mixture

I. Golutvin: "Let's tilt the chambers by whatever angle is comfortable, then make a gas with the same Lorentz angle."

O. Prokofiev
Yu. Bonushkin } => Yes, sir. Possible.

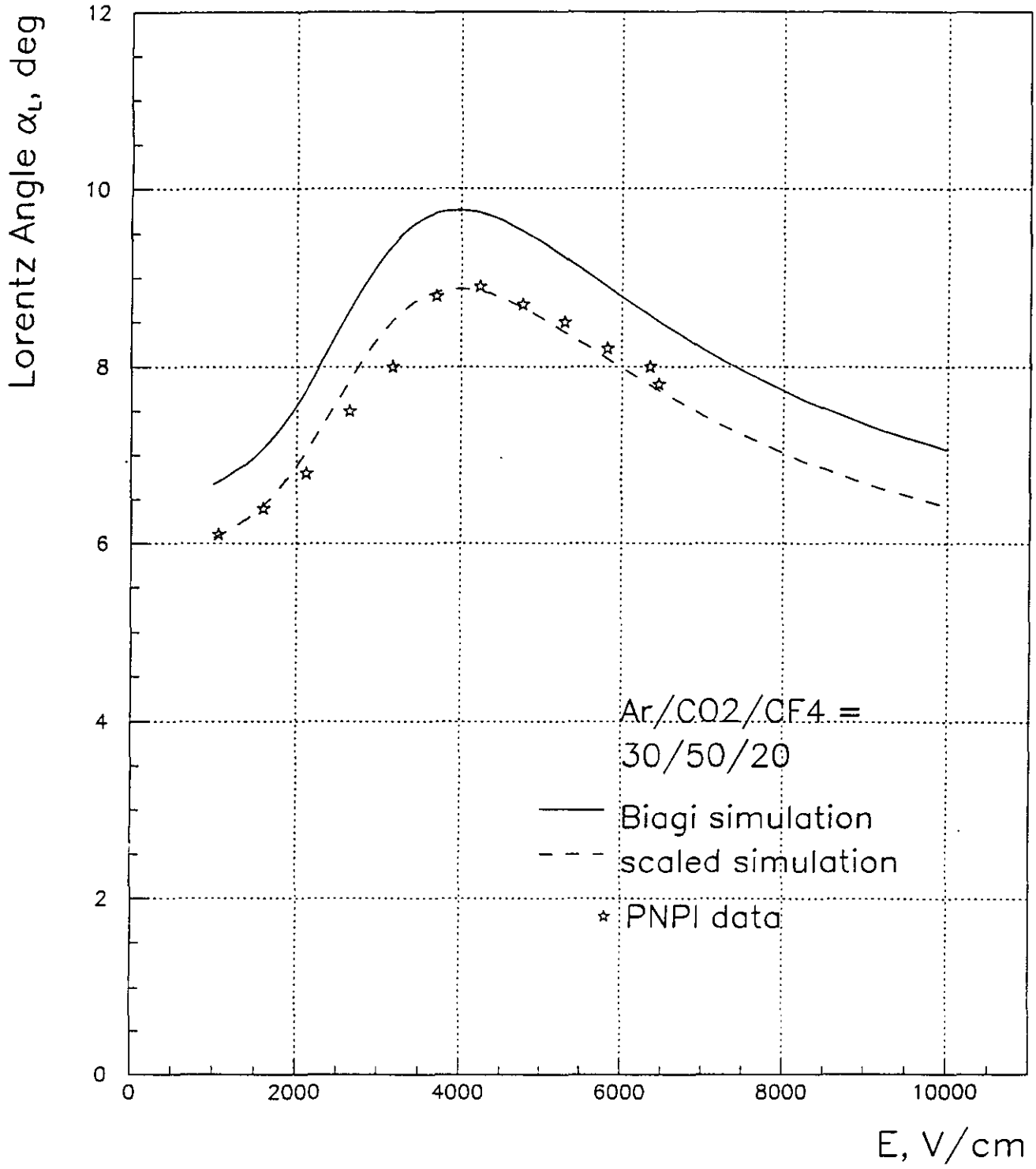
Lorentz Angle α_L, deg
12
10
8
6
4
2
0
0
2000
4000
6000
8000
10000
E, V/cm
Ar/CO2/CF4 =
30/50/20
Biagi simulation
scaled simulation
PNPI data

93/07/29 01.42

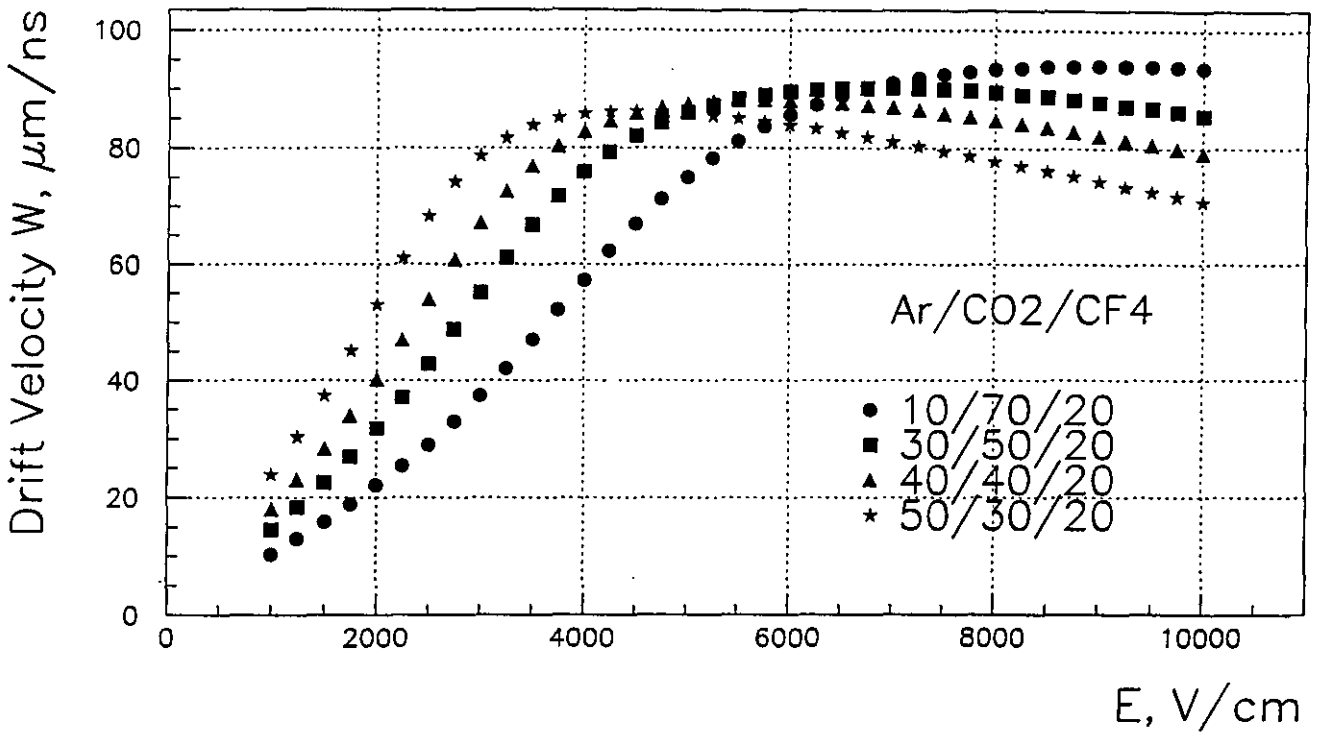
Drift Velocity W, μm/ns
100
80
60
40
20
0
0
2000
4000
6000
8000
10000
E, V/cm
Ar/CO2/CF4
10/70/20
30/50/20
40/40/20
50/30/20

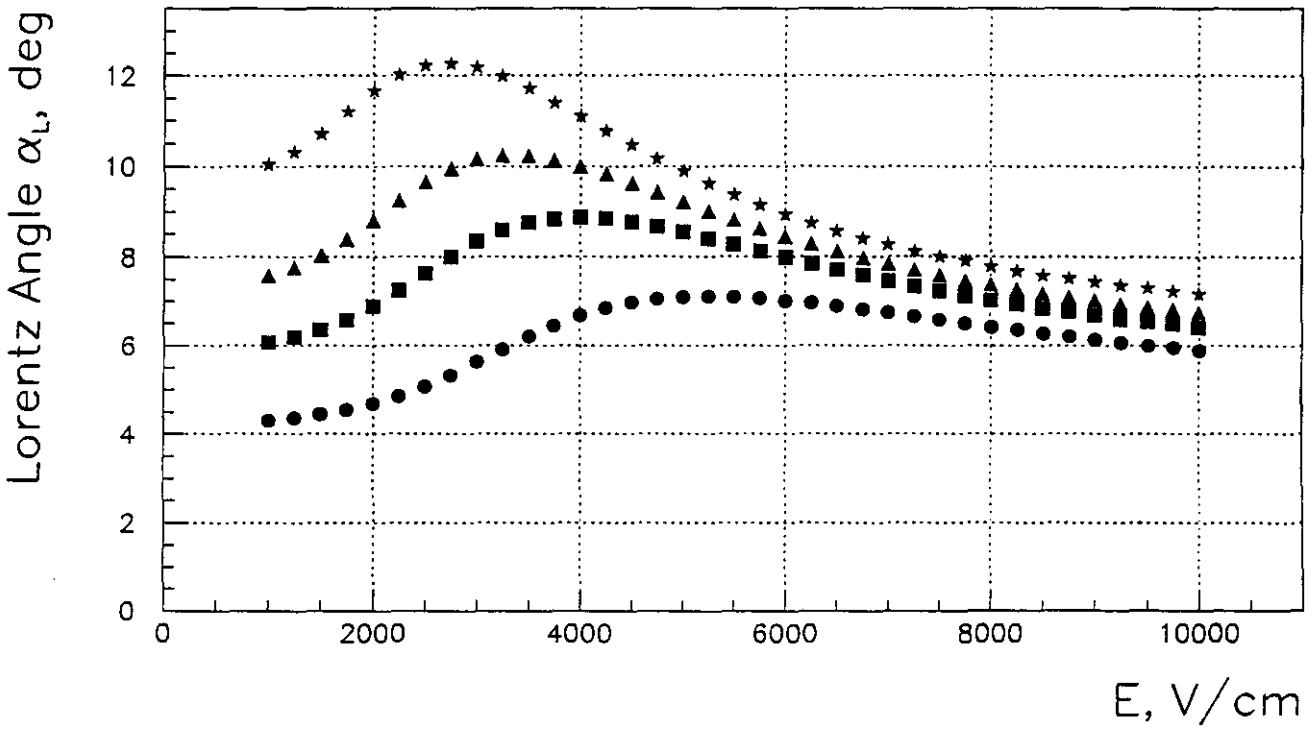
Lorentz Angle α_L, deg
12
10
8
6
4
2
0
0
2000
4000
6000
8000
10000
E, V/cm

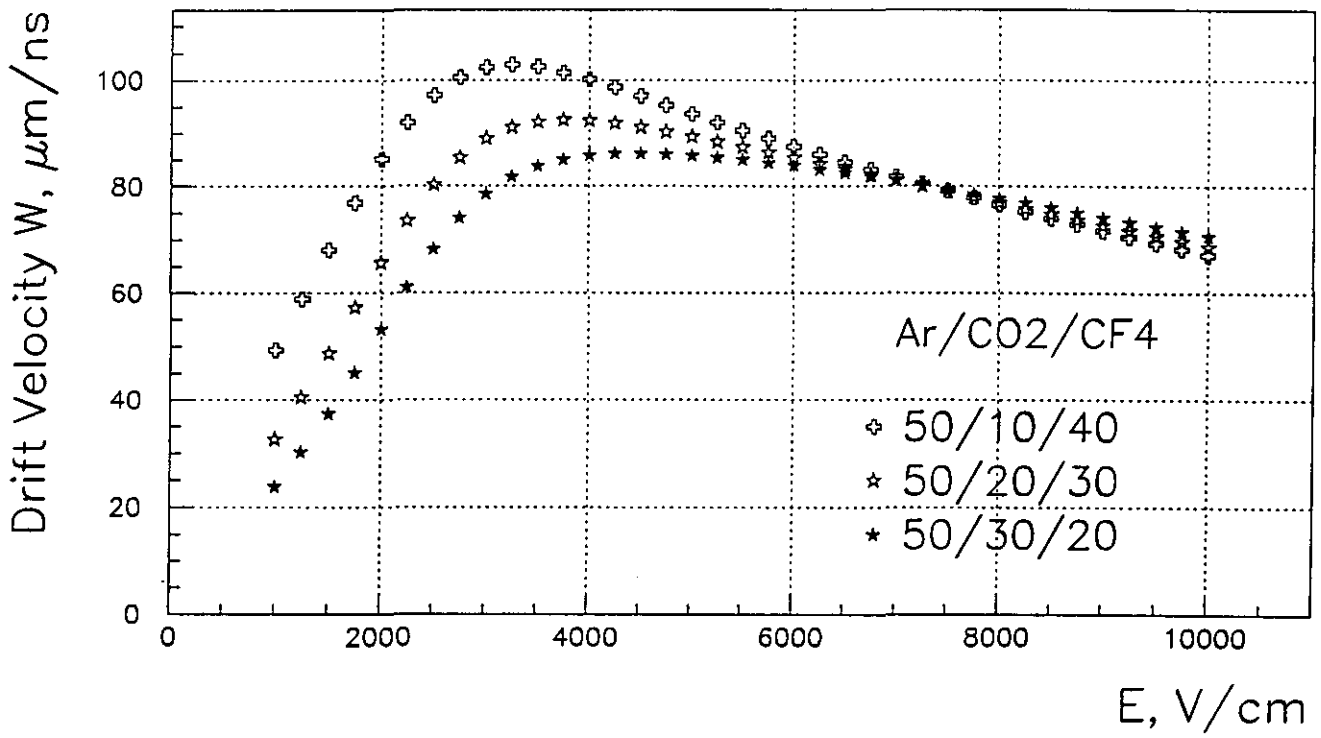
Drift Velocity W, μm/ns
100
80
60
40
20
0
0
2000
4000
6000
8000
10000
E, V/cm
Ar/CO2/CF4
50/10/40
50/20/30
50/30/20

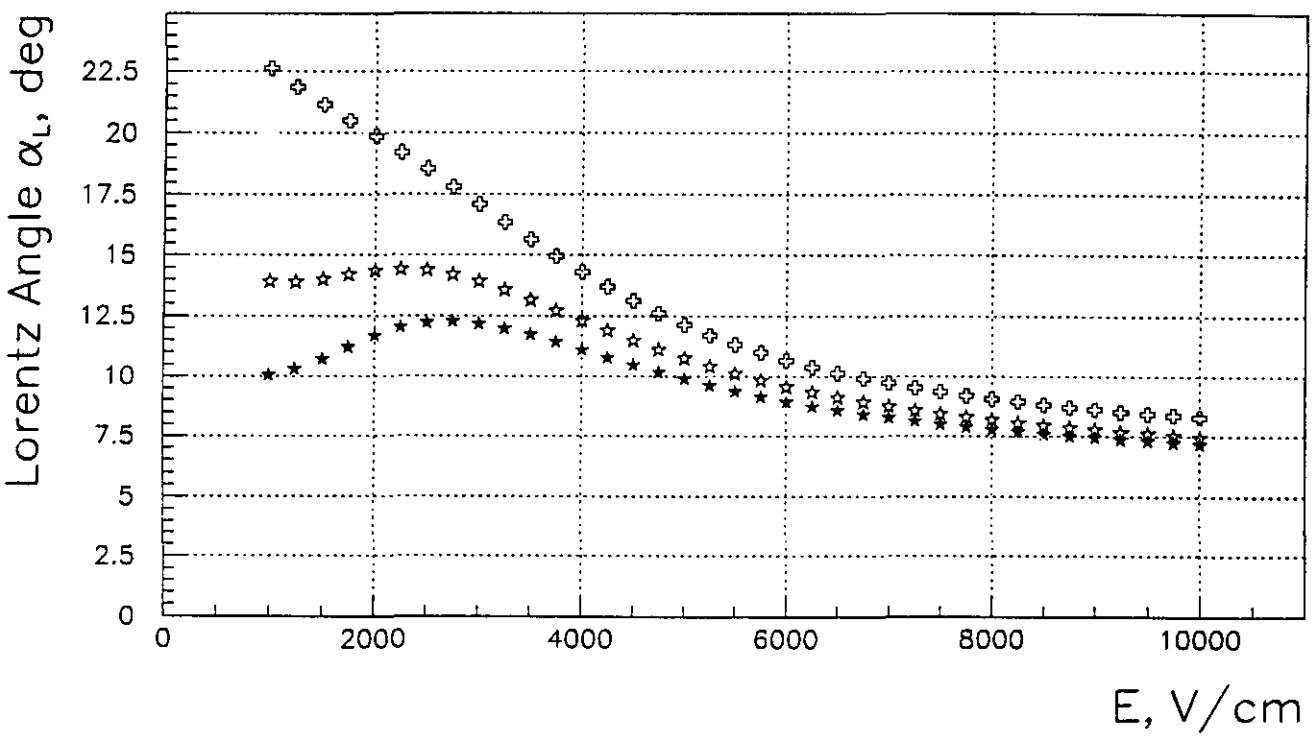
Lorentz Angle α_L, deg
22.5
20
17.5
15
12.5
10
7.5
5
2.5
0
0
2000
4000
6000
8000
10000
E, V/cm

93/07/29 02.13

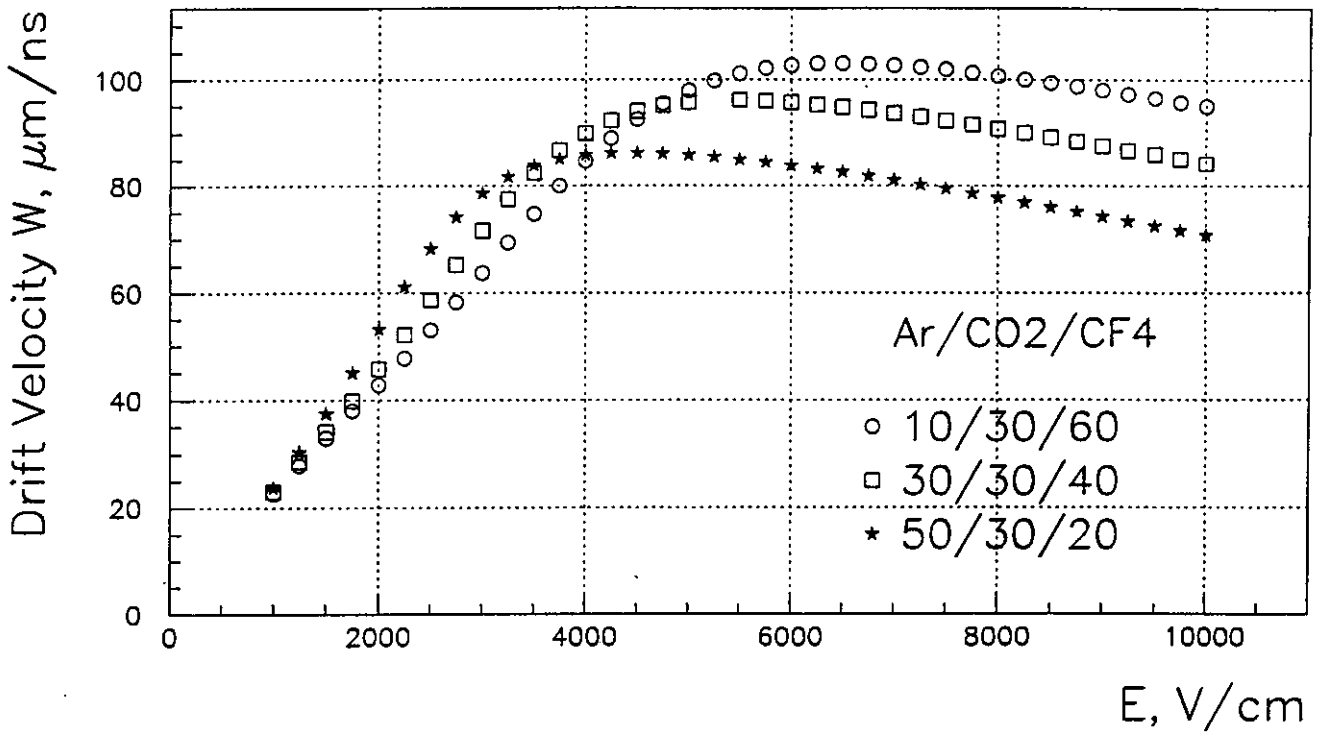
Drift Velocity W, μm/ns
100
80
60
40
20
0
0
2000
4000
6000
8000
10000
E, V/cm
Ar/CO2/CF4
10/30/60
30/30/40
50/30/20

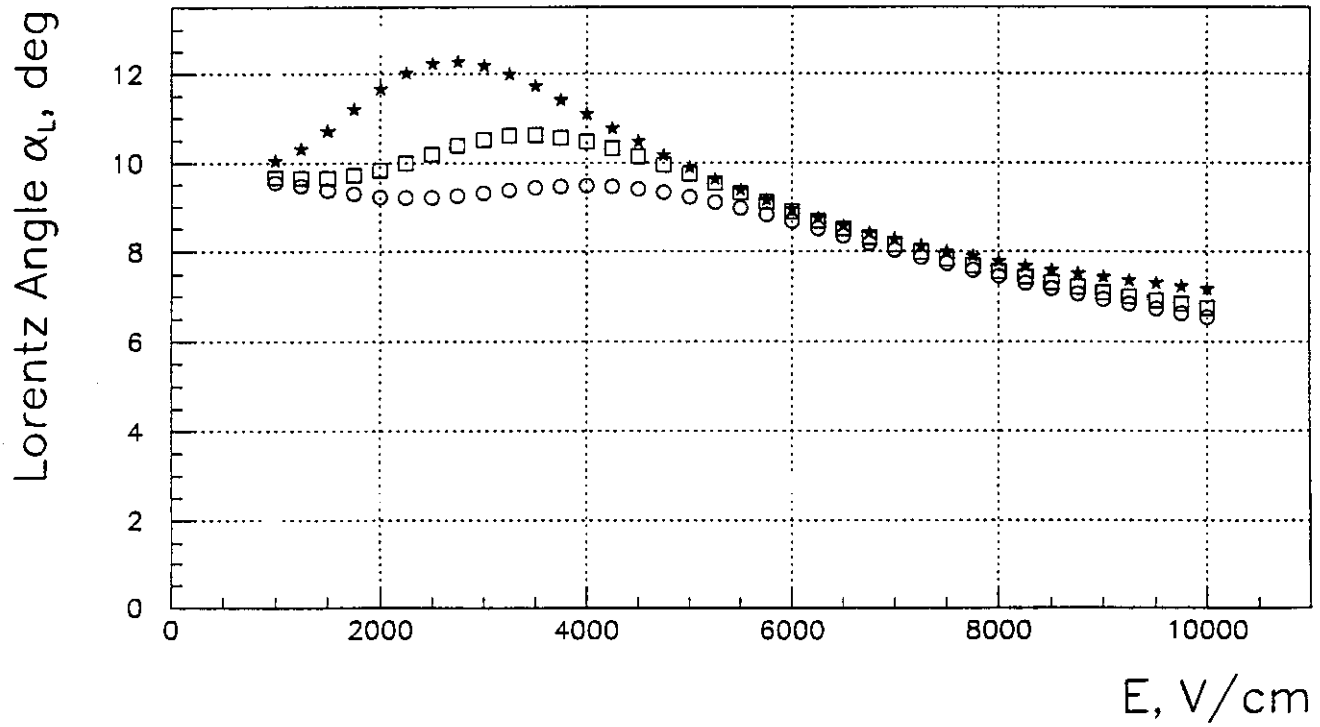
Lorentz Angle α_L, deg
12
10
8
6
4
2
0
0
2000
4000
6000
8000
10000
E, V/cm

Front Panel

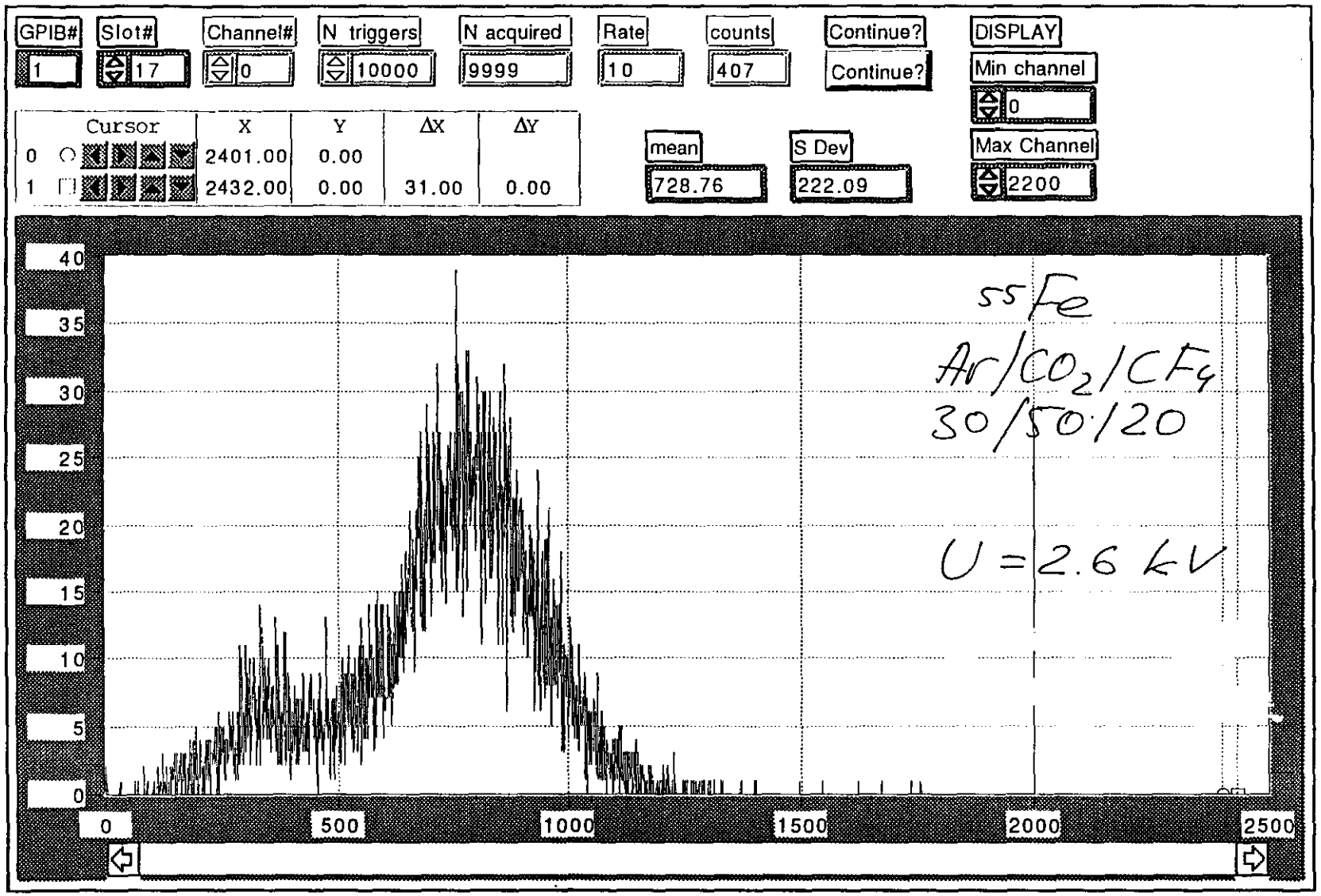
GPIB#
1
Slot#
17
Channel#
0
N triggers
10000
N acquired
9999
Rate
10
counts
407
Continue?
Continue?
DISPLAY
Min channel
0
Max Channel
2200
Cursor
X
Y
ΔX
ΔY
0
2401.00
0.00
1
2432.00
0.00
31.00
0.00
mean
728.76
S Dev
222.09
40
35
30
25
20
15
10
5
0
0
500
1000
1500
2000
2500
55Fe
Ar/CO2/CF4
30/50/20
U = 2.6 kV

Front Panel

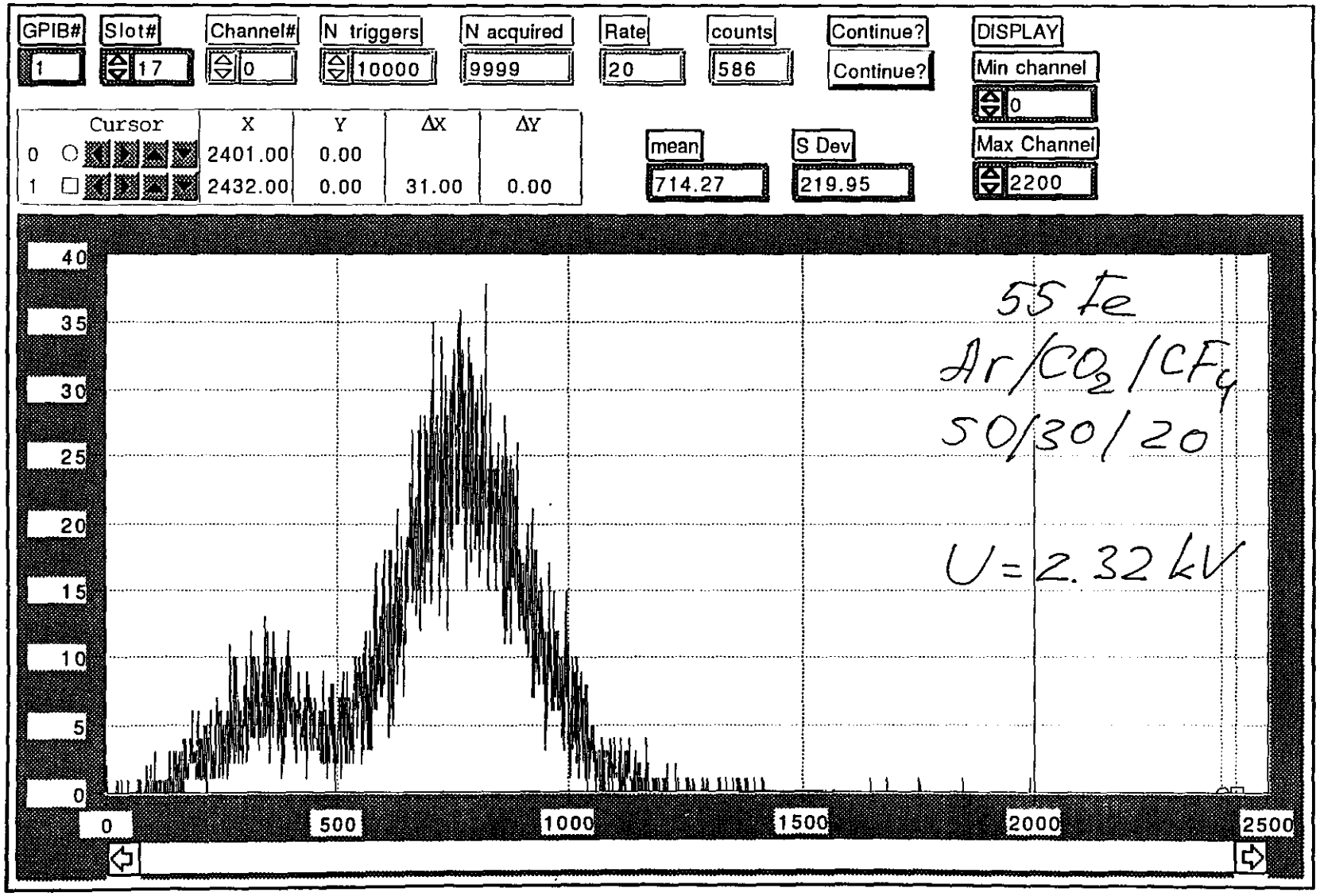
GPIB#
1
Slot#
17
Channel#
0
N triggers
10000
N acquired
9999
Rate
20
counts
586
Continue?
Continue?
DISPLAY
Min channel
0
Max Channel
2200
Cursor
X
Y
ΔX
ΔY
0
2401.00
0.00
1
2432.00
0.00
31.00
0.00
mean
714.27
S Dev
219.95
40
35
30
25
20
15
10
5
0
0
500
1000
1500
2000
2500
55 Fe
Ar/CO2/CF4
50/30/20
U = 2.32 kV

93/08/03 13.19

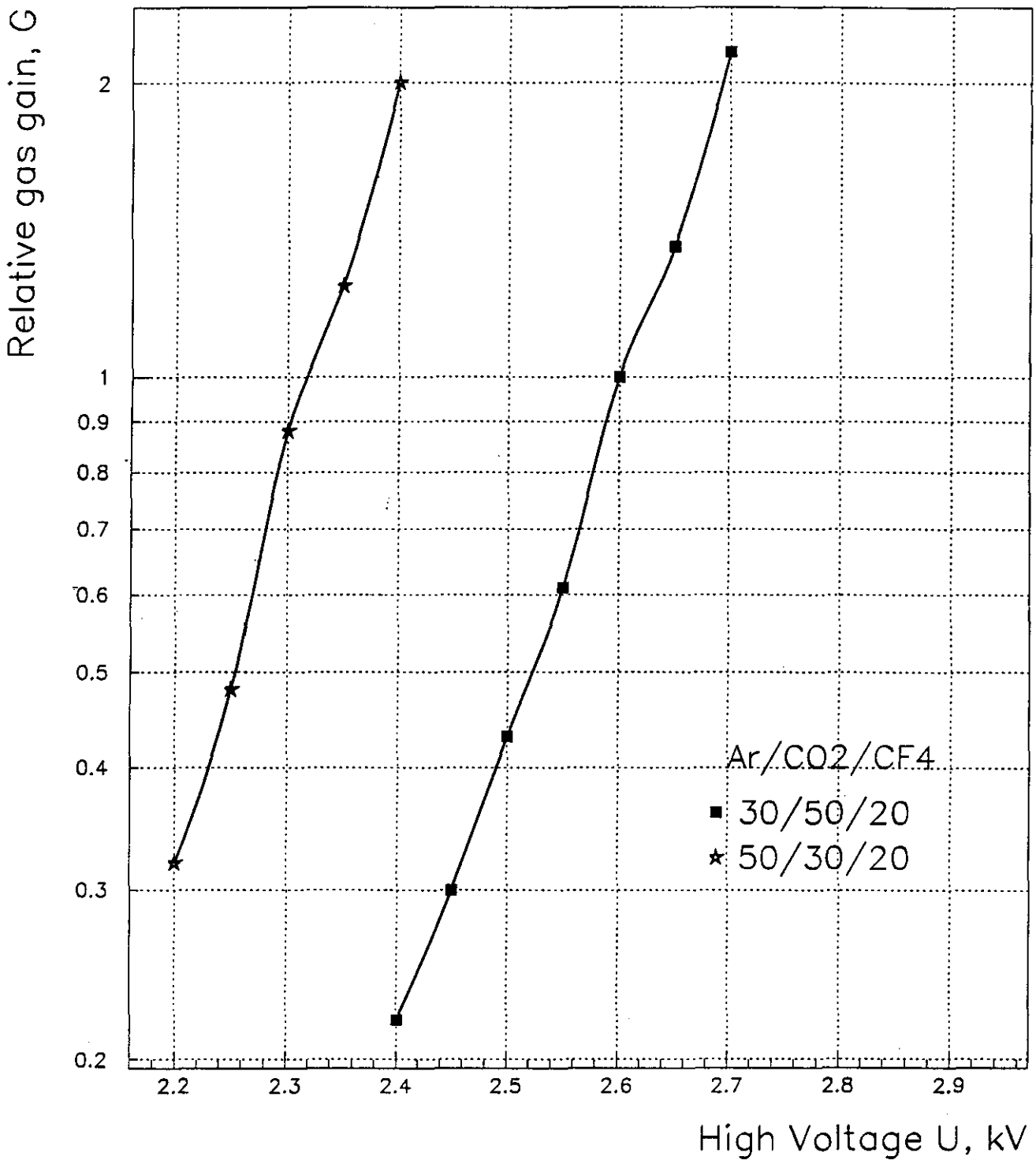
Relative gas gain, G
2
1
0.9
0.8
0.7
0.6
0.5
0.4
0.3
0.2
2.2
2.3
2.4
2.5
2.6
2.7
2.8
2.9
High Voltage U, kV
Ar/CO2/CF4
30/50/20
50/30/20

GEM MAGNETIC FIELD
(REFERENCE FOR THE MUON SYSTEM).

S.Timofeev
SSCL

ABSTRACT:

Overall map of the GEM magnetic field, radial distribution of the GEM magnetic field at Z positions correspond to the muon chamber superlayers positions, detailed distribution of the magnetic field in the barrel and endcap muon chambers, distribution and integral Bzdl of the magnetic field along the muon tracks at the different θ angles and axial nonsymmetry of the magnetic field are presented.

The 3-dimensional magnetic analysis of the GEM detector was carried out using the OPERA-3d prepocessor program, TOSCA analysis program and OPERA-3d postprocessor program on UNIX workstation.

Bz and Br components of the magnetic field have been calculated for the muon chambers placement regions.

GEM MAGNET SYSTEM.

GEM magnet system is a large superconducting solenoid assembly with field shaping in the forward region. The solenoid assembly is physically 31 m long with 18 m diameter inner bore and produces a central field of 0.8 Tesla. It consists of two half-length coil assemblies, each 14234 mm long, separated by a distance of 1532 mm at the midplane. In the forward direction the magnetic field is shaped to improve the muon resolution. This shaping is accomplished by large ferromagnetic structures, called Forward Field Shapers (FFS), which are roughly projective to the IP, coaxial with the beam axis, and occupy the volume from 10-18 m from the IP in both directions. The elevation view of the GEM magnet system is presented in Fig 1.

GEM MUON SYSTEM.

GEM muon system is a system of three superlayers, each containing multiple layers of detectors placed between the calorimeter and the solenoidal magnet coils. The positions of the muon chambers are indicated in Fig.2.

FEM MODEL

The procedure of the creating of the FEM model is described in (1). The final FEM-model that has been used for the analysis is presented in Fig.3. It consist from the 115710 elements (120120 nodes).

RESULTS.

The overall map of the GEM magnetic field is presented in Figs.4 Fig.4.1 represent the Bz component distribution, Fig.4.2 represent Br component distribution at the RZ plane of the half of the GEM sensitive volume (R=0-9000 mm; Z=0-17000 mm).The Forward Field Shapers (FFS) introduce a significant radial field component, the gap between the halfs of the coils lead to the decreasing of the field in this region, in the region of the last endcap muon chambers the radial component of the field change the sign that lead to the decreasing of the muon momentum resolution.

Figs.5 represent the radial distribution of the GEM magnetic field at Z positions correspond to the muon chamber superlayers positions (Z=0, -5760, -9950, -11250, -14750 and -16250 mm).

Figs.6 represent detailed distribution of the magnetic field in the barrel muon chambers and Figs.7 - in the endcap muon chambers.

The FFS support structure made from regular steel lead to the axial nonuniformity of the magnetic field in the endcap region. Figs.8 represent the worse case of the axial nonsymmetry of the magnetic field in the endcap region.

Distribution of the magnetic field along the muon tracks at the different θ angles (θ= 90; 29.60; 17.01; 9.75 and 9.45 grad) are presented in Figs.9.

Integrals Bzdl of the magnetic field along the muon tracks at the different θ angles (θ= 9.75; 30; 60; 90 grad) are presented in Fig.10.

REFERENCES:

1. S.Timofeev "Axial Symmetry of the GEM Magnetic Field" GEM TN--3-384.

LIST OF FIGURES:

Fig.1 The elevation view of the GEM magnet system .

Fig.2 The positions of the muon chambers.

Fig.3 FEM model.

Fig.4 Overall map of the GEM magnetic field.
Fig.4.1 Bz component distribution.
Fig.4.2 Br component distribution.

Fig.5 Radial distribution of the GEM magnetic field (Z positions correspond to the muon chamber superlayers positions).
Fig.5.1 Z=0 ; R=0-9000 mm.
Fig.5.2 Z=-5760 mm ; R=0-9000 mm.
Fig.5.3 Z=-9950 mm ; R=1450-9000 mm.
Fig.5.4 Z=-11250 mm ; R=1650-9000 mm.
Fig.5.5 Z=-14750 mm ; R=2250-9000 mm.
Fig.5.6 Z=-16250 mm ; R=2500-9000 mm.

Fig.6 Detailed distribution of the magnetic field in the barrel muon chambers.
Fig.6.1 Internal layer: R=3854 mm.
Fig.6.2 Middle layer: R=6282 mm.
Fig.6.3 Outer layer: R=8588 mm.

Fig.7 Detailed distribution of the magnetic field in the endcap muon chambers.
Fig.7.1 Z=-5760 mm.
Fig.7.2 Z=-6600 mm.
Fig.7.3 Z=-9950 mm.
Fig.7.4 Z=-11250 mm.
Fig.7.5 Z=-14750 mm.
Fig.7.6 Z=-16250 mm.

Fig.8 Axial nonsymmetry of the magnetic field in the endcap region.
Fig.8.1 overall picture of the local axial nonuniformity.
Fig.8.1 axial nonuniformity for the last muon chamber superlayer.

Fig.9 Distribution of the magnetic field along the muon tracks at the different θ angles.
Fig.9.1 θ= 90 grad.
Fig.9.2 θ= 29.60 grad
Fig.9.3 θ= 17.01 grad
Fig.9.4 θ= 9.75 grad
Fig.9.5 θ= 9.45 grad

Fig.10 Distribution and integral Bzdl of the magnetic field along the muon tracks at the different θ angles.

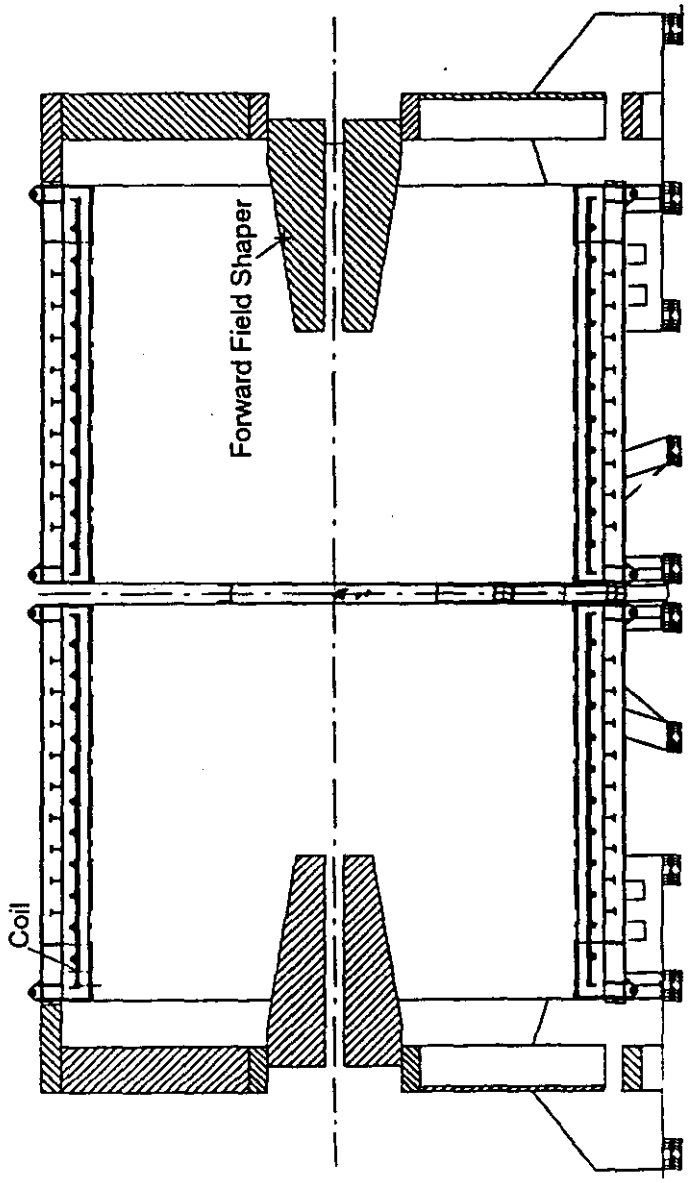

Fig.1

GEM DETECTOR PARAMETERS
BASELINE 2

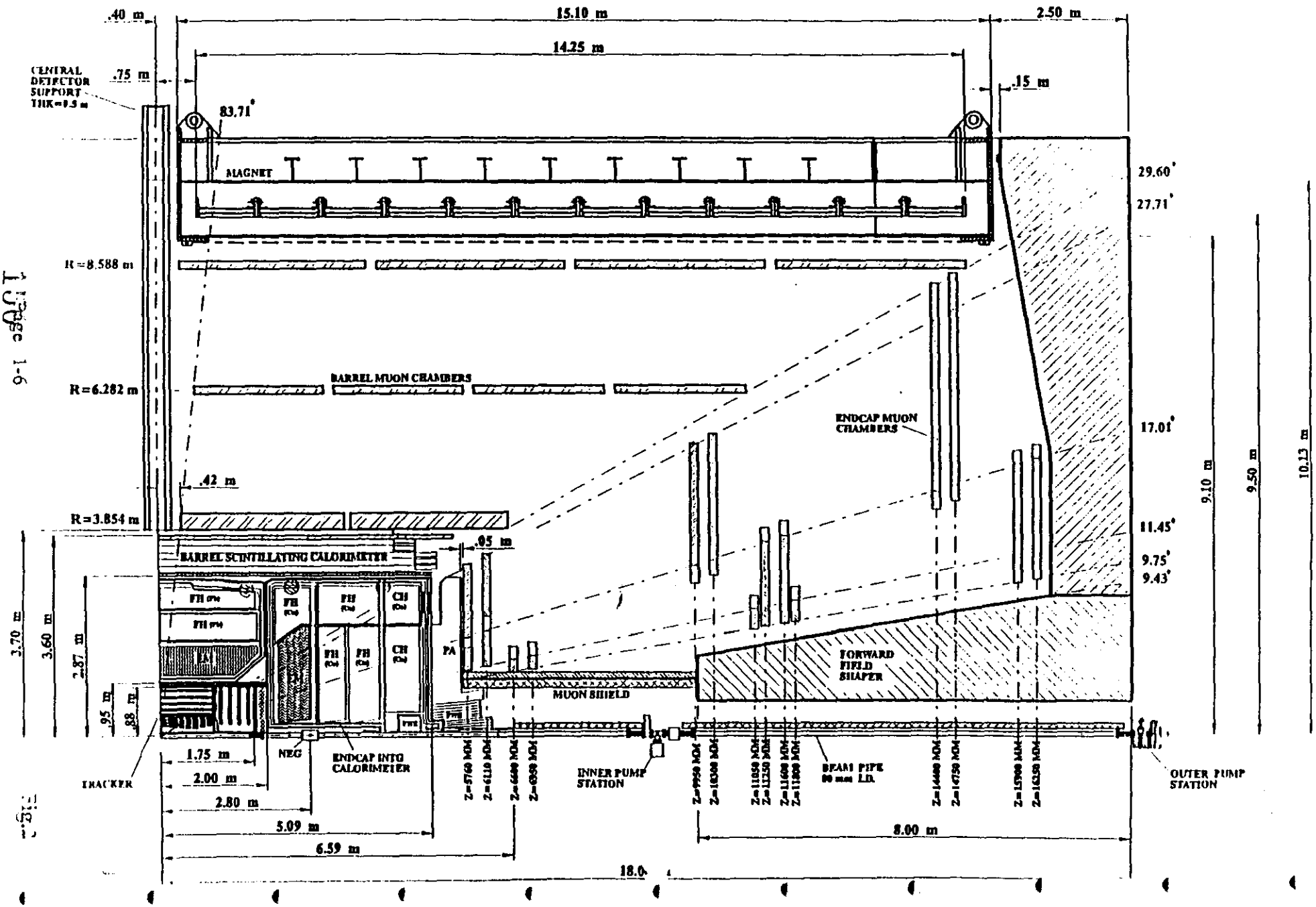

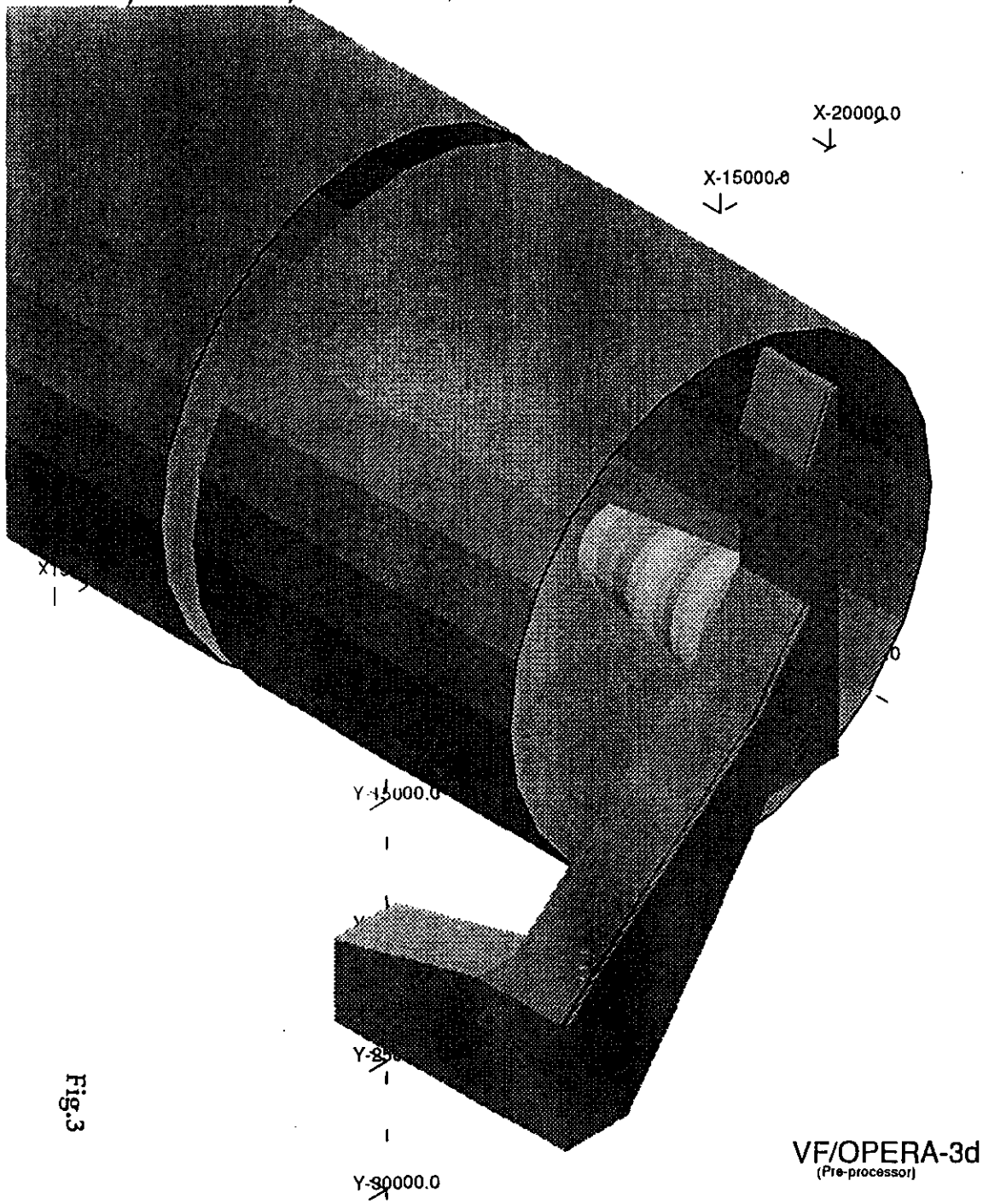

Fig.3

a.pic
27/Jul/93 15:51:21 Page 92 : hist comp=bz

Timofeev S.

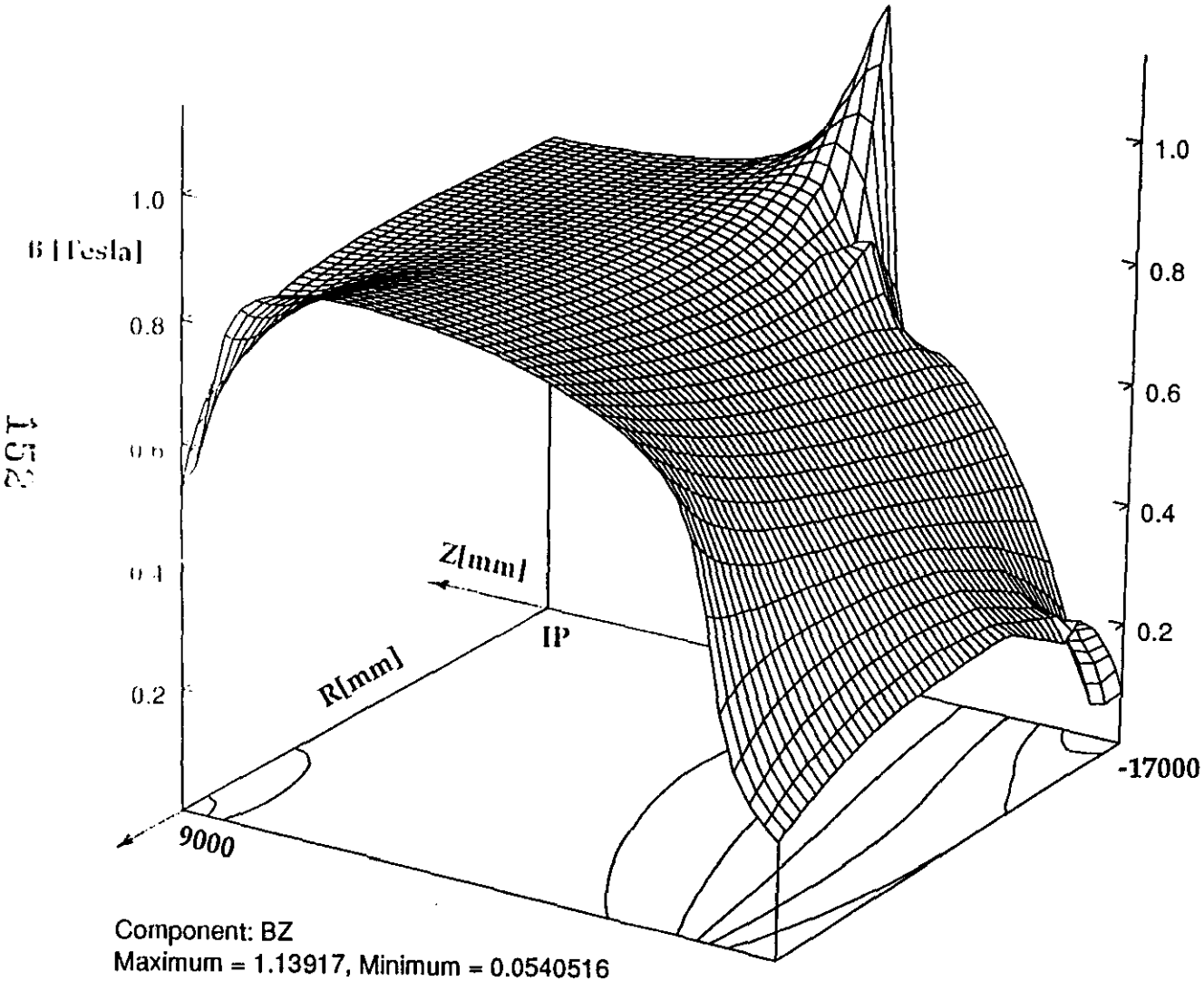

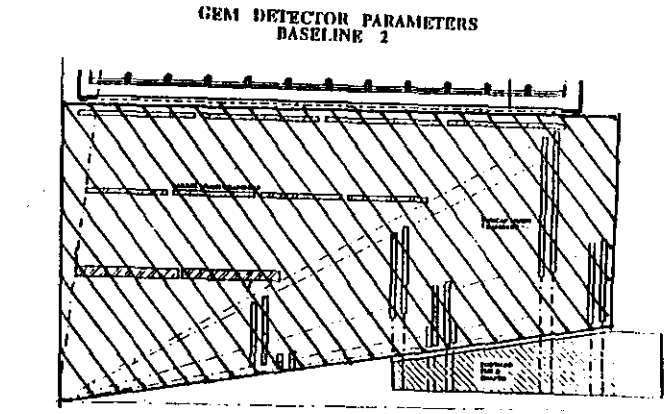

VF/OPERA-3d
(Post-processor)

Fig.4.1

a.pic
27/Jul/93 15:51:08 Page 91 : hist

Timofeev S.

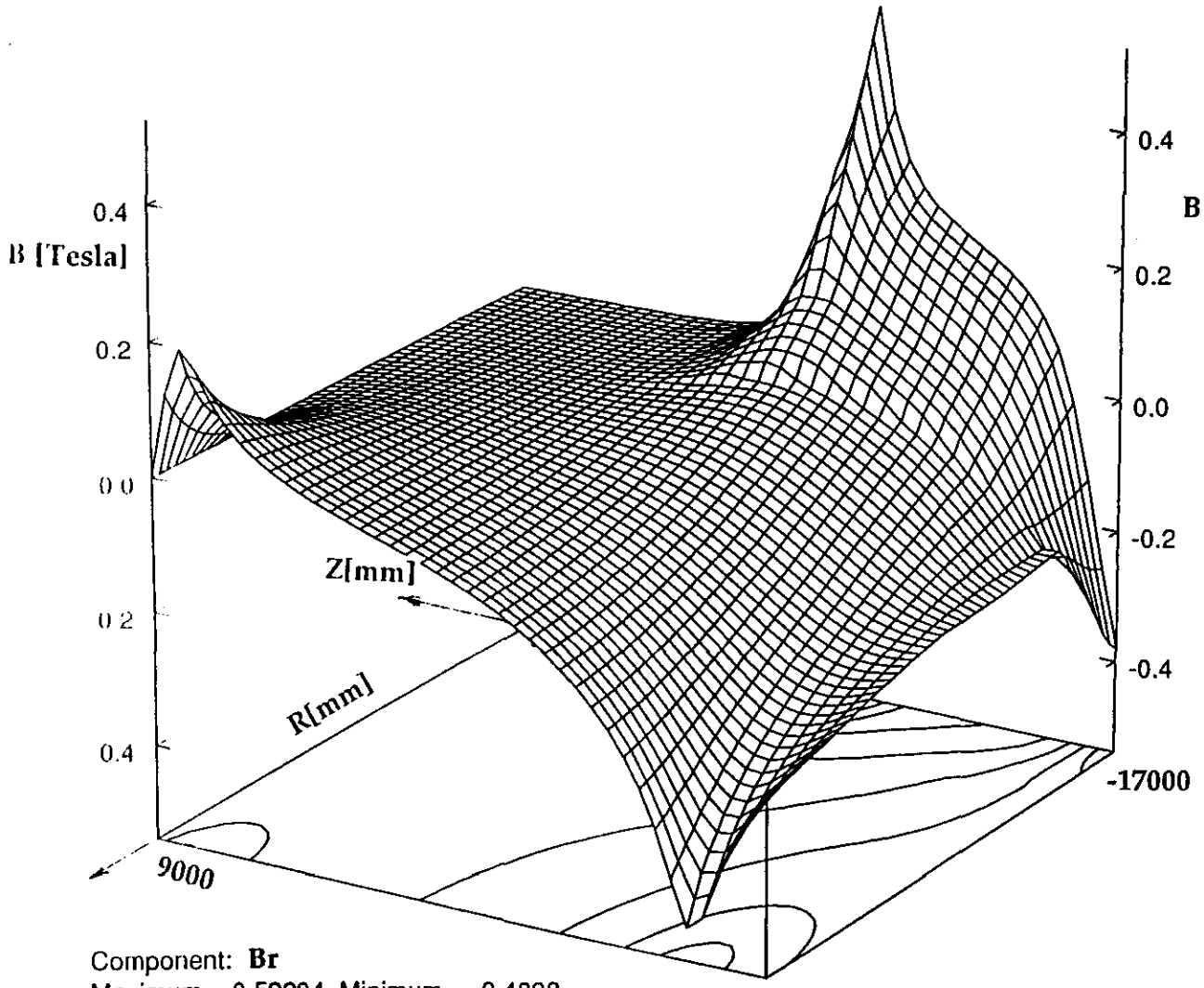

Component: **Br**
Maximum = 0.52234, Minimum = -0.4898
Integral = -3606425.0

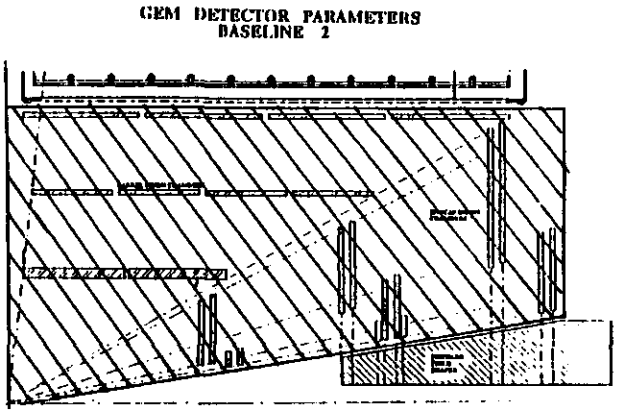

VF/OPERA-3d
(Post-processor)

Fig.4.2

z0.pic
27/Jul/93 15:05:12 Page 41 : plot comp=bz

Timofeev S.

Z=0 mm

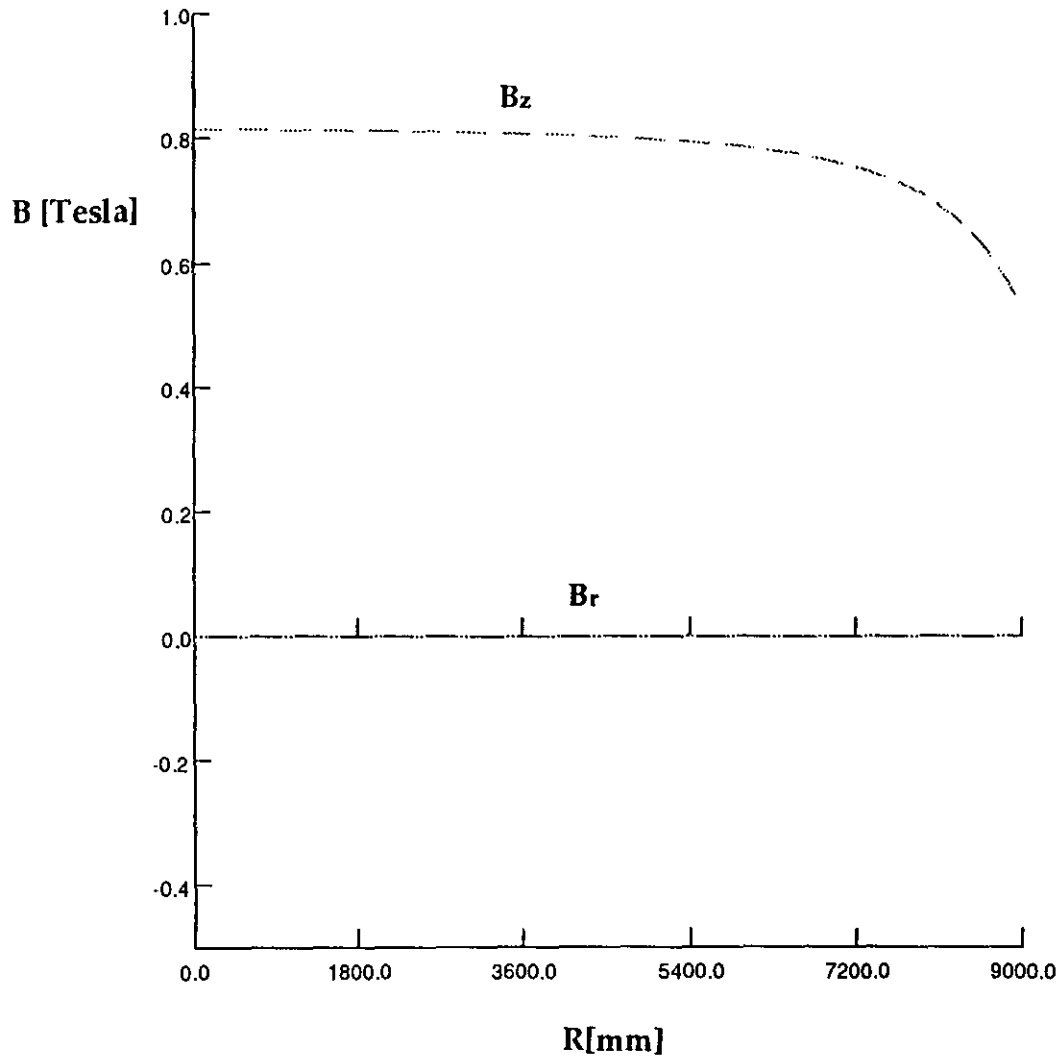

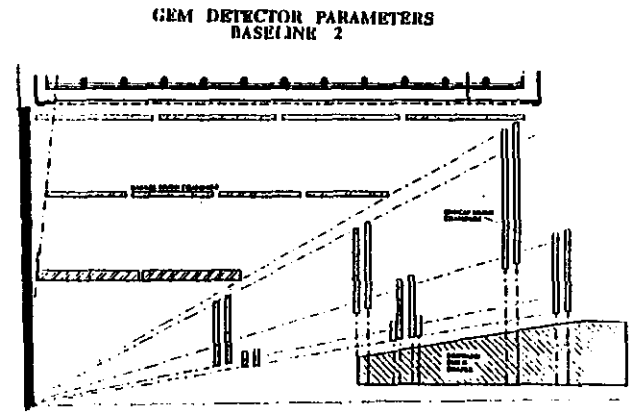

VF/OPERA-3d
(Post-processor)

Fig.5.1

z5760.plc
27/Jul/93 15:07:08 Page 44 : plot comp=bz

Timofeev S.

Z=-5760 mm

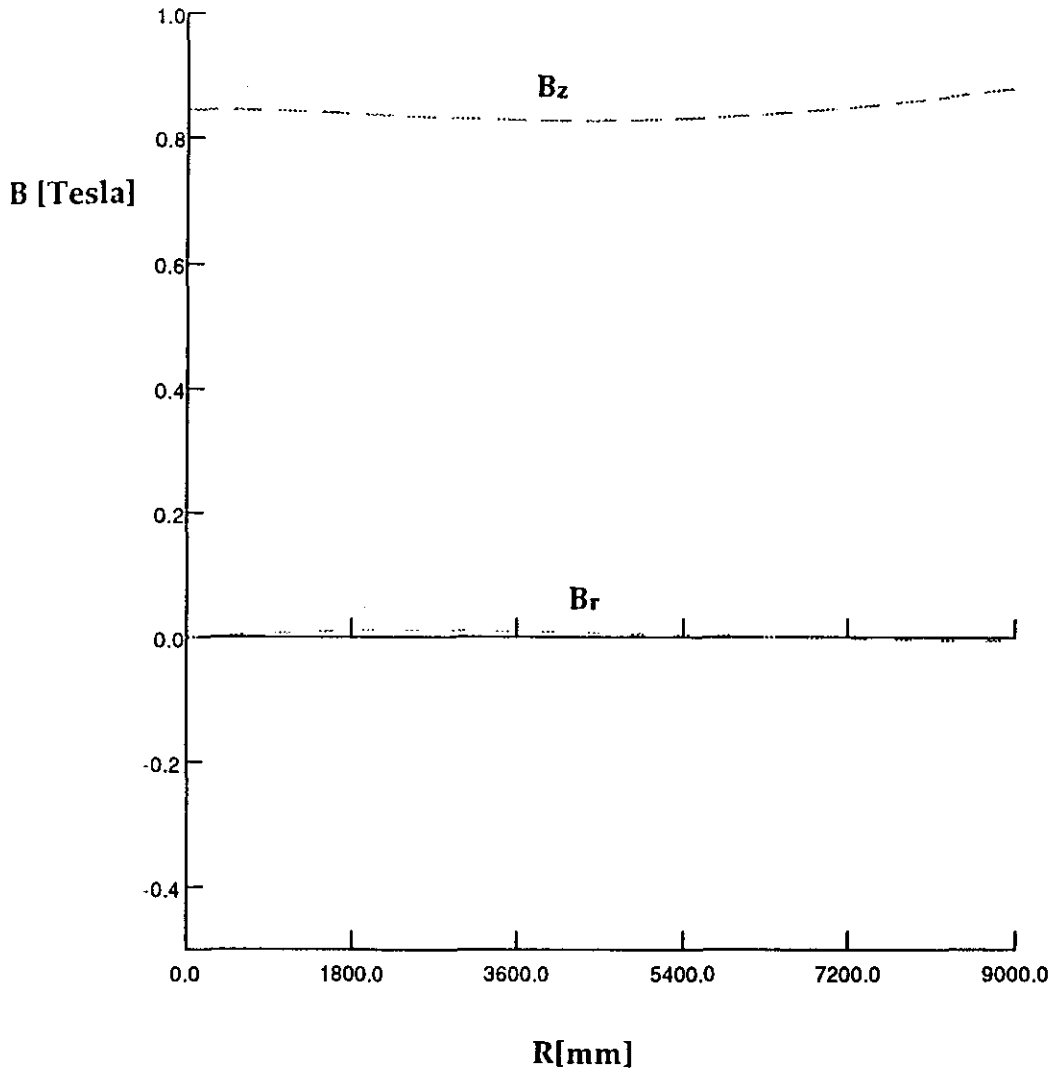

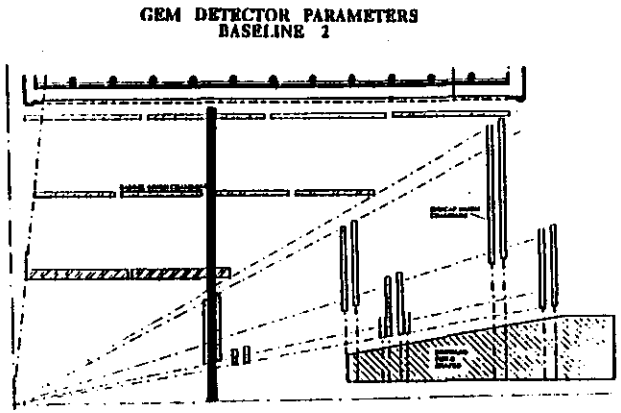

VF/OPERA-3d
(Post-processor)

Fig.5.2

z9950.pic
27/Jul/93 15:14:58 Page 53 : plot comp=bz

Timofeev S.

Z=-9950 mm

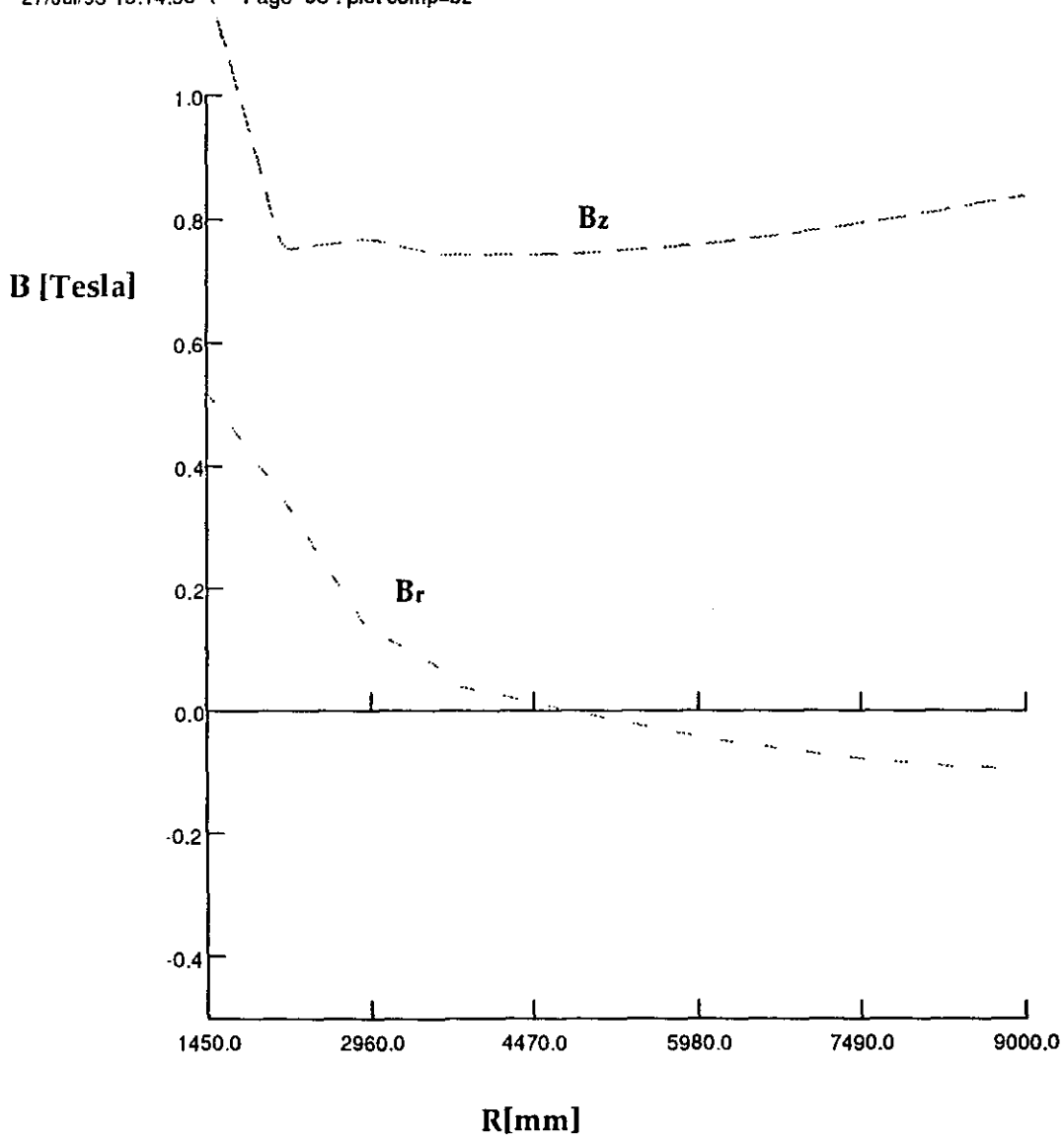

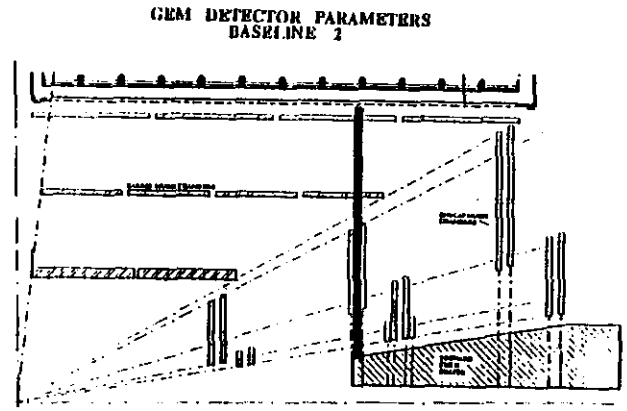

VF/OPERA-3d
(Post-processor)

Fig.5.3

z11250.pic
27/Jul/93 15:18:30 Page 62 : plot

Z=-11250 mm

Timofeev S.

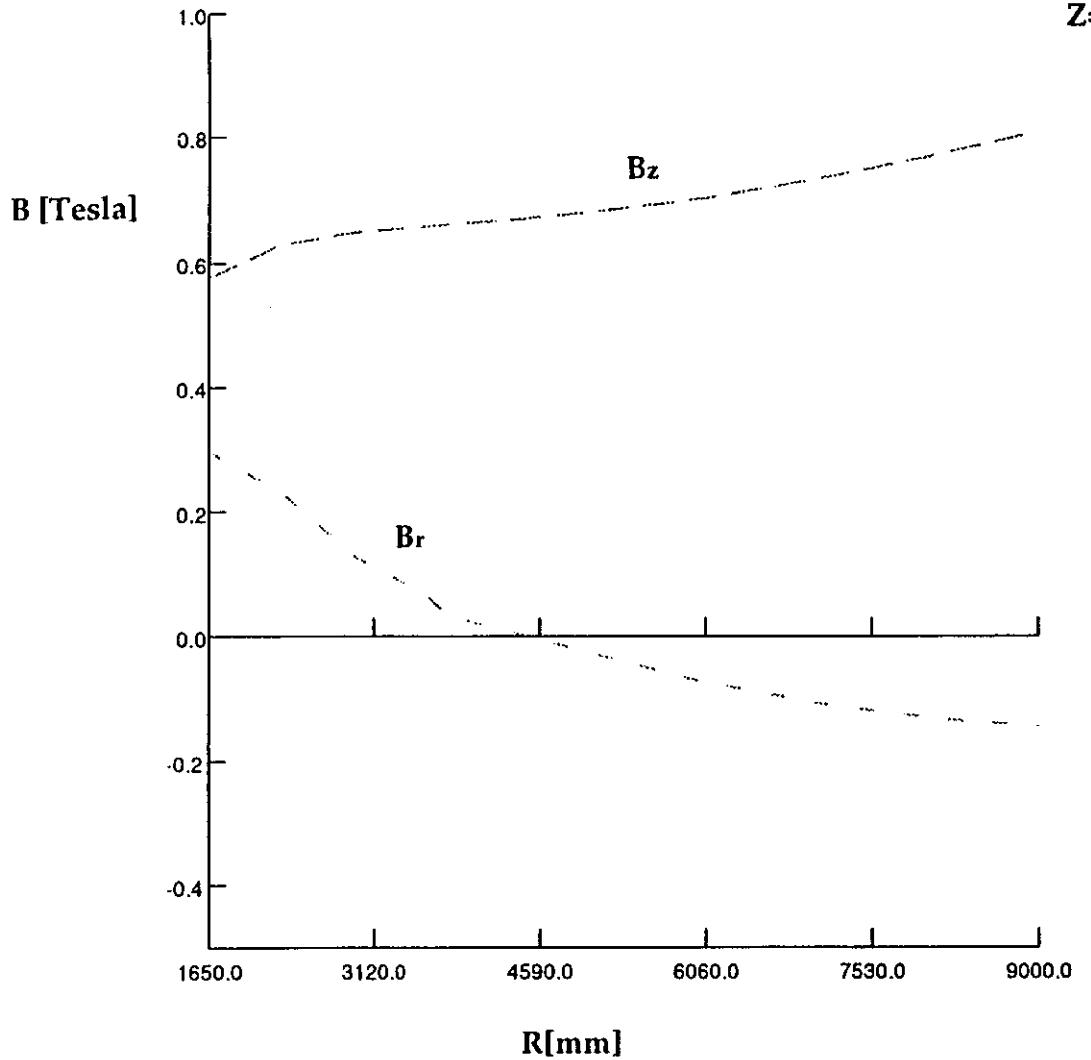

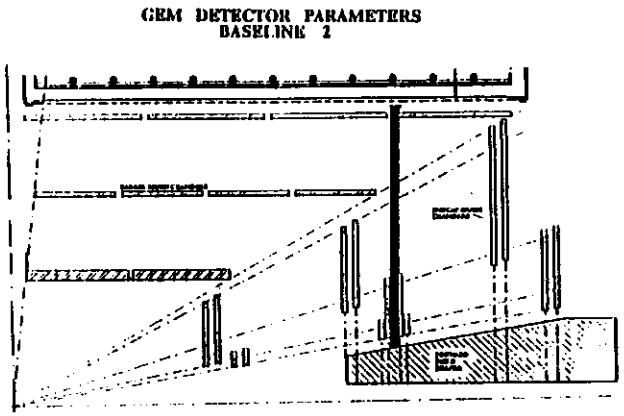

VF/OPERA-3d
(Post-processor)

Fig.5.4

z14750.pic
27/Jul/93 15:29:35 Page 71 : plot

Z=-14750 mm

Timofeev S.

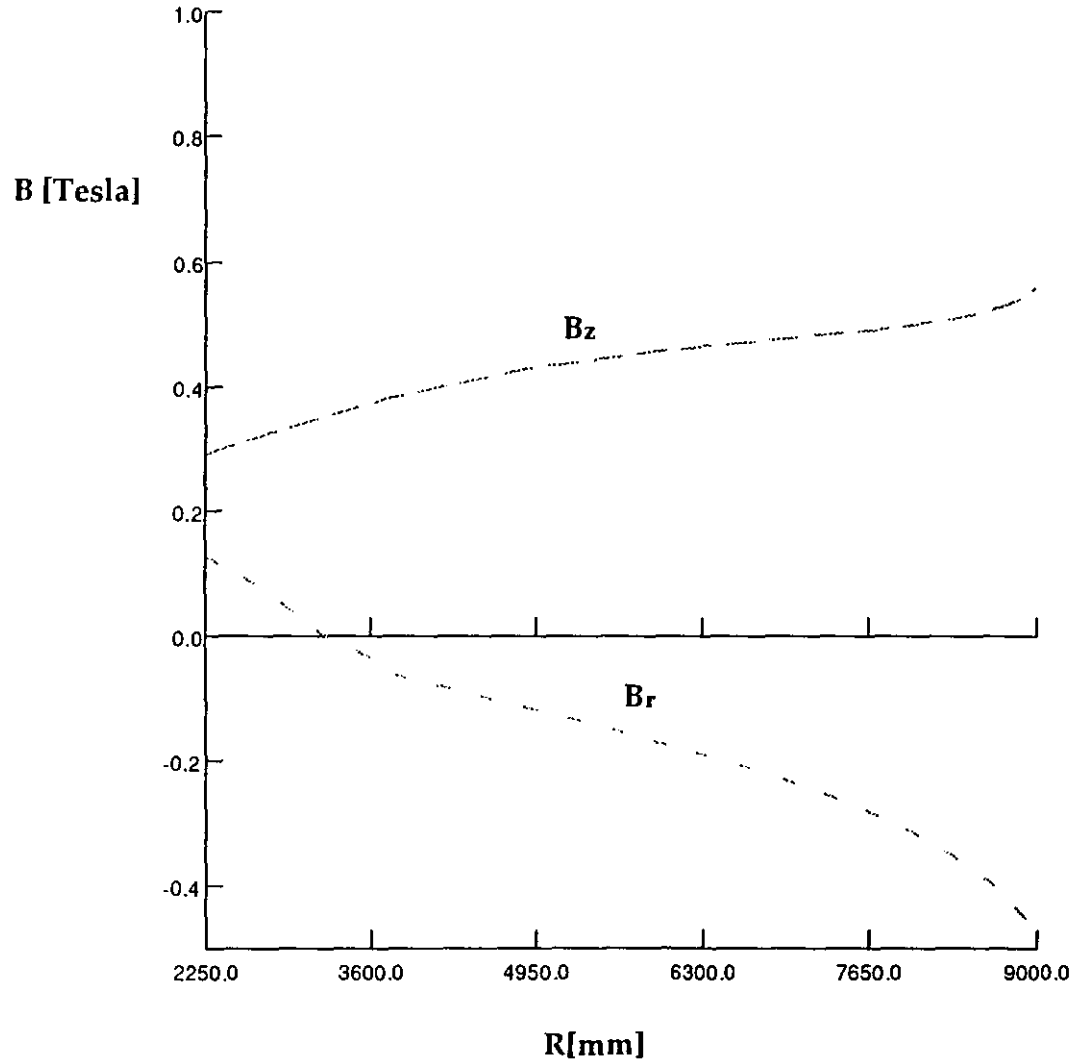

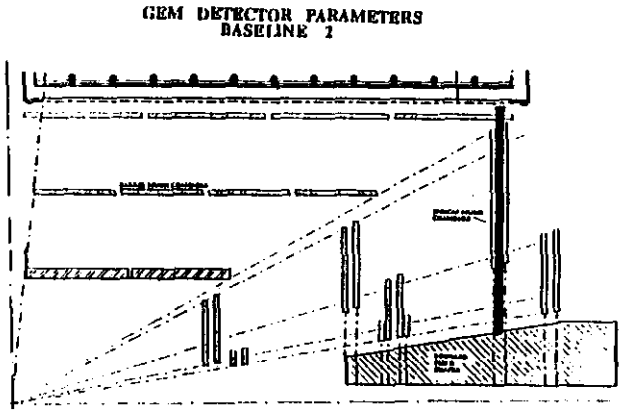

VF/OPERA-3d
(Post-processor)

Fig.5.5

z16250.pic
27/Jul/93 15:32:30 Page 79 : plot comp=bz

Timofeev S.

Z=-16250 mm

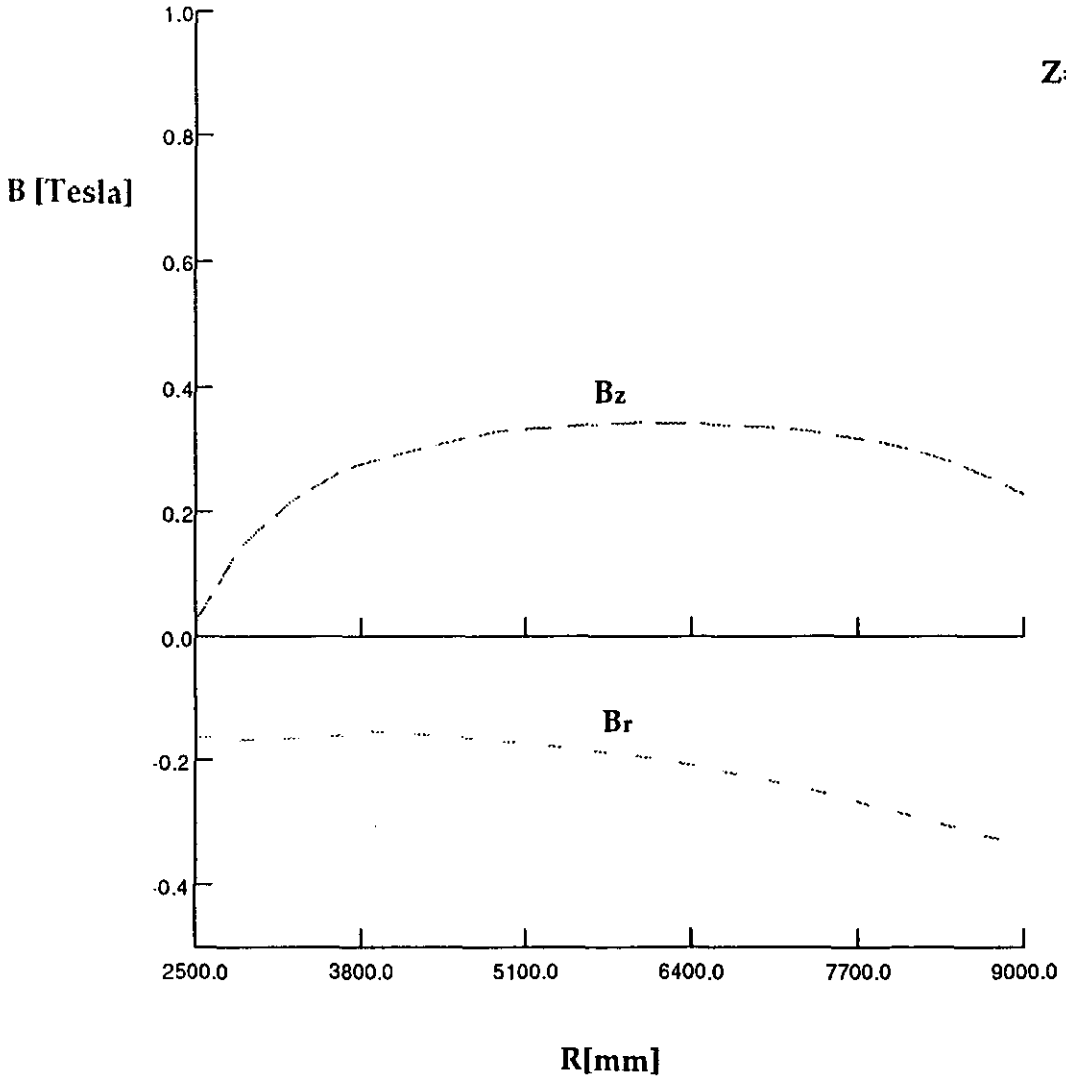

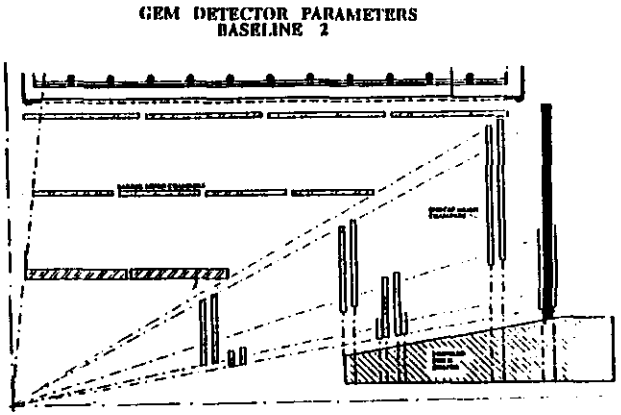

VF/OPERA-3d
(Post-processor)

Fig.5.6

r3854.pic
27/Jul/93 11:54:01 Page 35 : plot comp=bz

Timofeev S.

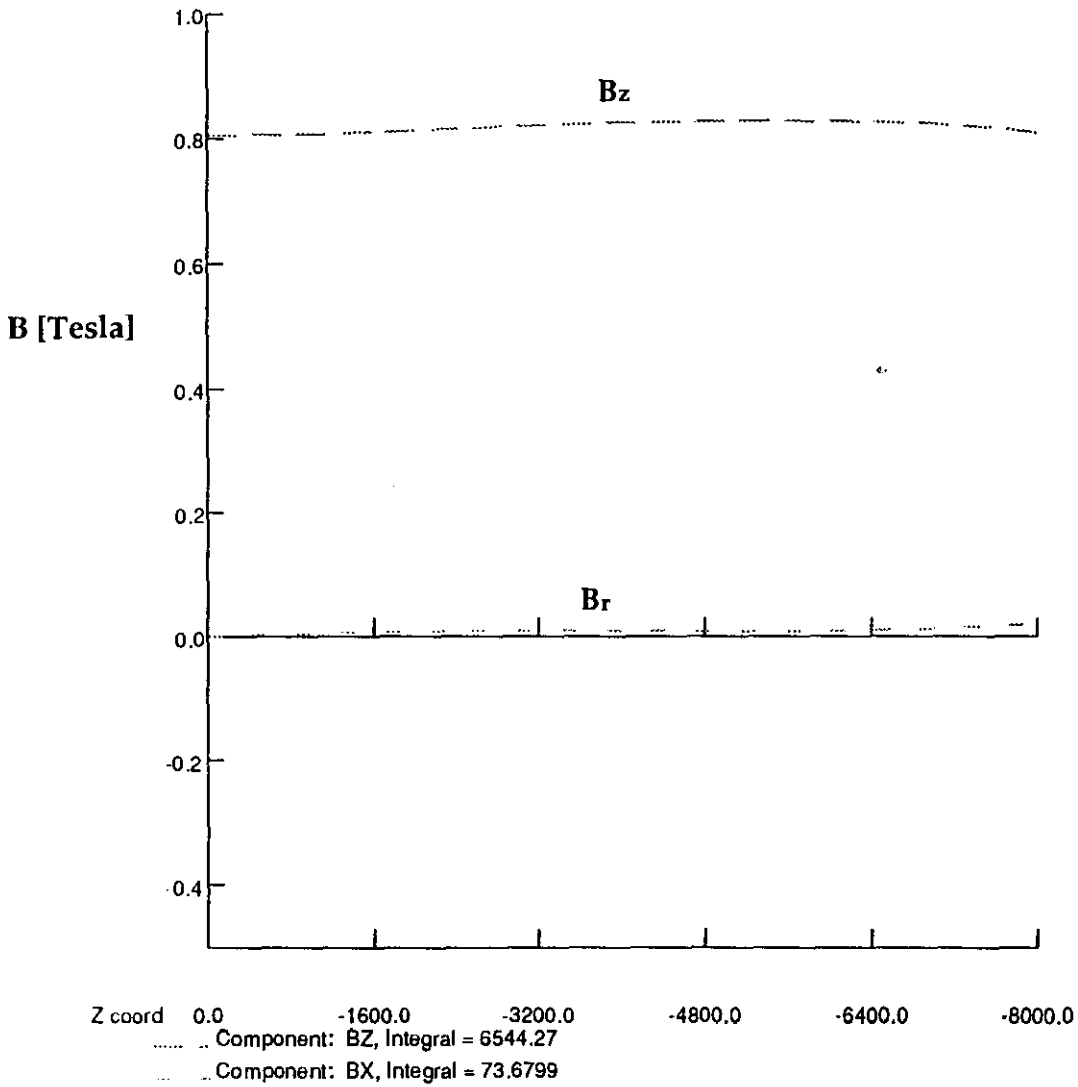

Barrel
R=3854 mm

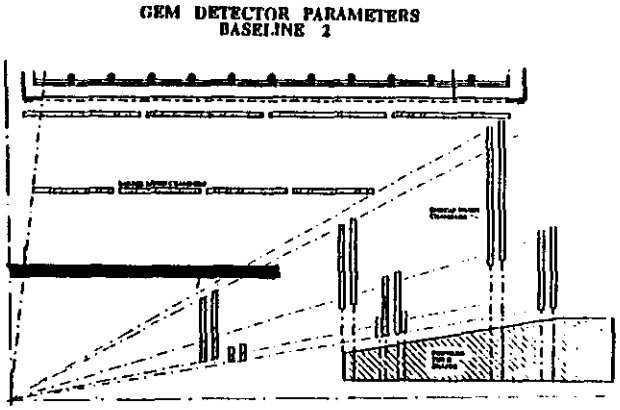

VF/OPERA-3d
(Post-processor)

Fig.6.1

r6282.pic
27/Jul/93 11:51:51 Page 32 : plot comp=bz

Timofeev S.

Barrel
R=6282 mm

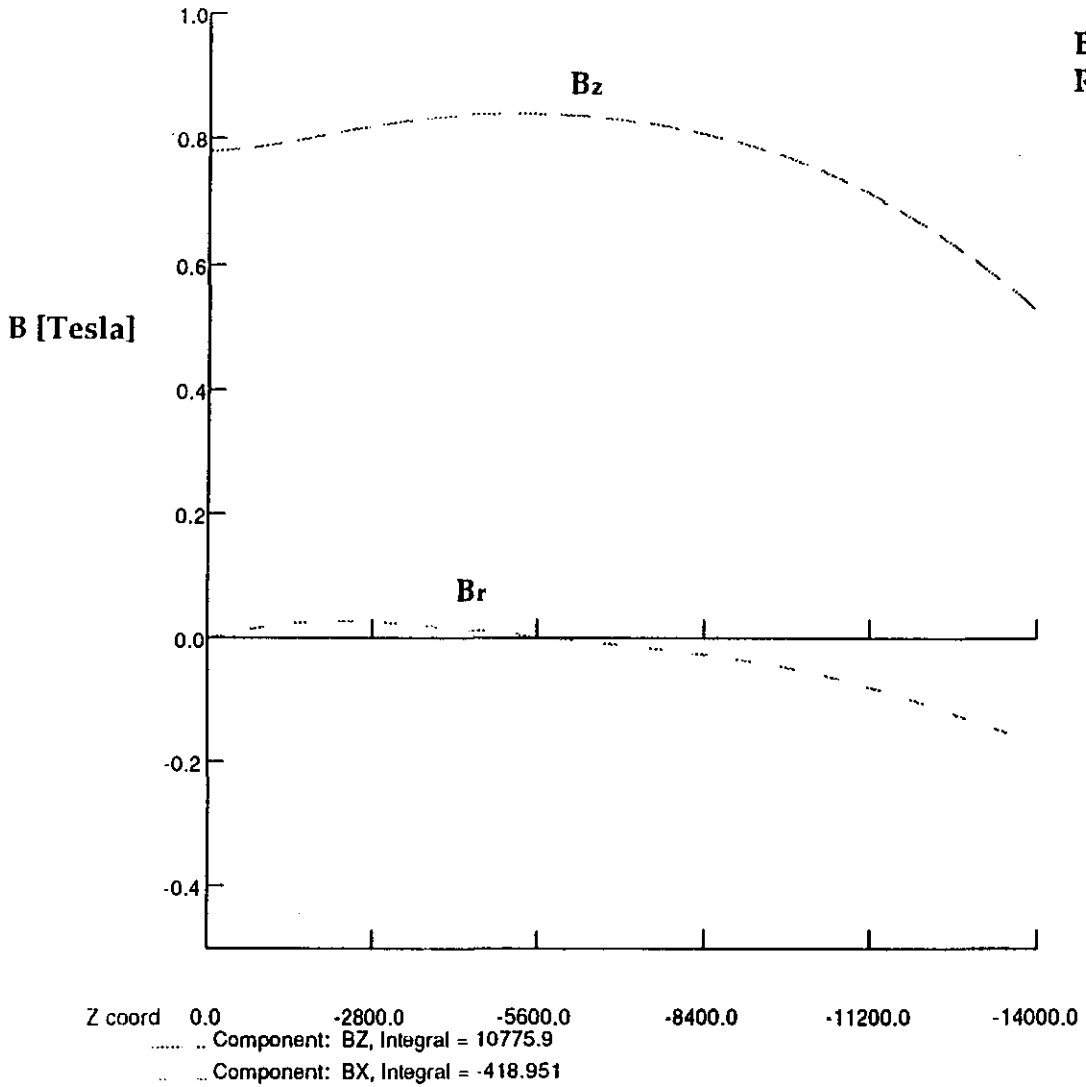

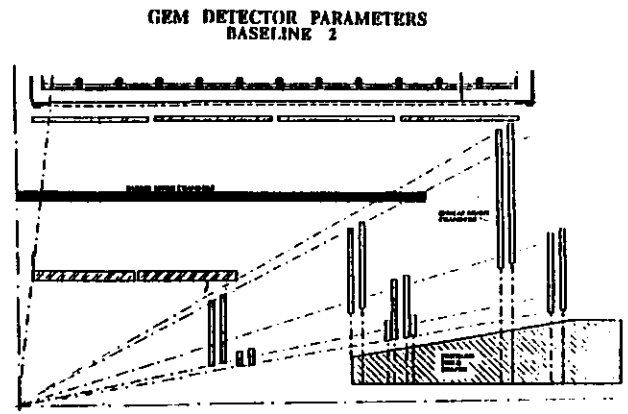

VF/OPERA-3d
(Post-processor)

Fig.6.2

r8588.pic
27/Jul/93 11:46:56 Page 29 : plot comp=bz

Timofeev S.

Barrel
R=8588 mm

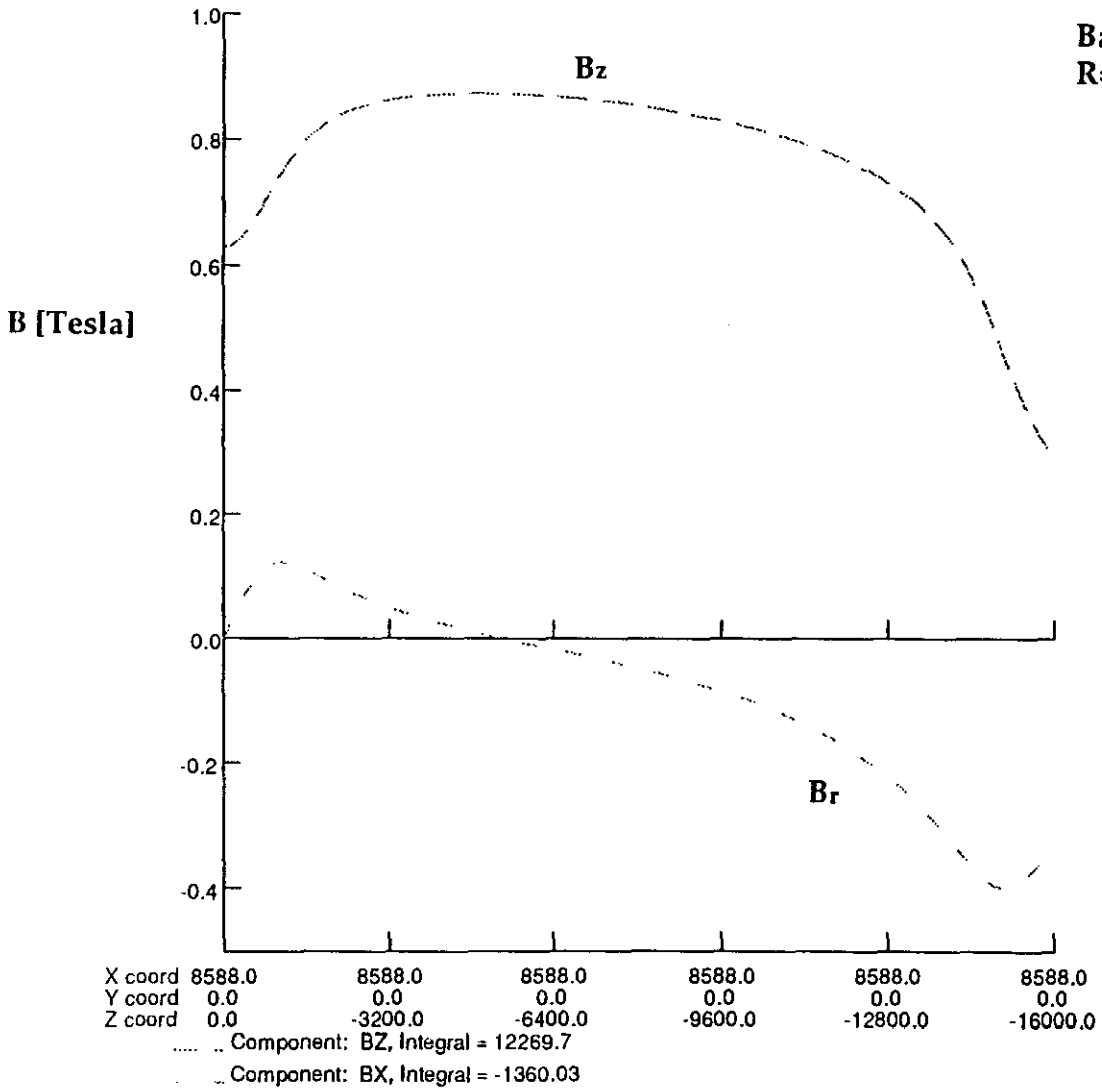

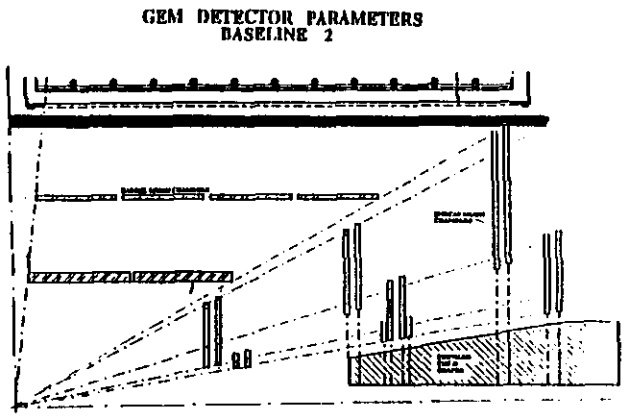

VF/OPERA-3d
(Post-processor)

Fig.6.3

z5760.plc
27/Jul/93 10:23:50 Page 6 : plot

Timofeev S.

Endcap
Z=-5760 mm

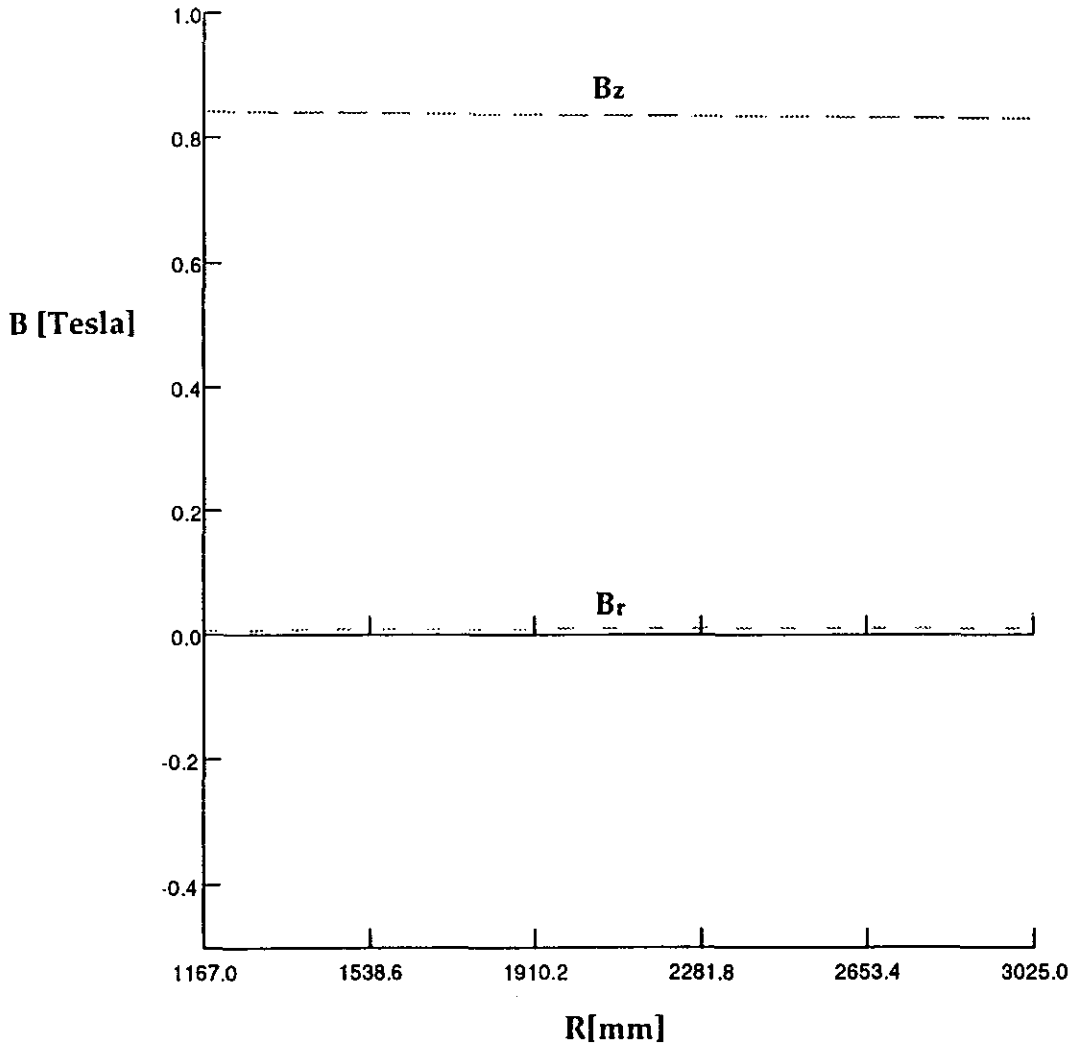

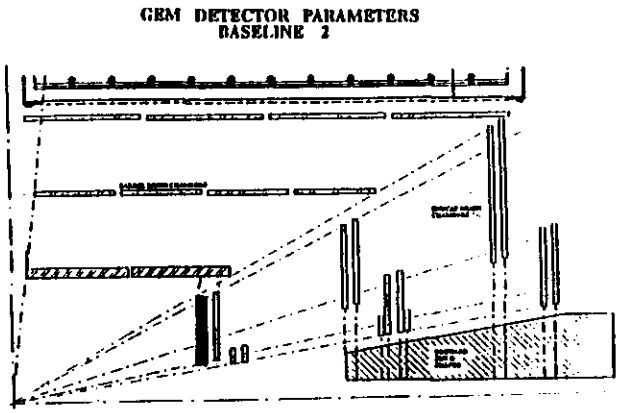

VF/OPERA-3d
(Post-processor)

Fig.7.1

z6600.pic
27/Jul/93 10:26:00 Page 9 : plot comp=bz

Timofeev S.

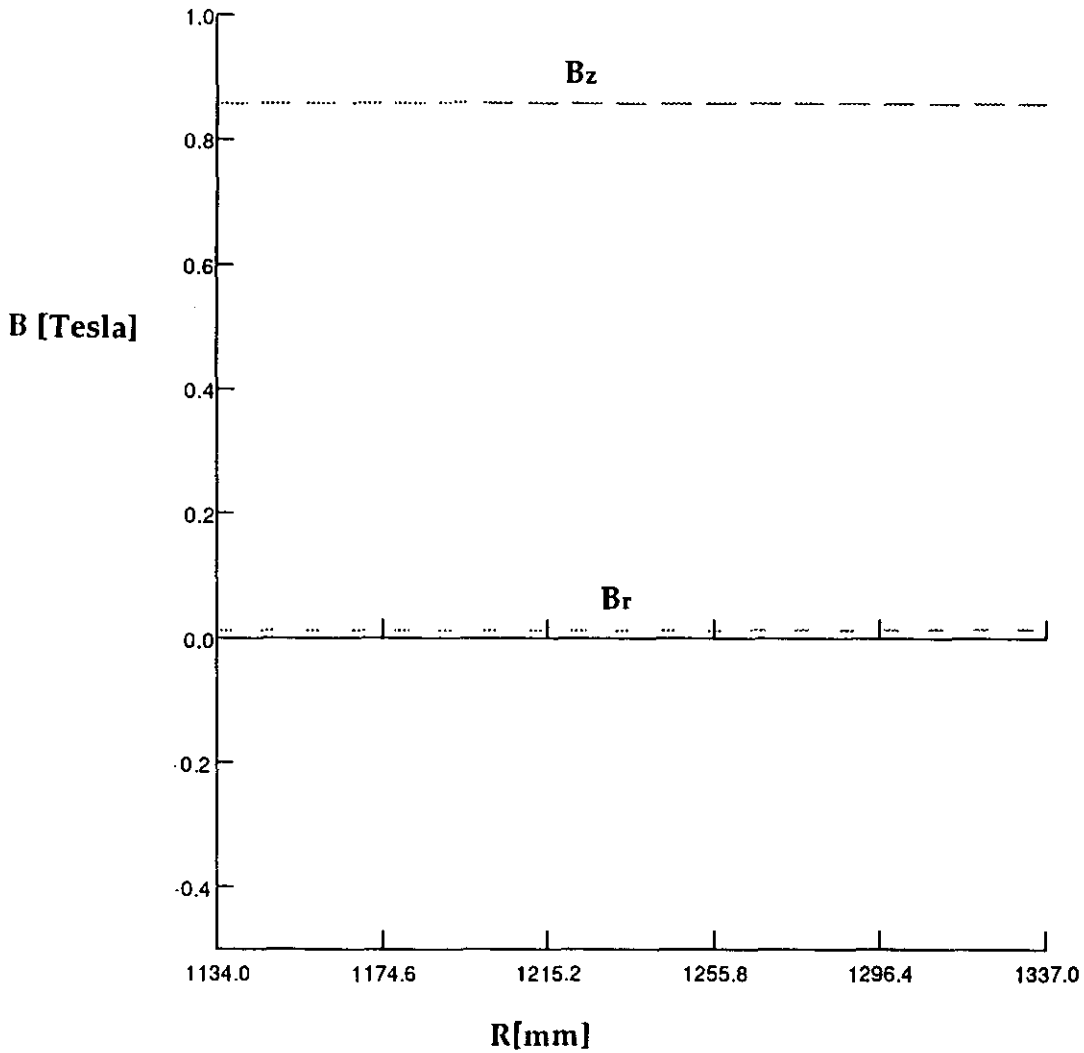

Endcap
Z=-6600 mm

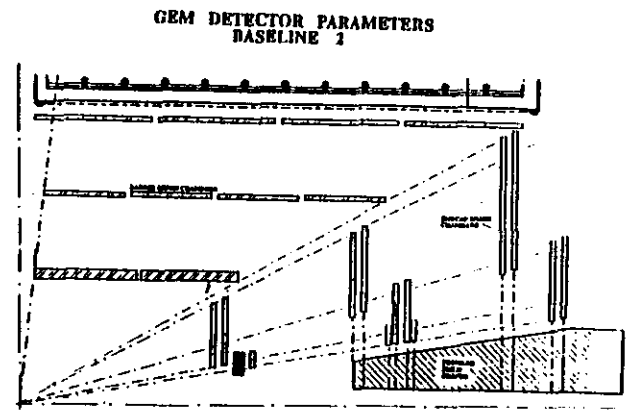

Fig.7.2

VF/OPERA-3d
(Post-processor)

z9950.pic
27/Jul/93 10:28:25 Page 12 : plot comp=bz

Timofeev S.

Endcap
Z=-9950 mm

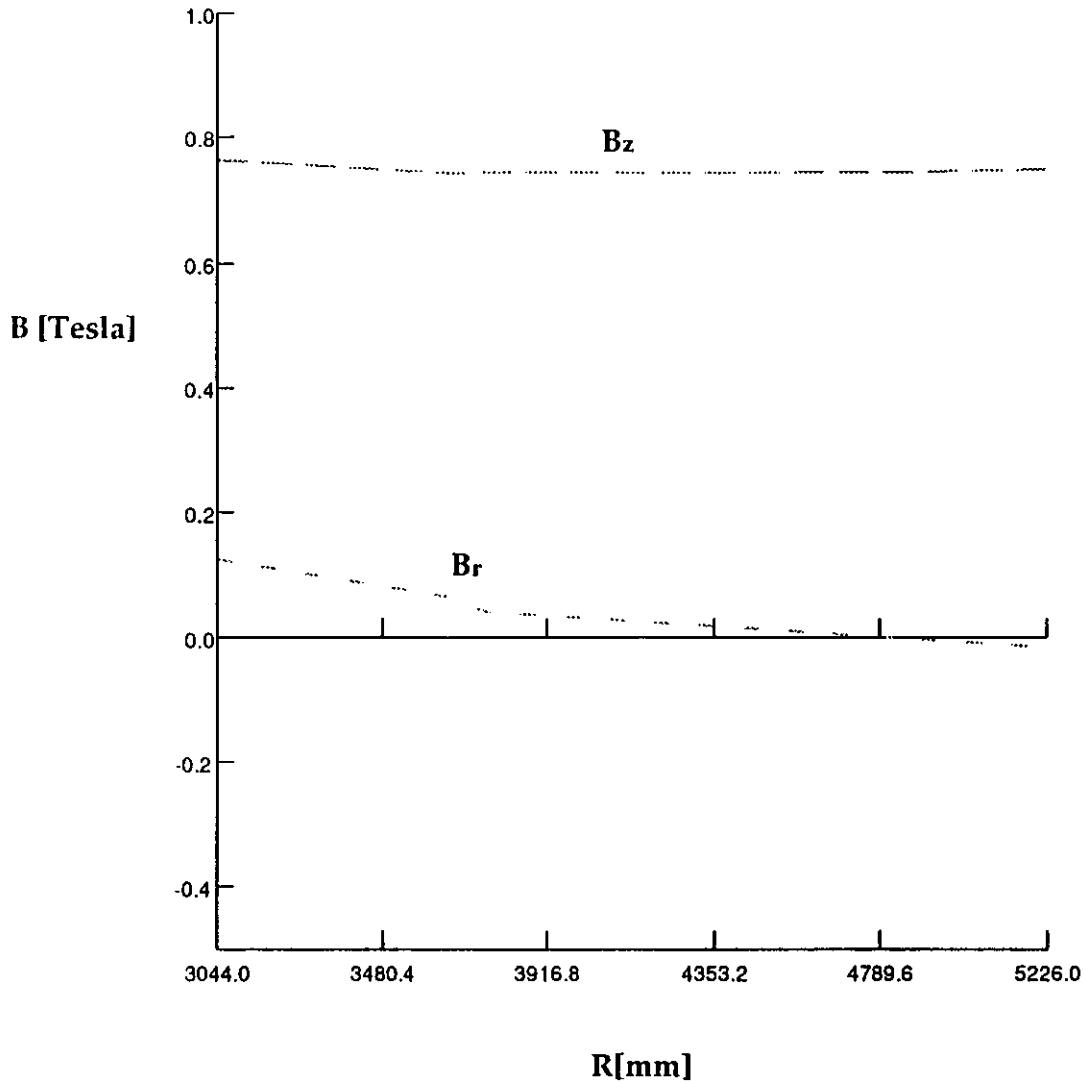

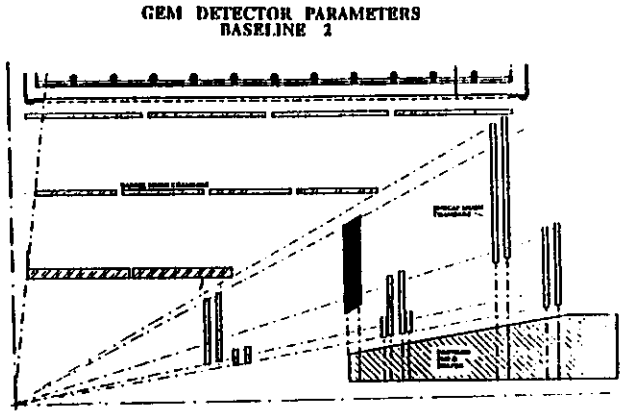

VF/OPERA-3d
(Post-processor)

Fig.7.3

z11250.pic
27/Jul/93 10:30:55 Page 15 : plot comp=bz

Timofeev S.

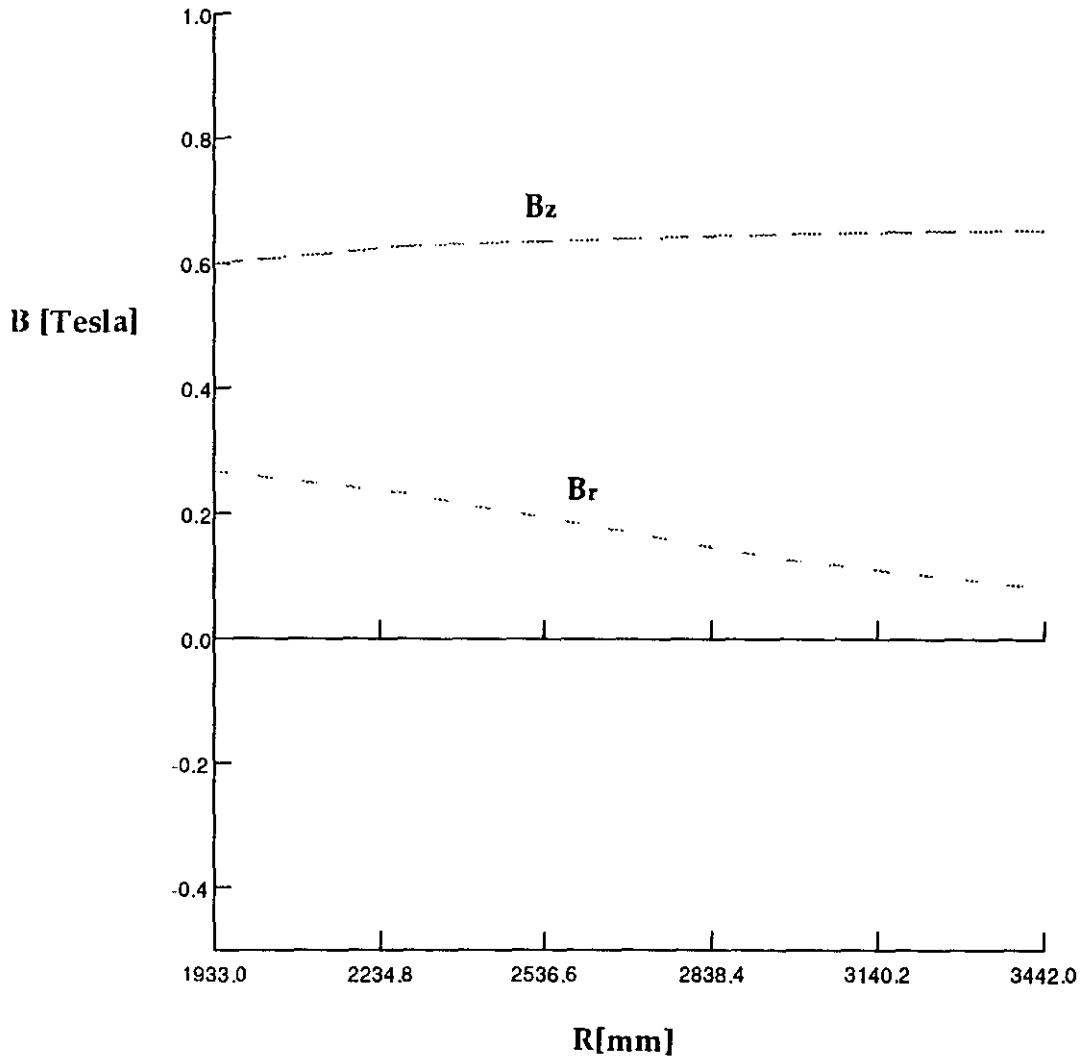

Endcap
Z=-11250 mm

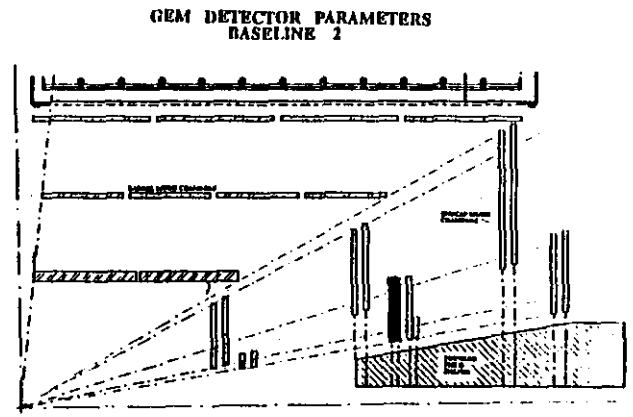

VF/OPERA-3d
(Post-processor)

Fig.7.4

z14750.pic
27/Jul/93 10:40:05 Page 18 : plot comp=bz

Timofeev S.

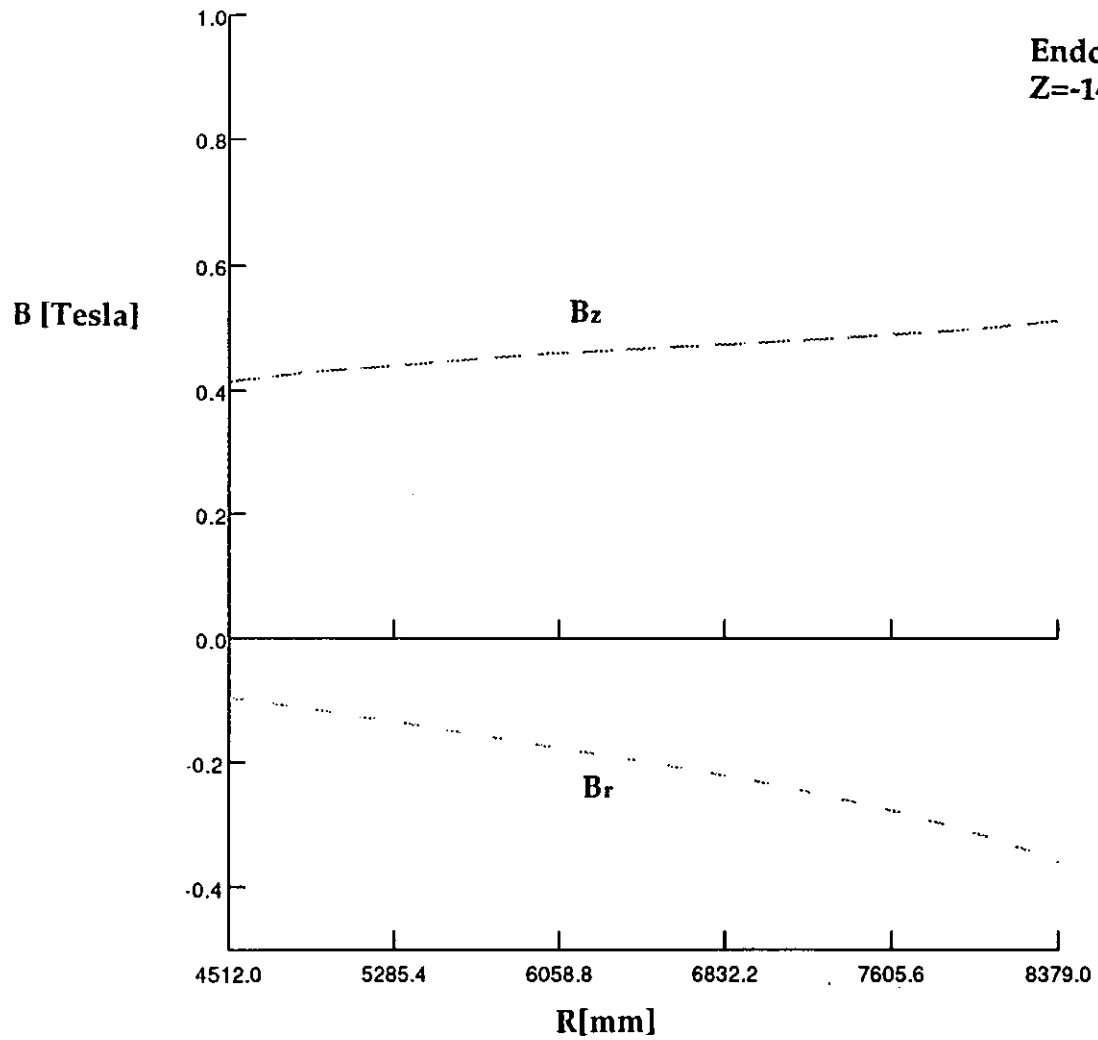

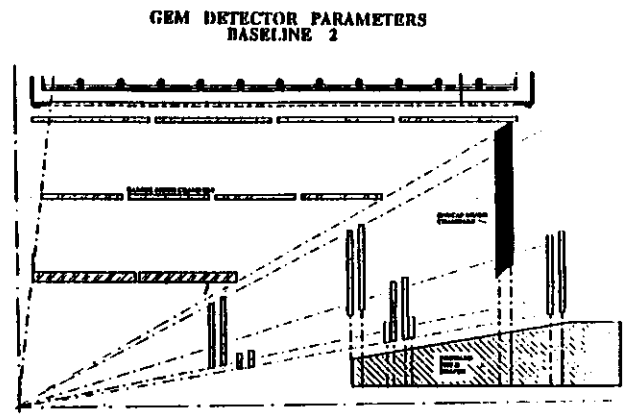

VF/OPERA-3d
(Post-processor)

Fig.7.5

z16250.pic
27/Jul/93 10:42:58 Page 21 : plot comp=bz

Timofeev S.

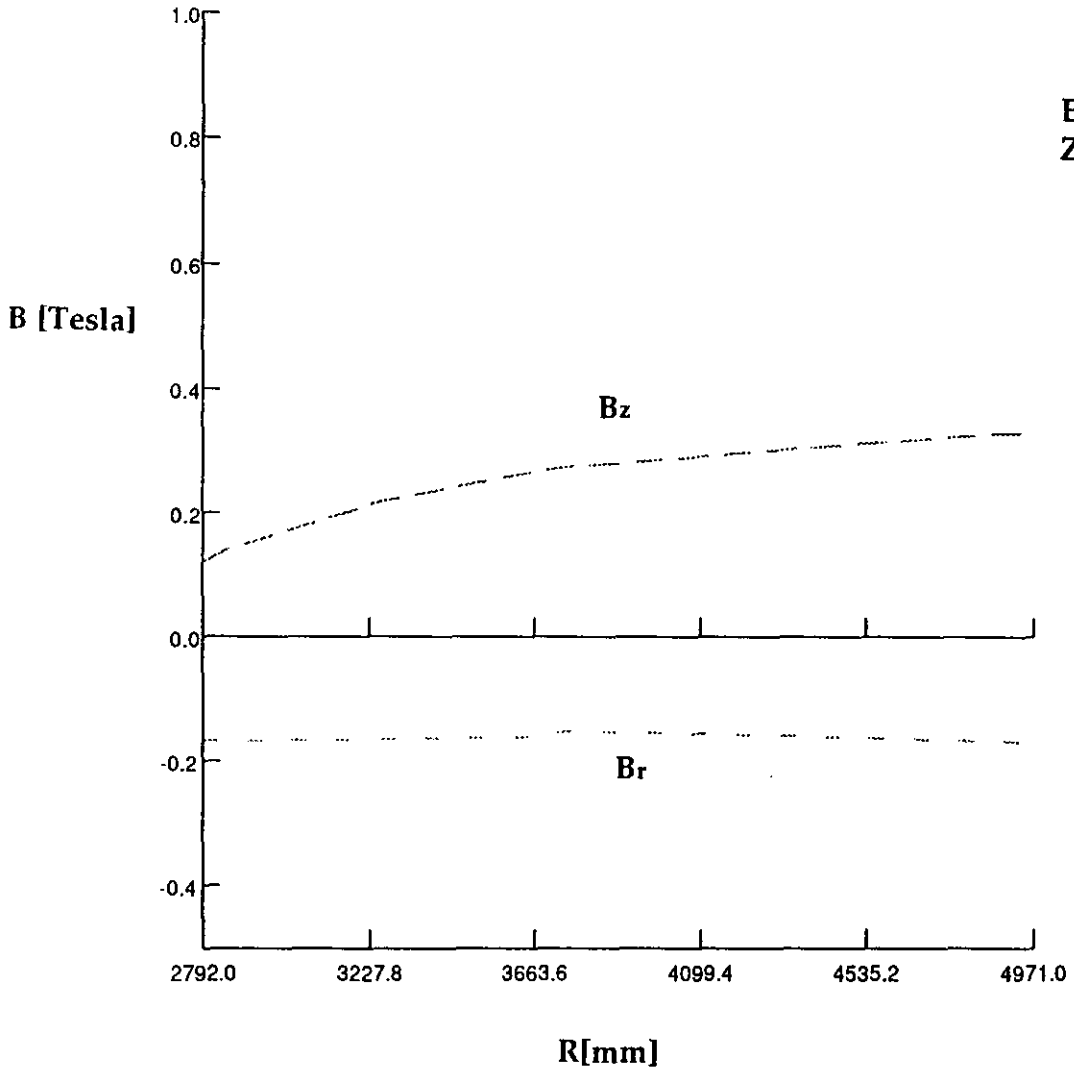

Endcap
Z=-16250 mm

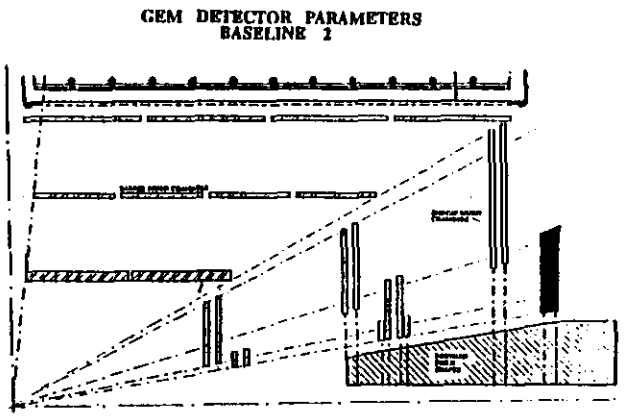

Fig.7.6

VF/OPERA-3d
(Post-processor)

a.pic
29/Jul/93 10:08:18 Page 7 : hist

Timofeev S.

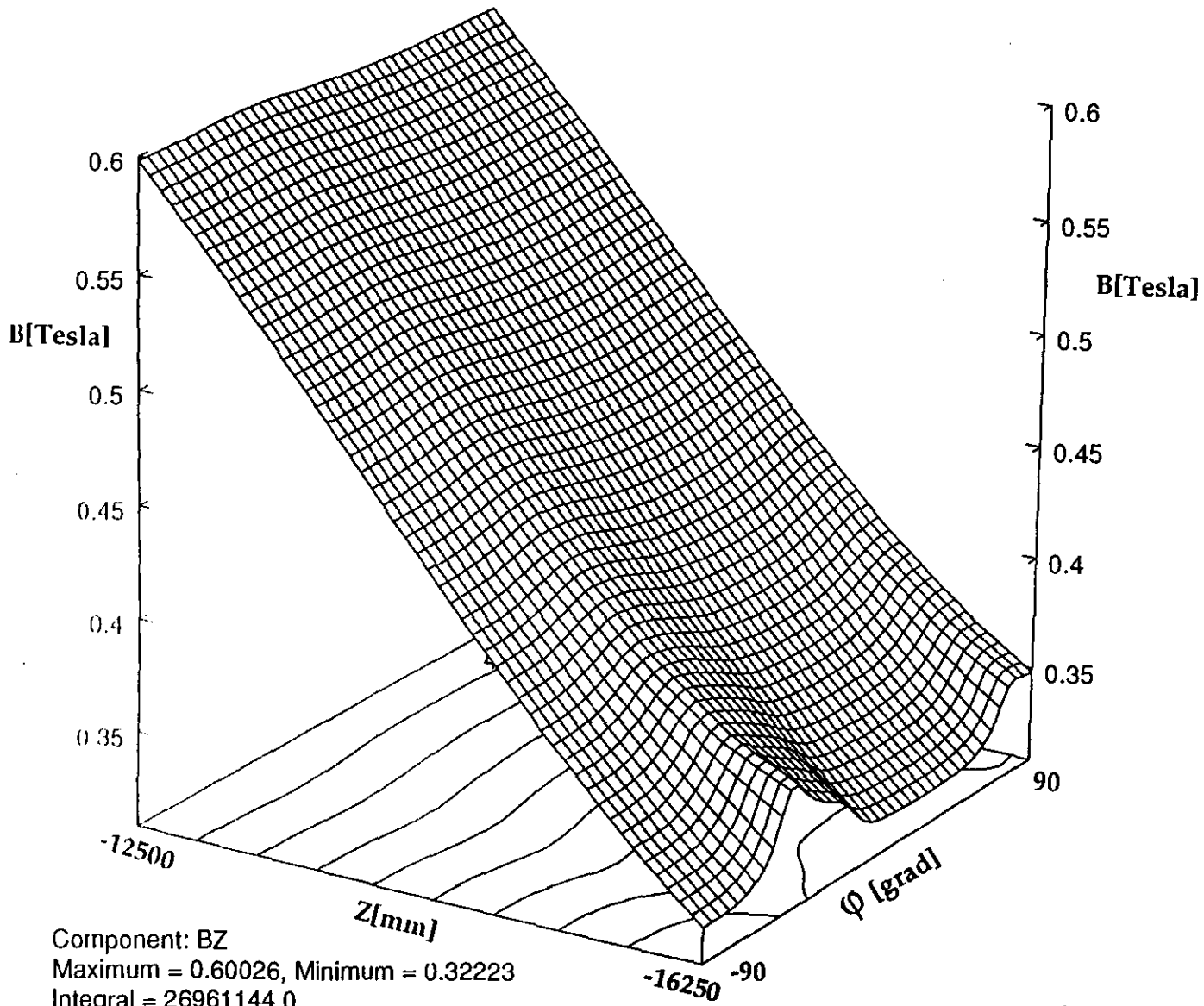

Component: BZ
Maximum = 0.60026, Minimum = 0.32223
Integral = 26961144.0

VF/OPERA-3d
(Post-processor)

Fig.8.1

axial.plc
29/Jul/93 10:13:29 Page 18 : plot

Timofeev S.

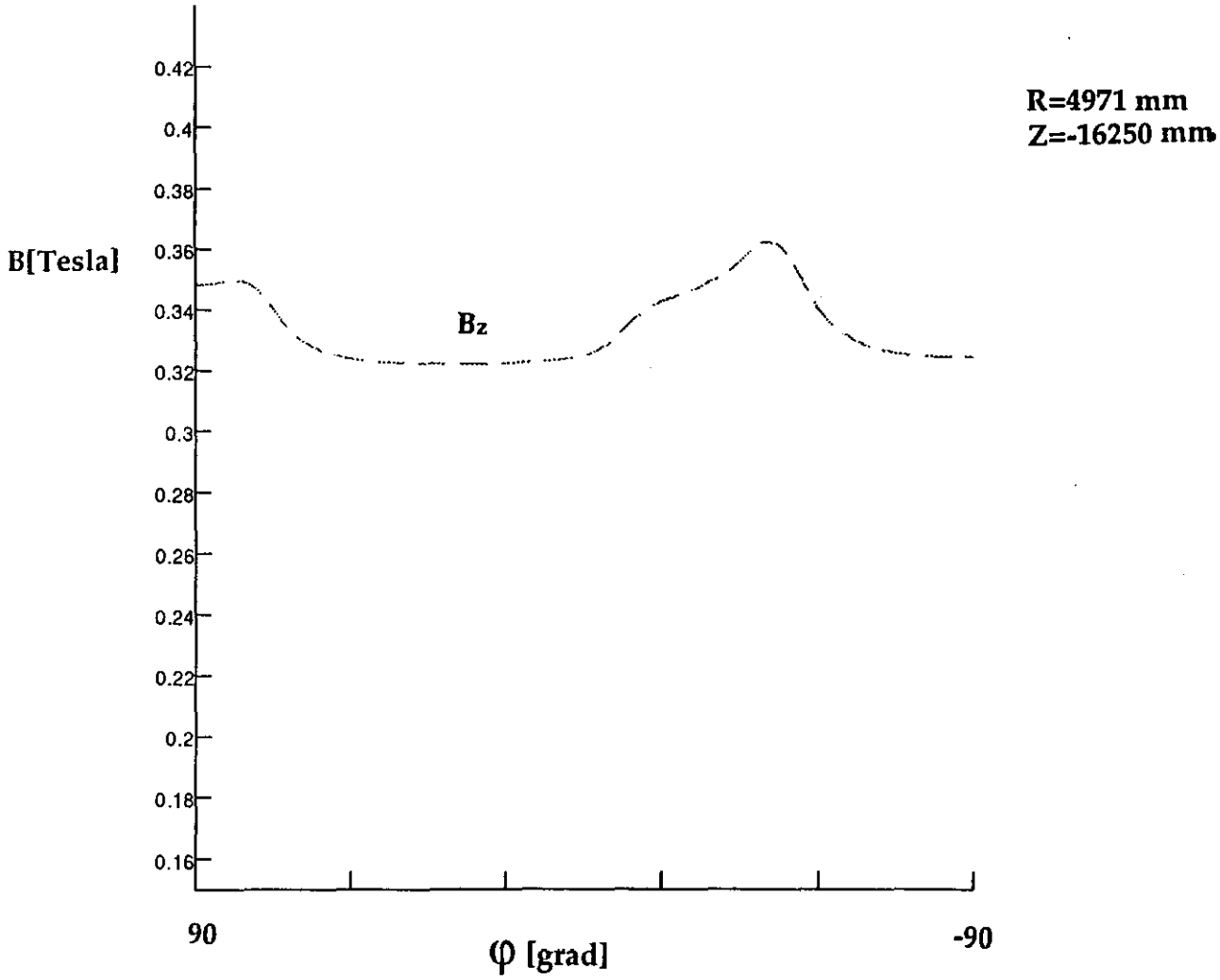

Fig.8.2

VF/OPERA-3d
(Post-processor)

thet90.pic
29/Jul/93 17:46:19 Page 53 : plot comp=bz

θ=90

Timofeev S.

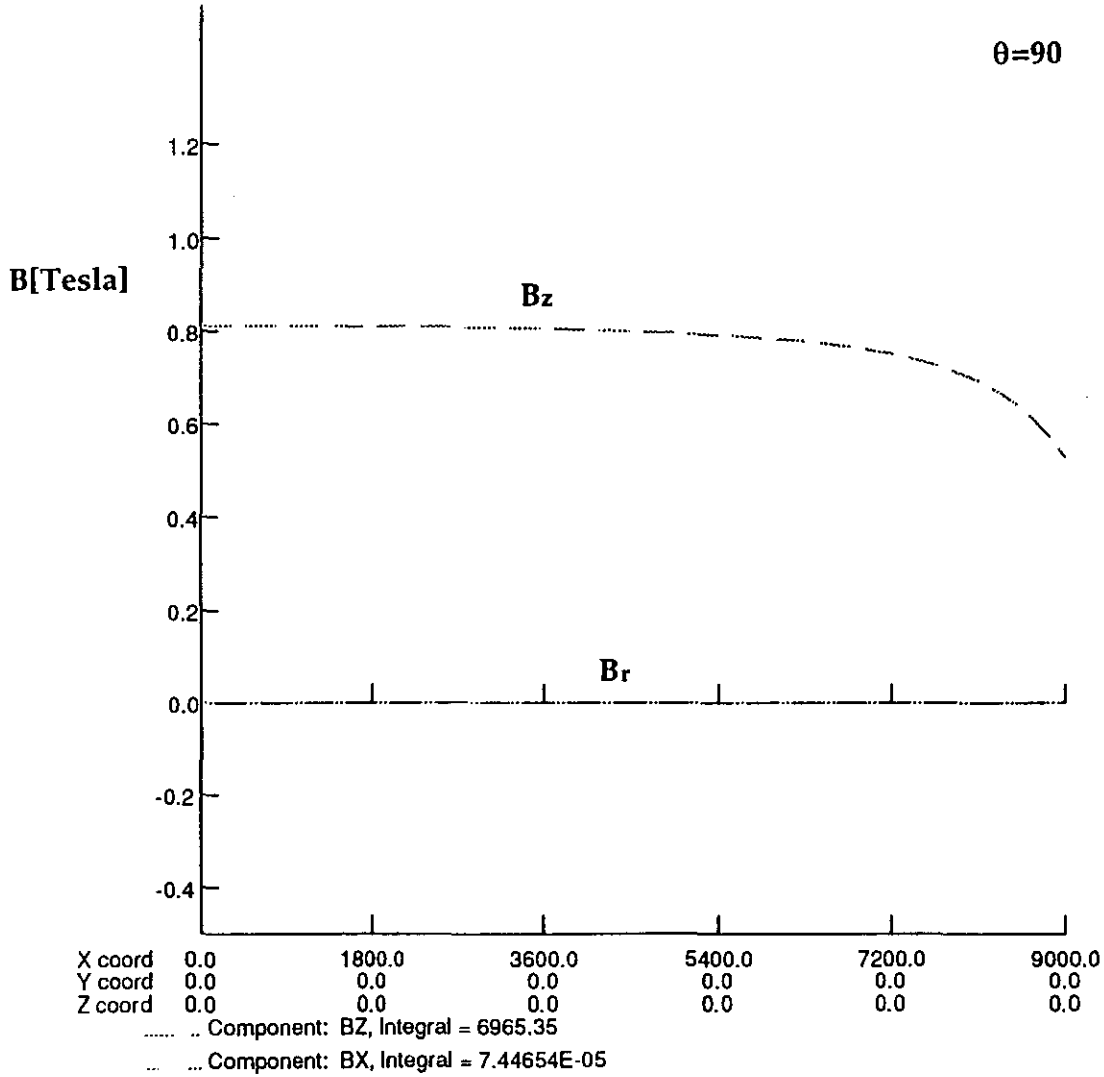

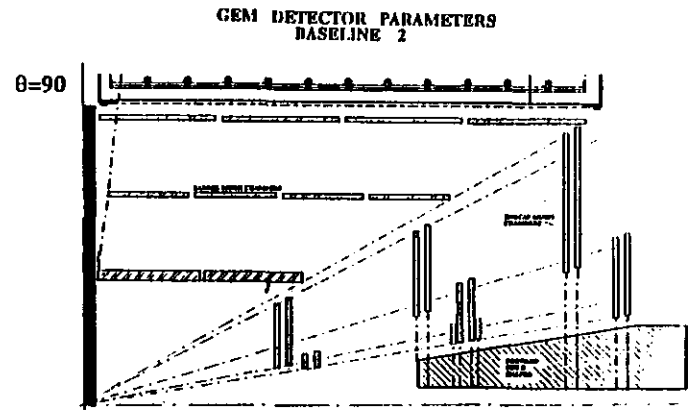

VF/OPERA-3d
(Post-processor)

Fig.9.1

thet29.pic
29/Jul/93 17:51:21 Page 56 : plot

θ=29.60

Timofeev S.

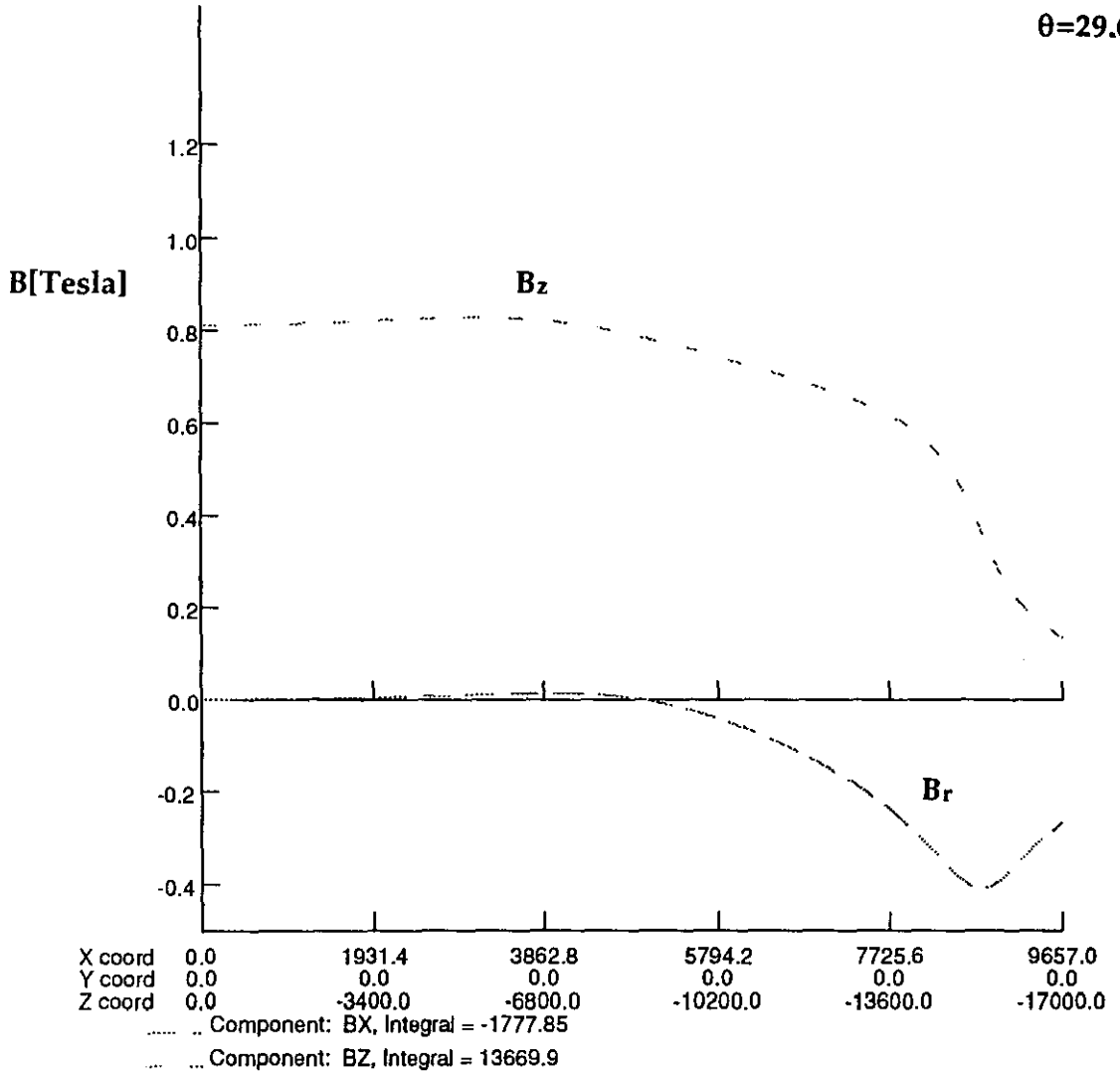

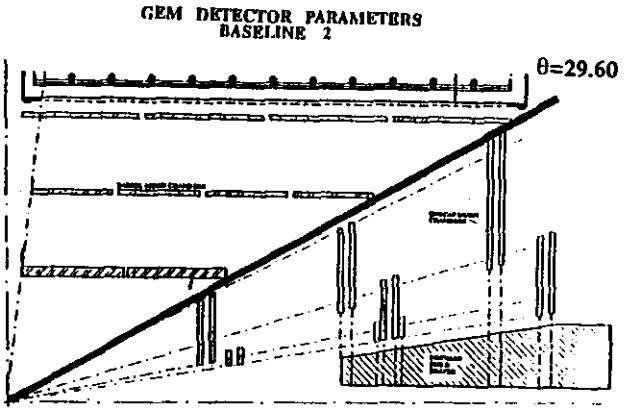

VF/OPERA-3d
(Post-processor)

Fig.9.2

thet17.pic
30/Jul/93 09:15:16 Page 59 : plot

θ=17.01

Timofeev S.

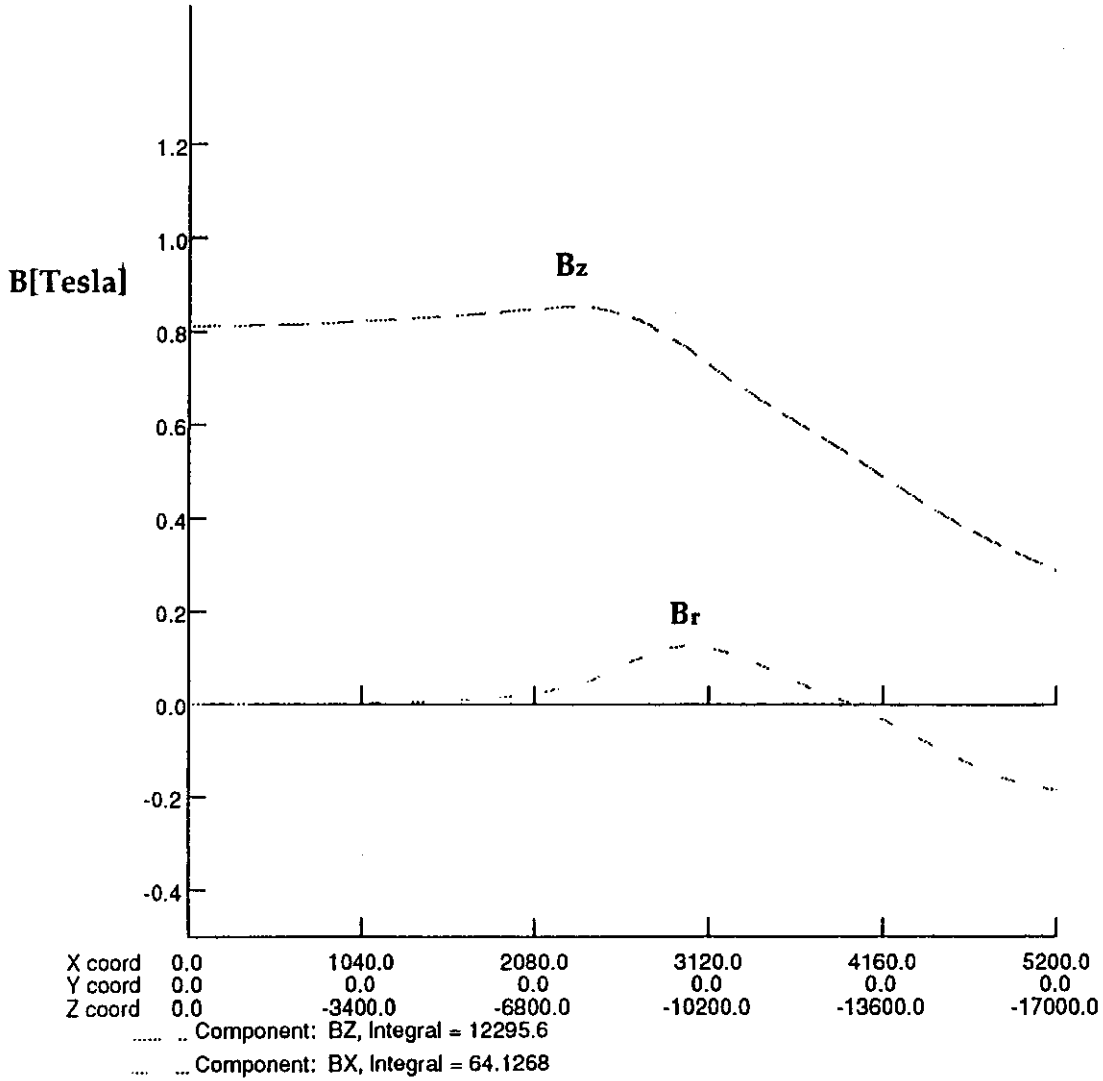

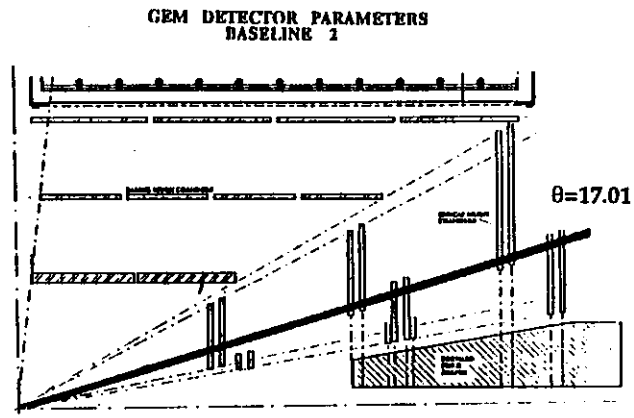

VF/OPERA-3d
(Post-processor)

Fig.9.3

thet9.pic
30/Jul/93 09:19:50 Page 62 : plot comp=bz

θ=9.75

Timofeev S.

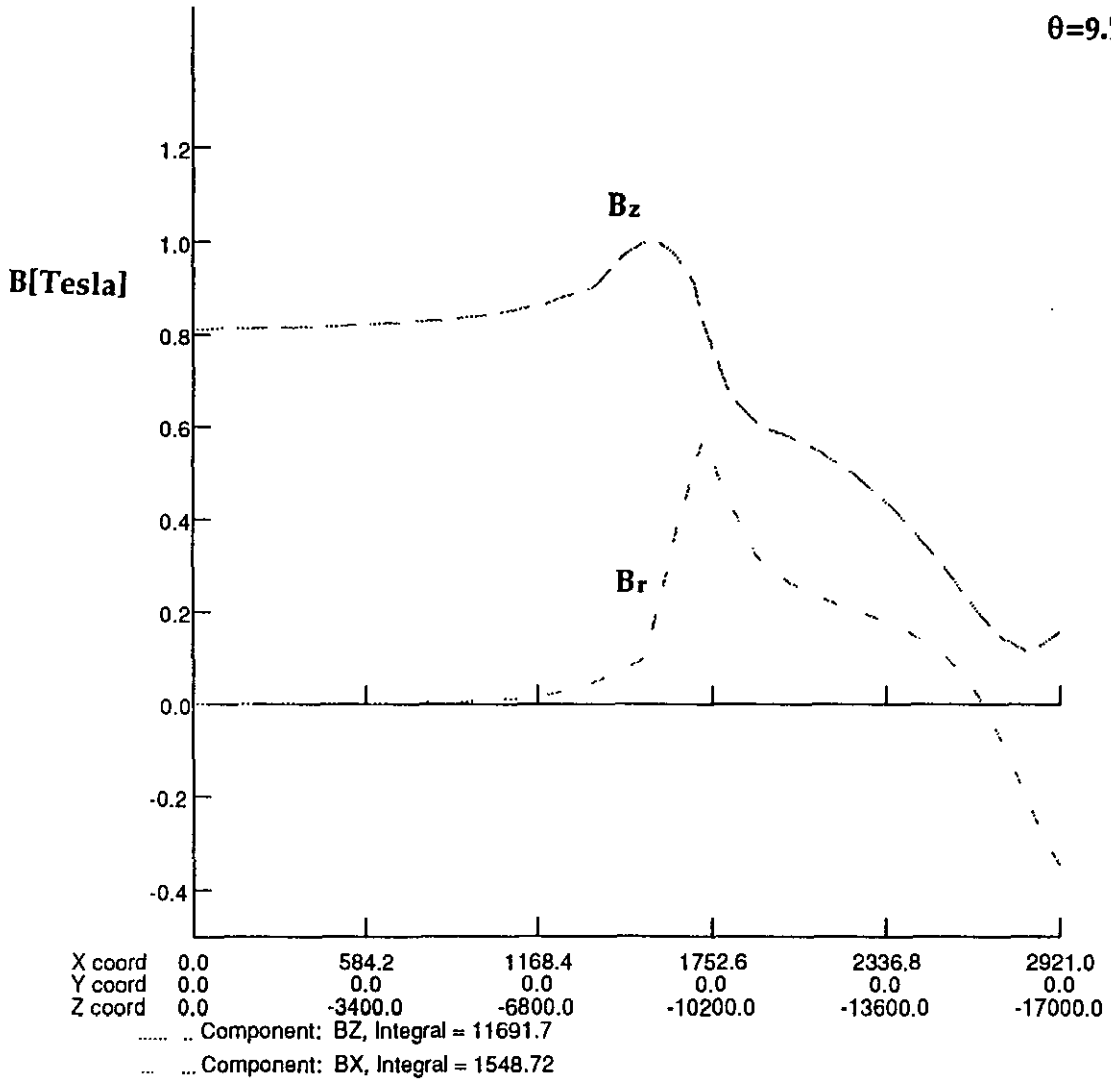

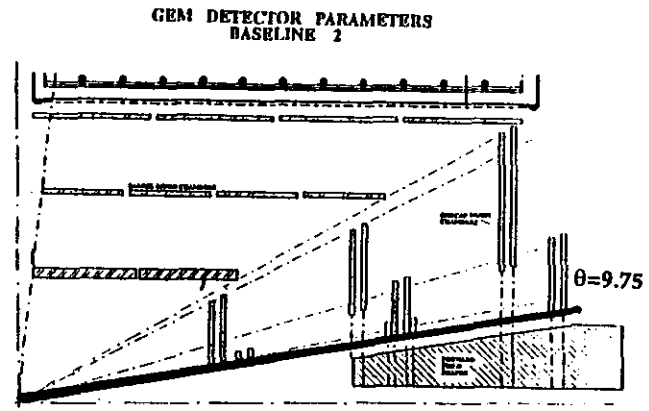

VF/OPERA-3d
(Post-processor)

Fig.9.4

a.pic
30/Jul/93 09:22:24 Page 65 : plot comp=bz

θ=9.45

Timofeev S.

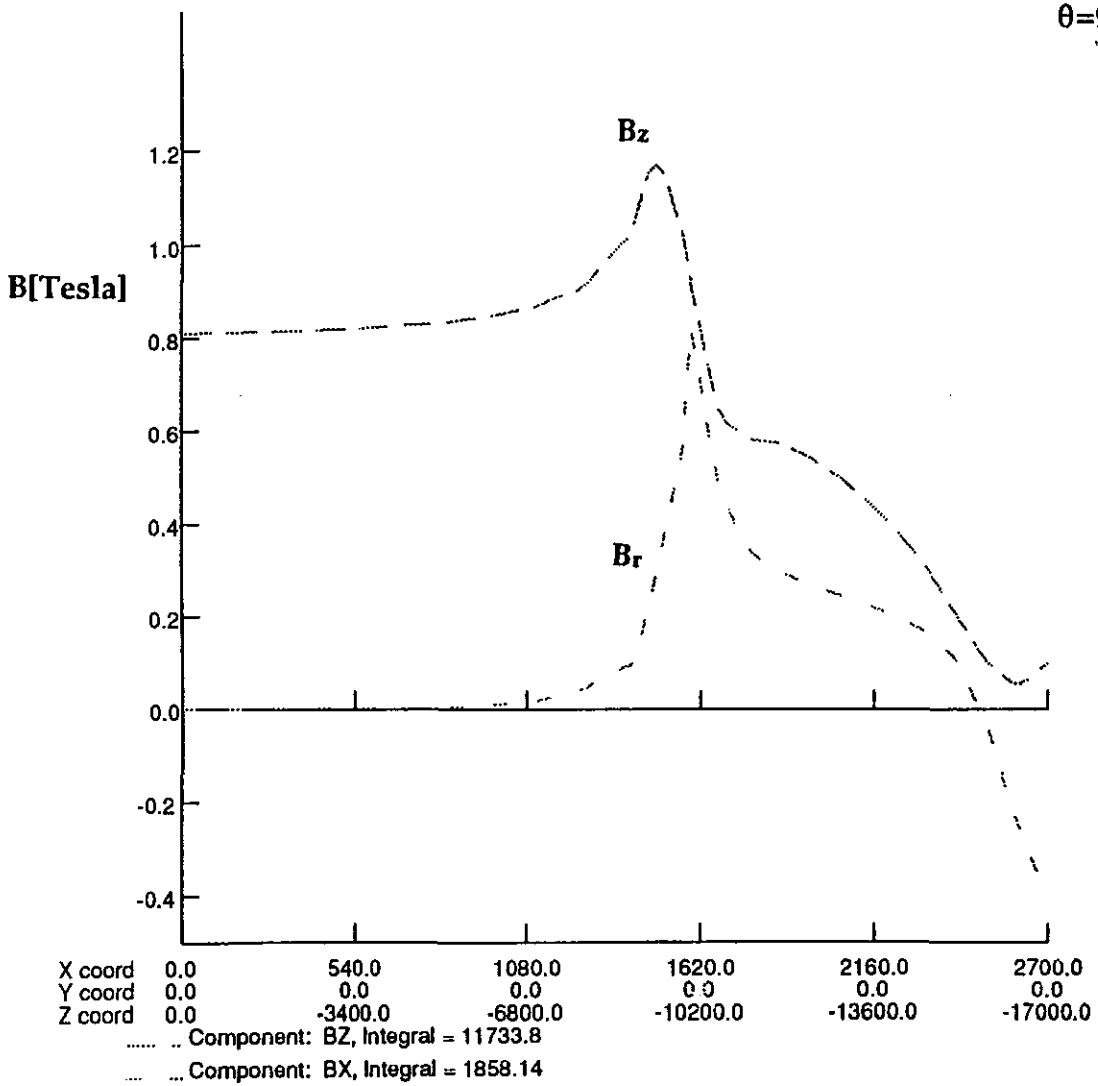

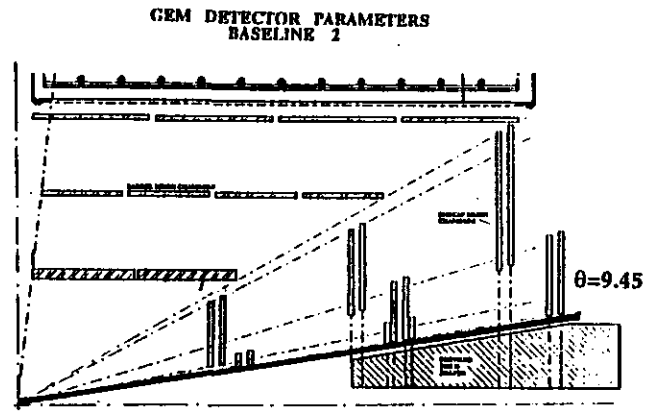

VF/OPERA-3d
(Post-processor)

Fig.9.5

a.pic
30/Jul/93 16:18:40 Page 98 : plot

Timofeev S.

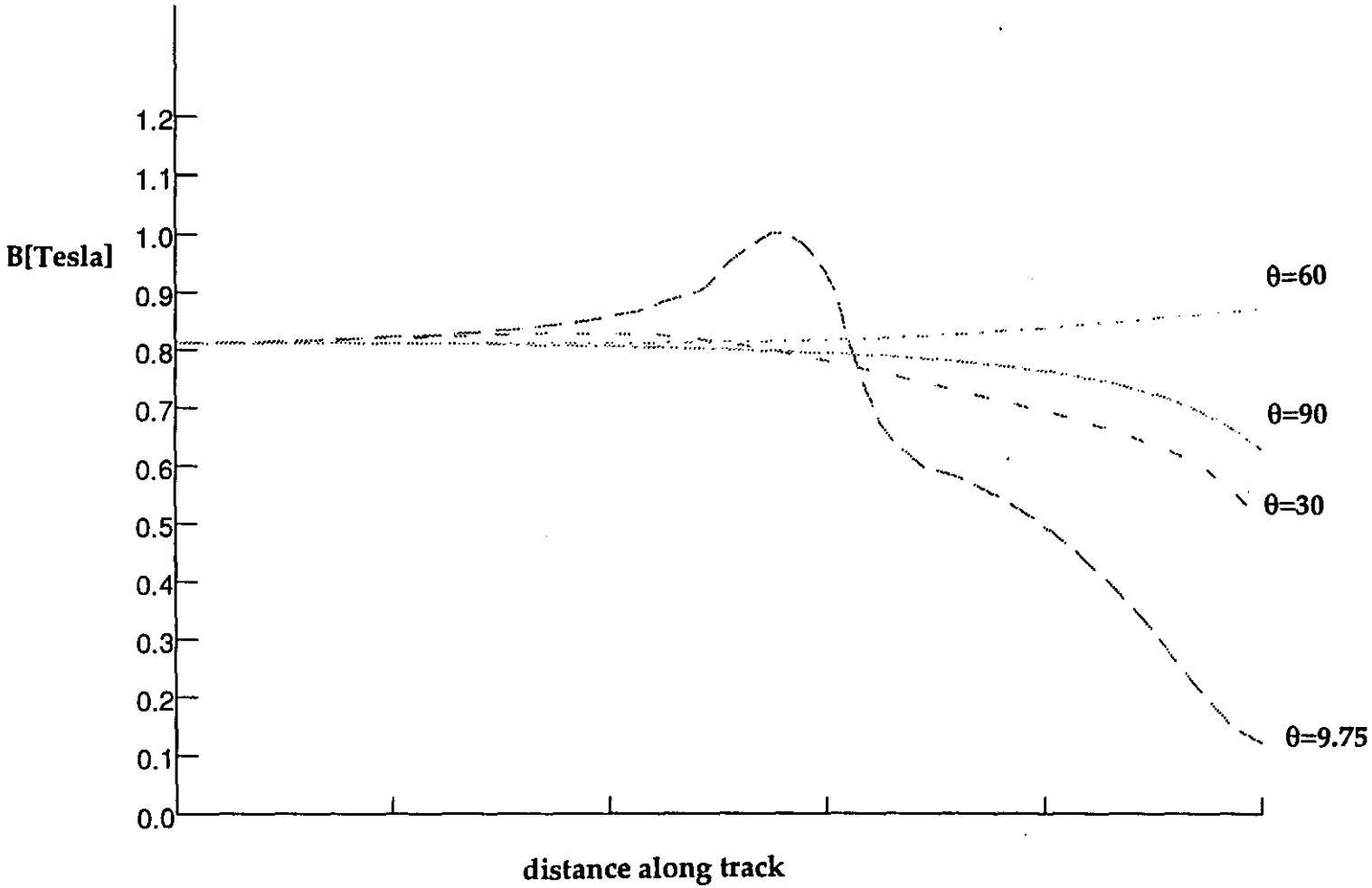

θ=9.75 Component: BZ, Integral = 11594.6
θ=30 Component: BZ, Integral = 13077.6
θ=60 Component: BZ, Integral = 8159.36
θ=90 Component: BZ, Integral = 6725.28

VF/OPERA-3d
(Post-processor)

Fig.10

FIELD INCREASE CONSEQUENCES:

Stored Energy goes as B^2

Forces goes as B^2

Stability drops some

CURRENT DESIGN OF THE GEM MAGNET MEETS REQUIREMENTS

COST (M$)=0.523[E(MJ)]* $^{2/3}$

INCREASE IN 20% OF THE MAGNETIC FIELD SHOULD COST

$1.2^{4/3}=1.275 \quad \Delta\approx 30M\$$

WITH THE SAME DESIGN APPROACH

Conductor

Stability

Protection

Joints

Cold mass design

Coil forms

Preloading

Attachment to cold mass support structures

Power supply system

Current supply

Bus work

Dump resistor

Vacuum vessel

Stability

Cryogenics

Current leads

STABILITY OF FORCED COOLED CONDUCTORS
vs COOLING AND JOULE'S HEAT RELEASE

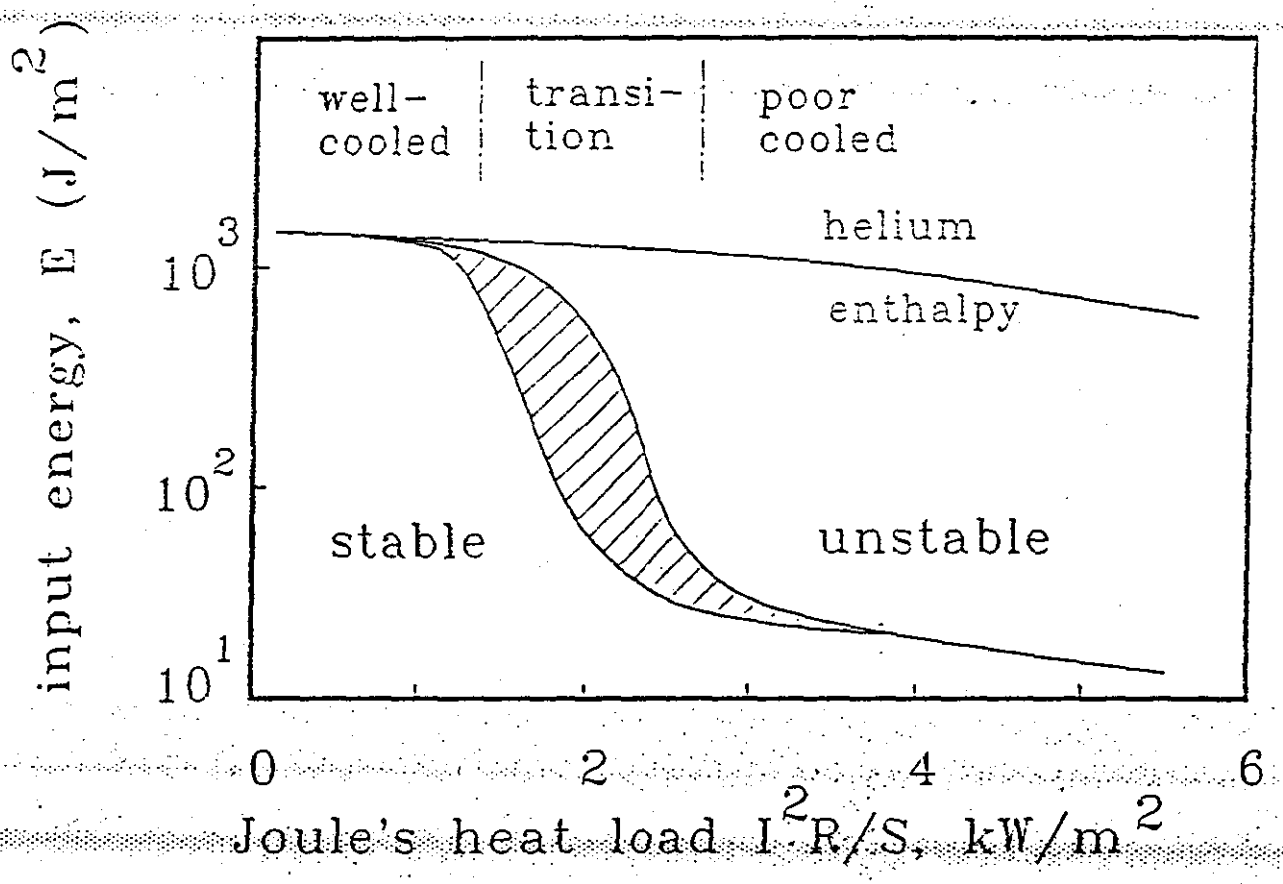

Fig. 5

STABILITY MARGIN

The stability margin is the largest sudden energy deposition to the conductor from which it can still recover the superconducting state.

It is normally expressed as energy per unit volume of cable (mJ/cc)

The limiting current defines the transition between the well-cooled and the ill-cooled stability regimes:

$$I_{lim} = \sqrt{\frac{h\, p\, A_{cu}(T_c - T_b)}{\rho_{cu}}}$$

Where,

h = heat transfer coefficient (W/m^2-K)
p = cooled perimeter (m)
A_{cu} = area of copper stabilizer in cable
ρ_{cu} = copper stabilizer resistivity (Ω-m)
T_c = critical temperature (K)
T_b = initial helium temperature (K)

General Requirements

1	Central field	T	0.8
2	Nominal field in winding	T	1.1
3	Peak field in winding	T	1.6
4	Operating temperature	K	4.5-4.8
5	Maximum hot spot temperature in a quench event	K	100
6	Maximum Dump Voltage to ground	V	500
7	Stored Energy	GJ	2.5
8	Number of charge/discharge cycles		200
9	Charging time	hr	8
10	Maximum number of quenches		100
11	Number of Cycles 293K/4.5K		100

HUGE STORED ENERGY AND LOW DUMPING VOLTAGE = LOW OVERALL CURRENT DENSITY

Design Criteria

HIGH RELIABILITY

high stability

good protection

RELATIVELY SIMPLE OPERATION

VERIFICATION IN LARGE SCALE APPLICATIONS

MODERATE COST

SHORT TERMS OF THE MANUFACTURE

CONVENIENT WINDING

Features:

STEADY STATE OPERATION IN RELATIVELY SMALL MAGNETIC FIELD (Jc is high)

NO INTENTION TO USE BATH COOLING (RISKY)

NO INTENTION TO USE CONDUCTOR AS A PIPING FOR COOLING DOWN AND TAKING MAJOR HEAT LEAKS

Conductor

Design features

- NbTi strand, 0.73 mm diameter
- 3.6:1 Cu:SC ratio
- 450 strands cabled in a 3x5x5x6 pattern
- 304L stainless steel conduit, two options
  > tube mill continuously welds conduit around cable (previous industrial experience)
  > tube lengths are butt welded and the cable is pulled through (development activity at Y-12)
- 1100 Al sheath
  > baseline design employs two symmetric halves, continuously longitudinally welded around the conduit (weld process development at Everson Electric and Y-12)
  > alternate of coextrusion requires industrial demonstration at this cross-section

Stability

- Energy margins
  > 300 J/m external disturbance
  > 250 J/m internal disturbance
- T_{cs} at 1.6 T peak field 7.5 K
- I_{op}/I_{cr} = 28.5%, I_{op} = 50.2 kA

Operation Current

Considerations calling for high current:

- Protection
- Smaller number of pieces
- Smaller number of turns
- Better mechanical integrity

Considerations calling for lower current:

- Lower cryogenic load due to current leads
- Easier manufacture
- Less expensive current source, distribution and protection equipment
- Easier transportation

50 kA is a reasonable compromise within manufacturing capability

Ic vs B
and load lines for
GEM conductor

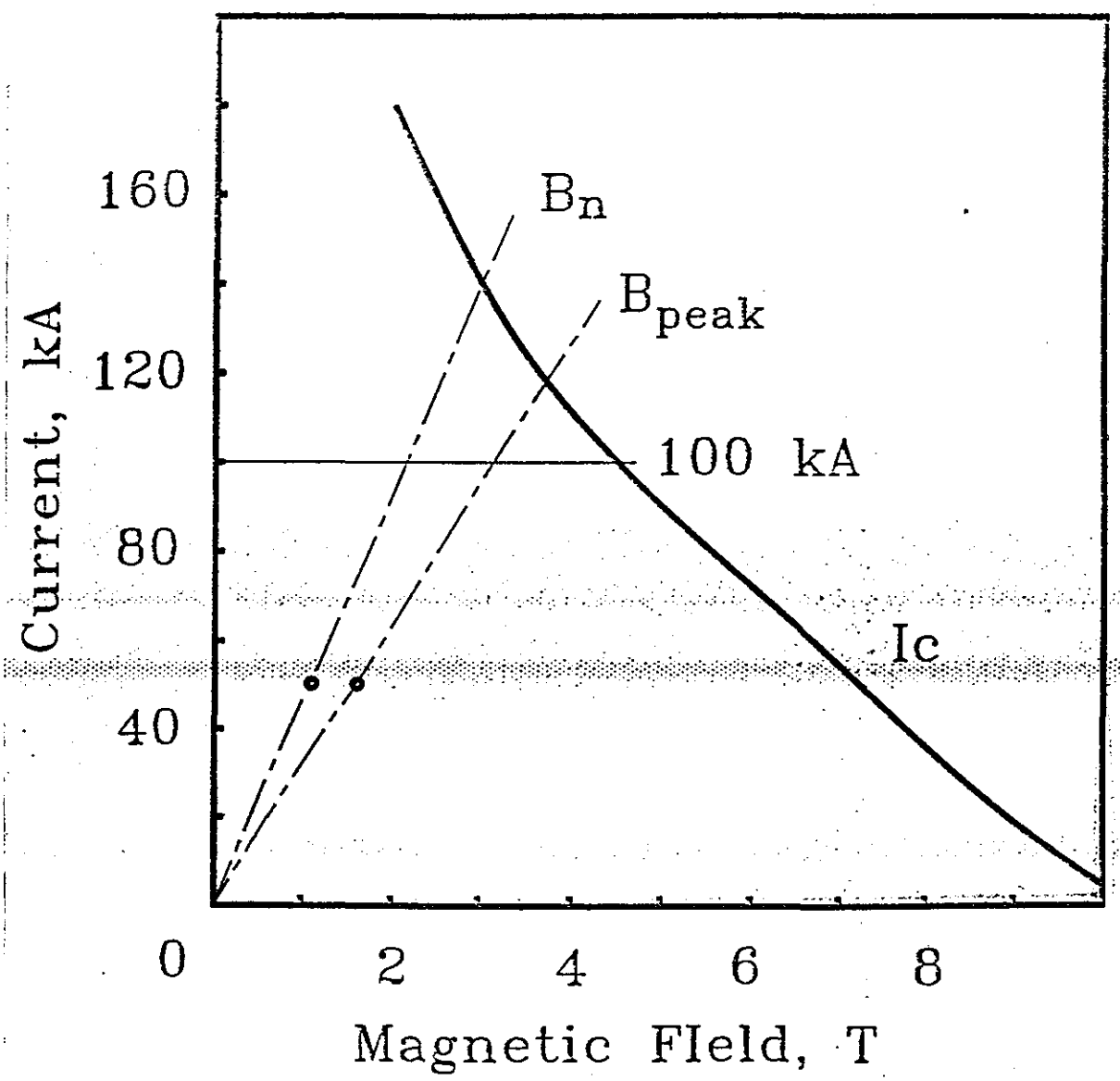

3 PANEL MEETINGS (Dec.91, Jan.92, March 92) WERE HELD DISCUSSING THE TYPE OF THE CONDUCTOR FOR GEM MAGNET:

Conductor Options:

A) INDIRECTLY COOLED CONDUCTOR (ICC)

B) FORCED FLOW COOLED CONDUCTOR (FFC)

C) CABLE-IN-CONDUIT CONDUCTOR (CICC)

Stability Against External Disturbances (20 kA option):

	ICC	FFC	CICC
Energy	7 J/m	50 J/m	300 J/m
Equivalent displacement	0.35 mm	2.5 mm	15 mm

No need for impregnation of the coil for the CICC

Conductor (cont.)

Quench Performance

- Terminal voltage = 1000V
- Dump time constant = 100 s
- Hot spot temperature = 100 K
- Helium pressure for a closed end fault condition = 45 MPa (6500 psi)

Full verification test of conductor and joint design with GEM Test Coil at the University of Wisconsin

CONDUIT

Should take pressure in the event of quench - 34 MPa

LENGTH

Maximum practicable 1139 m

SHEATH

For protection purposes only

Cost considerations - Al 1100 with RRR >17

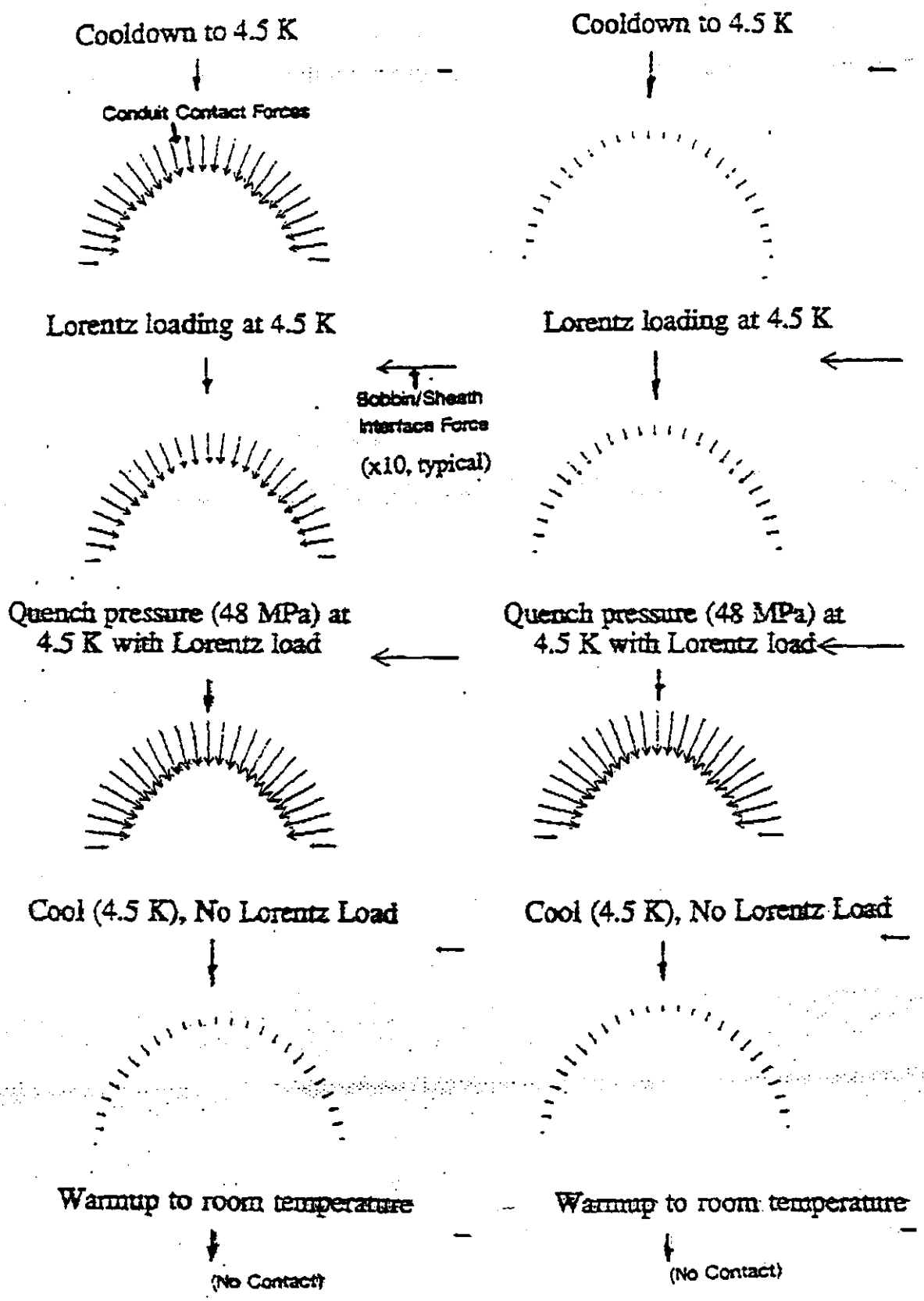

Sheath/Bobbin Contact Force Vectors for Each Load Step

Design Approach

- Single layer solenoid at 9.5 m mean winding radius, together with the FFS, provide required magnetic field quality

- Reliability is provided in several ways

  > Conductor design
    - CIC conductor provides high stability margin and minimum risk of magnet quench due to either small wire motions within the cable or frictional motions outside the sheath
    - Hot spot temperature following unlikely event of a quench is limited to a conservative 100 K by the Al sheath

  > Use of CIC conductor enables conservative insulation design for both the coil turn insulation and the ground insulation

  > Dump voltage during quench is limited to 1000 V across magnet terminals and 500 V to ground

Design Approach

Insulated bobbin quadrants improve availability

Energy deposited per bobbin during emergency discharge (τ = 100 s) if continuous = 30 MJ

Peak power per bobbin if continuous = 300 [illegible]

Design Approach (cont.)

- Reliability (cont.)

  > Conservative structural design
  - ASME Section VIII used as a guide
  - Winding is radially and axially constrained inside the bobbin and flange structure to minimize winding motion

  > Module-to-module electrical joints are designed to be cryostable

- Availability

  > Insulated bobbin quadrants save the magnet from quenching on emergency discharge, enabling rapid restart without need for magnet cooldown

  > High availability is derived from high reliability

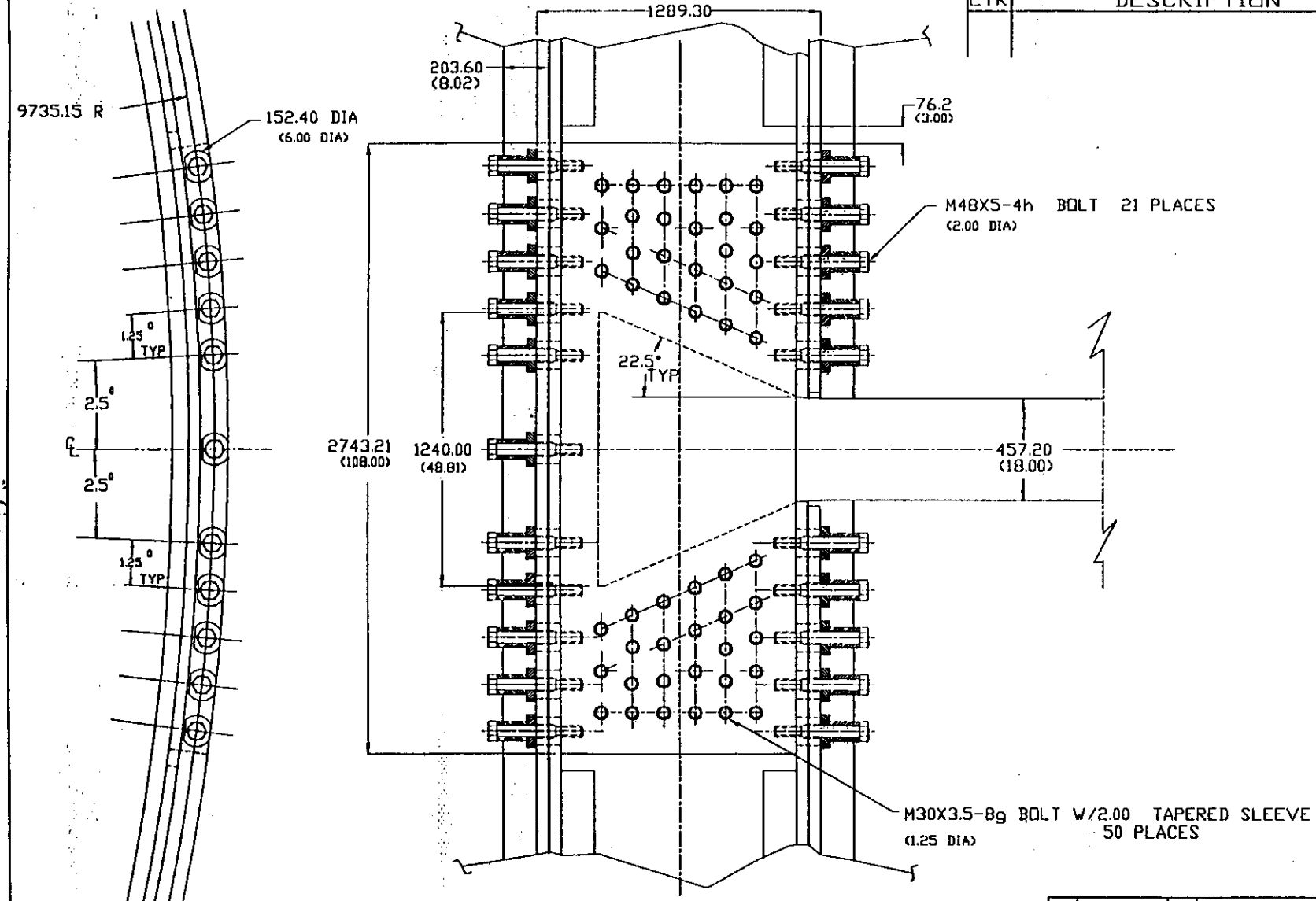

REVISIONS			
LTR	DESCRIPTION	DRN	DATE

REF NO	PART NO	NO REQ	DESCRIPTION

MATERIAL

FINISH

NEXT ASSY

REMOVE ALL BURRS AND SHARP EDGES

DIMENSIONS IN MILLIMETERS TOL UNLESS OTHERWISE SPECIFIED

XXX= ± .150 MM
XX= ± .50 MM
X= ± 1.5 MM

PLASMA FUSION CENTER
MASS INSTITUTE OF TECHNOLOGY

AXIAL SUPPORT
(TOP VIEW)

DRN ALEX R.	5-6-93	SCALE	SHT	OF
CHK		DWG SIZE		REV NO
APPD				

194

REVISIONS			
LTR	DESCRIPTION	DRN	DATE

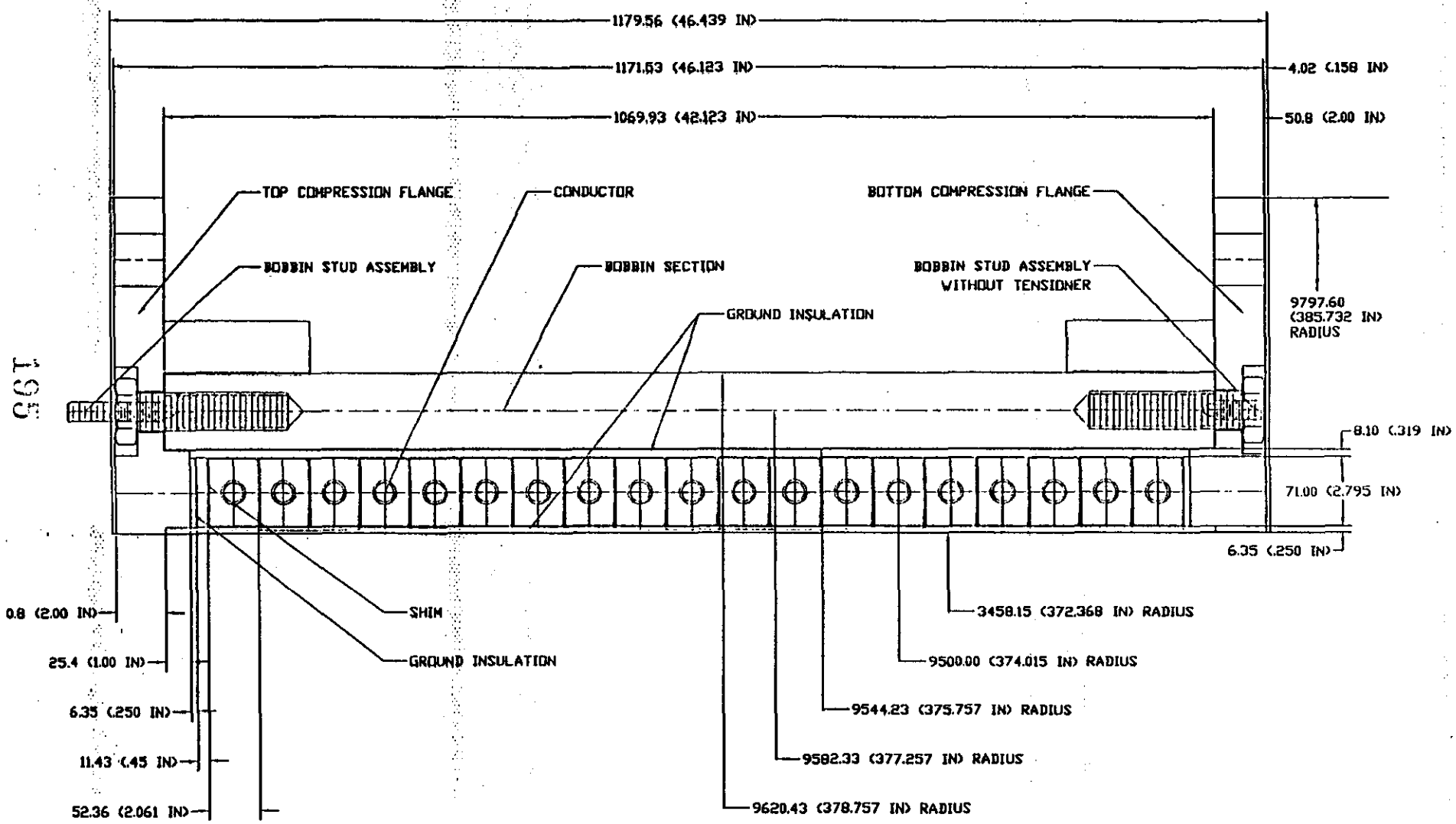

REF NO	PART NO	NO REQ	DESCRIPTION

MATERIAL	DIMENSIONS IN INCHES TOL UNLESS OTHERWISE SPECIFIED
FINISH	3 PLC DEC +/- .005 2 PLC DEC +/- .010 FRACTIONS +/- 1/64 ANGULAR +/- 1/2 DEG CONCENTRICITY .005 TIR MACHINE SURFACES 63
NEXT ASSY	
REMOVE ALL BURRS AND SHARP EDGES	

PLASMA FUSION CENTER
MASS INSTITUTE OF TECHNOLOGY

FULL BOBBIN MODULE ASSY

DRN W.J. MEANS	5-18-93	SCALE	SHT	OF
CHK		DWG SIZE		REV NO
APPD				

Coil Module Design

Design features

- 19 turns of conductor, 1134 m in length
- Conductor is preterminated in the factory
  - > Length adjustment of ±0.35 m built into termination and winding design
  - > Adequacy of adjustment will be proven during the dummy winding at Y-12
  - > Termination design does not preclude field termination
- Initial precompression applied during winding
- Final precompression applied at winding completion via flange bolts, stud tensioners and insulating shims

Supporting development activity

- Measurement of effective modulus of insulated conductor winding stack (6.4 GPa)

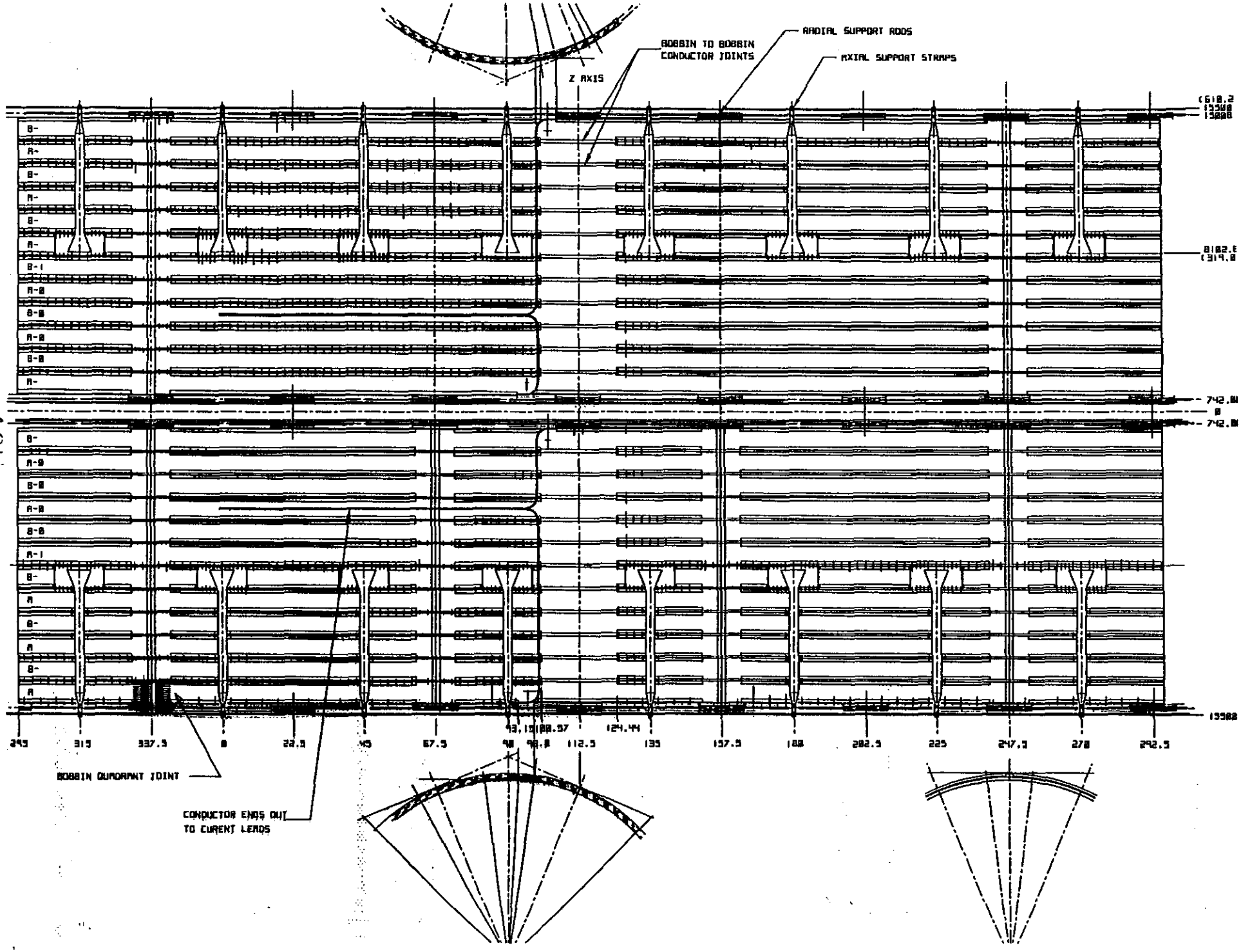
RADIAL SUPPORT RODS
BOBBIN TO BOBBIN CONDUCTOR JOINTS
AXIAL SUPPORT STRAPS
Z AXIS
BOBBIN QUADRANT JOINT
CONDUCTOR ENDS OUT TO CURENT LEADS

Structural Design (cont.)

Flange/Bobbin Bolt Loads

Loads	
Preload on coil	114 kN (26 kips)
Prying action of preload	245 kN (55 kips)
Differential thermal expansion	-17 kN (-4 kips)
Lorentz loads (always compressive)	0 kN
Deadweight (primarily causes shear)	0 kN
Lift loads (including prying)	
Single bobbin (concentrated load)	130 kN
Assembly (distributed load)	46 kN
Total (operational)	359 kN (81 kips)
Total (lift)	489 kN (111 kips)
Allowable Load, Inco LEA	487 kN (109 kips)
Bolt preload, Inco LEA	857 kN (109 kips)

Structural Design (cont.)

Stresses at Flex Plate Attachment (Preliminary)

	Stress (MPa)		Allowable Stress (MPa)
Bobbin (6061 T6 Aluminum)			
Membrane + bending (Pl + Pb)	208	<	225
Cover plate (6061 T6 Aluminum)			
Membrane + bending (Pl + Pb)	200	<	225
Bearing	260	<	321
Flanges (6061 T6 Aluminum)			
Membrane + bending (Pl + Pb)	188	<	321
Flex Plate (Titanium)			
Membrane + bending (Pl + Pb)	500	<	785
Bearing	260	<	1348

Structural Design (cont.)

Loss of Preload

Initial preload	8.3 MPa (1.2 ksi)

Low elastic modulus for coil stack
6.4 GPa (930 ksi) by test
Tolerant of displacement changes

Cooldown
In "normal" direction, G-11CR contracts more than 6061-T6

Loss =	1.2 MPa (175 psi)
Preload remaining	7.1 MPa (~~958~~ 1029 psi)
Preload required	6.6 MPa (~~958~~ psi)

Creep
Not significant at operating temperature
At room temperature, creep data are not available, and testing is required

Structural Design (cont.)

Bobbin Stresses (excluding quadrant joint)

	Stress (MPa)		Allowable Stress (MPa)
Preload on Coil			
Hoop direction	Negligible	<	150*
Transverse direction			
General membrane	7.4	<	150*
Membrane + Bending (Pl+Pb)	16	<	225
Differential thermal expansion	Small		
Lorentz loads			
Hoop direction			
General membrane	34	<	150*
Transverse direction			
General membrane	15	<	150*
Membrane + Bending	40	<	225
Deadweight			
Hoop direction			
General membrane	0	<	150*
Membrane + Bending	5	<	225

*6061-T6 (welded)

Structural Design (cont.)

Bobbin Quadrant Joint Stress-Flange Design

	Stress (MPa)		Allowable Stress (MPa)
Bobbin (6061 T6 Aluminum)			
General membrane	44	<	150*
Flange bolting (Nitronic 40)	292	<	345
Thermal Compensation Sleeve (Low Expansion Alloy)	281	<	427
Insulation			
At flange face	45	<	175
At washer	162	<	175

*6061-T6 if welded 128

CONCLUSION

GEM MAGNET DESIGN IS ROBUST TO MEET GIVEN REQUIREMENTS

DESIGN OF A NEW GEM MAGNET FOR HIGHER FIELD IS POSSIBLE

CHANGE IN REQUIREMENTS WILL COST

WAVING SOME REQUIREMENTS MIGHT SAVE SOME COST (like availability of the magnet)

SOME IMPROVEMENTS ARE POSSIBLE FOR THE PENALTY OF HIGHER RISK OR LOWER SAFETY MARGIN

EXTENSIVE REDESIGN AND ADDITIONAL R&D ARE NEEDED TO MEET NEW REQUIREMENTS FOR HIGHER FIELD

Outline of CSC Muon Detector Test Beam Program Document

I. General Description of the GEM Muon Subsystem (Fig. 1-3)

- A. Chamber Design
- B. Readout and Trigger Electronics
- C. Barrel and Endcap Chamber Layout
- D. Alignment Philosophy and Components

II. Goals of the Pre-Fermilab and Fermilab Test Program

- A. Pre-Fermilab goals
- B. Fermilab goals

III. Pre-Fermilab Test Program

A. Bench Tests (Fig. 4-5)
1. Cosmic Ray Tests (TTR, etc.)
2. Tests with Laser, Gas Choice
3. Alignment System Tests
4. Electronics prototypes tests

B. Low Energy Beam Tests (PNPI, ITEP, BNL(?)) (Fig. 6)
1. Studies of spatial and time resolution for CSC with various readout pitch widths and anode-cathode gaps at different beam angles in a Magnetic Field
2. Lorentz Angles studies
3. Double track resolution
4. Gas studies
5. Electronics Tests in Accelerator Environment

C. High Energy Beam Tests in RD5 (Fig. 7)
1. Punchthrough measurements
2. Muon Radiation Background
3. Studies of spatial and time resolution

IV. Fermilab Test Beam Program

A. High Energy (200-500 GeV) Muon Beam Tests with 40x40sqcm 6-Plane Module in a Magnetic Field (Fig. 8)
1. Test Muon Radiation Background
2. Repeat of Resolution Studies vs. Angles
3. Continuation of Electronics Tests

B. Punchthrough measurements on a High Energy Hadron Beam with 40x40sqcm 6-Plane Module in a Magnetic Field

C. Beam Tests of a Single Full-Scale Chamber Module (6-planes)
1. Resolution Measurements
2. Interlayer Alignment
3. Electronics Studies

D. Beam Tests of Barrel Muon 15-degree Sector (7.5-degrees instrumented) (Fig. 9)
1. Integrated Test of Detectors, Supports, Alignment, and Services.
2. X-ray Calibration of Global Alignment
3. Studies of Muon System sagitta measurements precision
4. Test Sagitta Correction with Tracks from a Simulated Focus
5. Tests of Time Resolution of the Muon System
6. Investigate Electronics and Trigger Prototypes

E. Beam Tests of GEM Sector, with Central Tracker, Calorimeter, and Muon

V. Requirements for Fermilab Program

A. Beam

1. General Requirements
   - a. Beam-Trigger Signal Properties
   - b. Momentum Measurement of Beam Particle in the Trigger
   - c. Direction Measurement of Beam Track in the Detector Hall
2. Muon Beam (Muon Tagging System and/or Hadron Filtering System?)
   - a. Spot Size -- Halo
   - b. Energies and dp/p
   - c. Minimum and Maximum Useful Intensities
   - d. Independent Beam Position System, Resolution, Location
   - e. Limitations on the Muon Beam contaminations with other particles
3. Hadron Beam (Electron, Muon Tagging Needed?)
   - a. Spot Size -- Halo
   - b. Energies and dp/p
   - c. Minimum and Maximum Useful Intensities
   - d. Independent Beam Position System, Resolution, Location
   - e. Limitations on the Hadron Beam contaminations with other particles

B. Chamber Test Facilities (Fig. 10)

1. Magnetic Field Tests
   - a. Design and Construction of Chamber Manipulator
   - b. Small Gas System (non-recovering ?)
   - c. LV, HV, Calibration and Readout Connections
   - d. Monitors for Temperature (local) and Pressure (once in building)
   - e. Facilities for Access to the Chamber
   - f. Calibrated Hall-probe Monitor
2. Sector Test
   - a. Design and Construction of Chamber, Alignment, Services Module
   - b. Design of Facility for Vertical and Horizontal Rotation of Module
   - c. Large Gas System (recirculating ?)
   - d. LV, HV, Calibration, Alignment and Readout Connections
   - e. Monitors for Temperature (local) and Pressure (once in building)
   - f. Facilities for Access to the Chambers (Scaffolds, etc.)

C. DAQ and Computers Requirements (Fig. 11)

1. Front End Electronics
2. Digitization Options
3. Calibration Procedure
4. DAQ System
5. Slow Control (EPICS) System
6. Online and Off-line computing

VI. Responsibilities

A. Detector Construction for Sector Tests
   1. Chamber Construction (3 or 6?)
   2. Alignment System Components
   3. Gas Supply and Monitoring System

B. Construction of Manipulators and Chamber Supports

C. Electronics
   1. Magnetic Field Tests
   2. Sector Tests

D. Data Aquisition, On-Line and Off-Line Analysis
   1. Magnetic Field Tests
   2. Sector Tests

E. Engineering Personel Needs
   1. Magnetic Field Tests
   2. Sector Tests

VII. Costs

VIII Schedule and Evolution of Fermilab Test Program

Figures:

1. General view of GEM Muon System
2. CSC Chamber designs
3. Alignment concept
4. TTR results on spatial resolution
5. Alignment tests results
6. Timing resolution of CSC
7. RD5 results
8. Sketch Showing Magnetic Field Test Configuration
9. Sketch of Showing 15 degree Sector Test Configuation
10. Design of Chamber Manipulator
11. Sketch of Muon DAQ and Monitoring subsystem

Chamber Interface with Support Structure

New "Baseline", preliminary decision (28 July 1993 video conference) ...

- Chambers are mounted at 4 points ("partial" kinematic mount) instead of at 3 points ("true" kinematic mount) presented to PAC Review.

- Chambers are supported at ends (~1mm sag for largest barrel chamber) instead of at "1/4 points", similar to PAC Review presentation.

Reasoning ...

- The chamber as a structure can accommodate any of the proposed support methods without being subject to unacceptable loads.

- Neither of the proposed support methods introduce significant, uncorrectable sagitta error.

- Practical engineering considerations (excluding chamber electronics) favor a 4 point support concept located at the ends of the chamber.
  - The addition of the fourth support point potentially introduces a small, correctable sagitta error as long as the support structure is "locally" stable. (The chamber would deform into a simple, predictable shape.)
  - End supports are most directly tied into the support structure providing a more stable, less massive interface structure.

Chamber Interface Structure and Kinematic Mounts

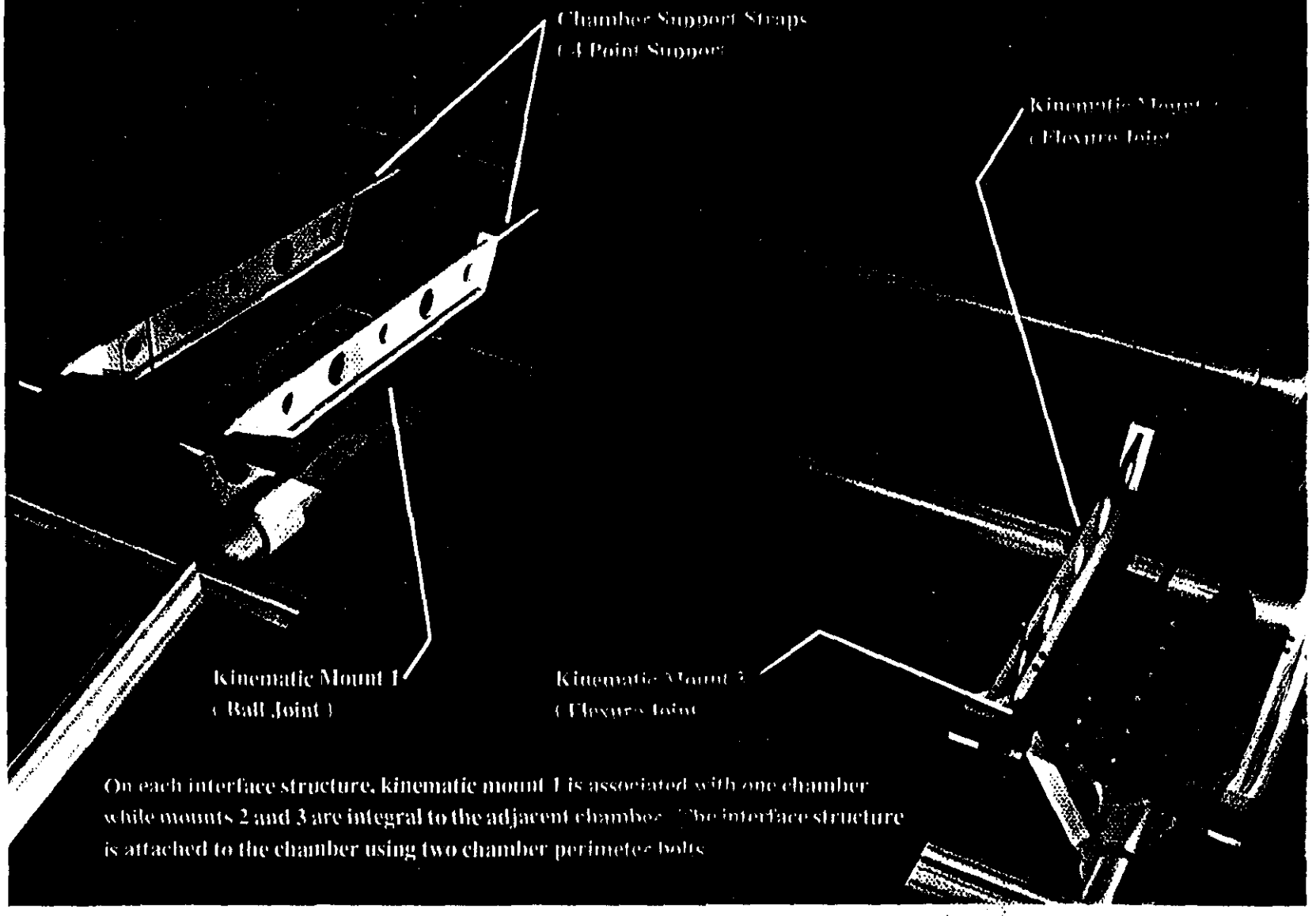

On each interface structure, kinematic mount 1 is associated with one chamber while mounts 2 and 3 are integral to the adjacent chamber. The interface structure is attached to the chamber using two chamber perimeter bolts.

Chamber Interface Structure

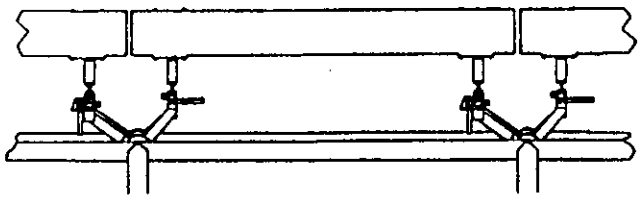

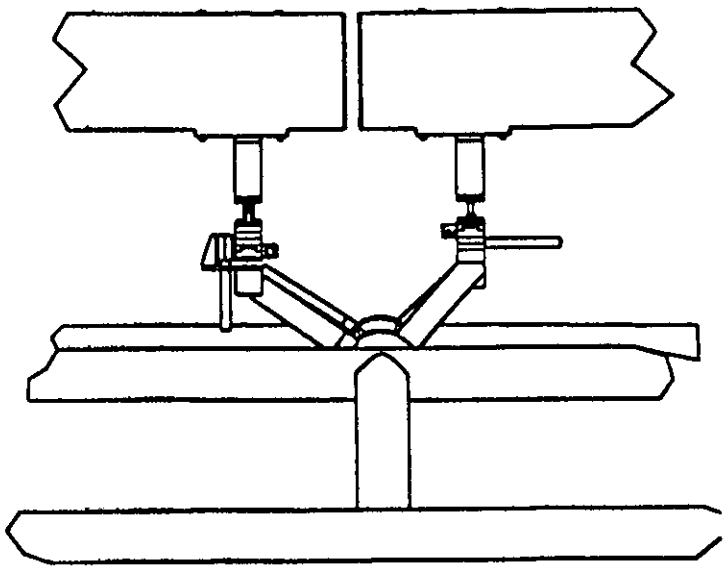

A view along the x-axis. Adjacent chambers along the x-axis are supported from a common interface structure.

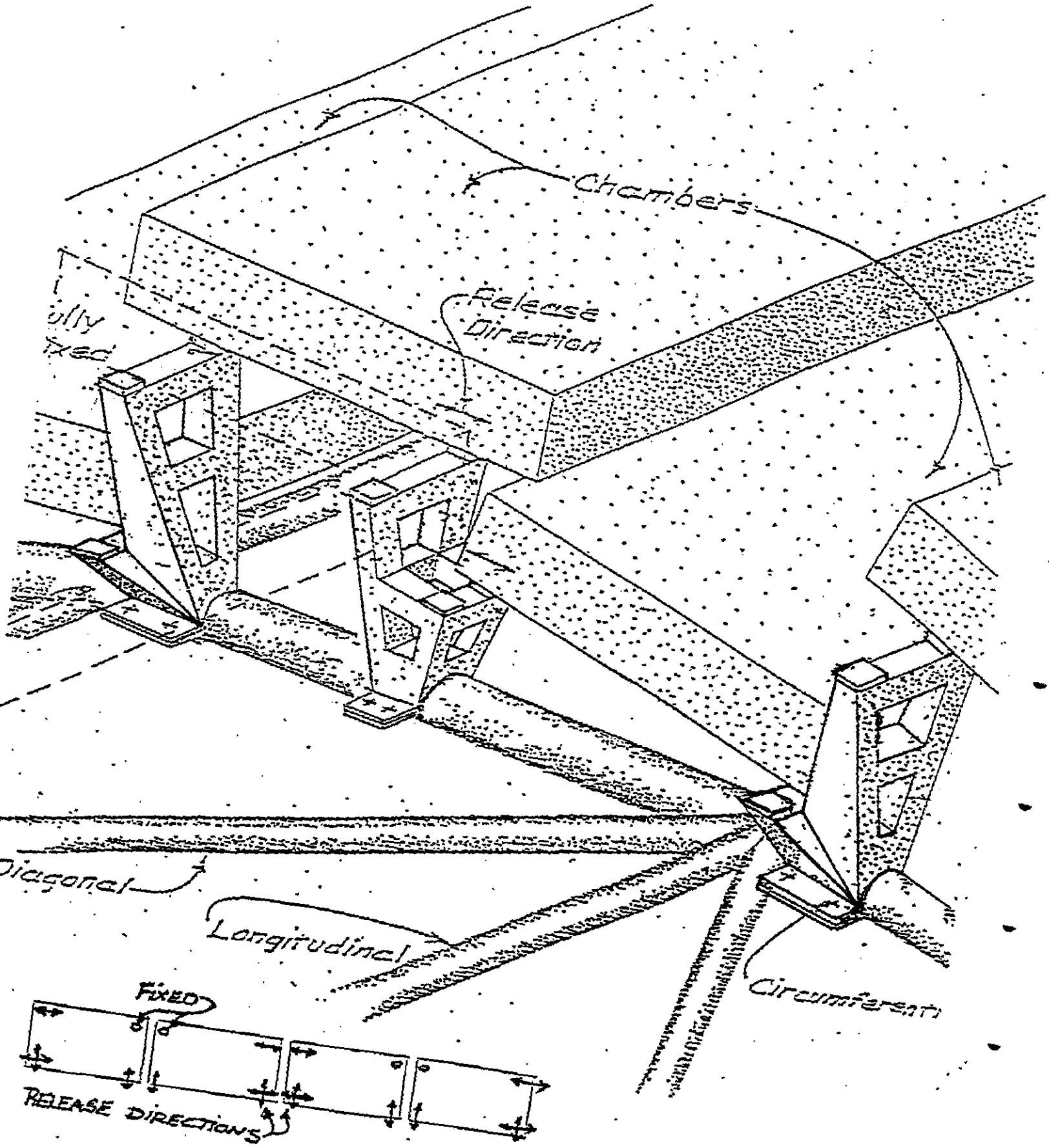

Barrel Chamber Mounting System

Chamber Interface with Support Structure (cont.)

- There are no compelling physics issues that favor one support method over another.

  - Compatible with "pure" projective and "hybrid" axial-projective alignment concepts.
  - Comfortable with ~1mm chamber sag as long as it is predictable to 10% or better, but verify!
  - Reasonably satisfied that the cumulative effects of all the minor uncertainties in sagitta error are understood.

Remaining issues ...

- Analyze dynamics of chamber-support structure interaction, although not thought be a problem (SG&H and LLNL)

- Creep tests to be performed on panel materials and assemblies to verify assumption that creep is not of concern, although a creep problem would favor the "1/4 point" support method (LLNL).

- Electronics, alignment components, and mount location on the chamber remains a severe design challenge even if electronics are moved from the edge to the face i.e. a "congested area" is created on the chamber face along the short edges (LLNL and SSCL).

Simulations

of the GEM

muon alignment system

Yu. Gershtein ITEP / SSCL

- The subject
- Projective v.s. axial
- Results
- Plans

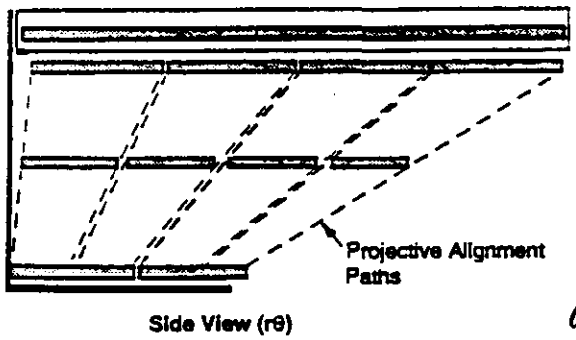

- Pure projective scheme:

⬇ loose efficiency due to gaps between chambers

Possible treatment:

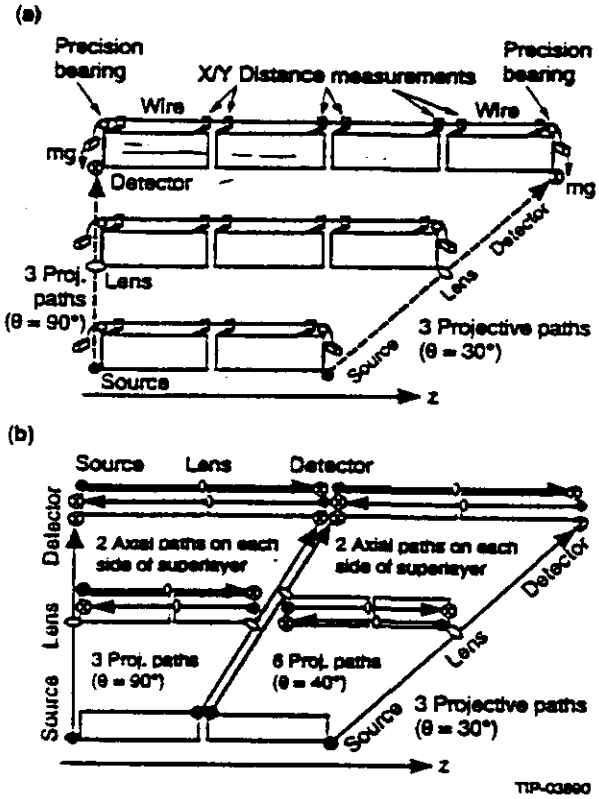

FIG. 4-69. Alternative schemes for local alignment of the GEM muon barrel.

Wire monitors:

⬆ no more gaps (just lead ends of the chambers)

⬆ 3 chambers in 2 SL

⬆ easy to place monitors

⬆ reduction of projective links number

Optical monitors

⬆ have to be used in the endcap alignment

Projective v.s. axial alignment

- False saggita method assumes that chambers are continous
- In proj. v.s. axial scheme false saggita is a non-continous function of angles θ and φ

HAVE TO:

- using axial monitor readings to project measured hits on a pseudo-chamber surface.
- then use projective monitor readings as in pure projective scheme.

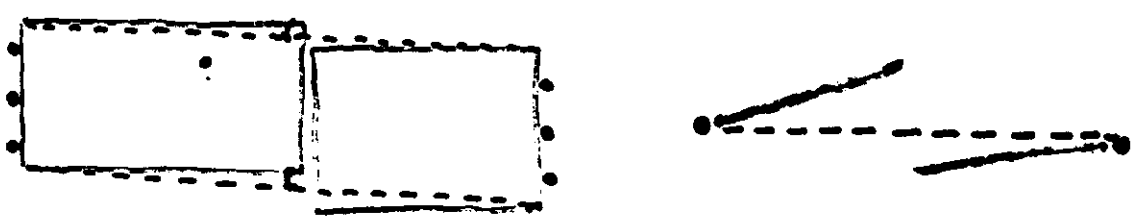

As the true chamber positions are not known we have to correct separately for relative chamber movements (with axial monitors) and for shifts and rotations of whole SL (with projective monitors).

In particular,

- take chambers in undisturbed positions
- move them to meet axial monitors readings
- assuming that track goes from IP calculate correction for relative chamber movements
  ! Approximate !
- interpolate projective monitor readings to corrected point
- calculate correction for movement of whole SL.

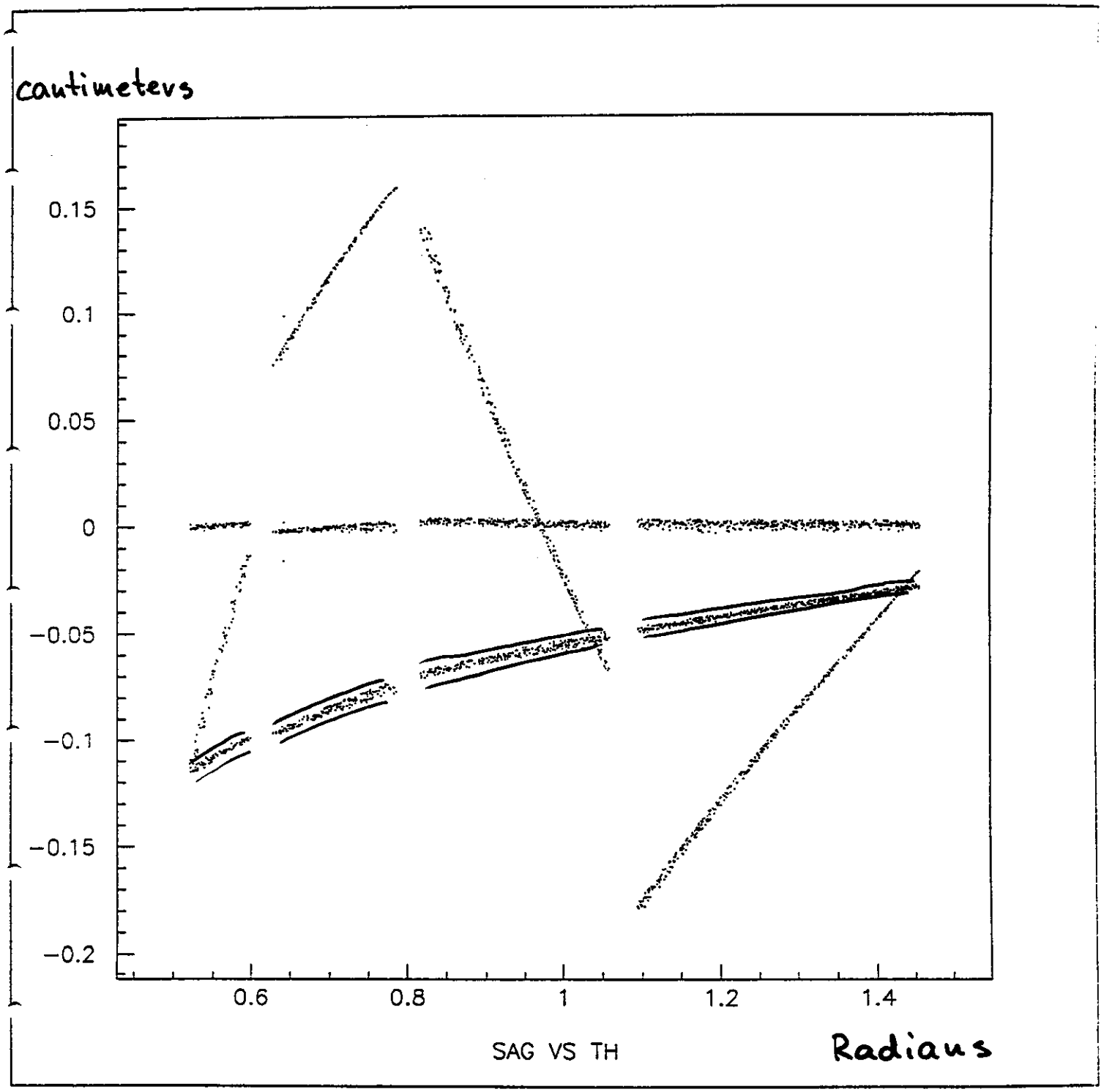
cautimeters
0.15
0.1
0.05
0
−0.05
−0.1
−0.15
−0.2
0.6
0.8
1
1.2
1.4
SAG VS TH
Radians

Coordinate system:

GEM:

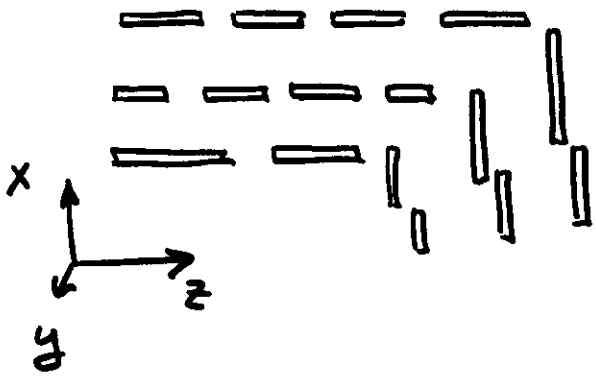

Chamber:

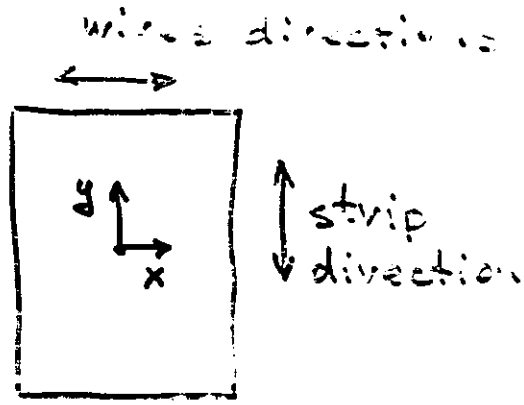

Projective monitors:

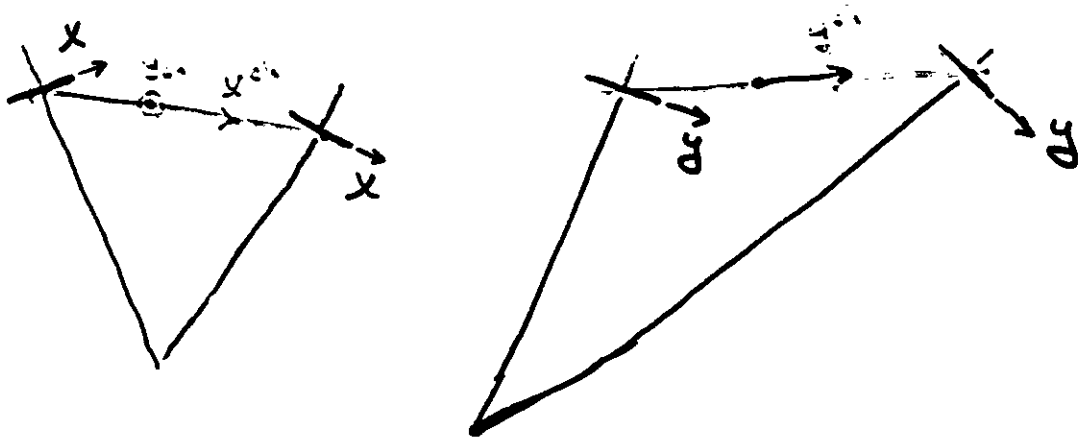

Axial Monitors:

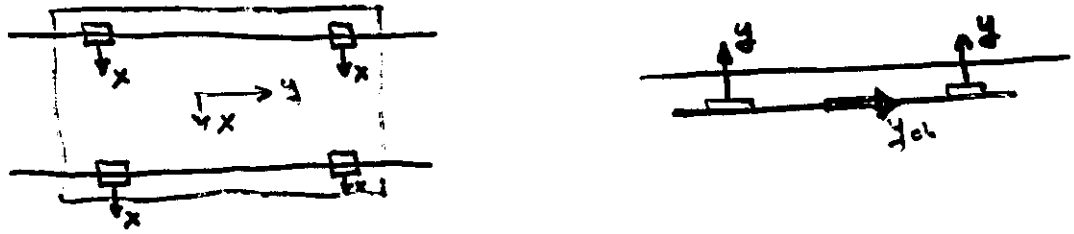

Defenitions:

Chamber movements:

1 SL shifts $x, y, z \pm 3.0$ mm
rotations $x, y \pm 2$ mrad ; $z \pm 7$ mrad

2 SL shifts $x, y, z \pm 1.5$ mm
rotations $x, y \pm 1$ mrad ; $z \pm 3$ mrad

3 SL shifts $x, y, z \pm 3.0$ mm
rotations $x, y \pm 1.5$ mrad ; $z \pm 5$ mrad

Non-bend resolution:

Readout 10 cm $\Rightarrow \sigma = 10 \cdot \frac{1}{2\sqrt{12}} = 1.44$ cm

Monitors:

Optical $\sigma_x = \sigma_y = 25\ \mu m$

Wire $\sigma_x = 10 \mu m$ $\sigma_y = 100 \mu m$

Non-projectivity:

bunch size $\sigma_x = \sigma_y = .2$ mm $\sigma_z = 5$ cm

center of GEM shift $\sigma_x = \sigma_y = \sigma_z = 3$ cm

Assumptions:

- tracks distributed uniformly over the tower (angles θ and φ)
- All numbers were obtained in 50 runs of 50 events $\Rightarrow$
  $\Rightarrow$ statistical error $\sim 10-15\%$

Table 1.

		method	proj. monitors resolution	non-projectivity	proj.mon + non-project.	axial mon. resolution	All
pure projective	tower 1	2.2	13.1	18.6	21.6		23.3
	tower 2	2.5	12.5	18.6	19.4		22.4
	tower 3	3.0	13.1	20.2	22.8		22.8
	tower 4	3.2	12.4	19.1	22.7		24.9
optical ax. mon	tower 12	4.1	10.6	15.9	19.3	5.7	22.5
	tower 34	3.5	11.1	17.7	19.0	4.8	21.5
wire	tower 1234	5.6	11.7	14.0	16.1	13.2	22.2
	tower 123	6.0	12.0	13.4	17.6	12.	22.1

tower 123 - gapless configuration with 3 chambers in second SL

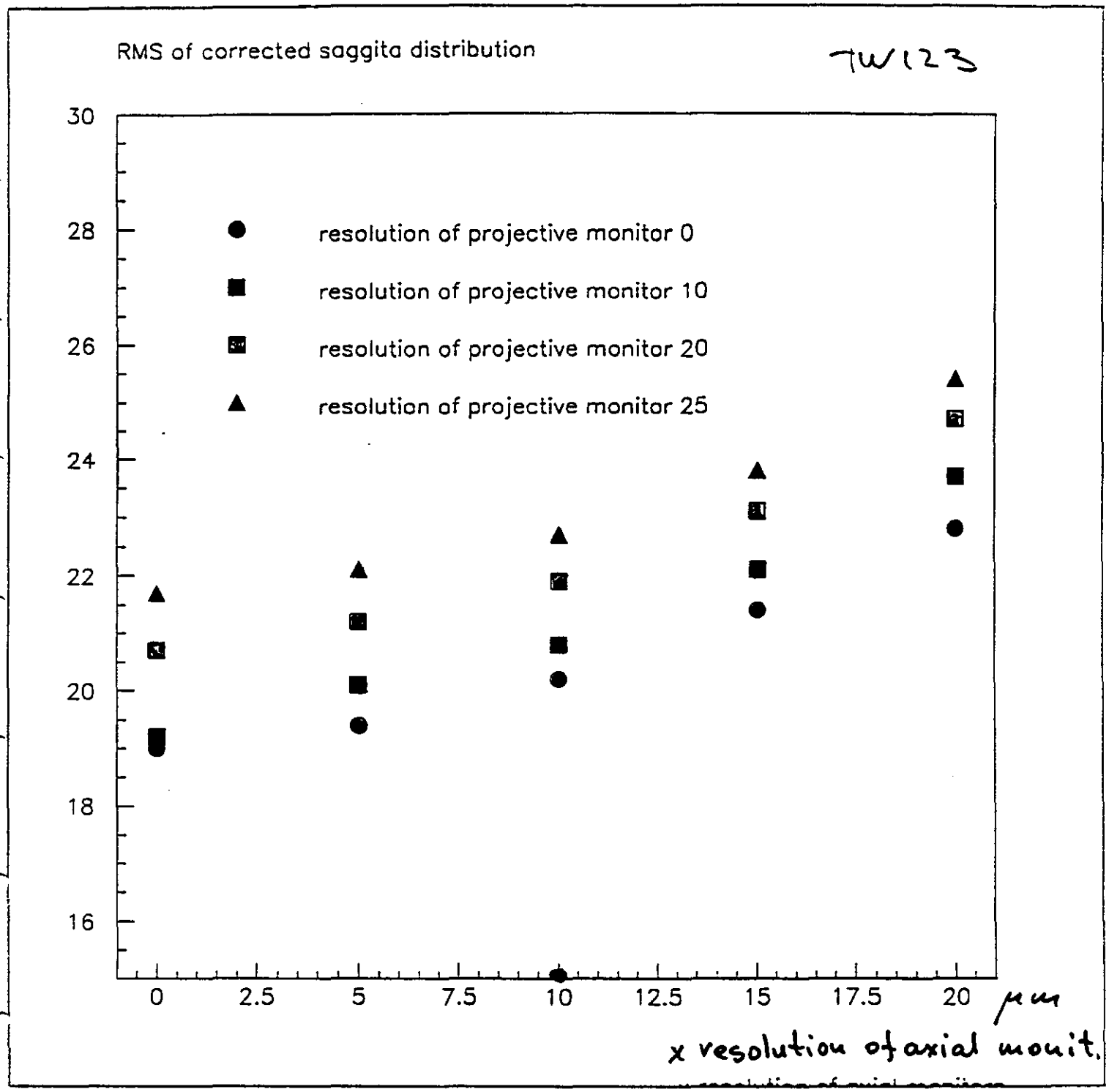

All other parameters - BASELINE

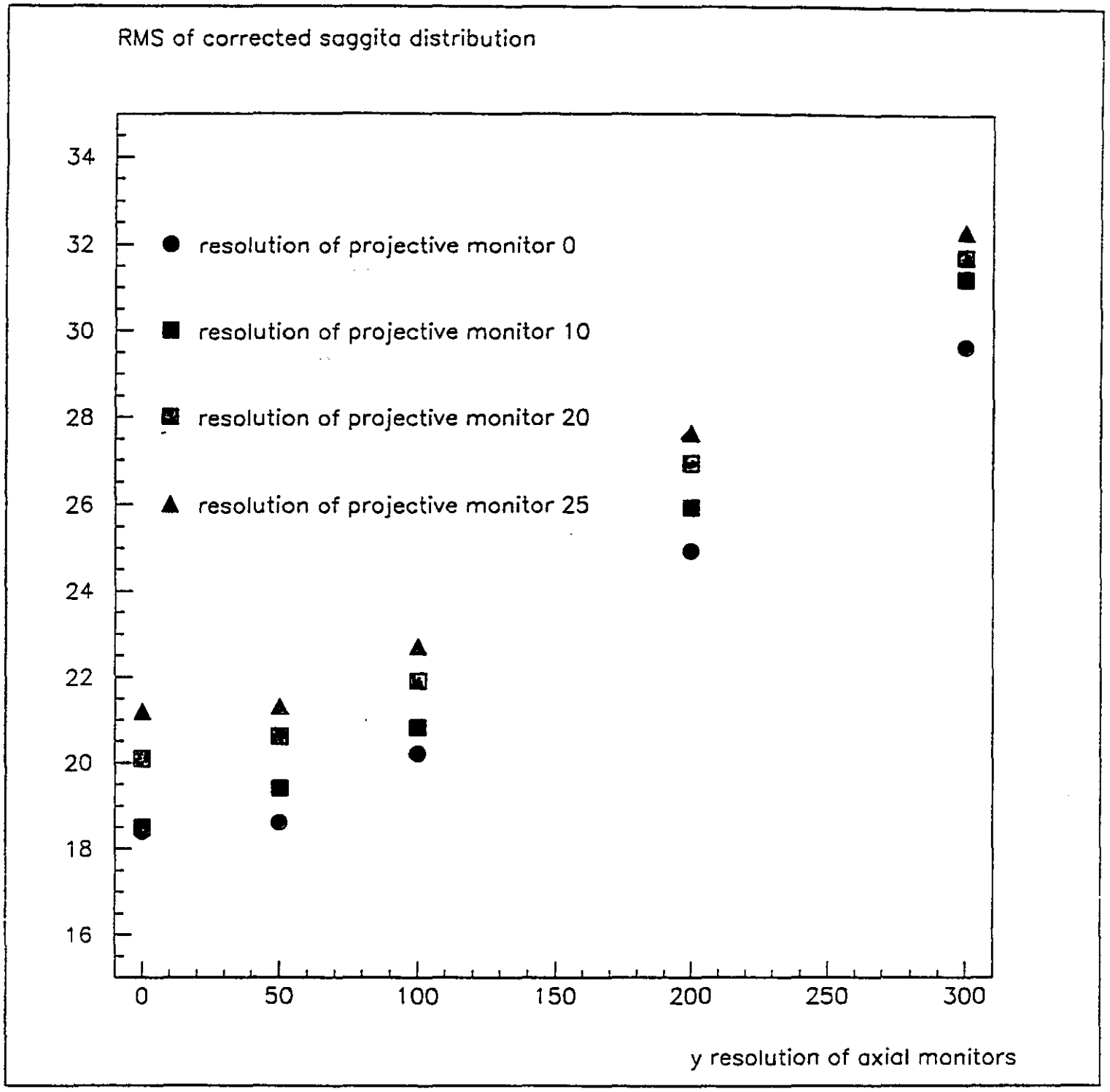

All other parametevs - BASELINE

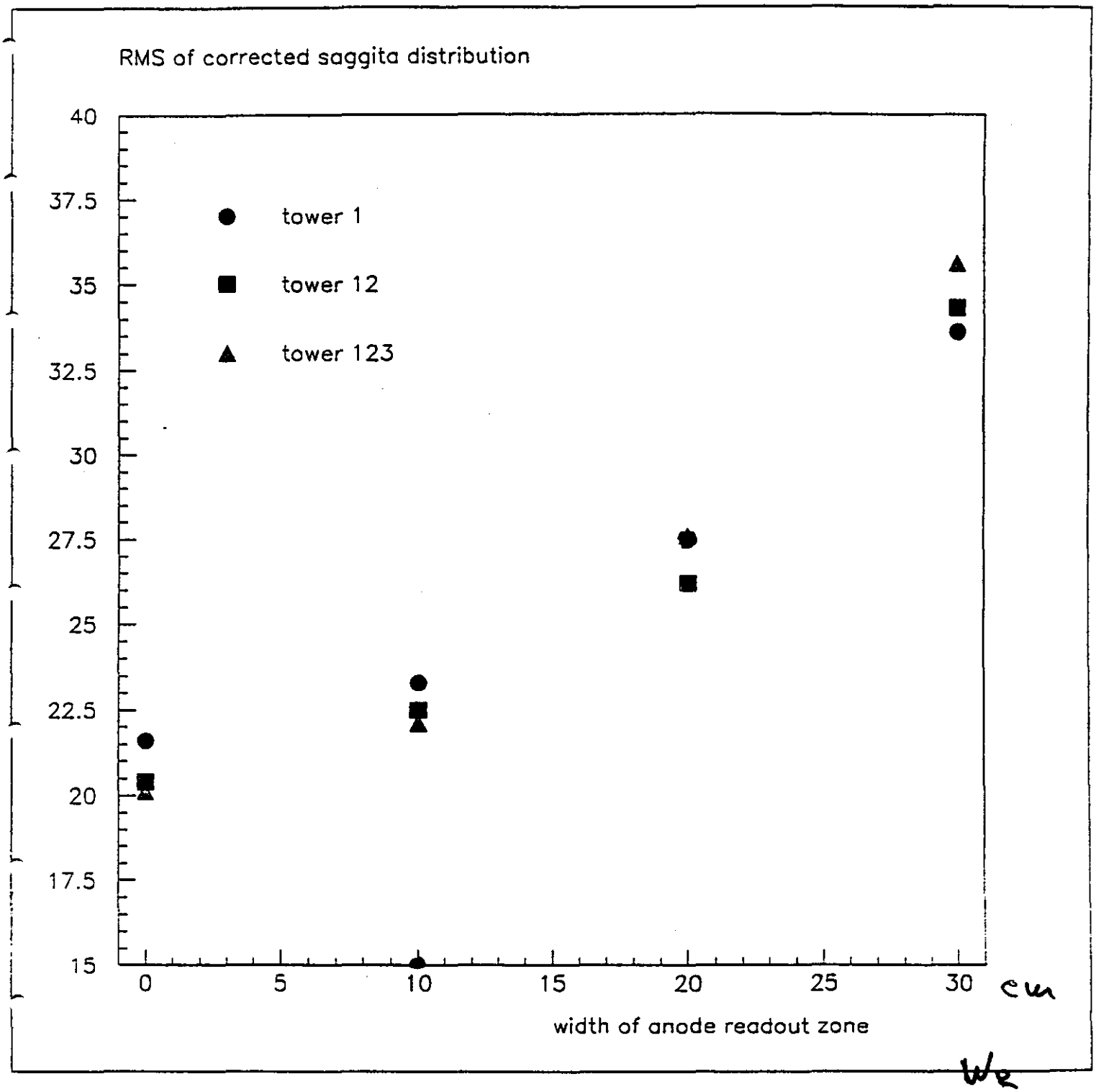

$\sigma_z = \frac{W_R}{2\sqrt{12}}$

All other parameters – BASELINE

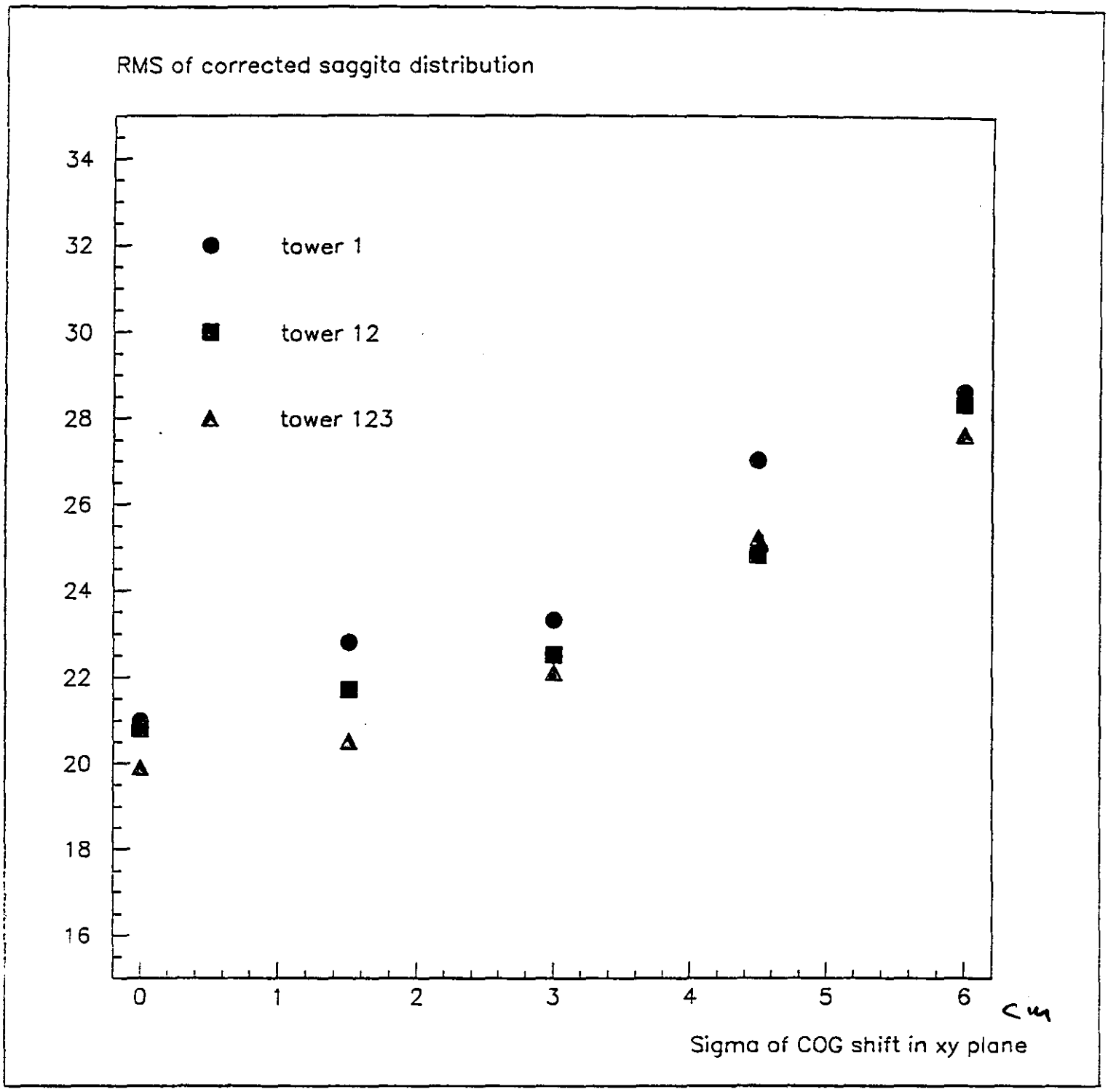

All other parameters - BASELINE

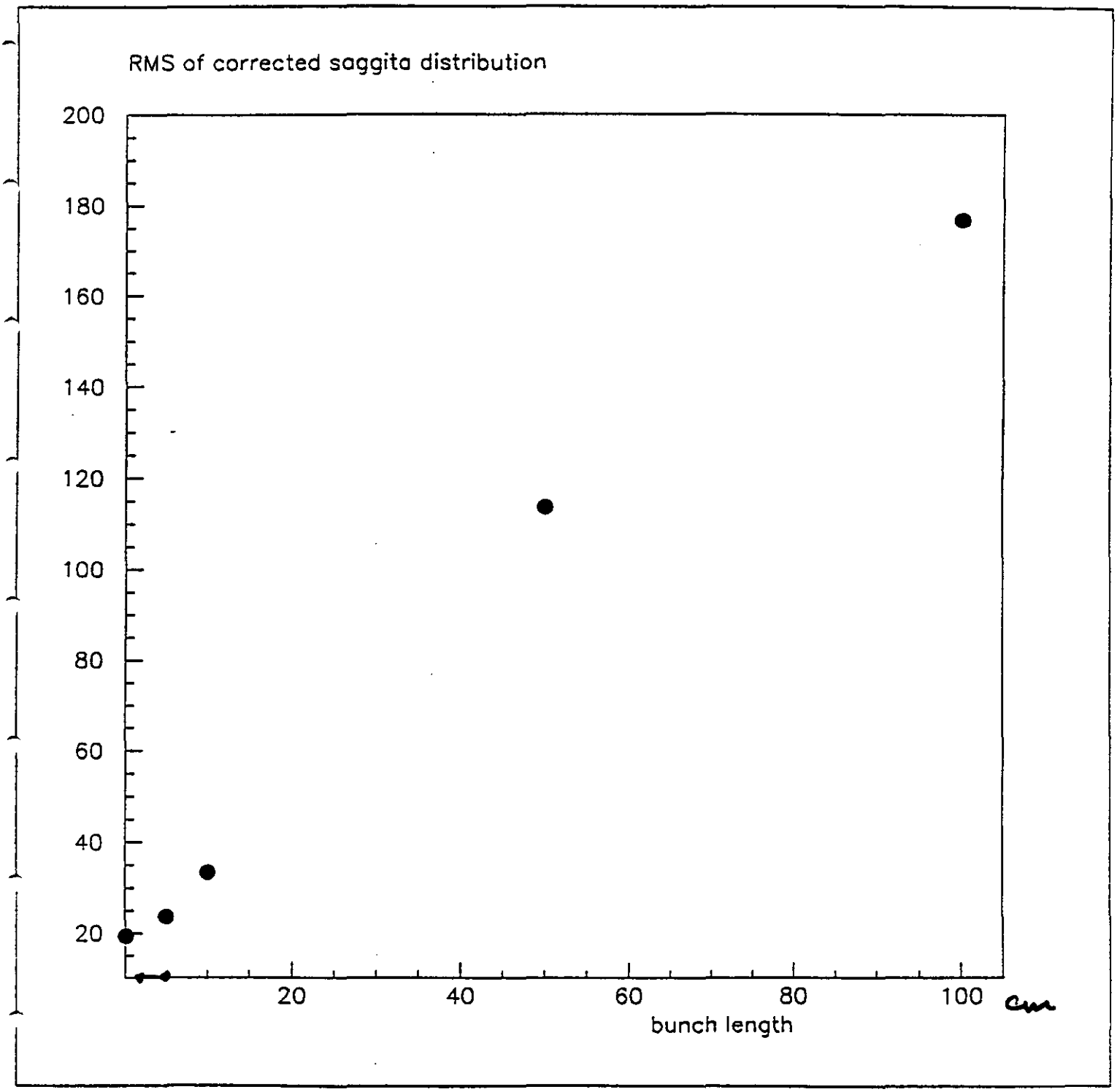

TOWER 1 — BASELINE

Conclusion

- Projective v.s. axial alignment scheme works as good as pure projective (and may be better)
- Available accuracy of axial monitors is safely below the required.
- Still to be done

  Correct endcap geometry

  Alignment of 32:32:48 configuration

SIGEM status

Yuri Fisyak

The SIGEM release 2.2 has been announced 10 days ago. This status is described in GEM TN-93-438. This release includes:

- Digitization for CSC and IPC based on program V.Cherniatin, A.Chikanian and V.Balagura
- Convolution of "trigger" event with pile-up events (on the level of HITS)
- Reconstruction as stand alone procedure which uses geometry data base (RZ-file) and input with hits (FZ-file)
- Global fit of muon track in Muon system with Central tracker. This procedure has been checked with single muon at $p_T = 25$, 100 and 1000 GeV/c. For the moment the calorimeter is considered as a passive detector. No calorimeter information is used so far in the reconstruction.

p_T−resolution for μ^+ with p_T = 25 GeV/c $N_{seg} \geq 2$

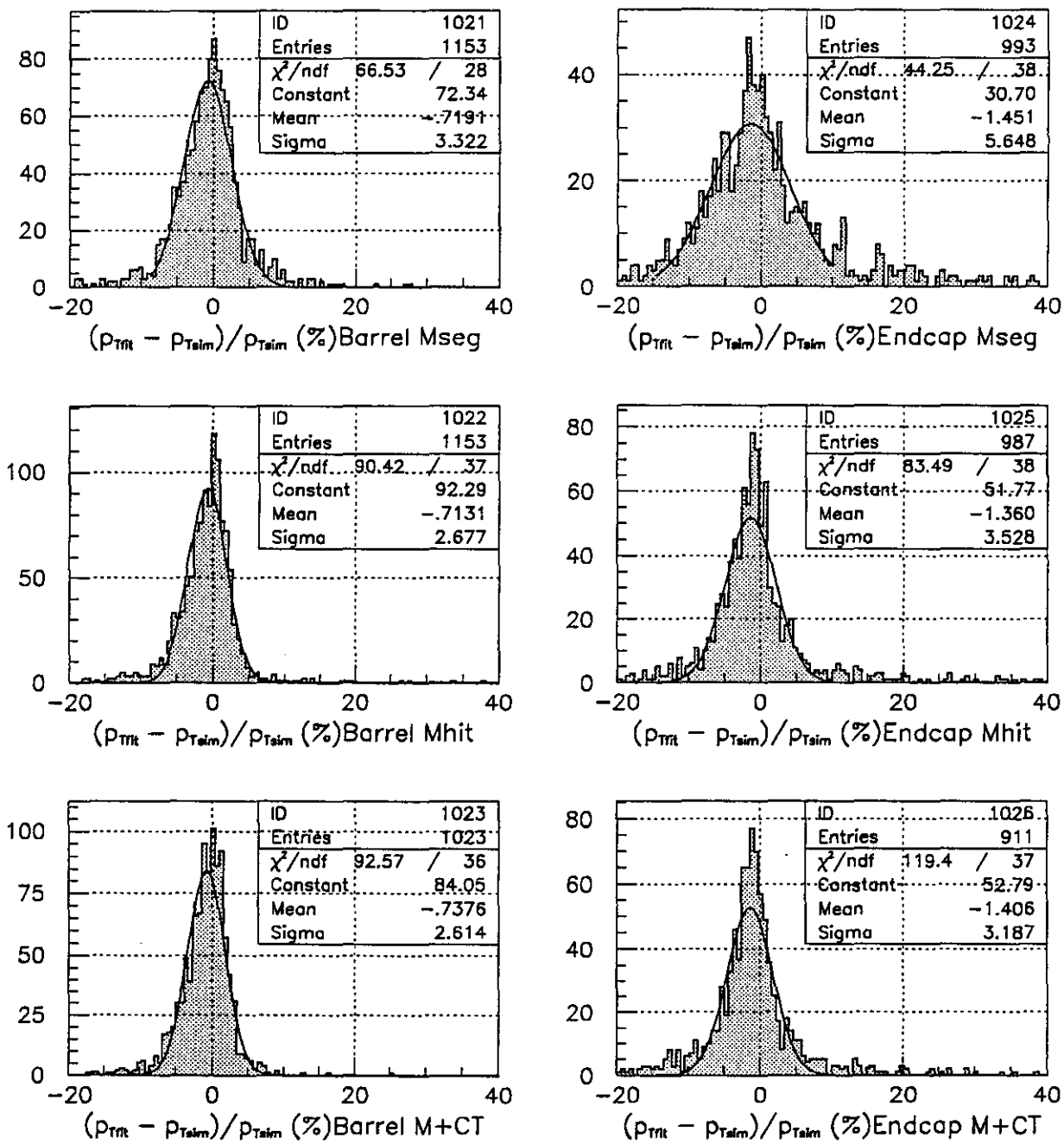

p_T−resolution for μ^+ with p_T = 25 GeV/c $N_{seg} \geqq 3$

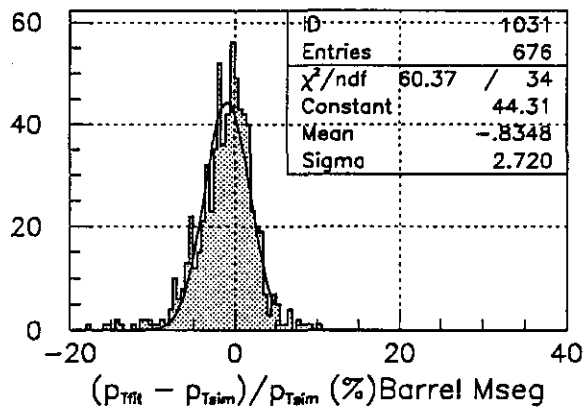

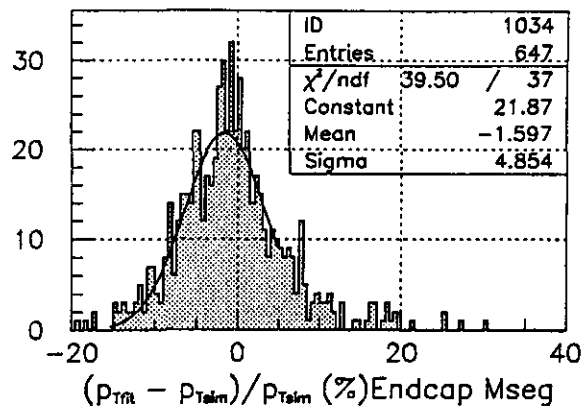

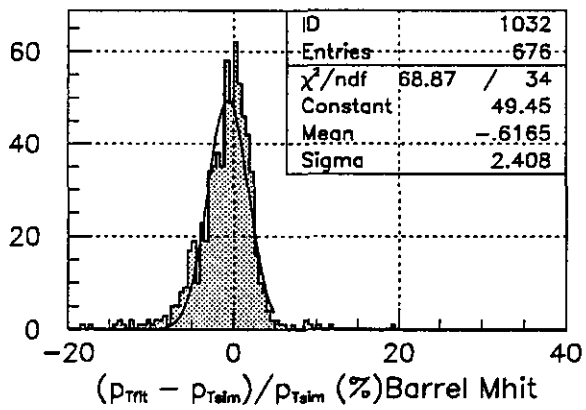

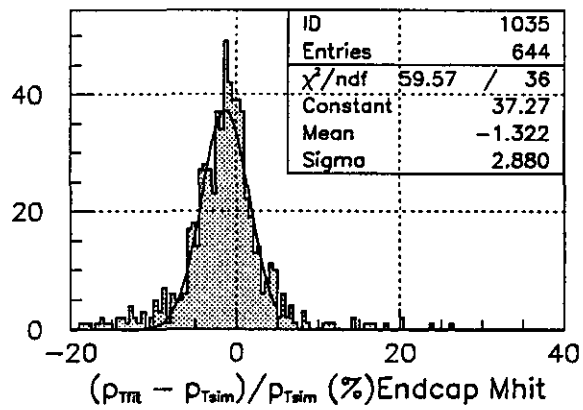

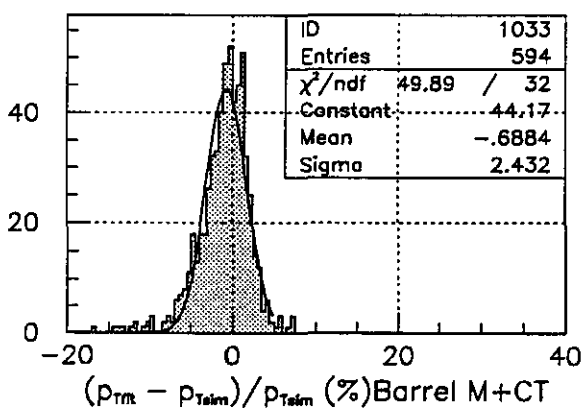

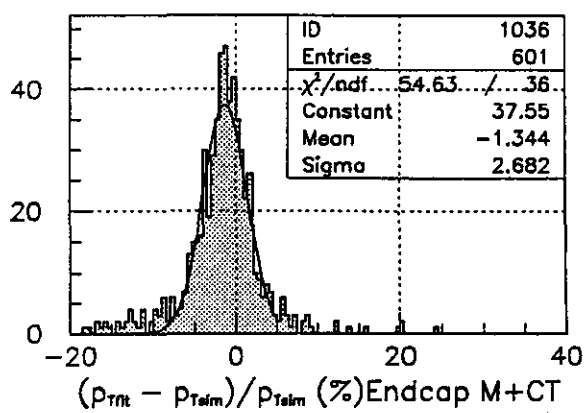

Transverse momentum pulls for μ^+ with p_T = 25 GeV/c

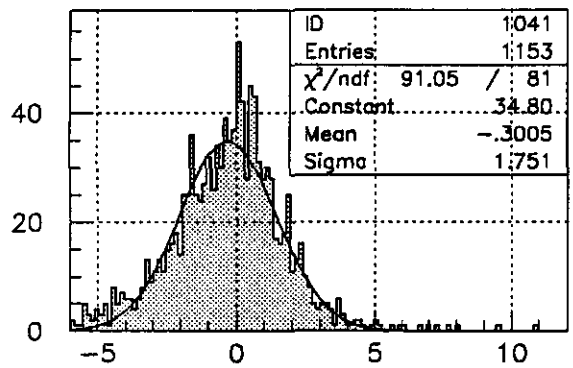

inv. momentum pull inBarrel Mseg

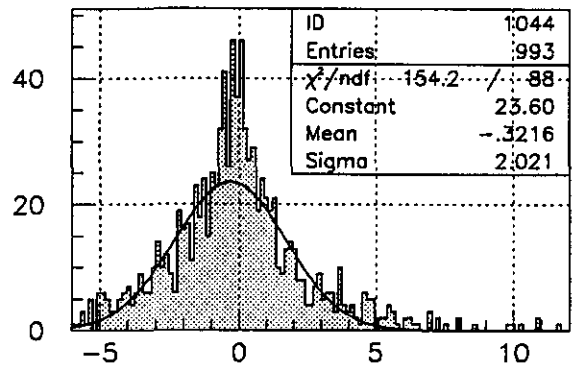

inv. momentum pull inEndcap Mseg

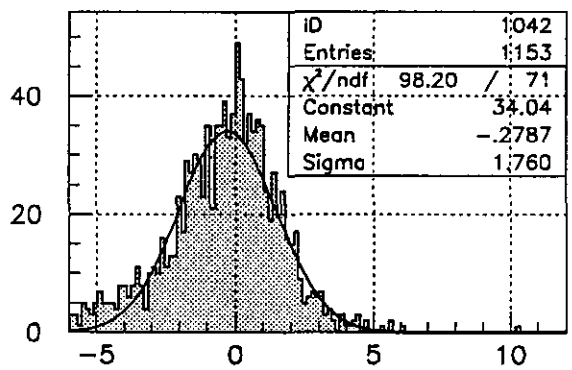

inv. momentum pull inBarrel Mhit

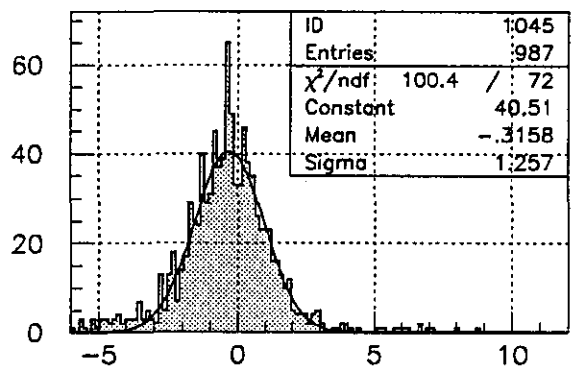

inv. momentum pull inEndcap Mhit

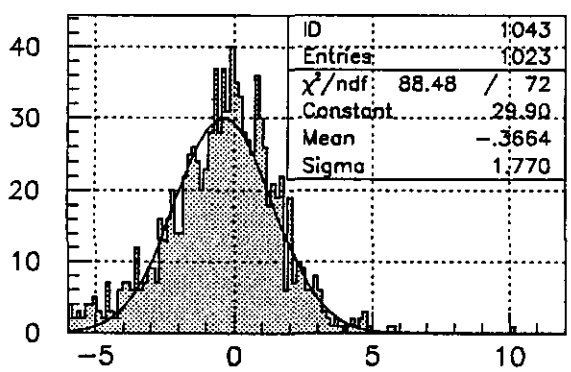

inv. momentum pull inBarrel M+CT

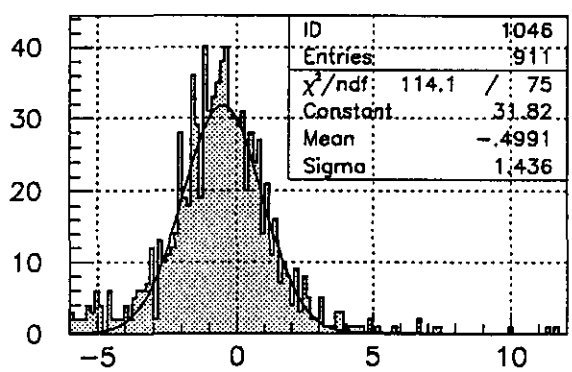

inv. momentum pull inEndcap M+CT

93/08/03 21.14

Estimated p_T resolution for μ^+ with p_T = 25 GeV/c

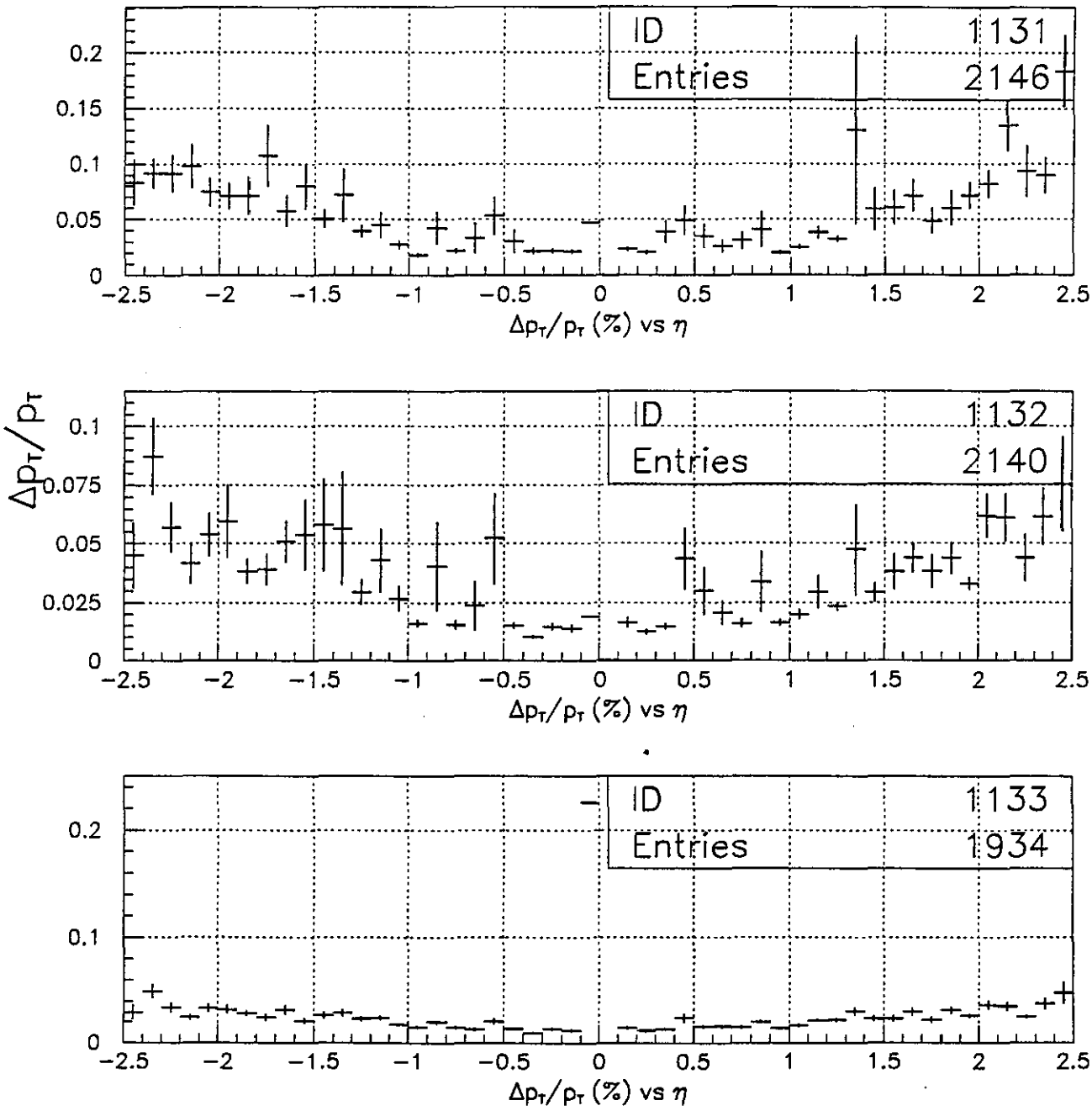

p_T−resolution for μ^+ with p_T = 100 GeV/c $N_{seg} \geqq 2$

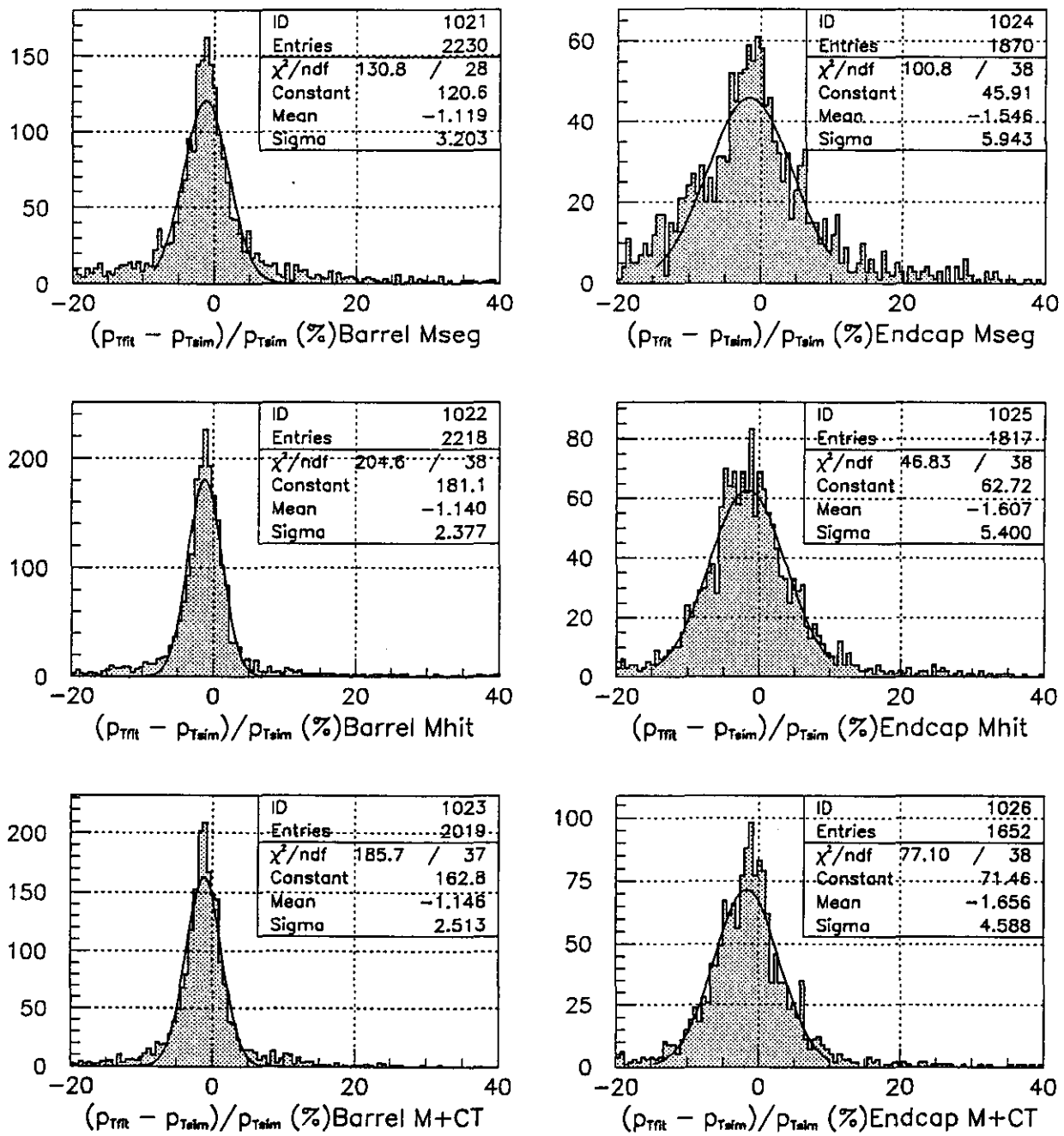

p_T−resolution for μ^+ with p_T = 100 GeV/c $N_{seg} \geq 3$

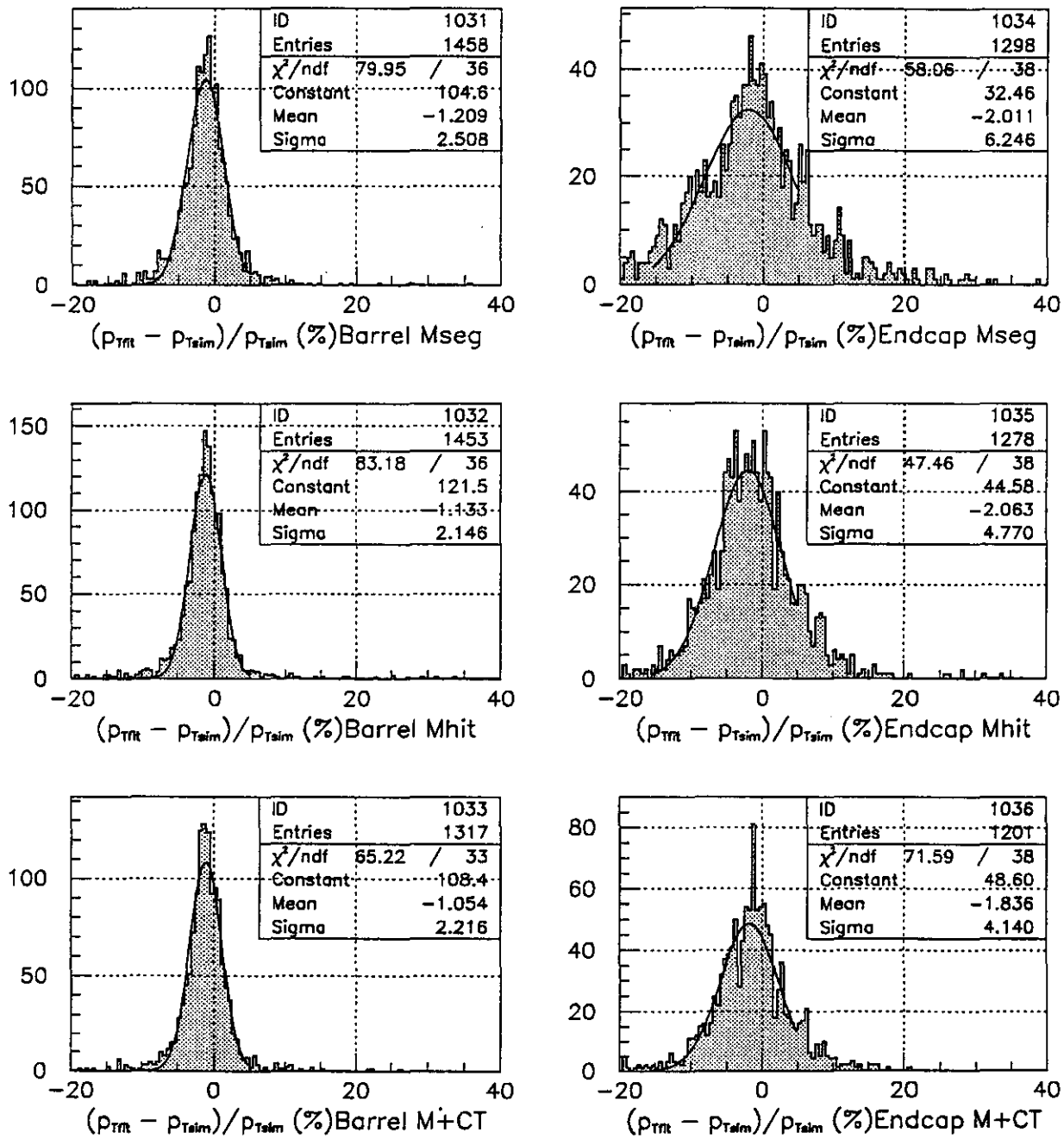

p_T pulls for μ^+ with p_T = 100 GeV/c

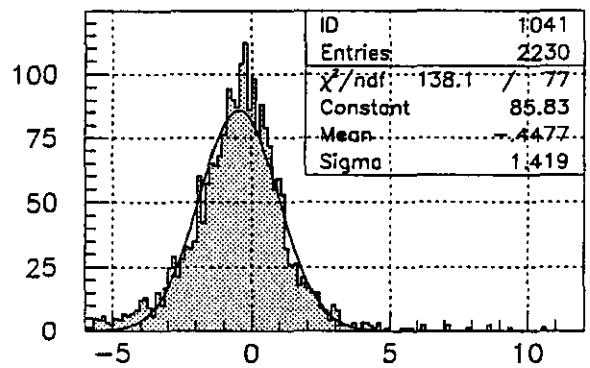

inv. momentum pull inBarrel Mseg

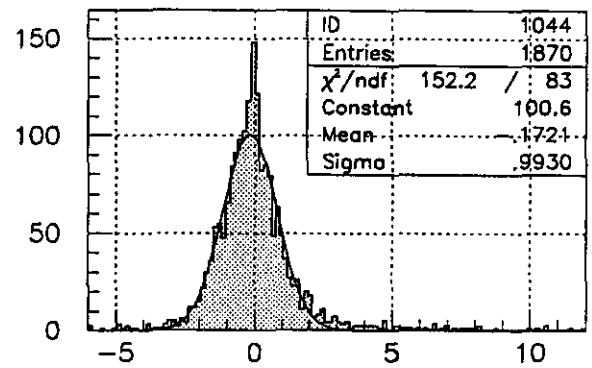

inv. momentum pull inEndcap Mseg

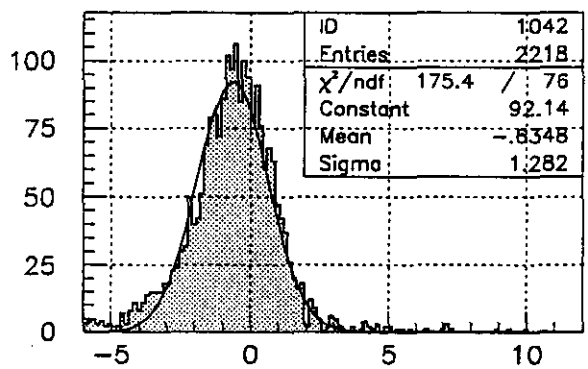

inv. momentum pull inBarrel Mhit

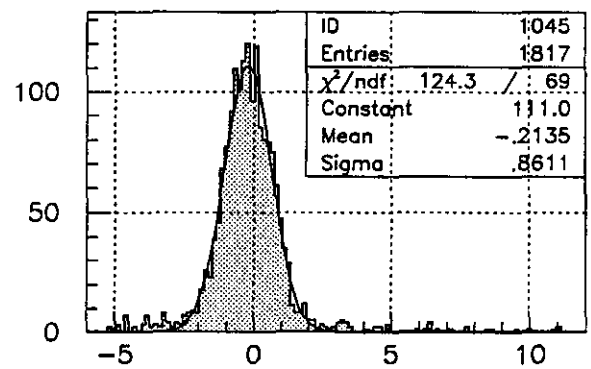

inv. momentum pull inEndcap Mhit

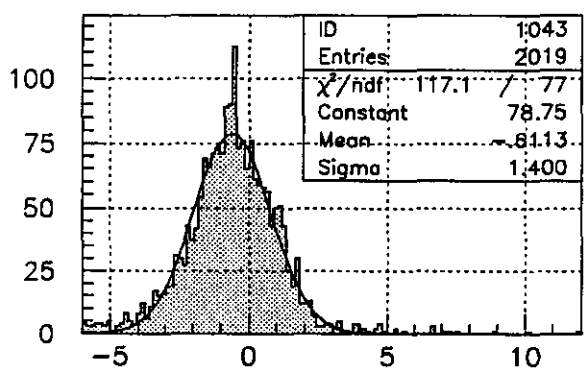

inv. momentum pull inBarrel M+CT

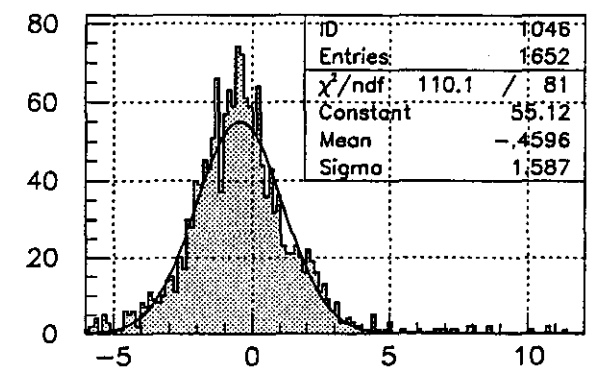

inv. momentum pull inEndcap M+CT

93/08/03 21.18

Estimated p_T resolution for μ^+ with p_T = 100 GeV/c

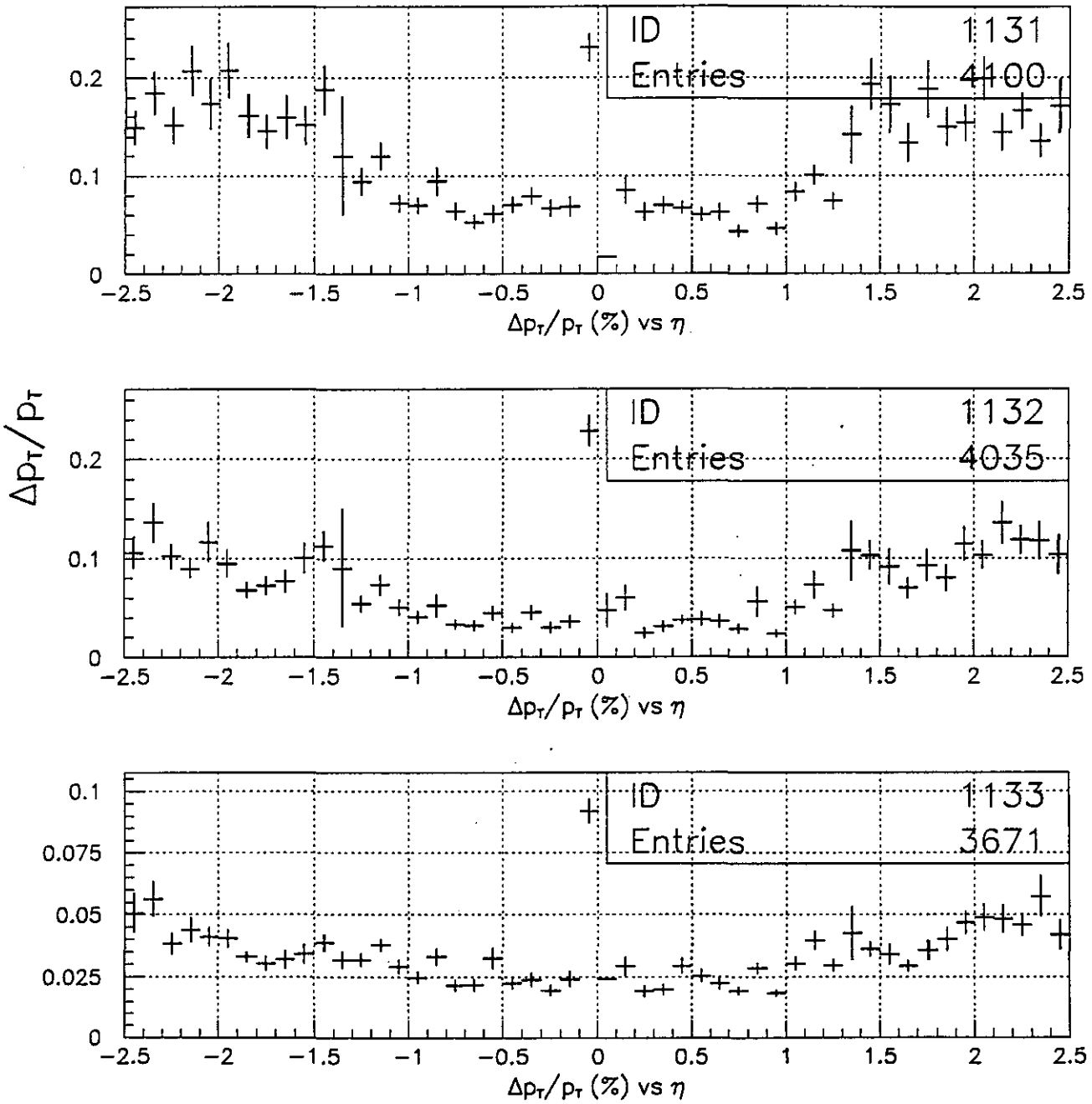

p_T−resolution for μ^+ with p_T = 1 TeV/c $N_{seg} \geqq 2$

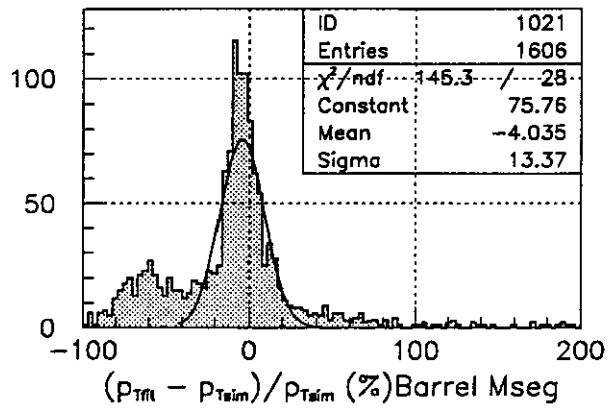

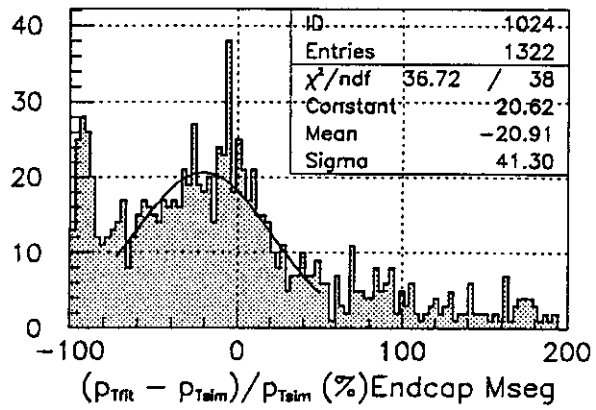

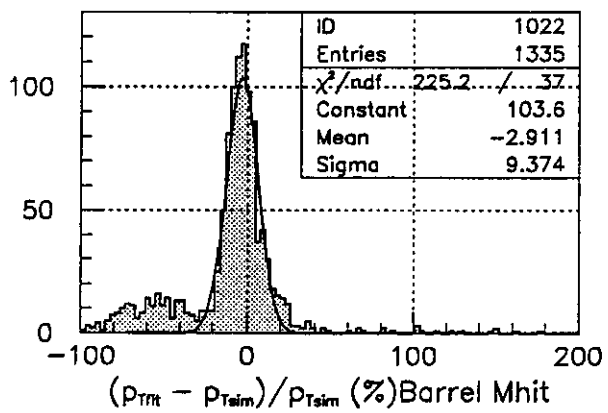

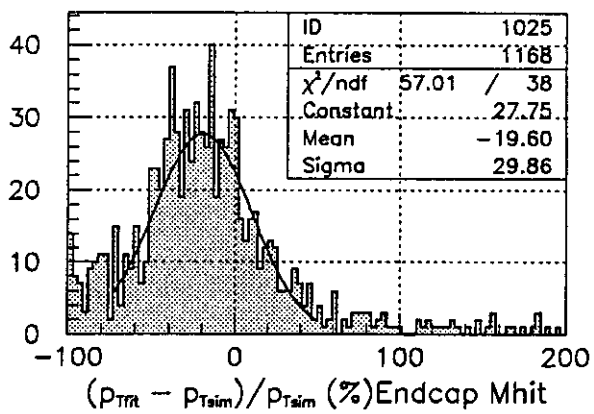

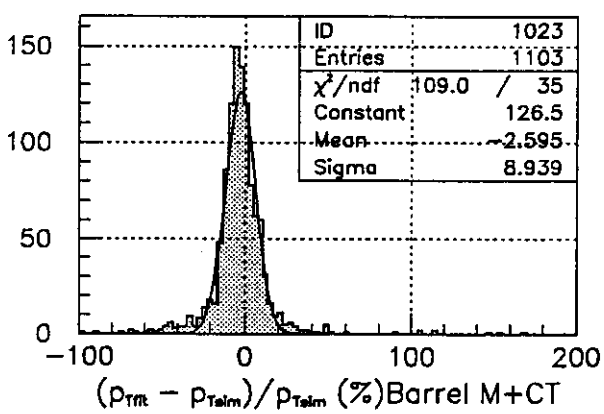

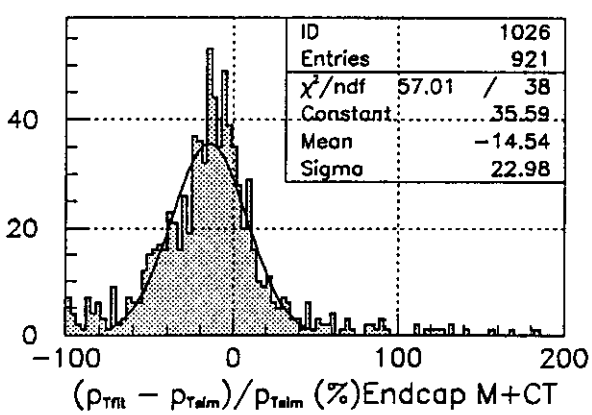

p_T−resolution for μ^+ with p_T = 1 TeV/c $N_{seg} \geqq 3$

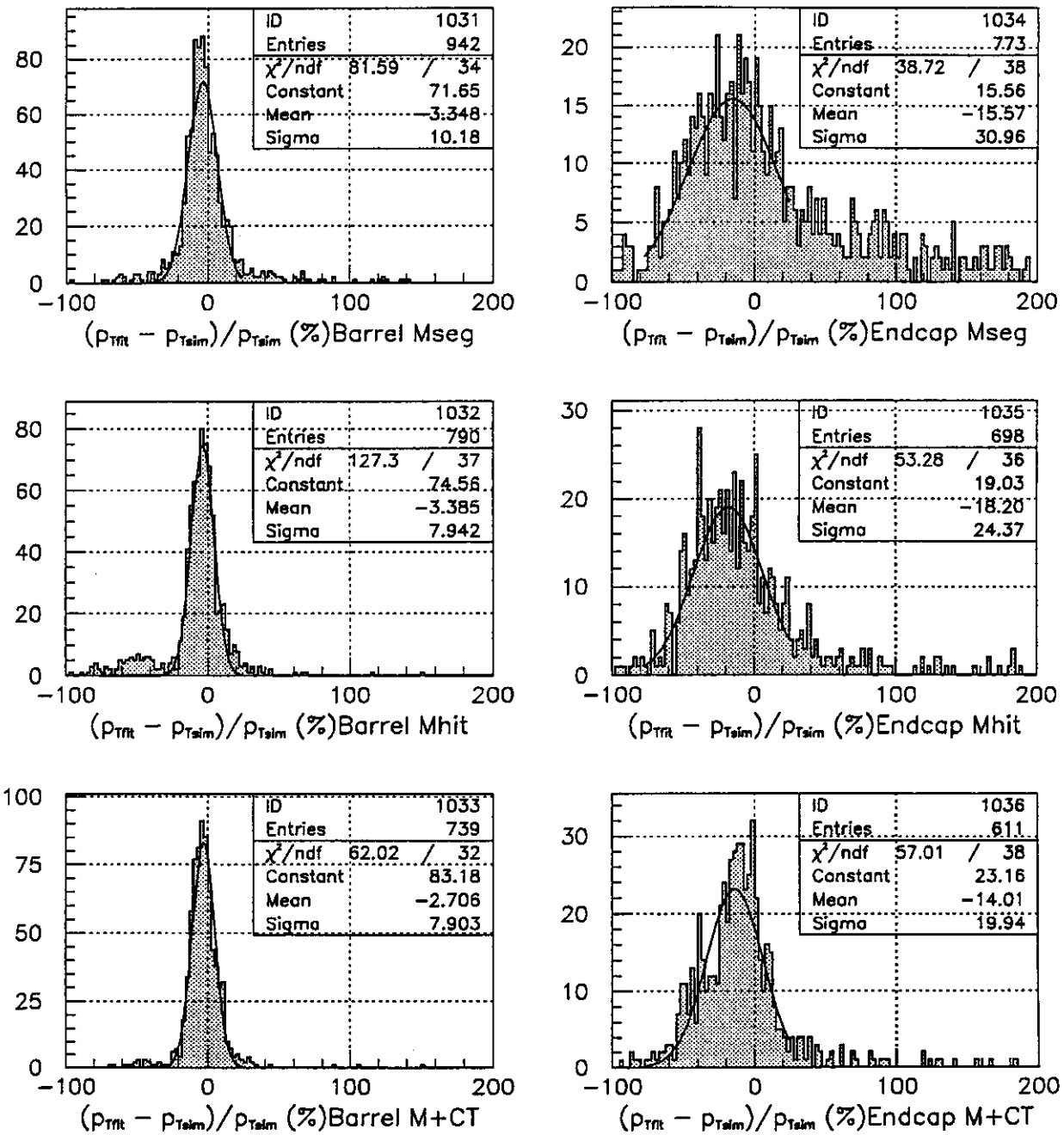

93/08/04 08.17

Fit probability for μ^+ with p_T = 1TeV/c

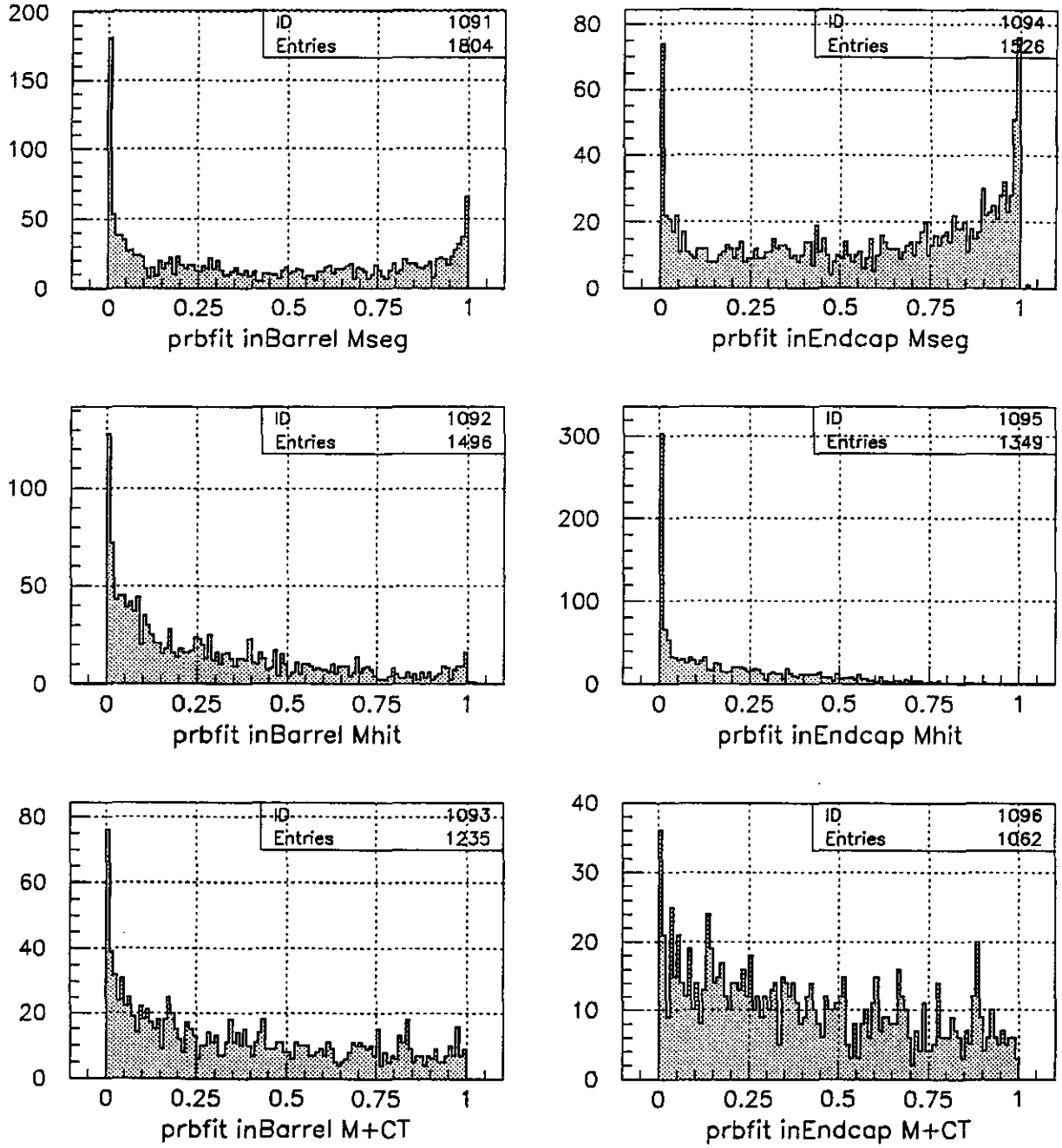

p_T pulls for μ^+ with p_T = 1 TeV/c

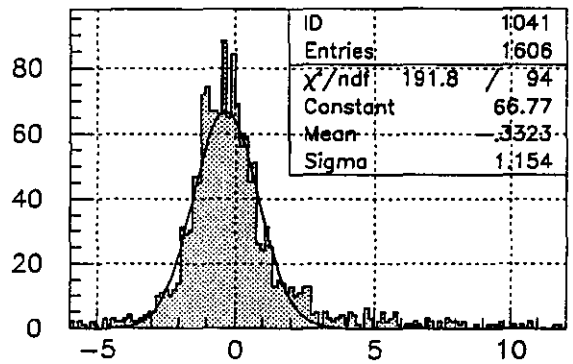

inv. momentum pull inBarrel Mseg

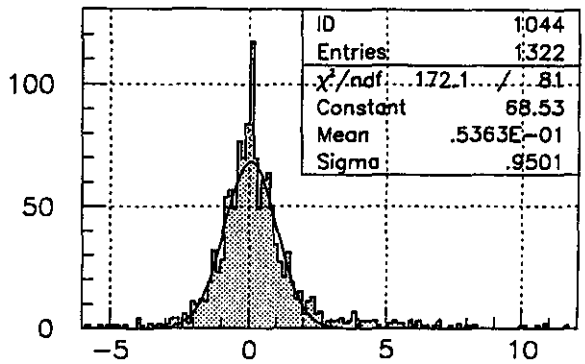

inv. momentum pull inEndcap Mseg

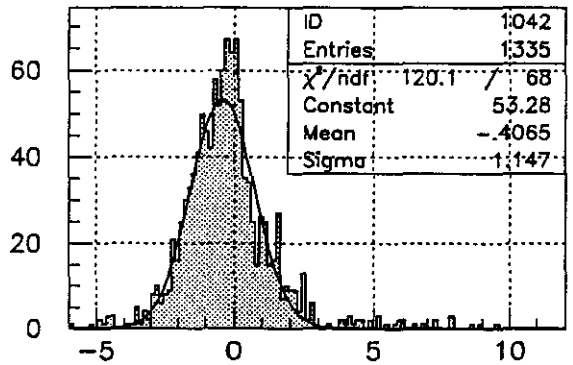

inv. momentum pull inBarrel Mhit

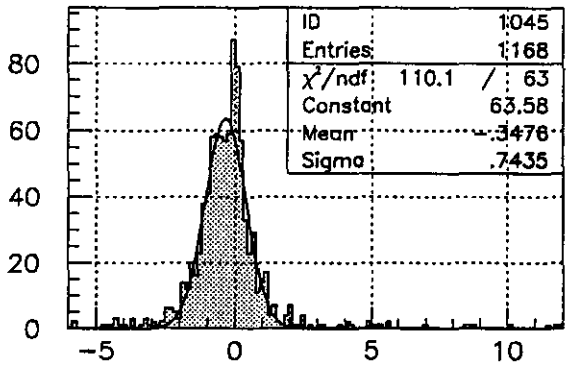

inv. momentum pull inEndcap Mhit

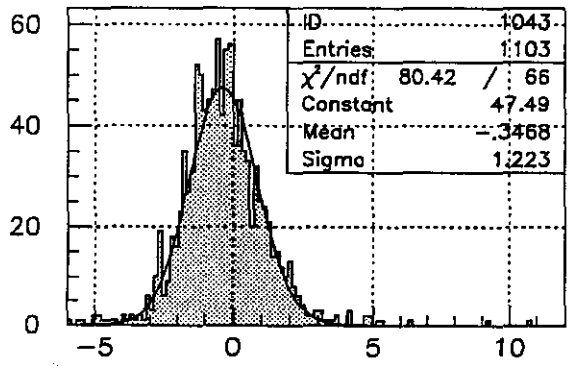

inv. momentum pull inBarrel M+CT

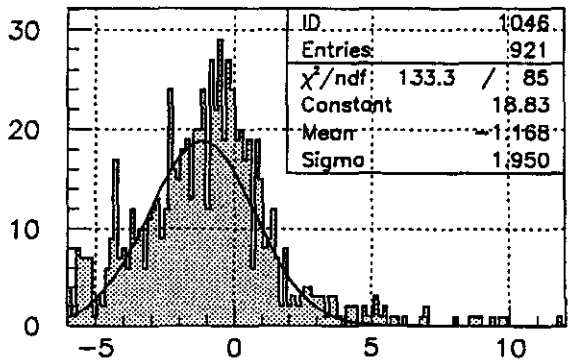

inv. momentum pull inEndcap M+CT

Estimated p_T resolution for μ^+ with p_T = 1 TeV/c

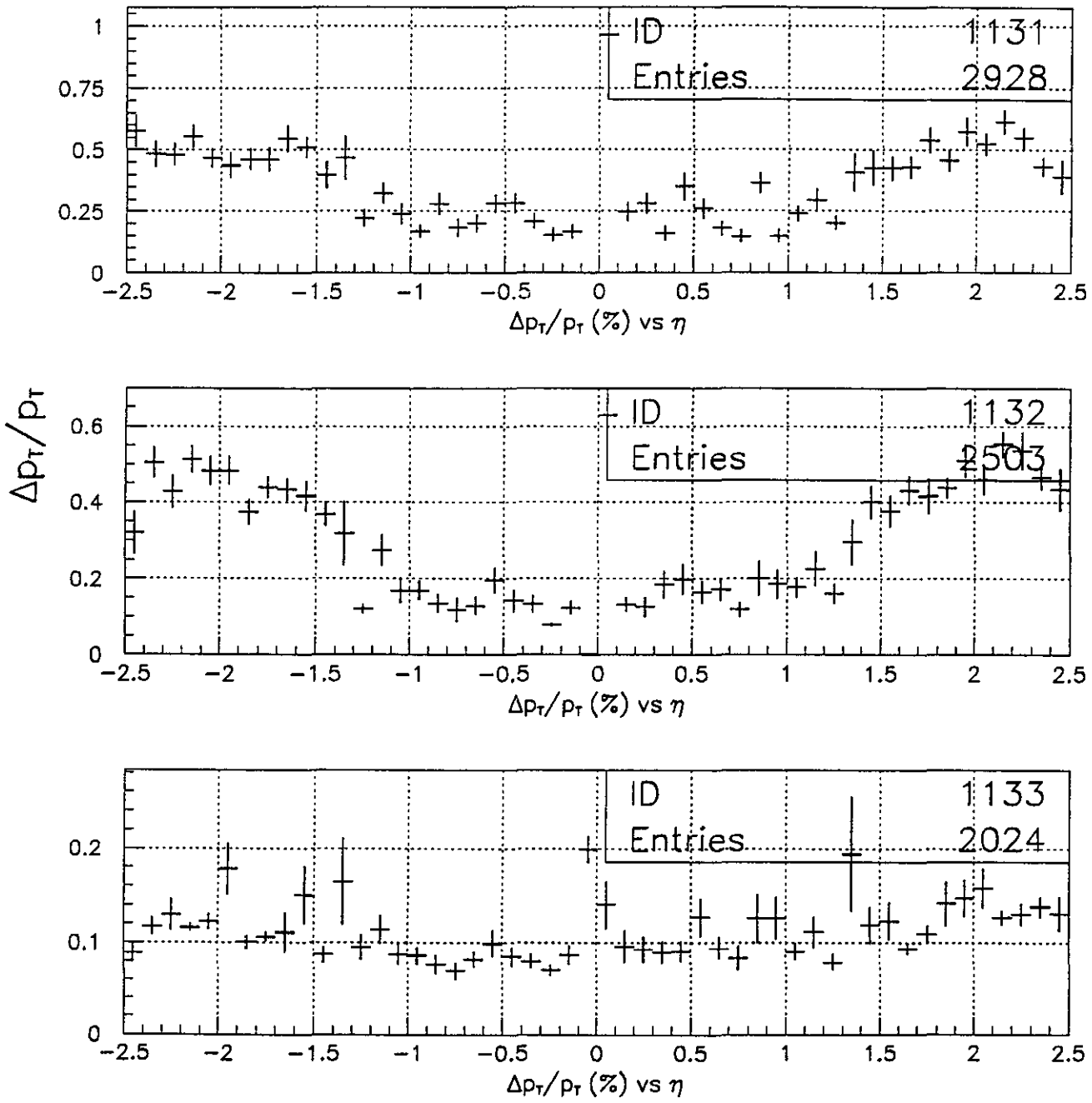

93/08/03 21.14

Efficiency for μ^+ with p_T = 25 GeV/c

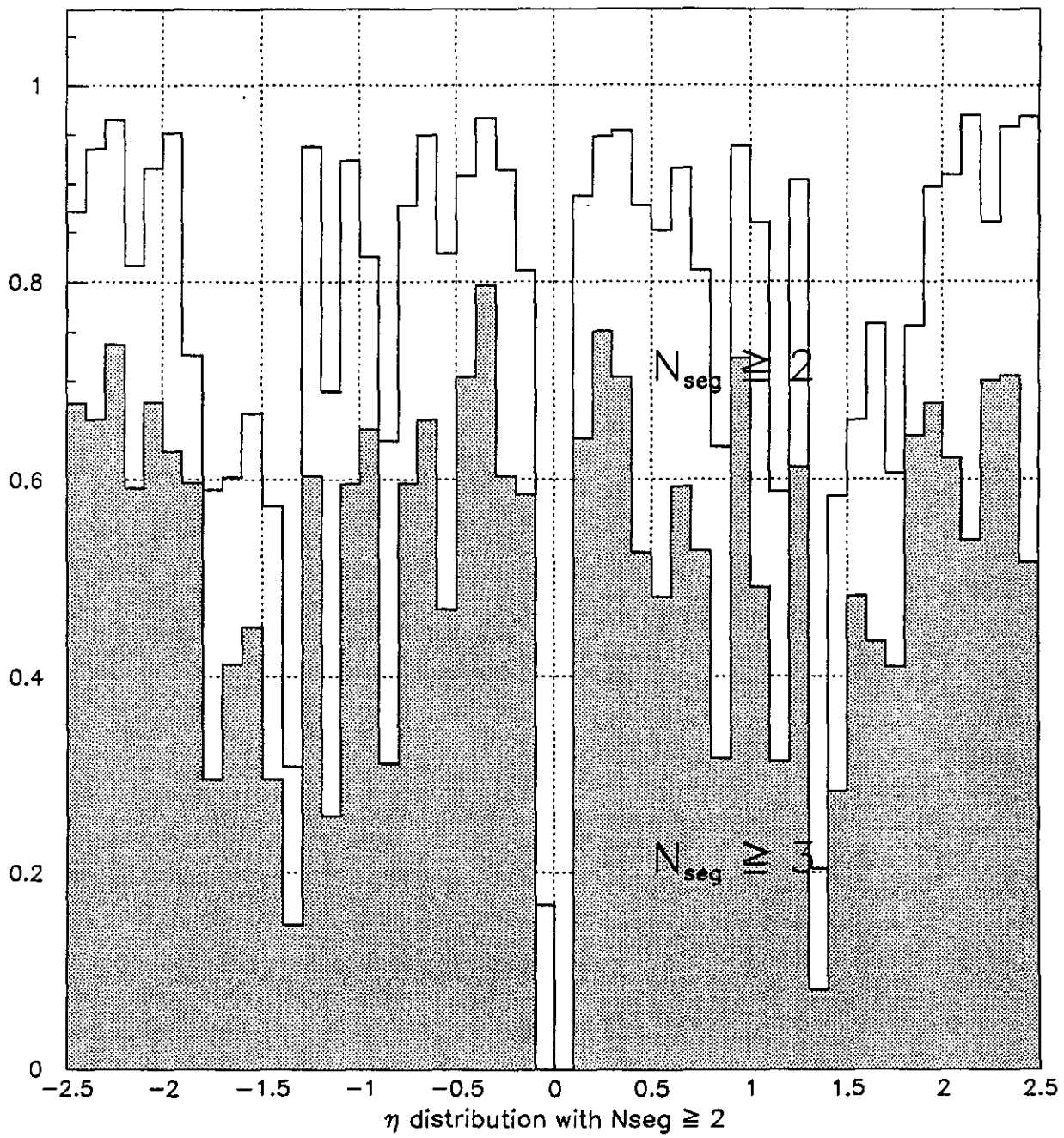

93/08/03 21.18

Efficiency for μ^+ with p_T = 100 GeV/c

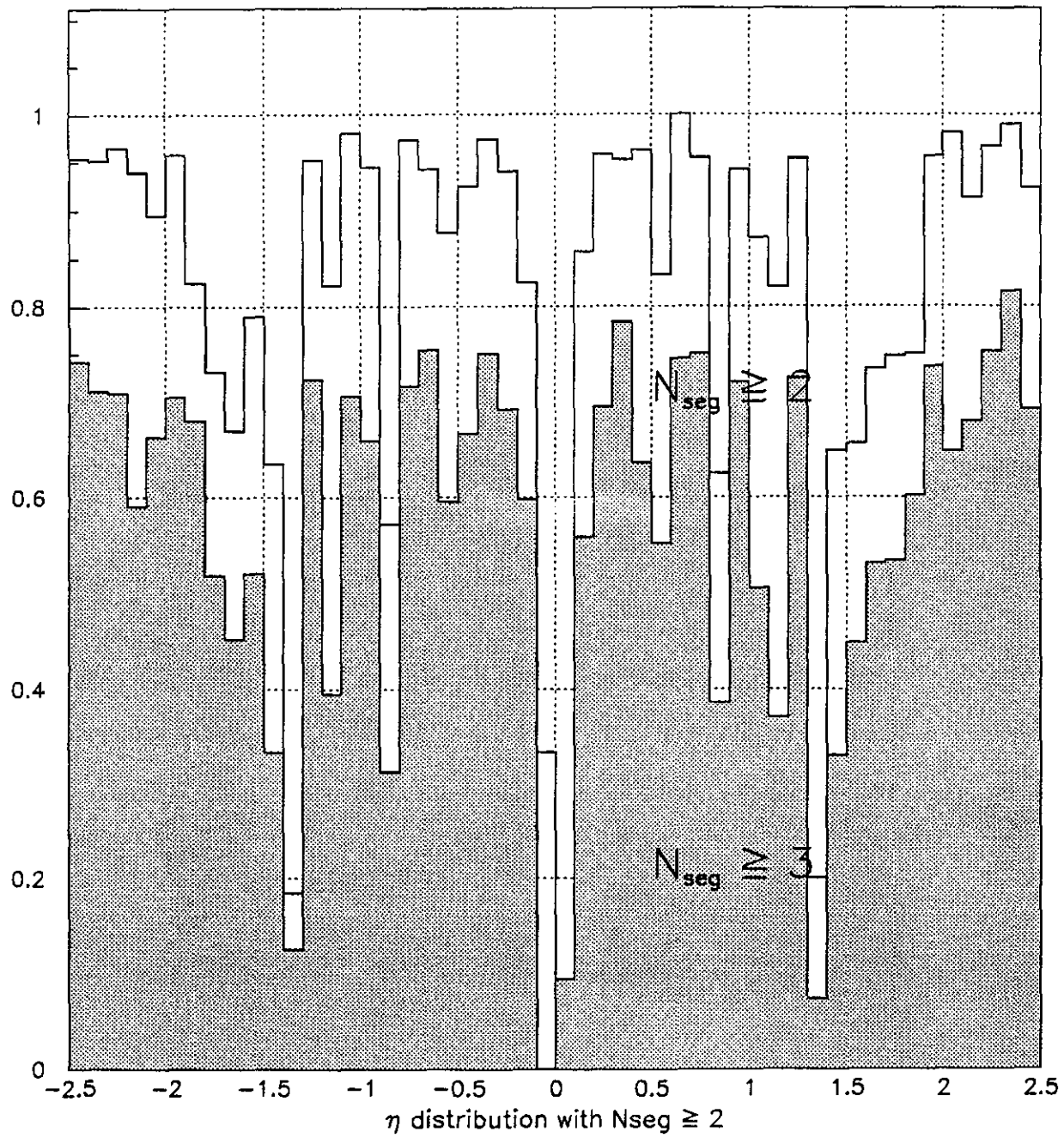

93/08/03 21.27

Efficiency for μ^+ with p_T = 1 TeV/c

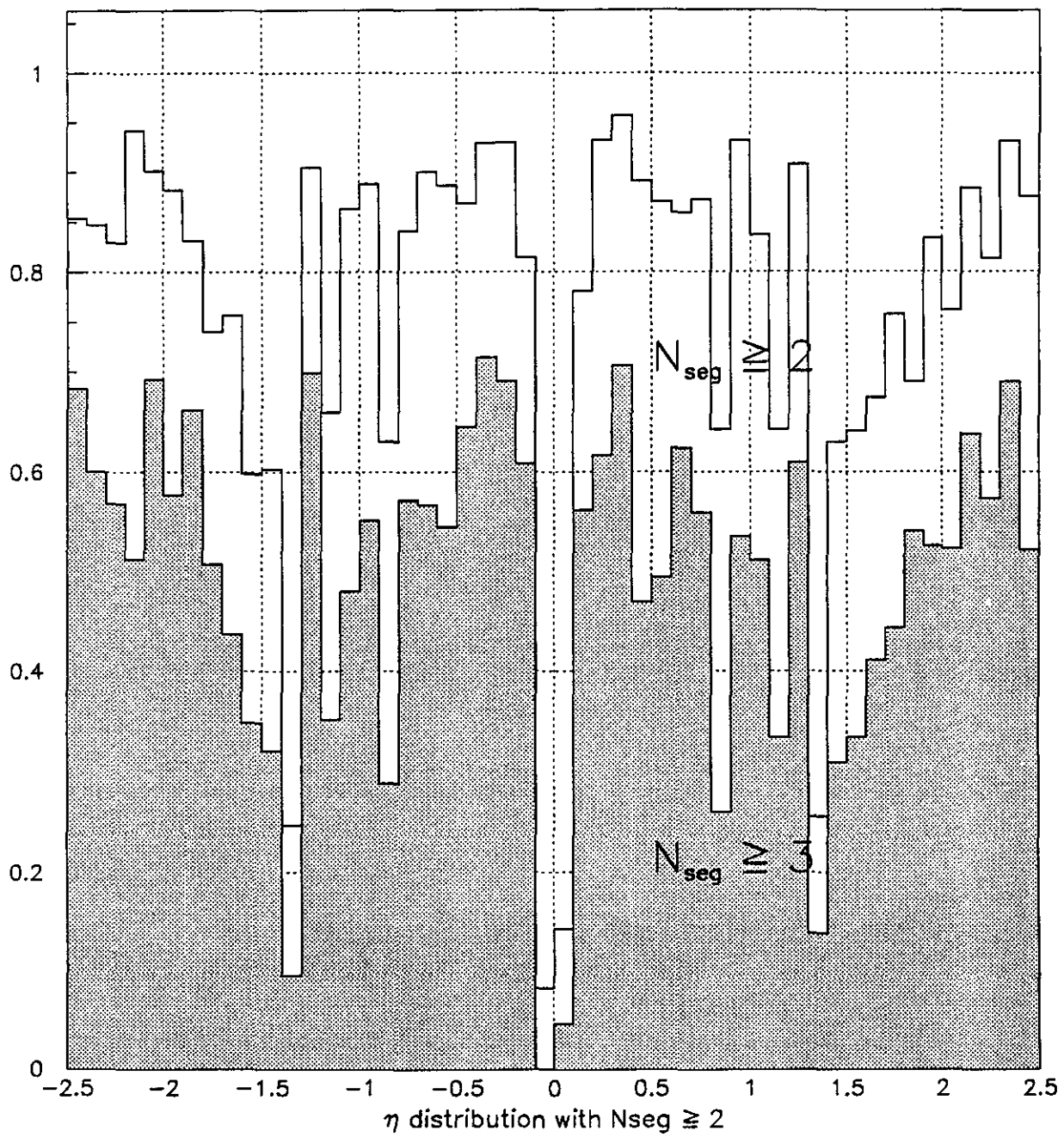

93/08/03 21.27

Impact parameter resolution for μ^+ with p_T = 1 TeV/c

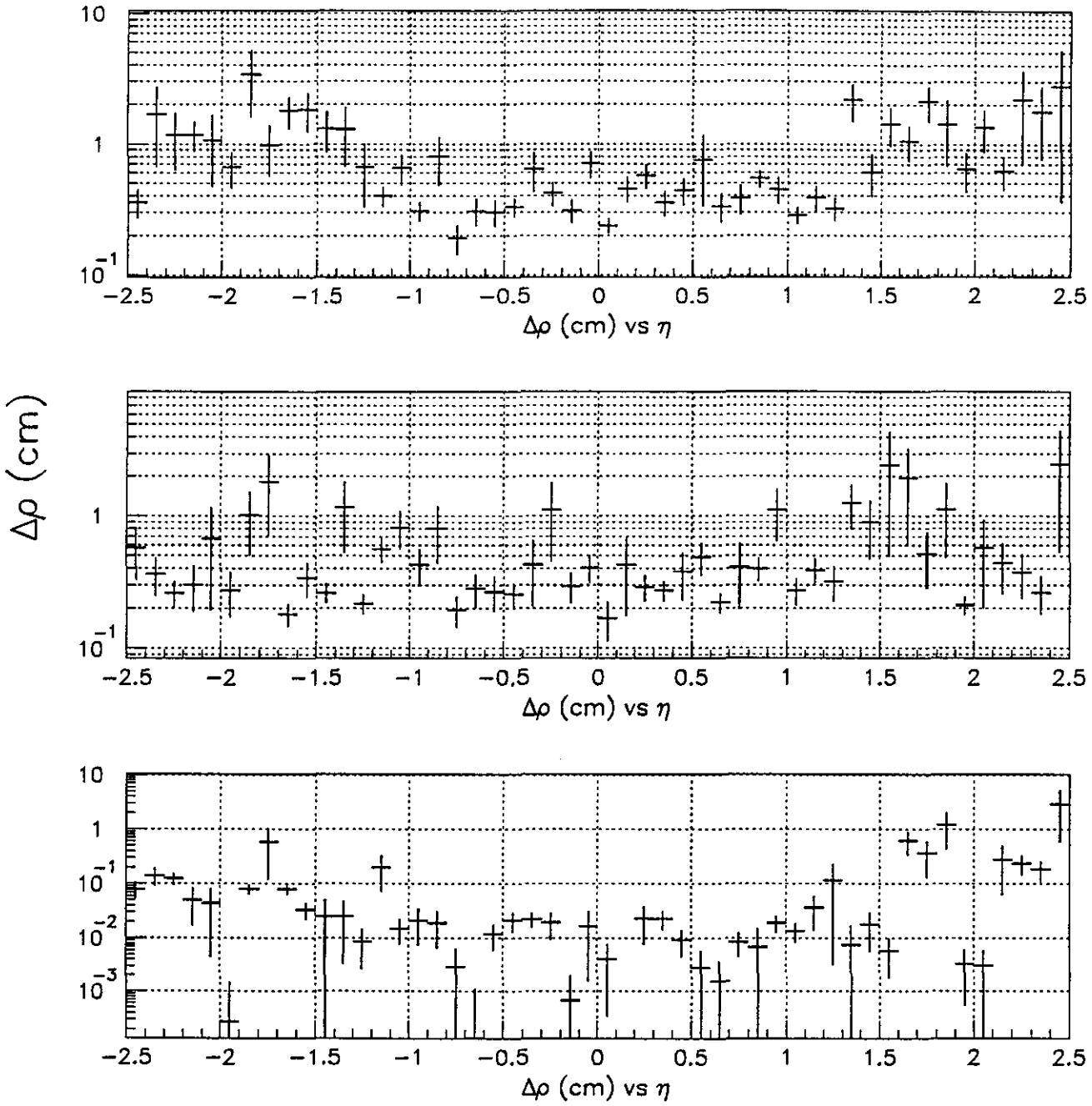

93/08/03 21.27

Z vertex resolution for μ^+ with p_T = 1 TeV/c

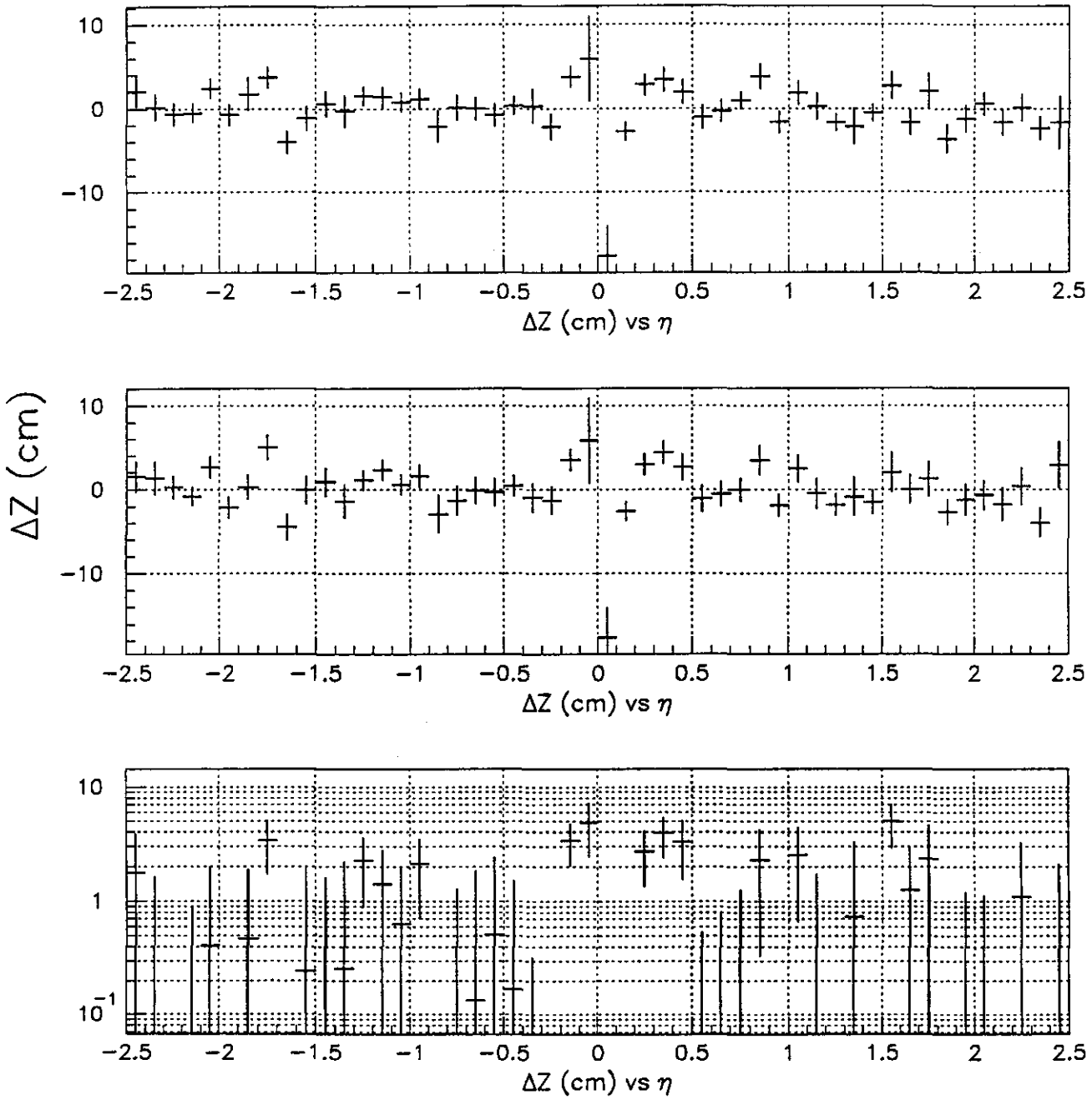

The nearest plans include:

- New baseline for Muon system. This work has been started but for the moment this baseline is too flexible. Apparently this new baseline requires some structural changing of the geometry tree — additional chamber in order to cover gaps.

- Extend reconstruction for event with more than 1 muon.

- For reconstruction it is necessary to introduce and to fix data structure tree and "title" constant structure. Presumably it will be Zebra structure. I am contacting with SDC to try understand what we can use from their experience. This has to be completed as a creation of GEM data base "prototype".

- Recover the calorimeter as an active detector. This requires using of new GEANT 3.20. This work has been started.

μ STUDIES UPDATE

- ACCEPTANCE

  SIGEM v2.1

- μ RECONSTRUCTION RESULTS
  - $H \to 4\mu$ ACCEPTANCE
    - 150, 400, 800 GeV
    - v2.1 + CLOSING OF CRACKS
    - TRIPLETS, DOUBLETS, CT
  - $H \to 4\mu$ RESOLUTION
    - ΔM_H, 150 GeV
    - μ RESOLUTION

- E LOSS CORRECTION

TORRE WENAUS
LLNL

4 AUG 92

SIGEM v2.1 BUG

$P_T = 100$ GeV

$\theta = 14°$

Gaps in phi

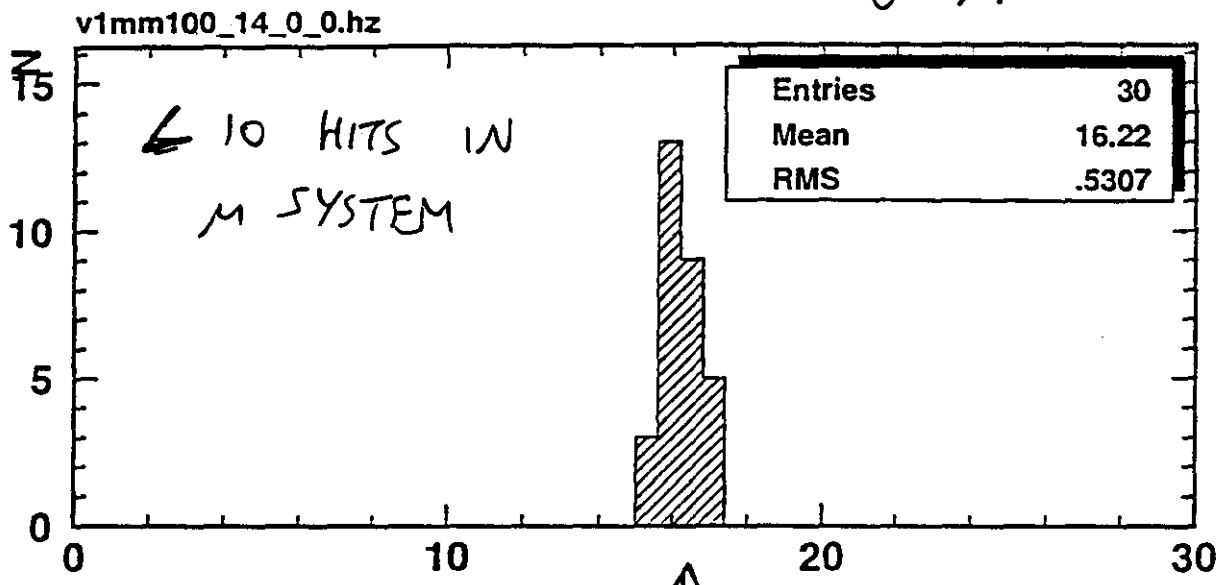

!!

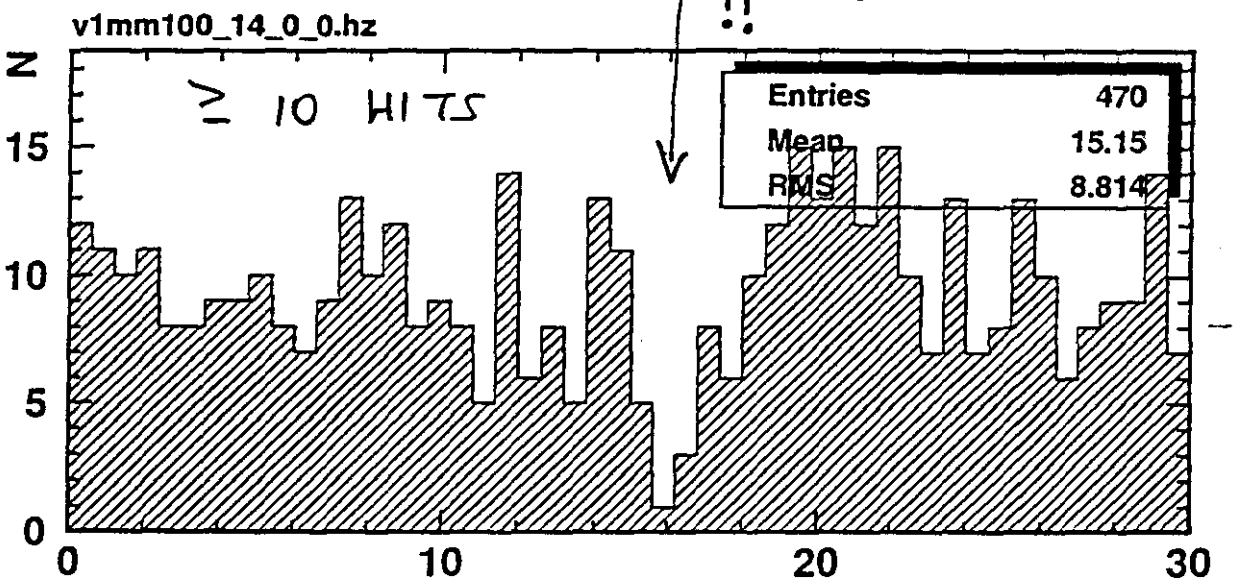

mod (φ, 30°)

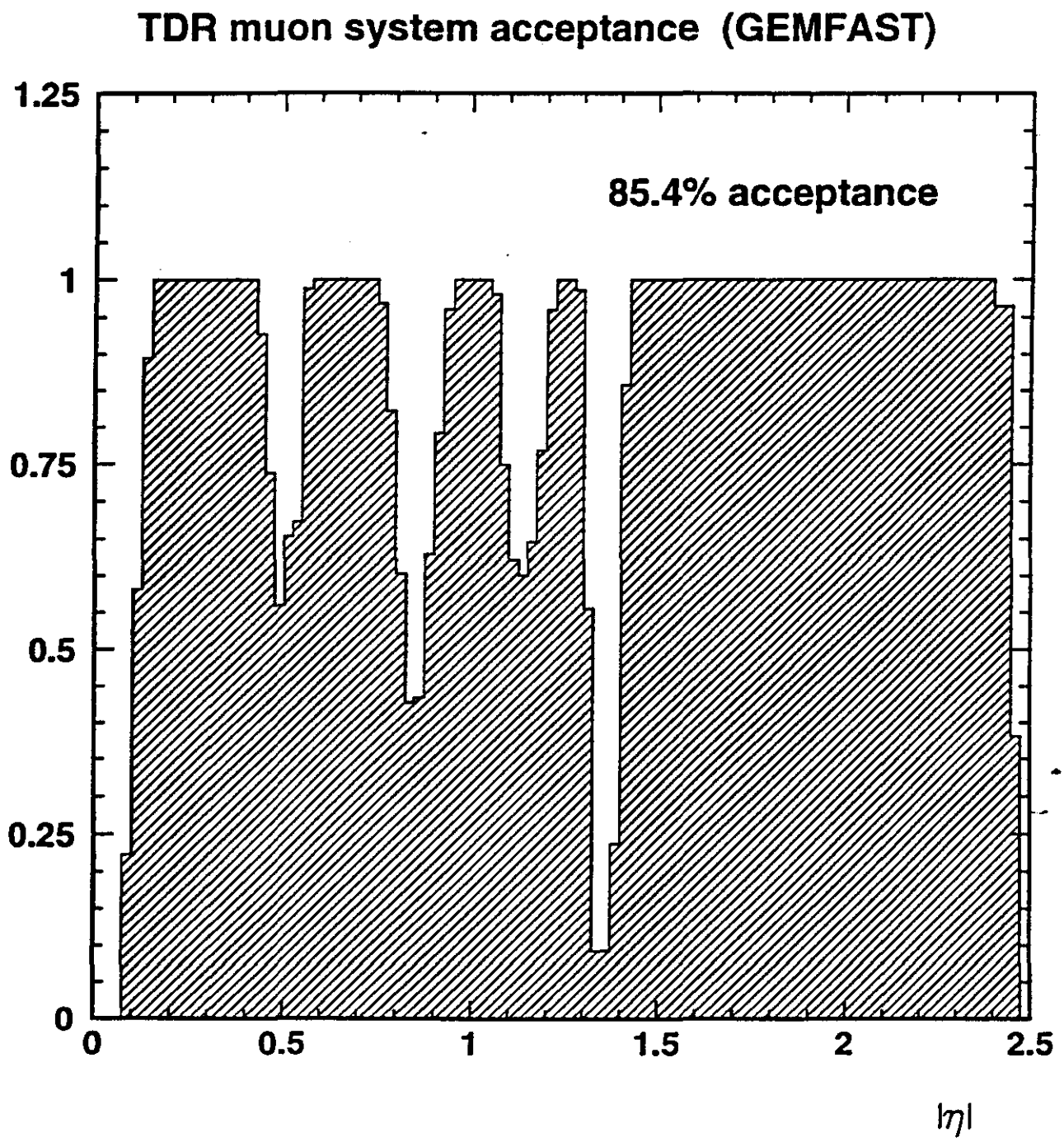
TDR muon system acceptance (GEMFAST)
85.4% acceptance
1.25
1
0.75
0.5
0.25
0
0
0.5
1
1.5
2
2.5
|η|

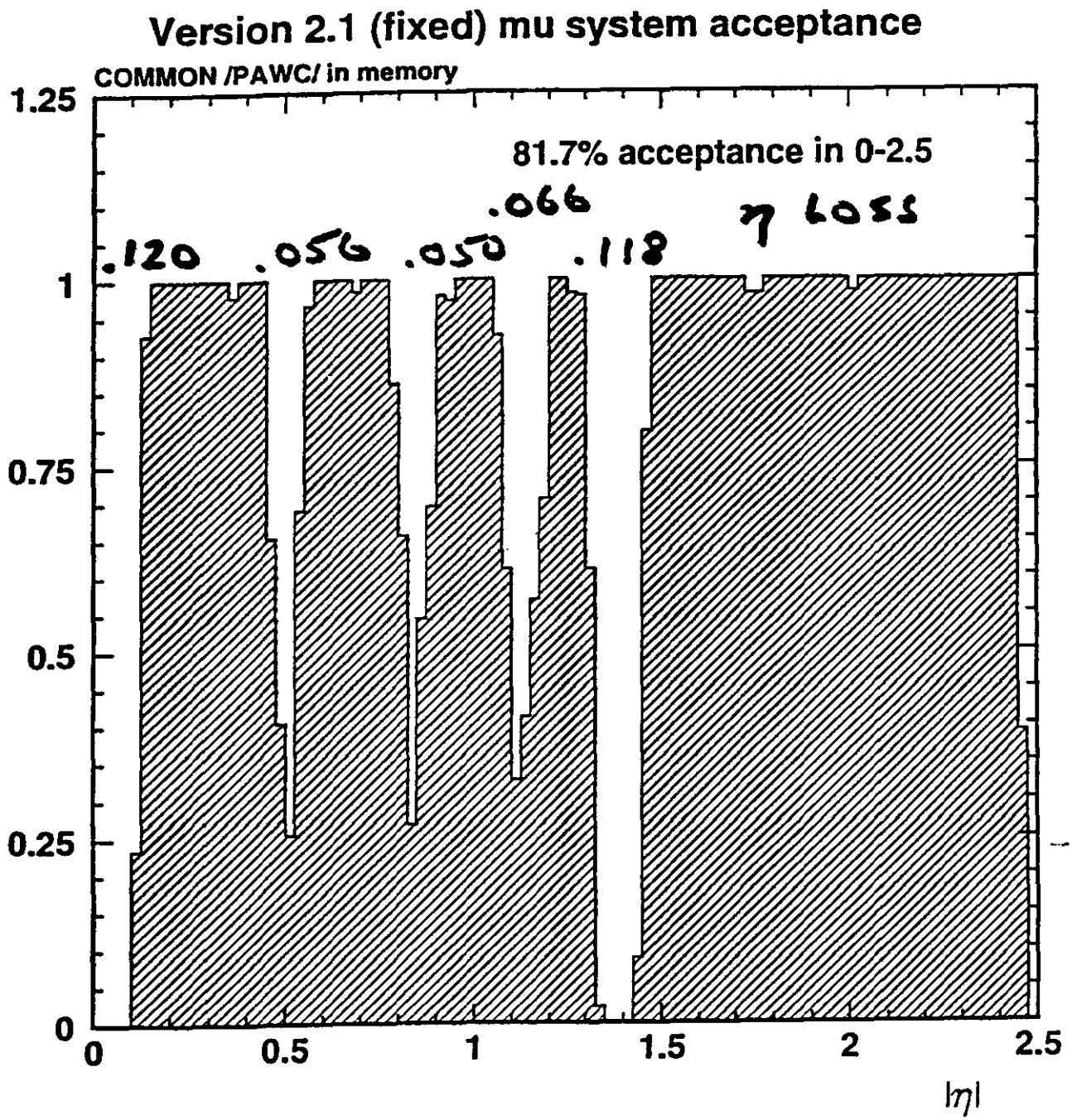
Version 2.1 (fixed) mu system acceptance
COMMON /PAWC/ in memory
81.7% acceptance in 0-2.5
.120
.056
.050
.066
.118
η loss
1.25
1
0.75
0.5
0.25
0
0
0.5
1
1.5
2
2.5
|η|

T. Wenaus 7/93

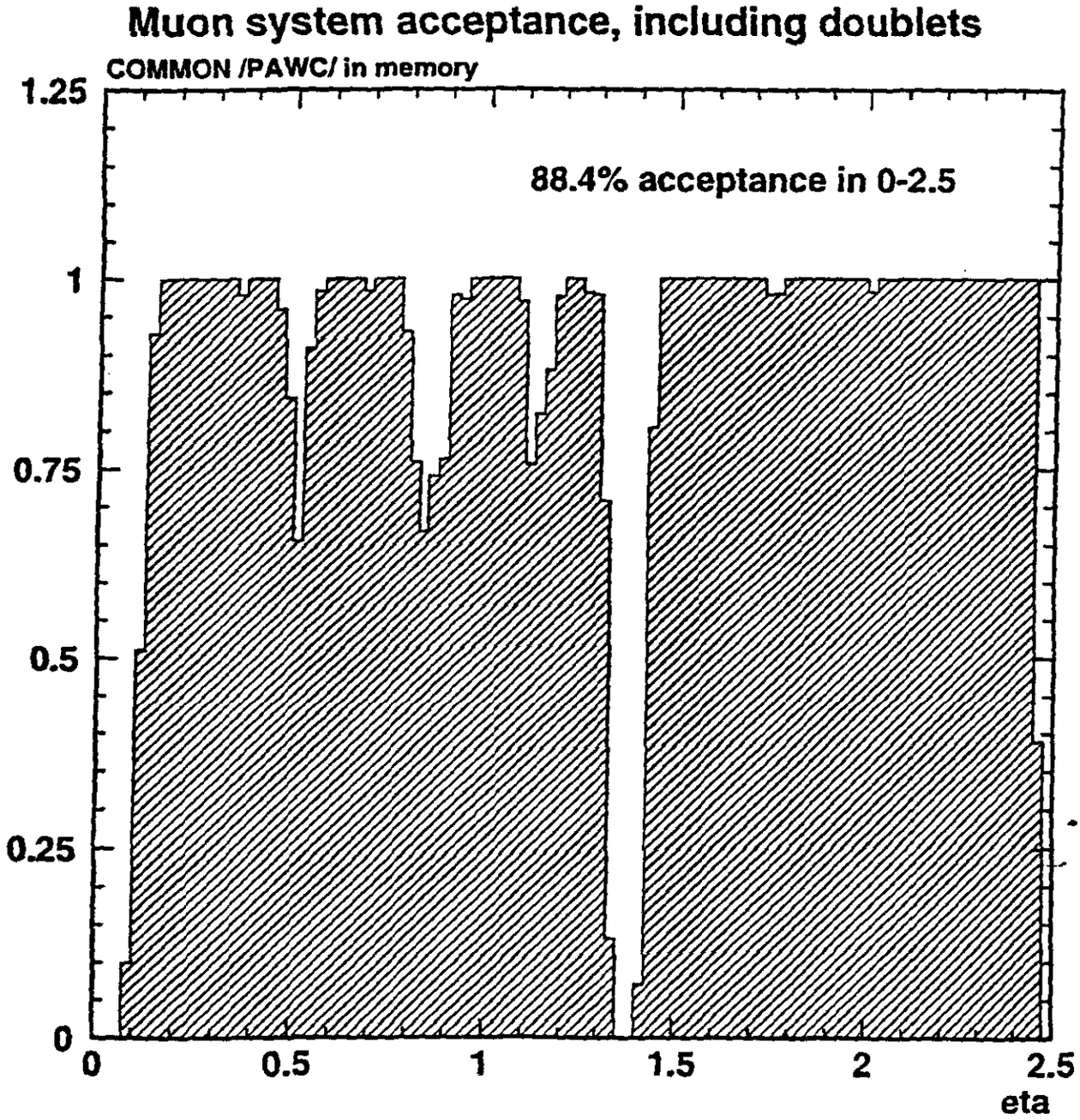
Muon system acceptance, including doublets
COMMON /PAWC/ in memory
88.4% acceptance in 0-2.5
1.25
1
0.75
0.5
0.25
0
0
0.5
1
1.5
2
2.5
eta

$H \to 4\mu$

COVERAGE RESULTS FROM FULL RECONSTRUCTION OF $H \to 4\mu$

DETECTOR MODEL: SLGEM v2.1 (FIXED)
1000 EVS.

150 GeV HIGGS

4μ WITH $|\eta| < 2.46$: 50% OF EVENTS IN 4π

COVERAGE WITHIN $|\eta| < 2.46$:

	TDR	v2.1	+BAR	+CDS	+30°	+BAR,30°	+BAR,CDS
3 SL	43%	36%	56%	48%	49%	73%	75%
2,3 SL	54%	55%	63%	71%	69%	78%	81%
3 SL + CT	80%	60%	83%	68%	68%	91%	90%
2,3 SL + CT	87%	90%	93%	96%	95%	97%	98%

(*)

(*) MODIFIED v2.1 GEOM:

+BAR : FULL ACCEPTANCE BARREL. NO PROJ ALIGN GAPS

+CDS : FULL COVERAGE AT $\eta = 0$

+30° : " " AT BAR/CAP INTERFACE

400 GeV

~~70%~~ 61% OF EVS IN $\eta < 2.46$

	v2.1	+BAR	+CDS	+30°	+BAR,30°	+BAR,CDS
3 SL	35%	53	51	46	67	76
2,3 SL	56	63	77	66	74	86
3 SL + CT	57	78	66	66	87	87
2,3 SL + CT	88	92	97	93	96	98

800 GeV

70% OF EVS IN $\eta < 2.46$

	TDR	v2.1	+BAR	+CDS	+30°	+BAR,30°	+BAR,CDS
3 SL	47%	33	55	48	44	70	75
2,3 SL	59	56	64	74	68	77	84
3 SL + CT	83	58	81	65	65	89	88
2,3 SL + CT	89	90	94	96	94	97	98

⇒ CLOSURE OF ALIGNMENT GAPS

IMPROVES TRIPLET COVERAGE 1.6 x

CLOSURE OF 30° AS WELL IMPROVES 2 x

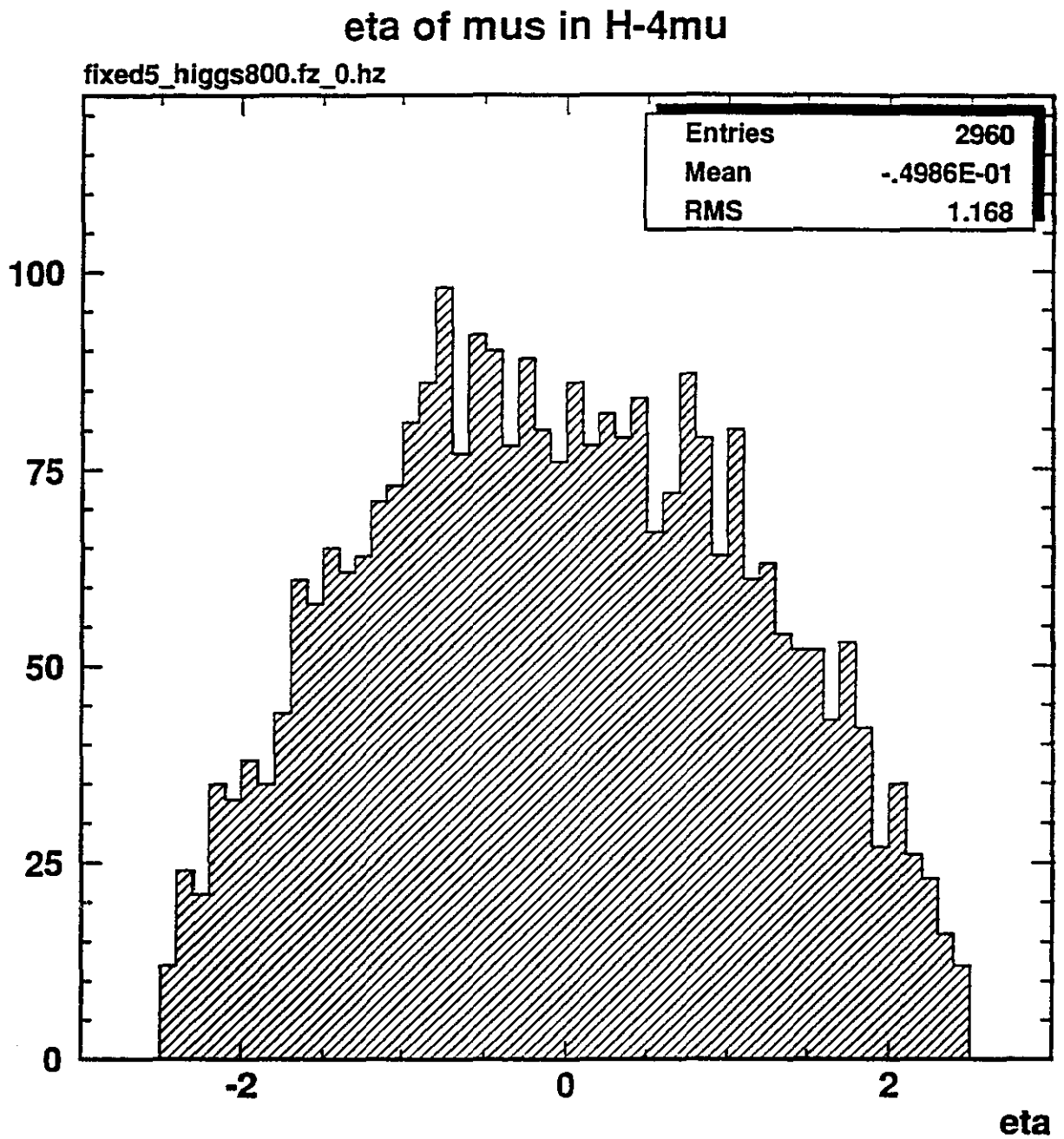
eta of mus in H-4mu
fixed5_higgs800.fz_0.hz
Entries 2960
Mean -.4986E-01
RMS 1.168
100
75
50
25
0
-2
0
2
eta

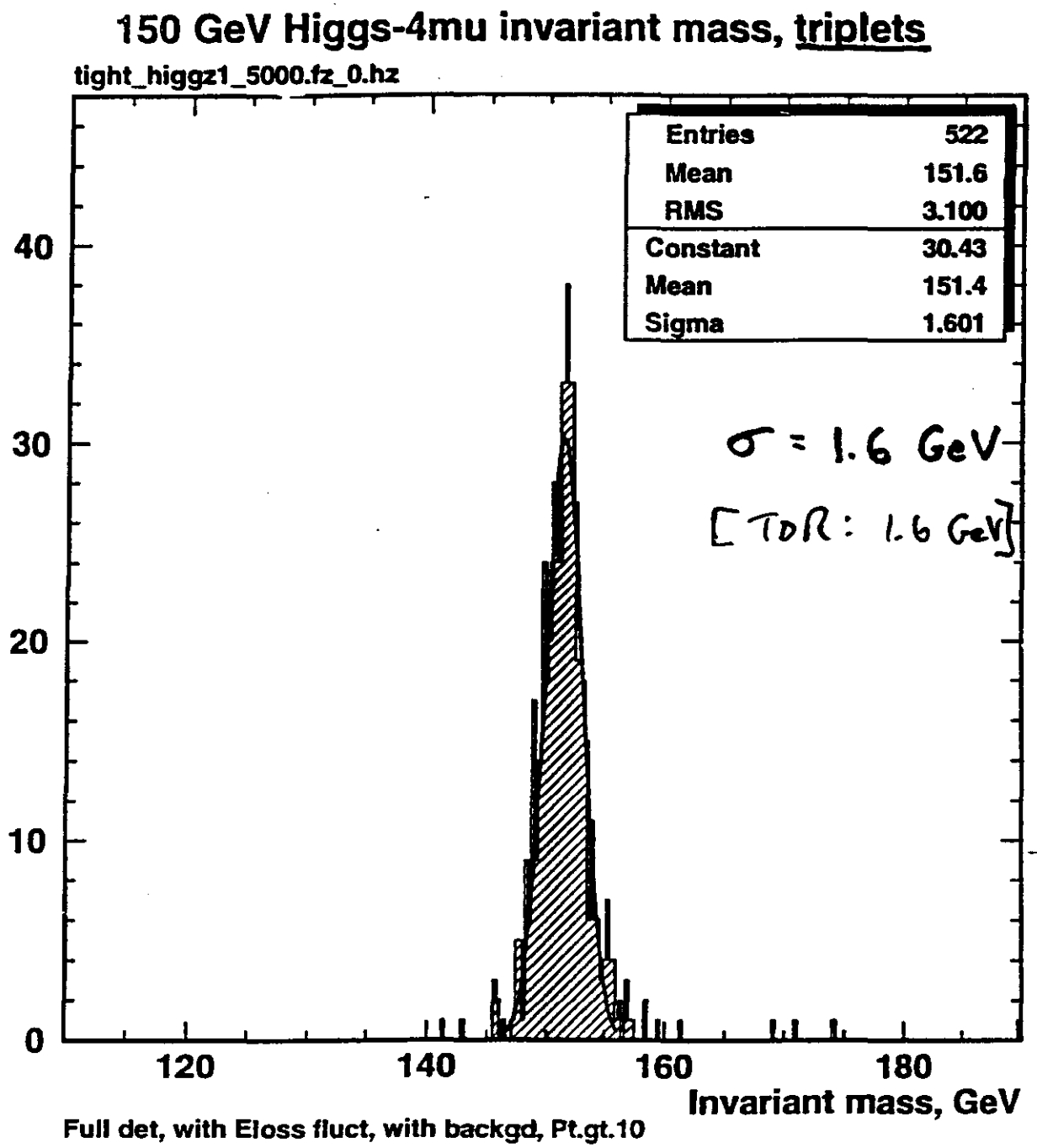
150 GeV Higgs-4mu invariant mass, triplets
tight_higgz1_5000.fz_0.hz
Entries 522
Mean 151.6
RMS 3.100
Constant 30.43
Mean 151.4
Sigma 1.601
σ = 1.6 GeV
[TDR: 1.6 GeV]
0
10
20
30
40
120
140
160
180
Invariant mass, GeV
Full det, with Eloss fluct, with backgd, Pt.gt.10

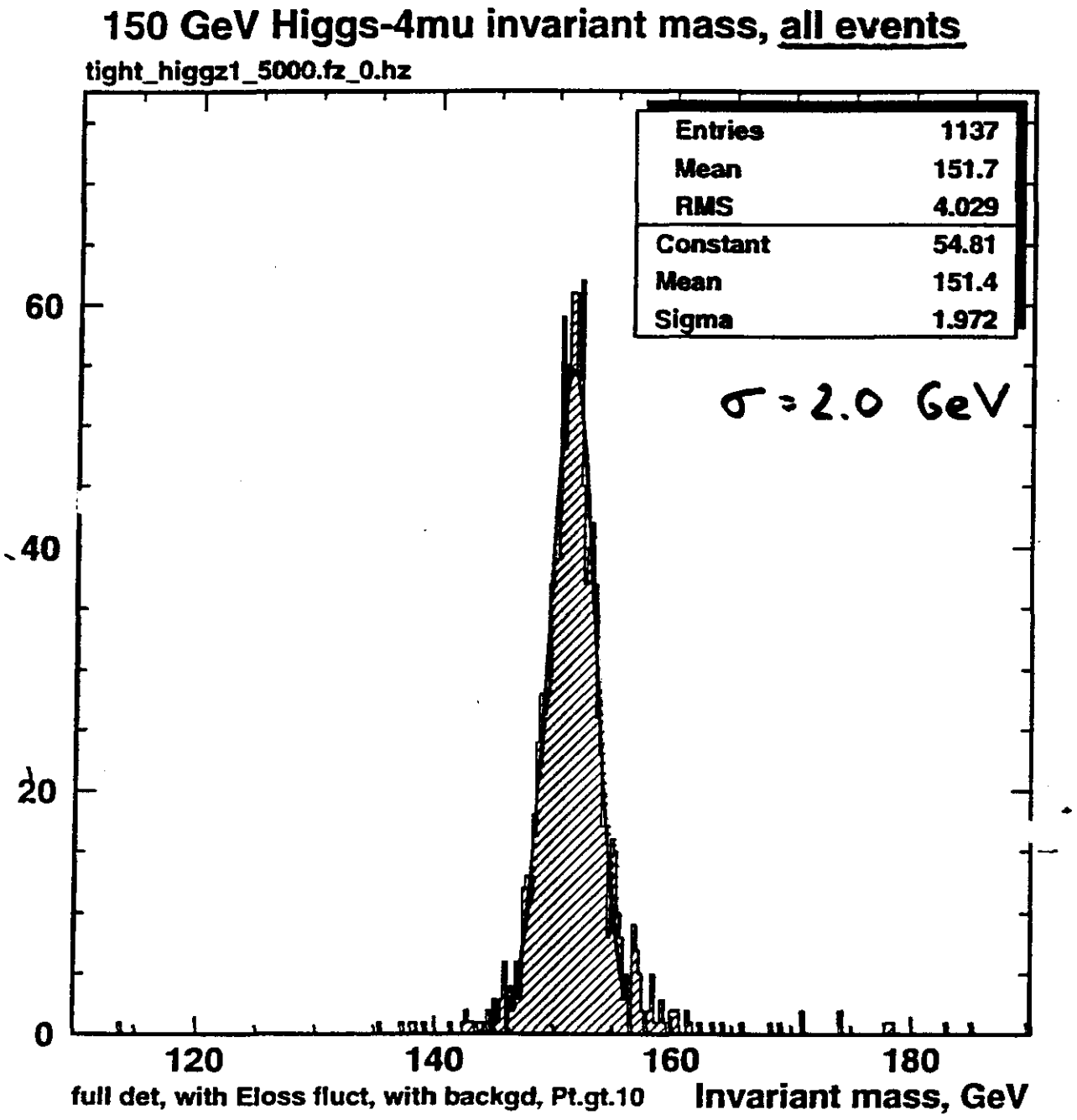
150 GeV Higgs-4mu invariant mass, all events
tight_higgz1_5000.fz_0.hz
Entries 1137
Mean 151.7
RMS 4.029
Constant 54.81
Mean 151.4
Sigma 1.972
σ = 2.0 GeV
60
40
20
0
120
140
160
180
full det, with Eloss fluct, with backgd, Pt.gt.10
Invariant mass, GeV

150 GeV Higgs-4mu invariant mass, triplets

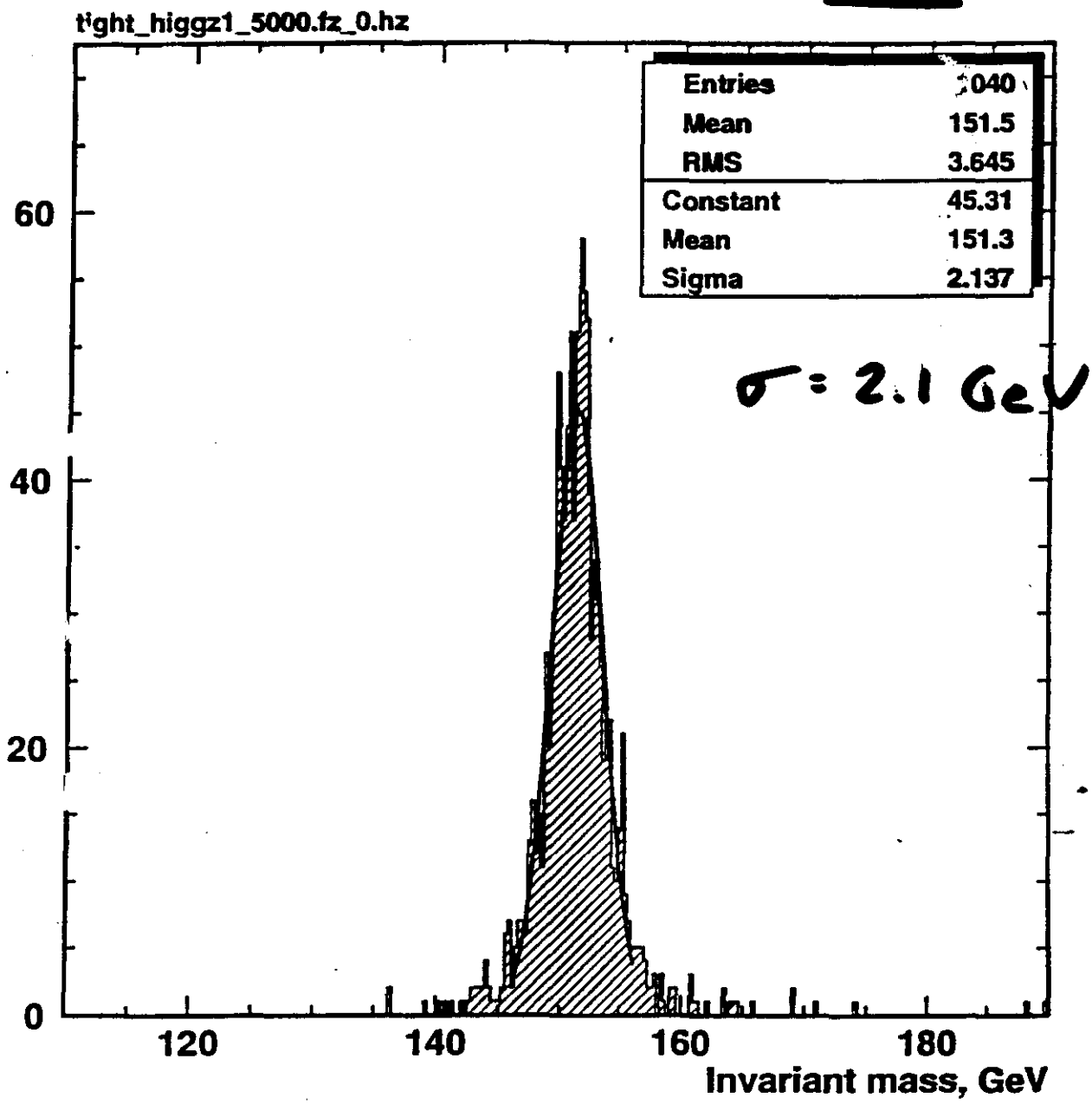

Full det, with Eloss fluct, with backgd, Pt.gt.10, CT used

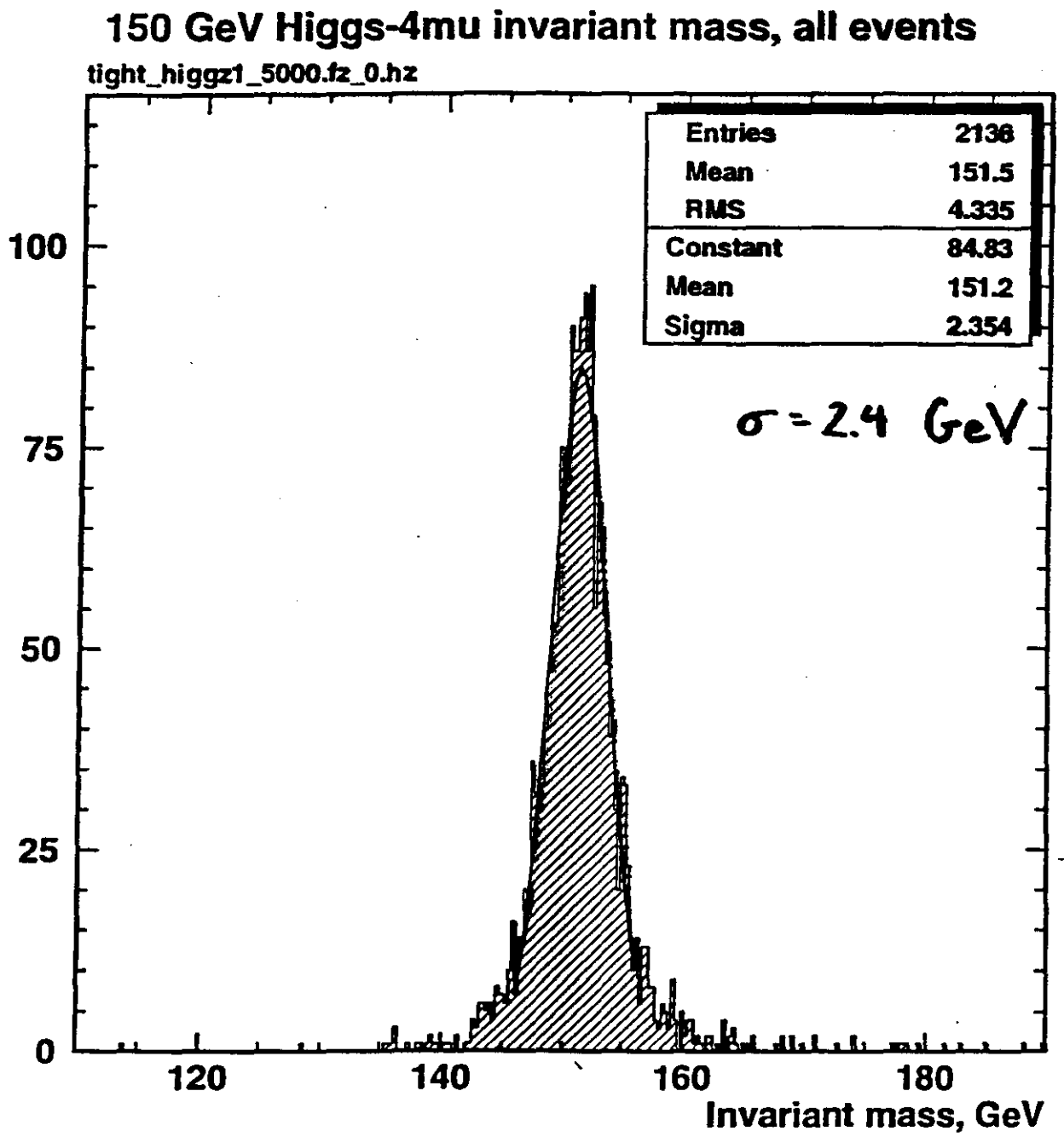

full det, with Eloss fluct, with backgd, Pt.gt.10, CT used

EFFECT OF DOUBLET, CT INCLUSION ON SIGNAL SIGNIFICANCE

ASSUME SIGNIFICANCE $\sim \frac{S}{\sqrt{B}} \sim \frac{N_{events}}{\sqrt{\Delta M_H}}$

	ΔM_H	N	$N/\sqrt{\Delta M_H}$ NORMALIZED
3 SLs	1.6 GeV	522	1.0
2,3 SLs	2.0	1137	1.9
3 SLs + CT	2.1	1040	1.7
2,3 SLs + CT	2.4	2136	3.3

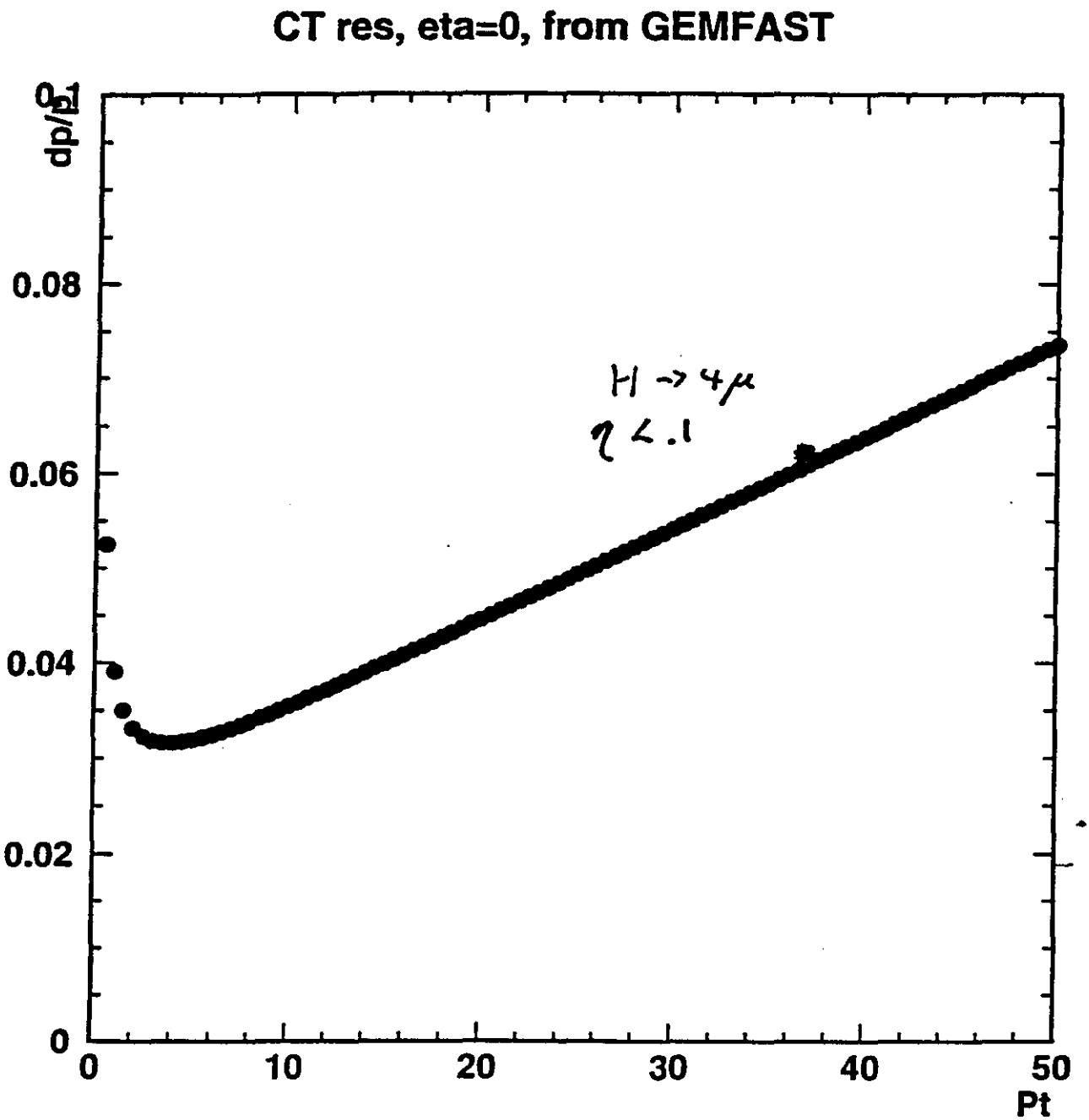
CT res, eta=0, from GEMFAST
dp/p
0.08
0.06
0.04
0.02
0
0
10
20
30
40
50
Pt
H -> 4μ
η < .1

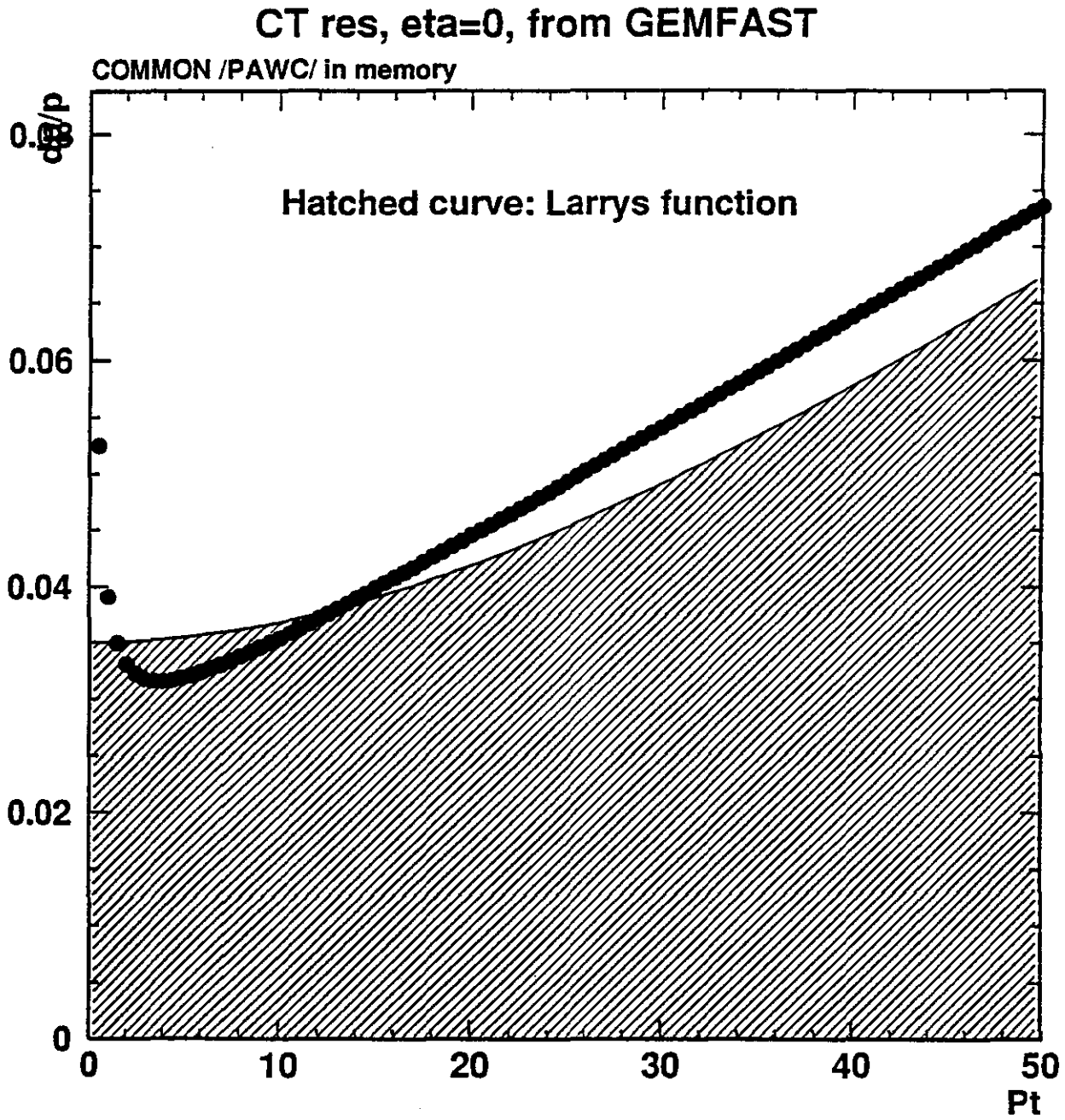
CT res, eta=0, from GEMFAST
COMMON /PAWC/ in memory
dp/p
Hatched curve: Larrys function
0.08
0.06
0.04
0.02
0
0
10
20
30
40
50
Pt

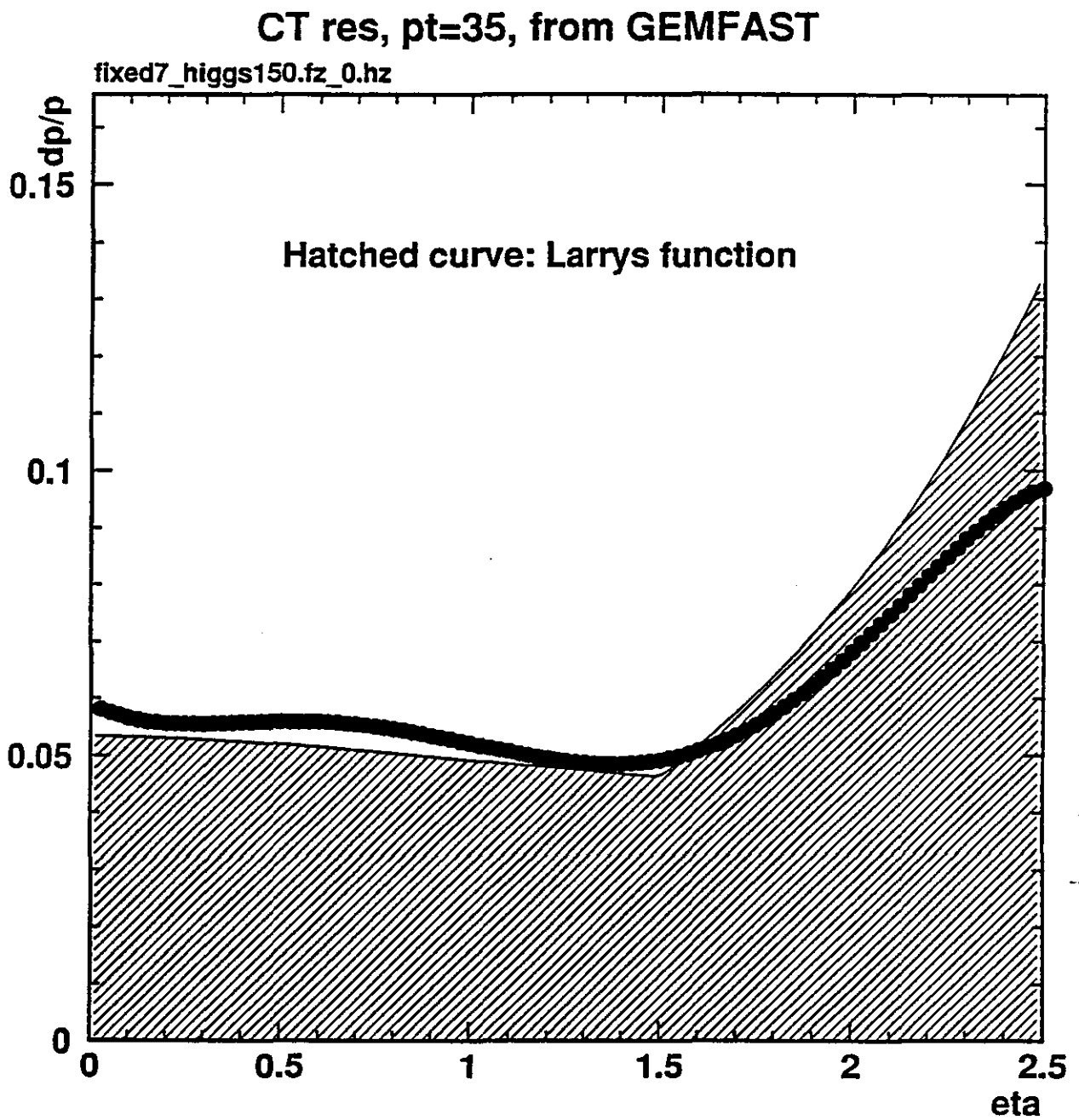
CT res, pt=35, from GEMFAST
fixed7_higgs150.fz_0.hz
dp/p
0.15
0.1
0.05
0
Hatched curve: Larrys function
0
0.5
1
1.5
2
2.5
eta

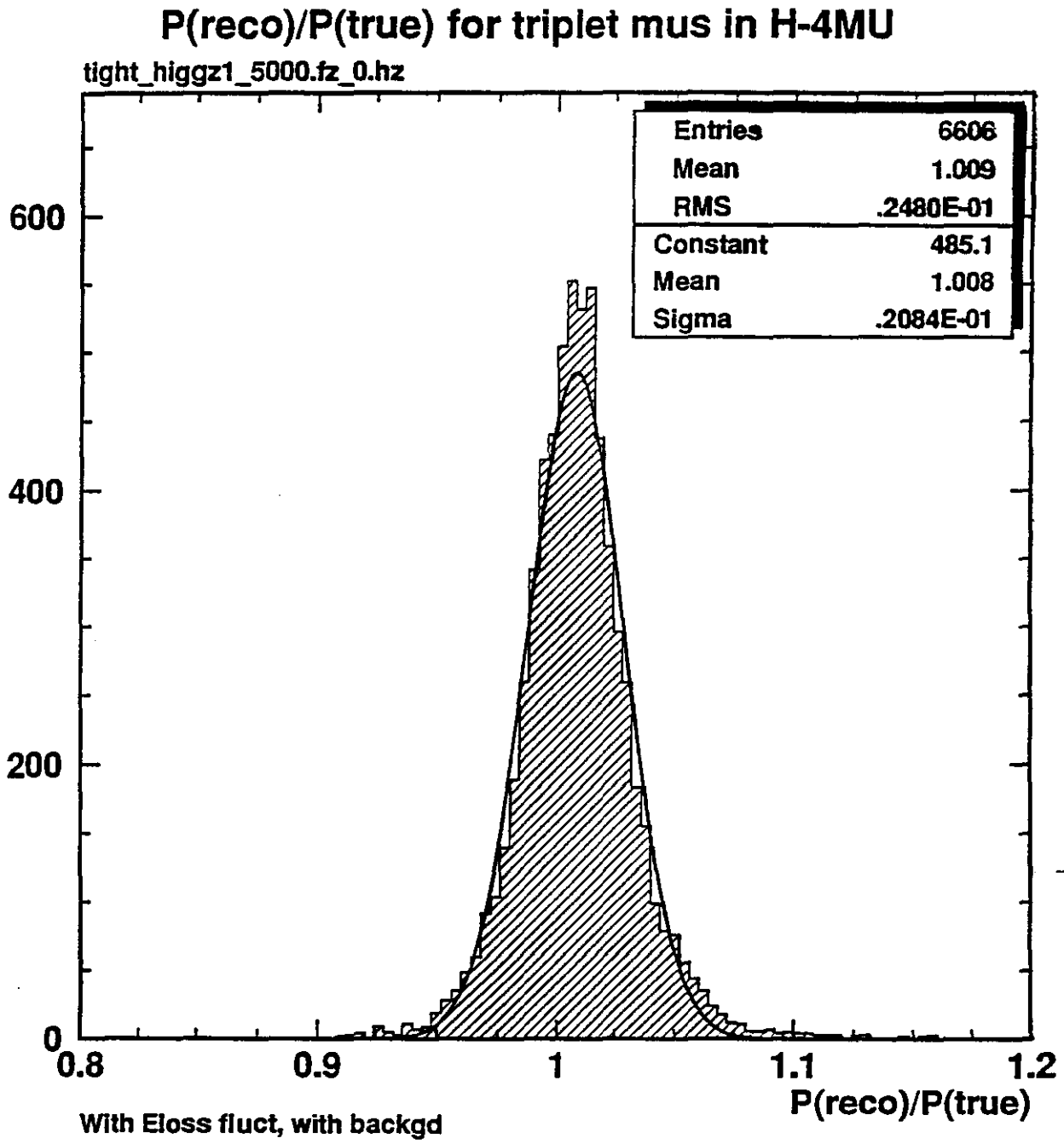
P(reco)/P(true) for triplet mus in H-4MU
tight_higgz1_5000.fz_0.hz
Entries 6606
Mean 1.009
RMS .2480E-01
Constant 485.1
Mean 1.008
Sigma .2084E-01
600
400
200
0
0.8
0.9
1
1.1
1.2
P(reco)/P(true)
With Eloss fluct, with backgd

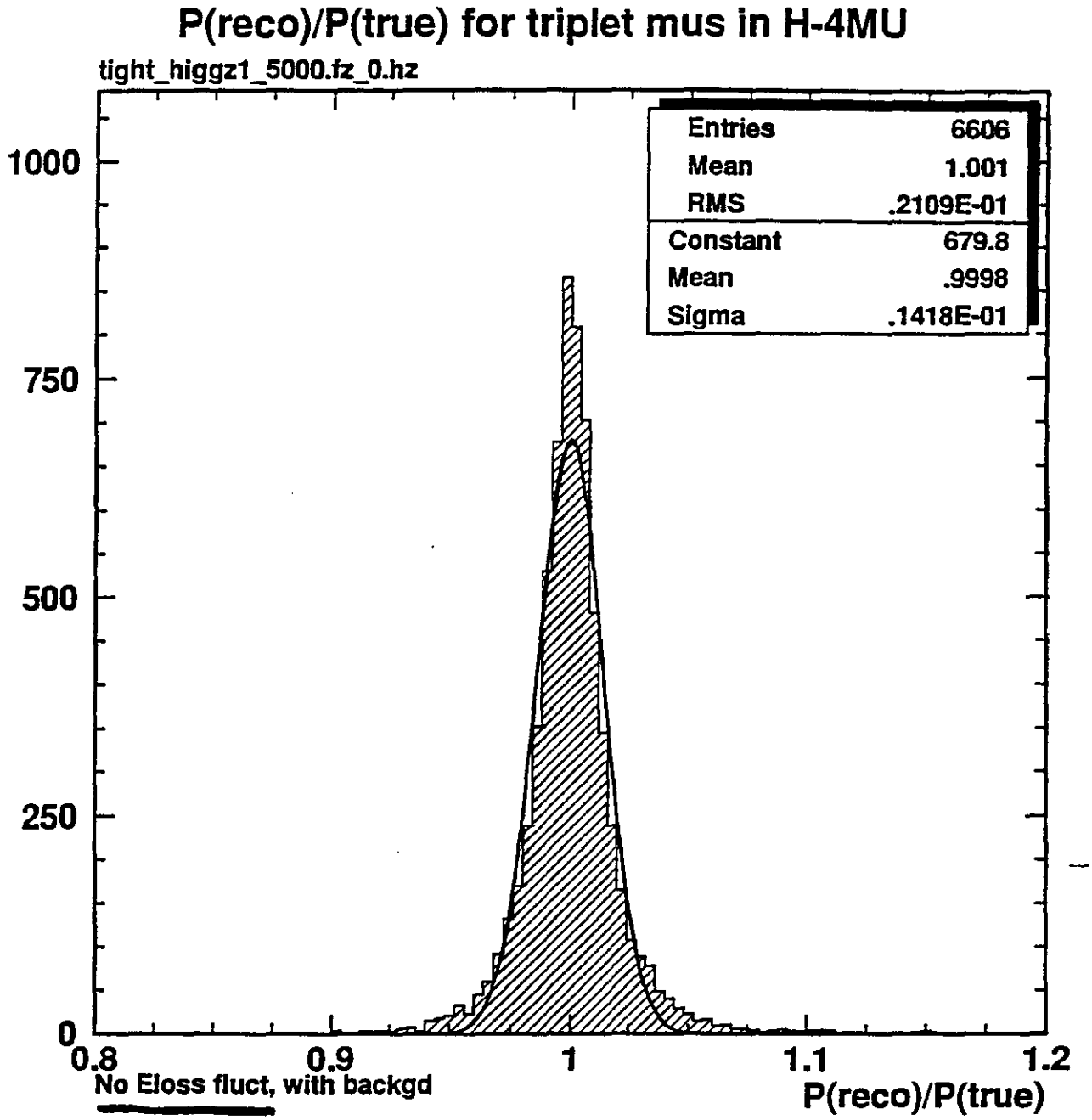
P(reco)/P(true) for triplet mus in H-4MU
tight_higgz1_5000.fz_0.hz
Entries 6606
Mean 1.001
RMS .2109E-01
Constant 679.8
Mean .9998
Sigma .1418E-01
1000
750
500
250
0
0.8
0.9
1
1.1
1.2
No Eloss fluct, with backgd
P(reco)/P(true)

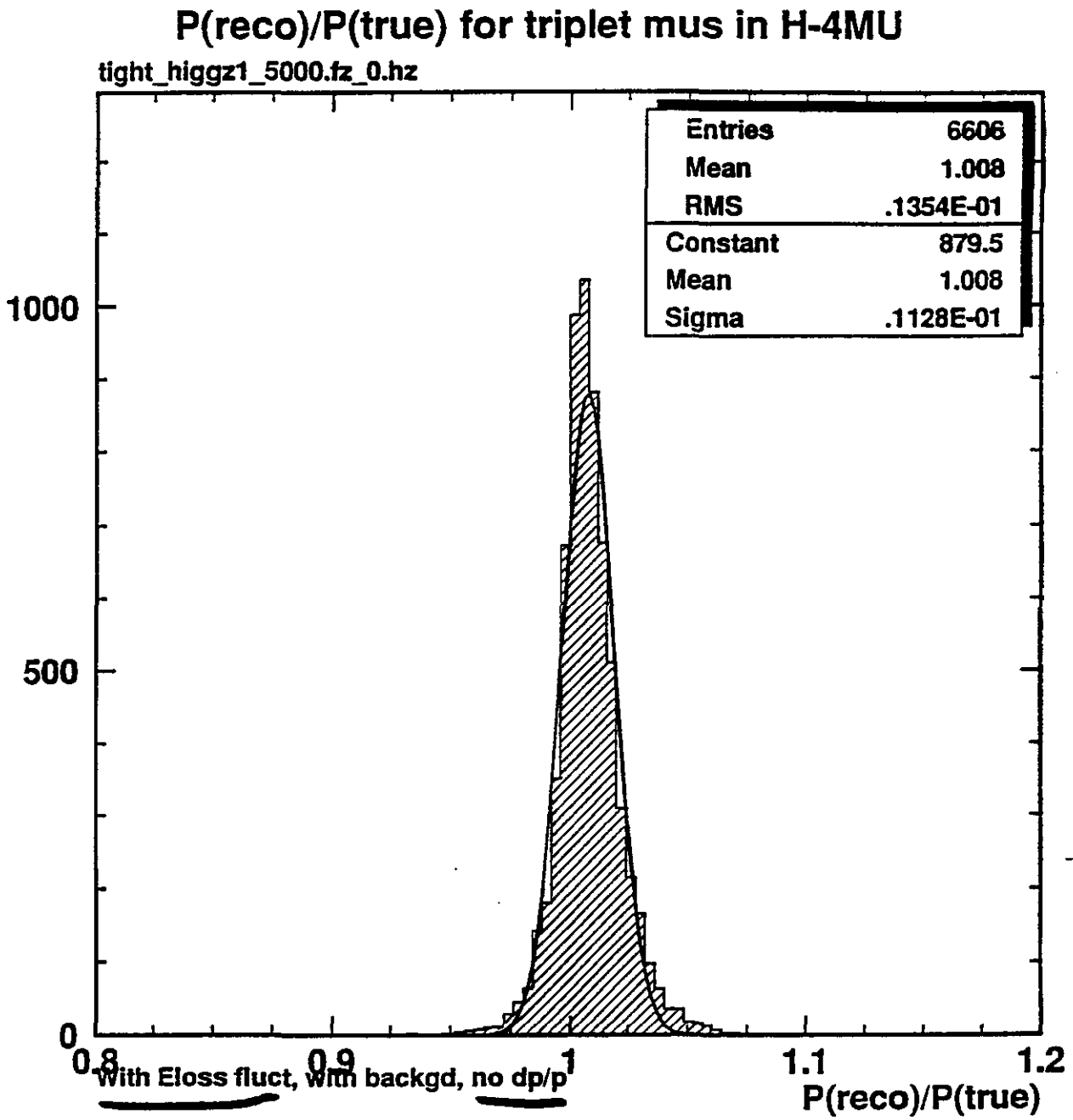
P(reco)/P(true) for triplet mus in H-4MU
tight_higgz1_5000.fz_0.hz
Entries 6606
Mean 1.008
RMS .1354E-01
Constant 879.5
Mean 1.008
Sigma .1128E-01
1000
500
0
0.8
0.9
1
1.1
1.2
With Eloss fluct, with backgd, no dp/p
P(reco)/P(true)

MUON MEASUREMENT IN $H(150) \to 4\mu$

	$\sigma(p(\text{RECO})/p(\text{TRUE}))$
WITH μ SYSTEM AND E LOSS RESOLUTIONS	2.1%
μ SYSTEM RES ONLY, NO E LOSS FLUCT	1.4%
E LOSS FLUCT ONLY	1.1%

- E LOSS FLUCT DOES NOT DOMINATE M_H RESOLUTION
- CANNOT ADD $\sigma(\mu\ \text{SYS})$ AND $\sigma(\text{ELOSS})$ IN QUAD; THEY ARE CORRELATED.

FIT: $y = \frac{x - x_0}{\sigma}$

$y \le y_0$: $A \exp(-y^2)$

$y \ge y_0$: $A \exp(-2yy_0 + y_0^2)$

$x = E_{loss} / \langle E_{loss} \rangle$

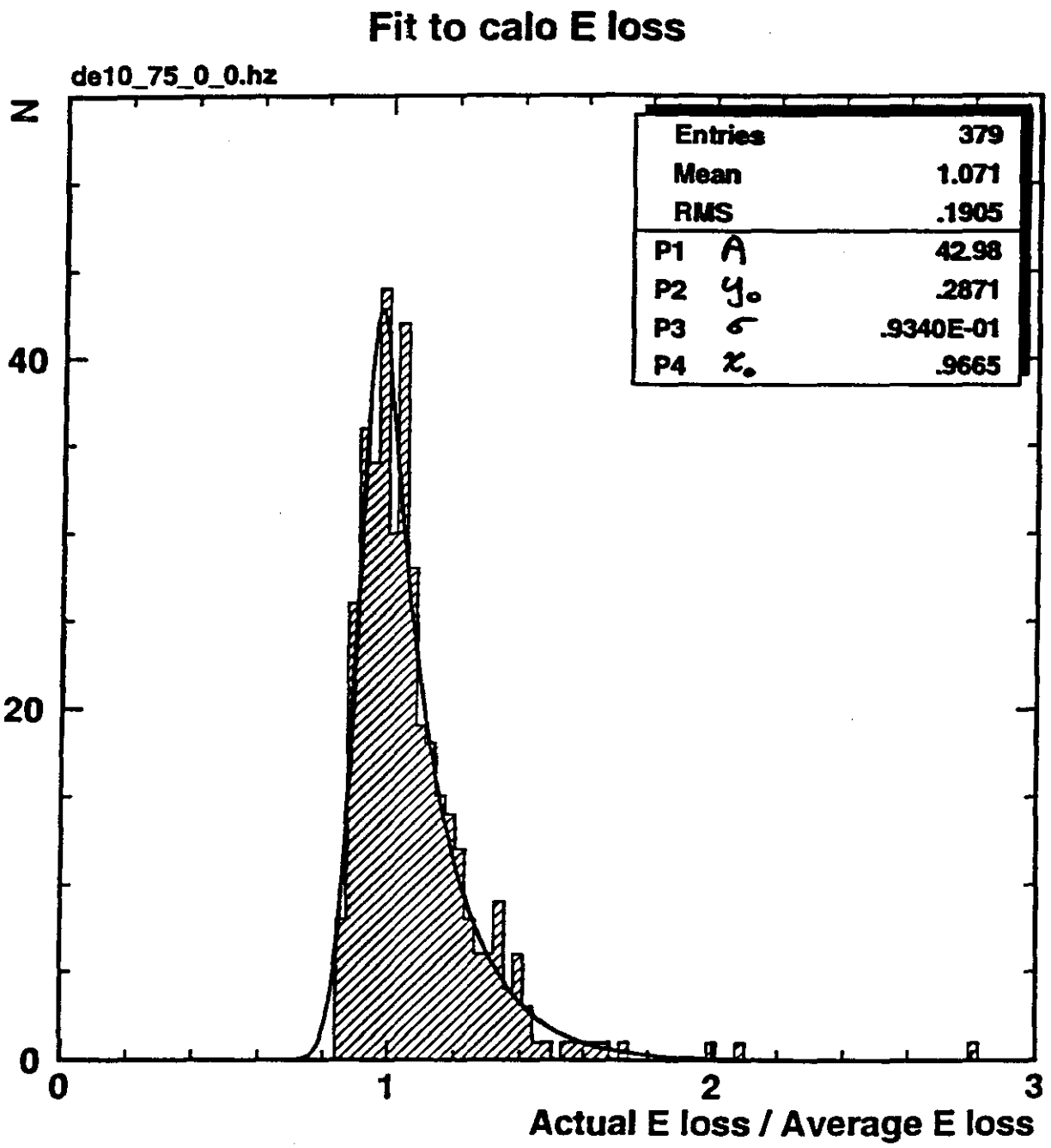

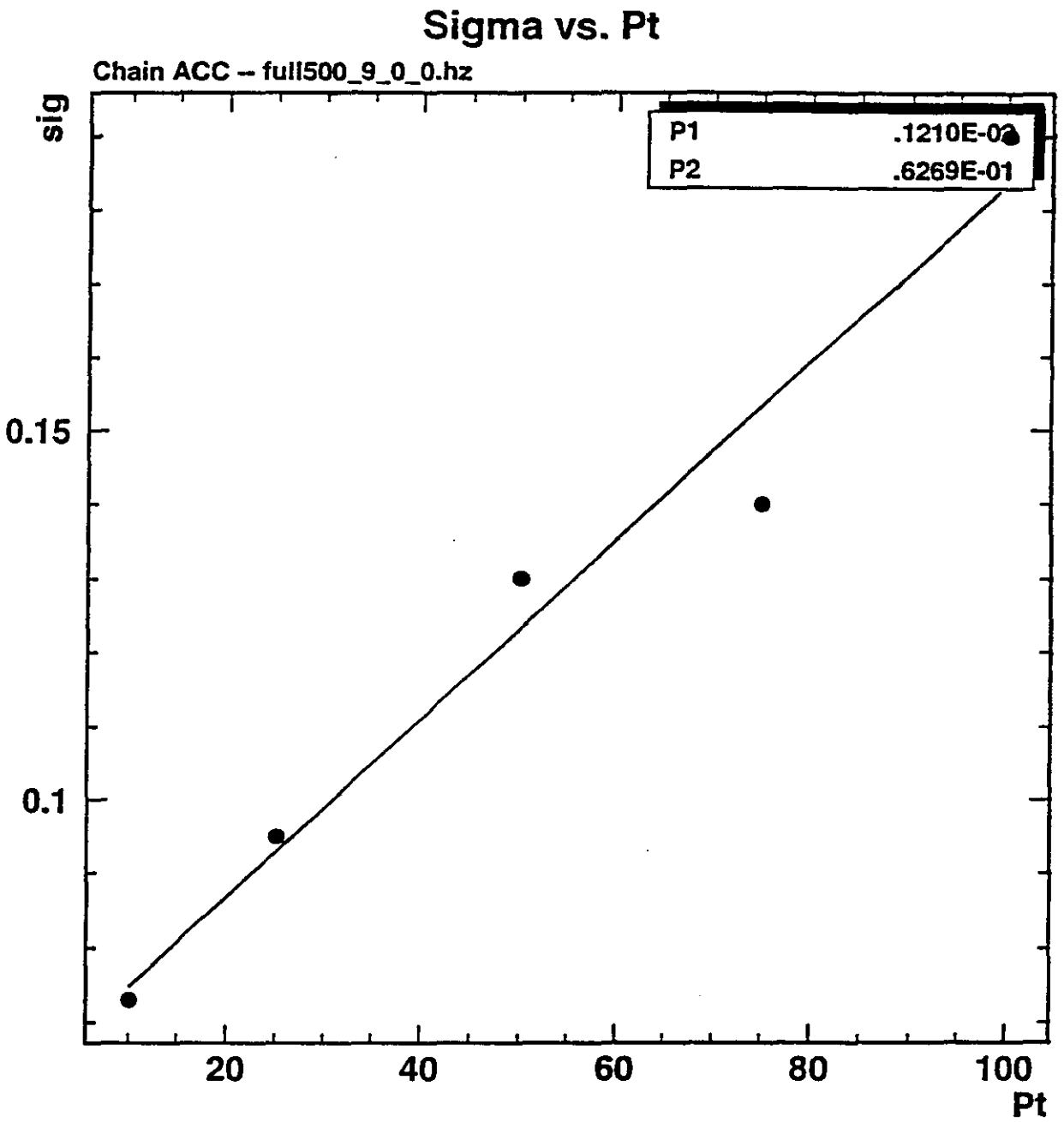
Sigma vs. Pt
Chain ACC -- full500_9_0_0.hz
sig
P1 .1210E-02
P2 .6269E-01
0.15
0.1
20
40
60
80
100
Pt

CALO E LOSS CORR'N -
VLADIMIR'S METHOD.

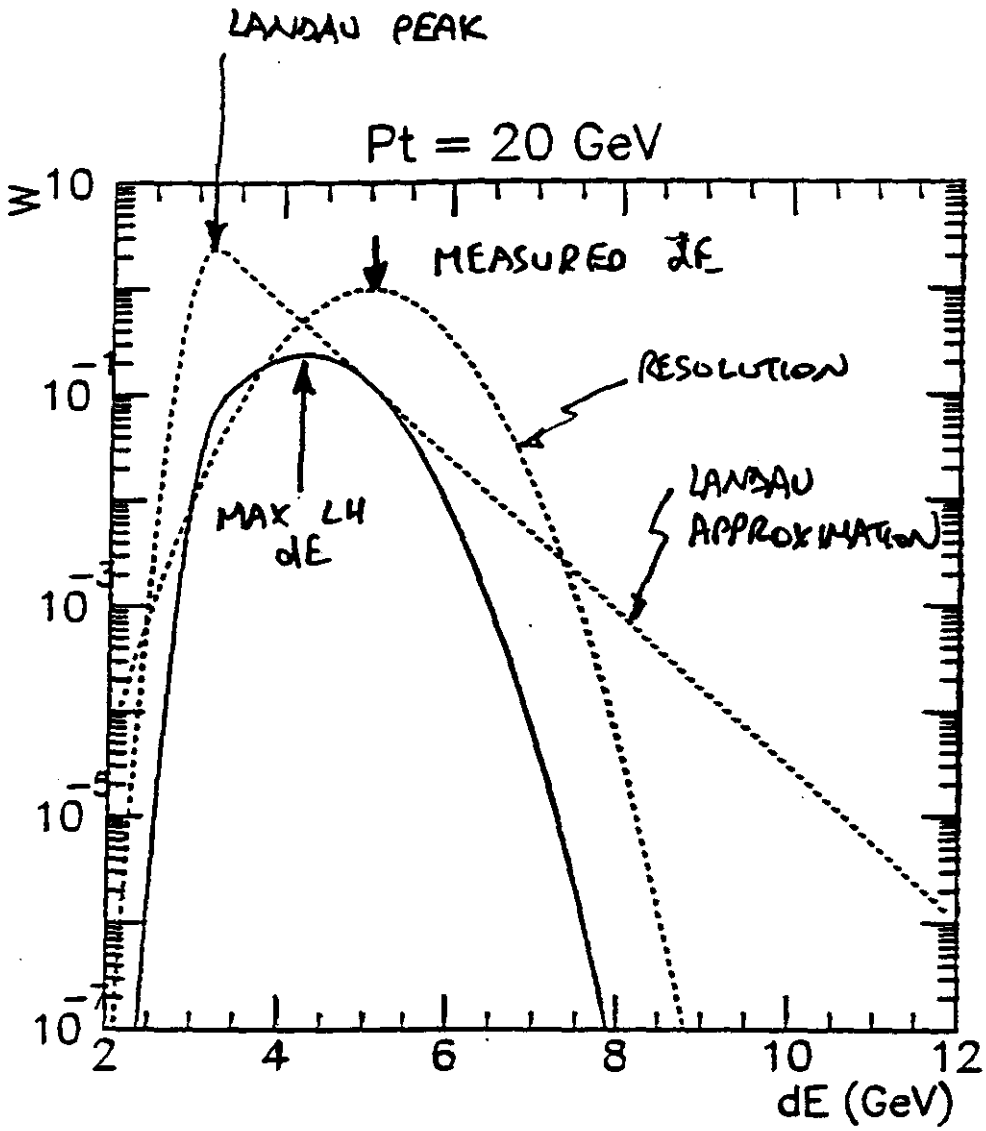

V. GAVRILOV

E LOSS CORRECTION

20 GeV p_T, BARREL ($\theta \sim 75°$)

σ OF dE/E =

2.9% FOR dE = UNCORRECTED E LOSS

2.3% FOR $\frac{\text{MEAS}}{\text{PROB}}$ RATIO CORR.

→ 1.8% FOR MAX LH CORR. + $\frac{\text{MAXLH}}{\text{PROB}}$ RATIO

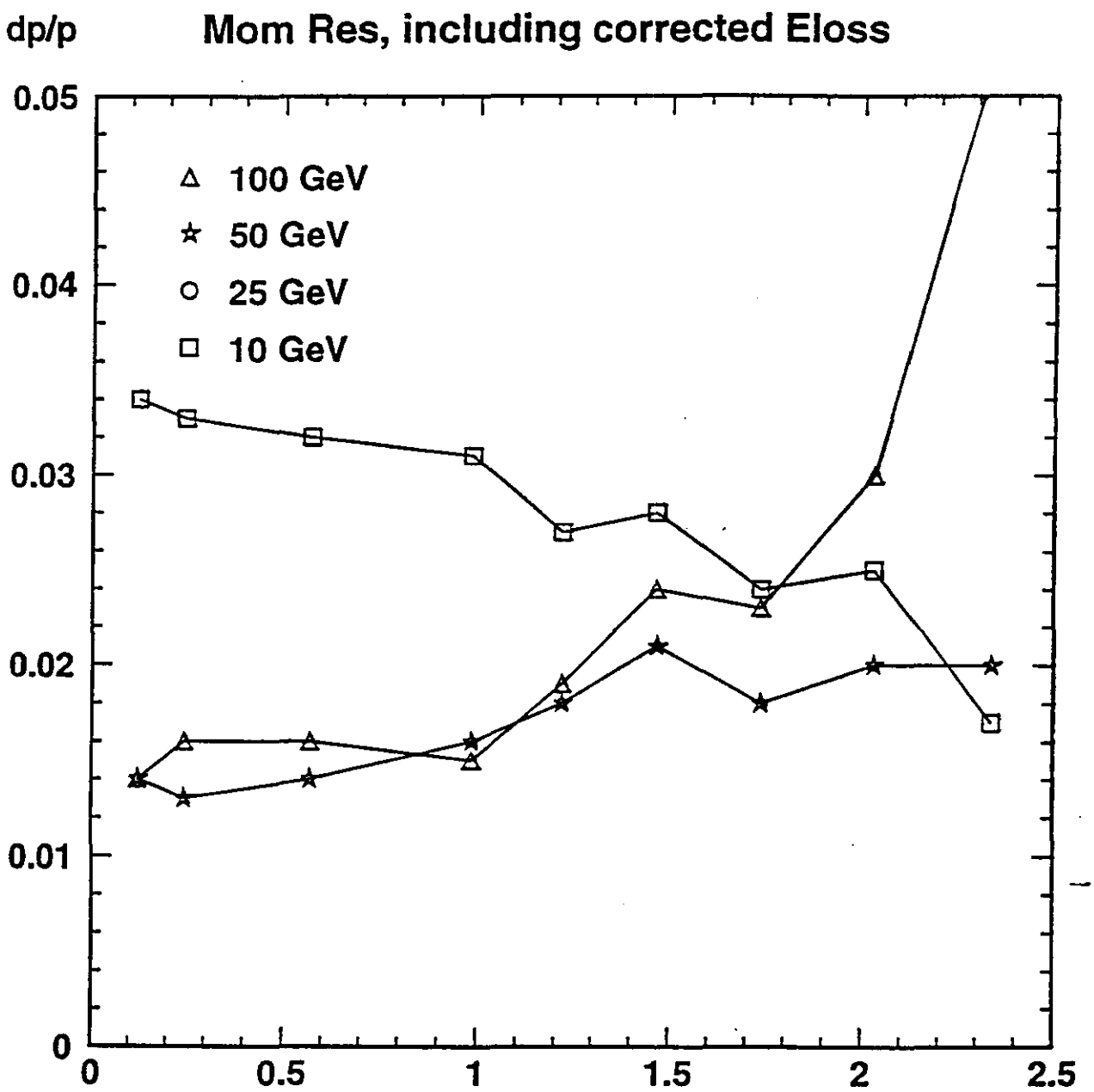
dp/p
Mom Res, including corrected Eloss
0.05
0.04
0.03
0.02
0.01
0
0
0.5
1
1.5
2
2.5
100 GeV
50 GeV
25 GeV
10 GeV

IN PROGRESS:

- INTEGRATING CT SIMU/RECO OF MELYNDA et al INTO SIGEM + MY μ RECO
- IMPLEMENTING MODEL OF NEW μ SYSTEM DESIGN FOR RESOLUTION + ACCEPTANCE STUDIES
  - WHEN DESIGN 'STABILIZES' WILL RELEASE GEMFAST μ PARAMS UNLESS THERE IS DEMAND FOR IT EARLIER
  - GEMFAST PARAM WILL INCLUDE DOUBLETS, VTX CONSTRAINT, CT

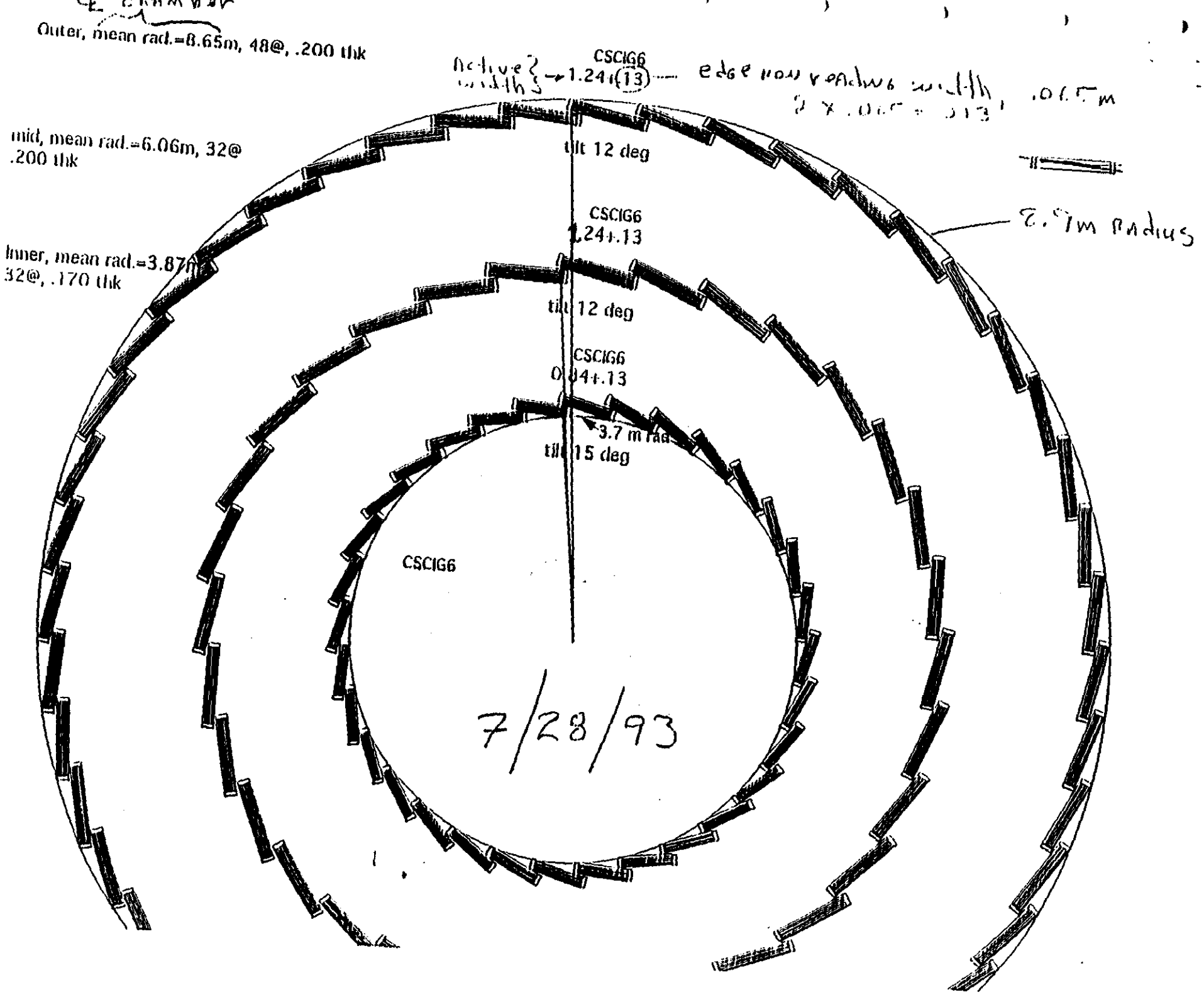
℄ chamber
Outer, mean rad.=8.65m, 48@, .200 thk
active? widths
CSCIG6
1.24+(13)
edge non radius width, .015m
2 x .015 = .013
mid, mean rad.=6.06m, 32@
.200 thk
tilt 12 deg
CSCIG6
1.24+.13
8.65m radius
inner, mean rad.=3.87m
32@, .170 thk
tilt 12 deg
CSCIG6
0.84+.13
3.7 m rad
tilt 15 deg
CSCIG6
7/28/93

287

Optimizing the Calorimeter depth

Calorimeter depth requirement established for TDR utilized Conservative approach

Calorimeter depth is maximum imposed by 3 criteria

1. Punchthrough rate < ½ real muon rate

2. Punchthrough rate with $P_T > 10$ GeV/c < ½ real muon rate $P_T < 10$

3. 4-strip CSC occupancy from charged particles 9×10^{34} is < 1% ⇒ reconstruction eff > 97%

Table 4-7. Depth Requirements imposed by criteria 1, 2, and 3.

Criteria	Minimum Depth required		
	$0.1 < \lvert\eta\rvert < 1.34$	$1.38 < \lvert\eta\rvert < 1.86$	$1.86 < \lvert\eta\rvert < 2.46$
1	11	11	11
2	10	10	10
3	10	12	16
Overall	11	12	16

GEM TDR Calor. is $\gtrsim 11\lambda$ $\gtrsim 14\lambda$ $\gtrsim 16\lambda$

What if we are not so conservative ?

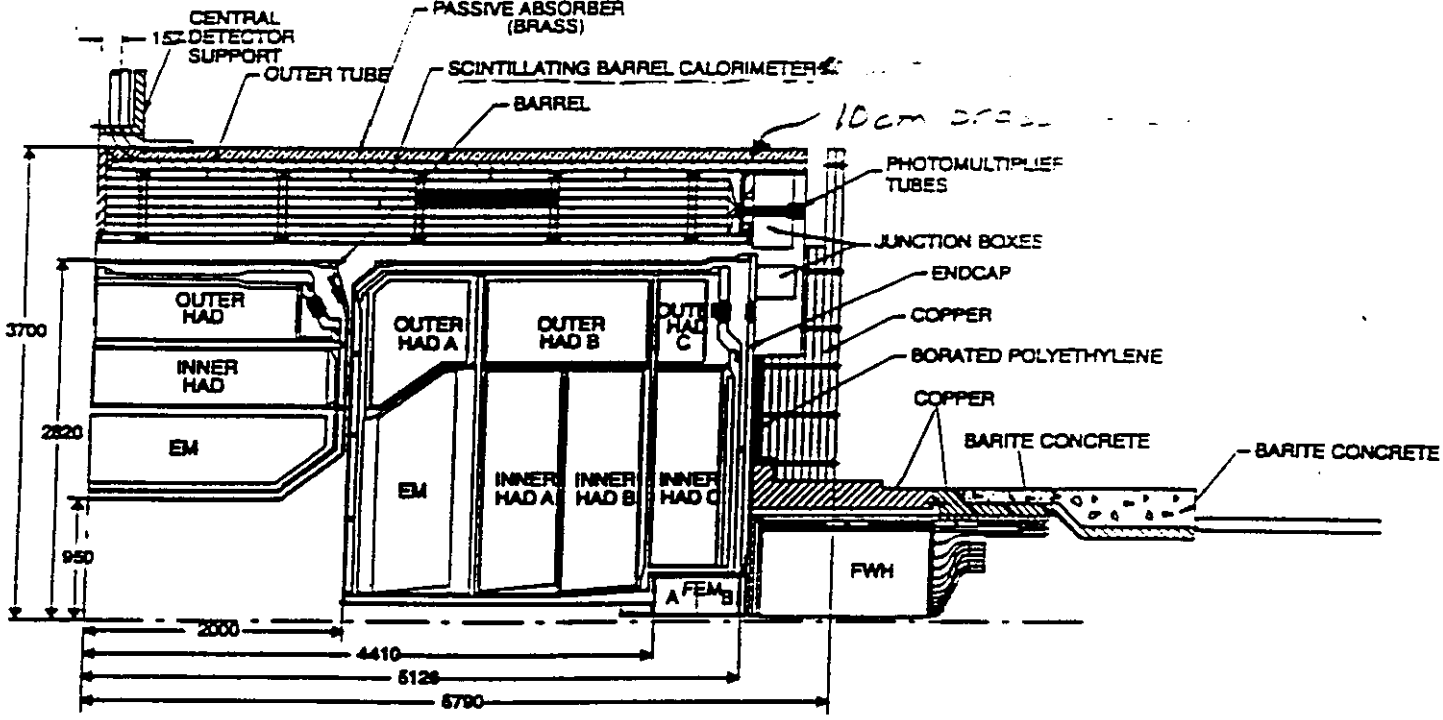

TDR

FIG. 5-1. Overall layout of GEM Calorimeter showing the Inner Barrel with LKr, the Outer Scintillating Barrel Calorimeter, and the Endcap with LAr.

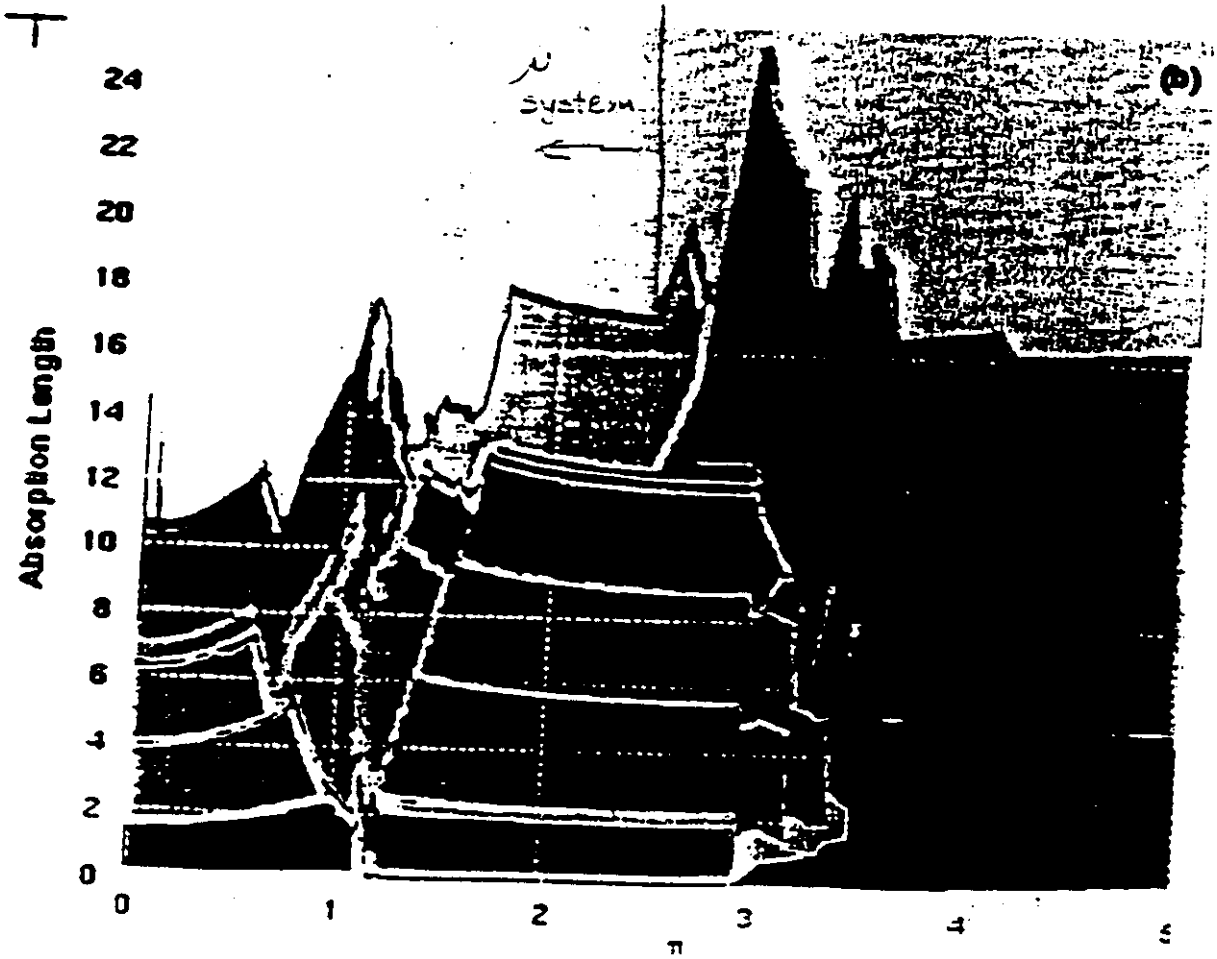

In the barrel the muon system design parameters are not set by hadron punchthrough. The are set by

- resolution - strip size, number of layers, lever arm, # sectors
- mechanical constraints - # sectors, chamber lengths/widths, ...
- EM backgrounds - strip size, number of layers, z-track resol.

Barrel muon system specification set

In the endcap, Criterion 3 determines calorimeter thickness

Relax the requirements for the barrel: Use <u>only</u> criteria 3

Keep 4-strip occupancy below 1% at $10^{34} s^{-1} cm^{-2}$

<u>Dangers</u>

- If criteria 1 & 2 not satisfied, then punchthrough rate will dominate the occupancy; rely more on punchthrough simulation ⇒ greater uncertainty

- For thin calorimeters ($\ll 12\lambda$) hadron punchthrough has large hadron/electron component ⇒ higher multiplicity, harder to simulate (neutrons, δ, etc.). For thick calorimeters ($\gg 12\lambda$), punchthrough is usually a single muon from decay of primary or secondary hadron ⇒ simulations agree better, easier

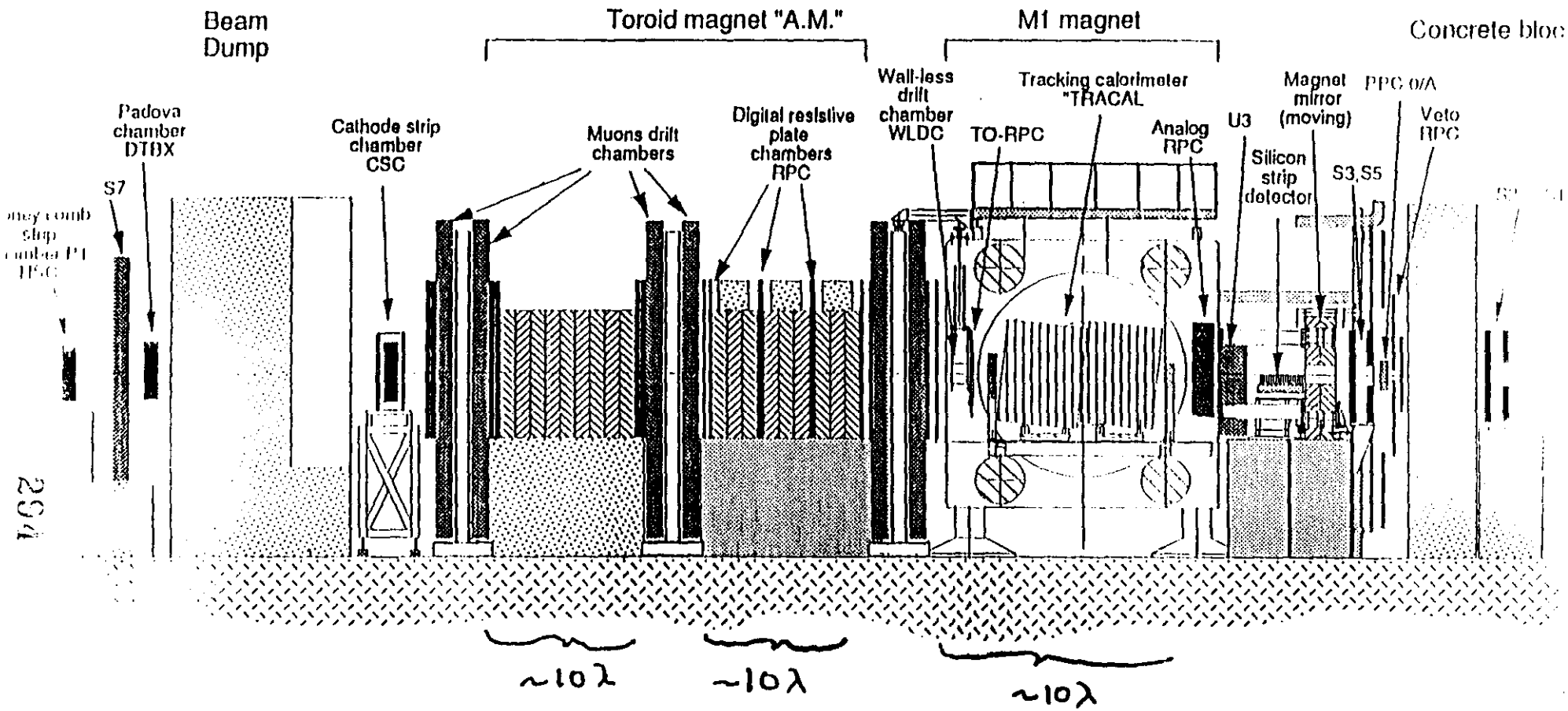

PLAN D'ENSEMBLE EXPERIENCE RD5
Situation 09/92

Chris Lyndon performed GEANT simulation
Update from June 29 results presented

Dessiné :P. PETIOT
CERN le 28/9/92

GEANT V3.15 w/ GHEISHA
GEANT Cut offs
all 1MeV in Absorber
10 KeV in sensitive volumes

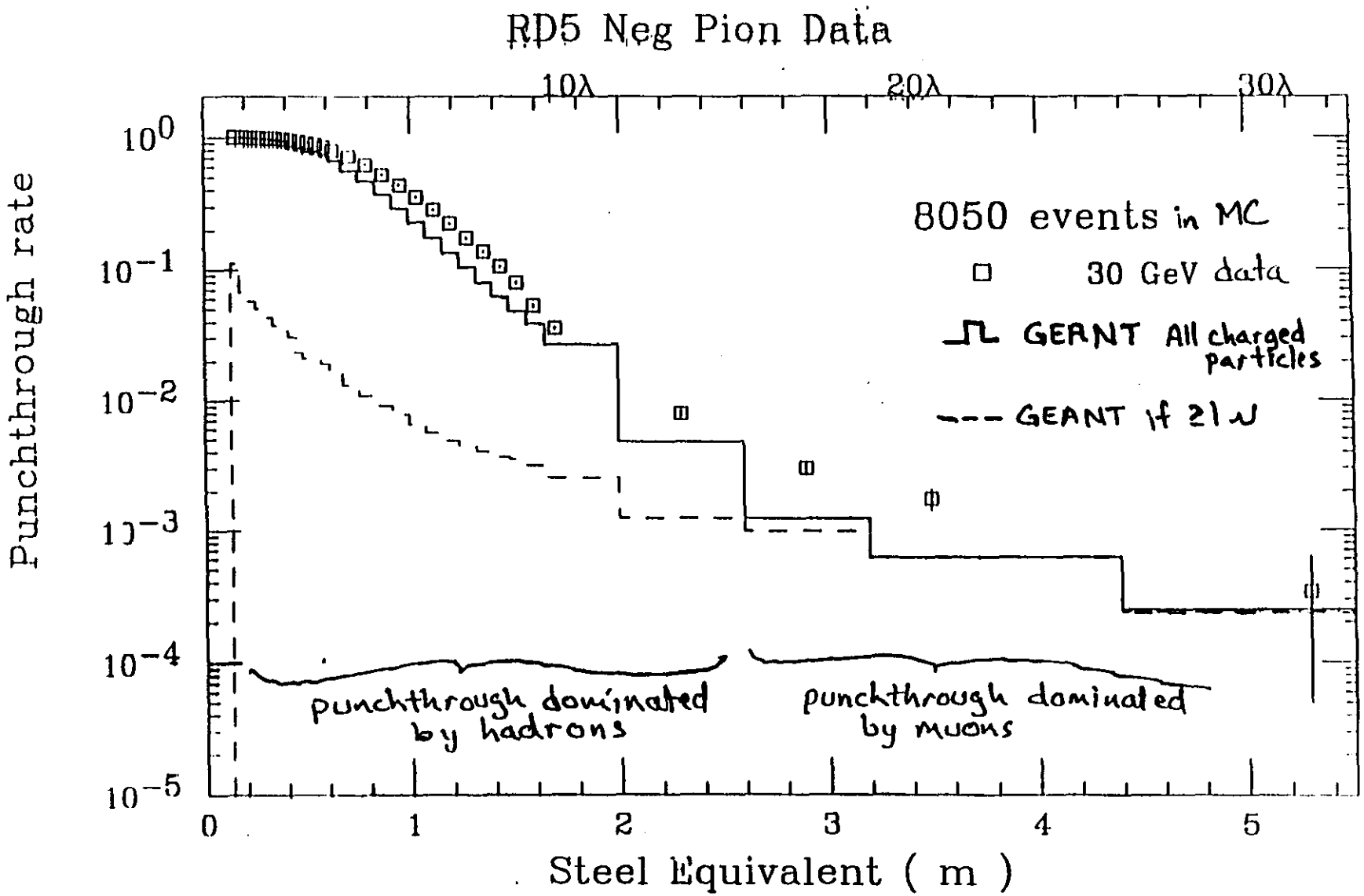

at 10-12λ, GEANT is ~factor of 2 low

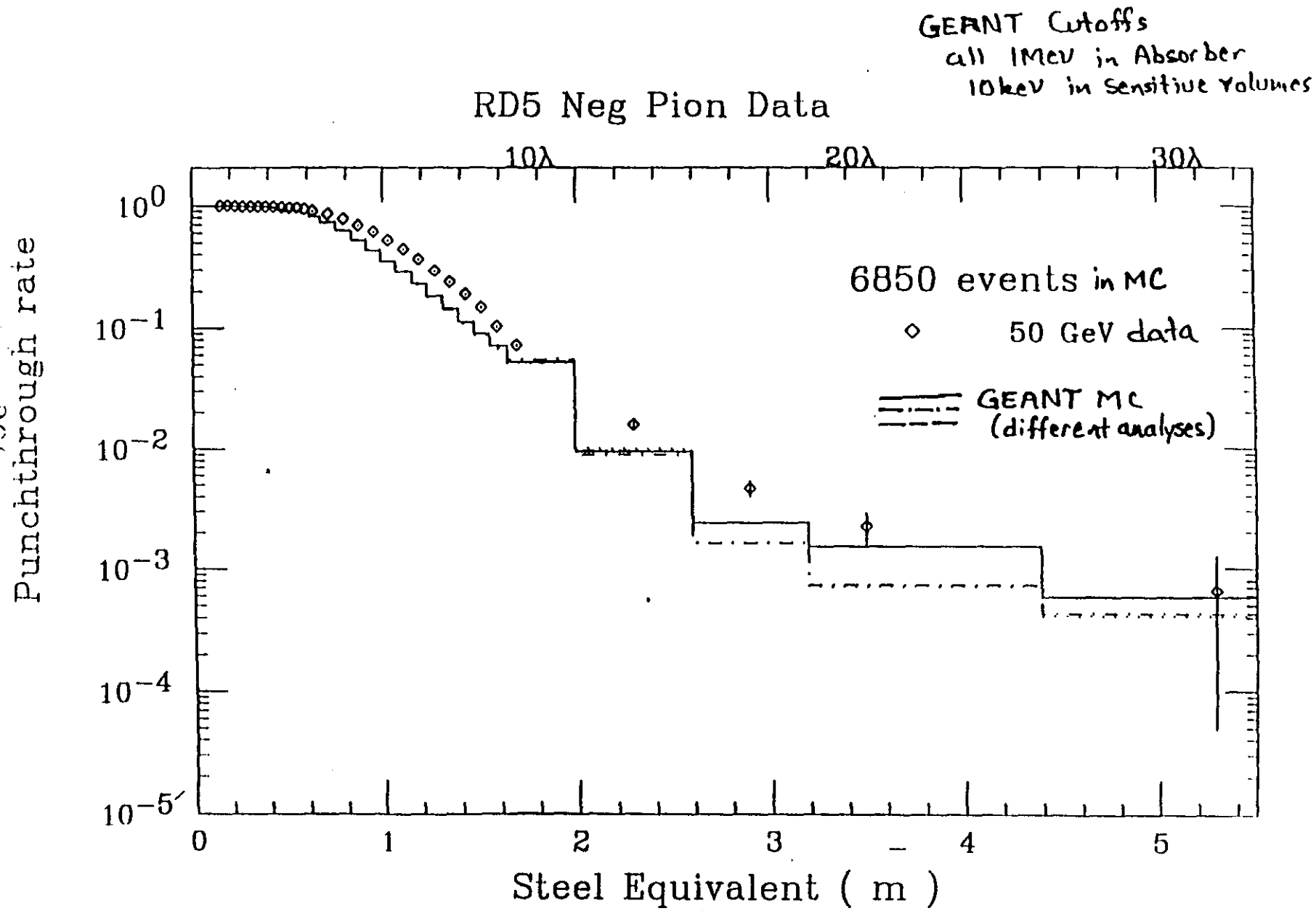
GEANT Cutoffs
all 1MeV in Absorber
10keV in Sensitive Volumes
RD5 Neg Pion Data
10λ
20λ
30λ
6850 events in MC
50 GeV data
GEANT MC
(different analyses)
Punchthrough rate
10^0
10^{-1}
10^{-2}
10^{-3}
10^{-4}
10^{-5}
0
1
2
3
4
5
Steel Equivalent (m)

GEANT Cutoffs All 1MeV in Absorber

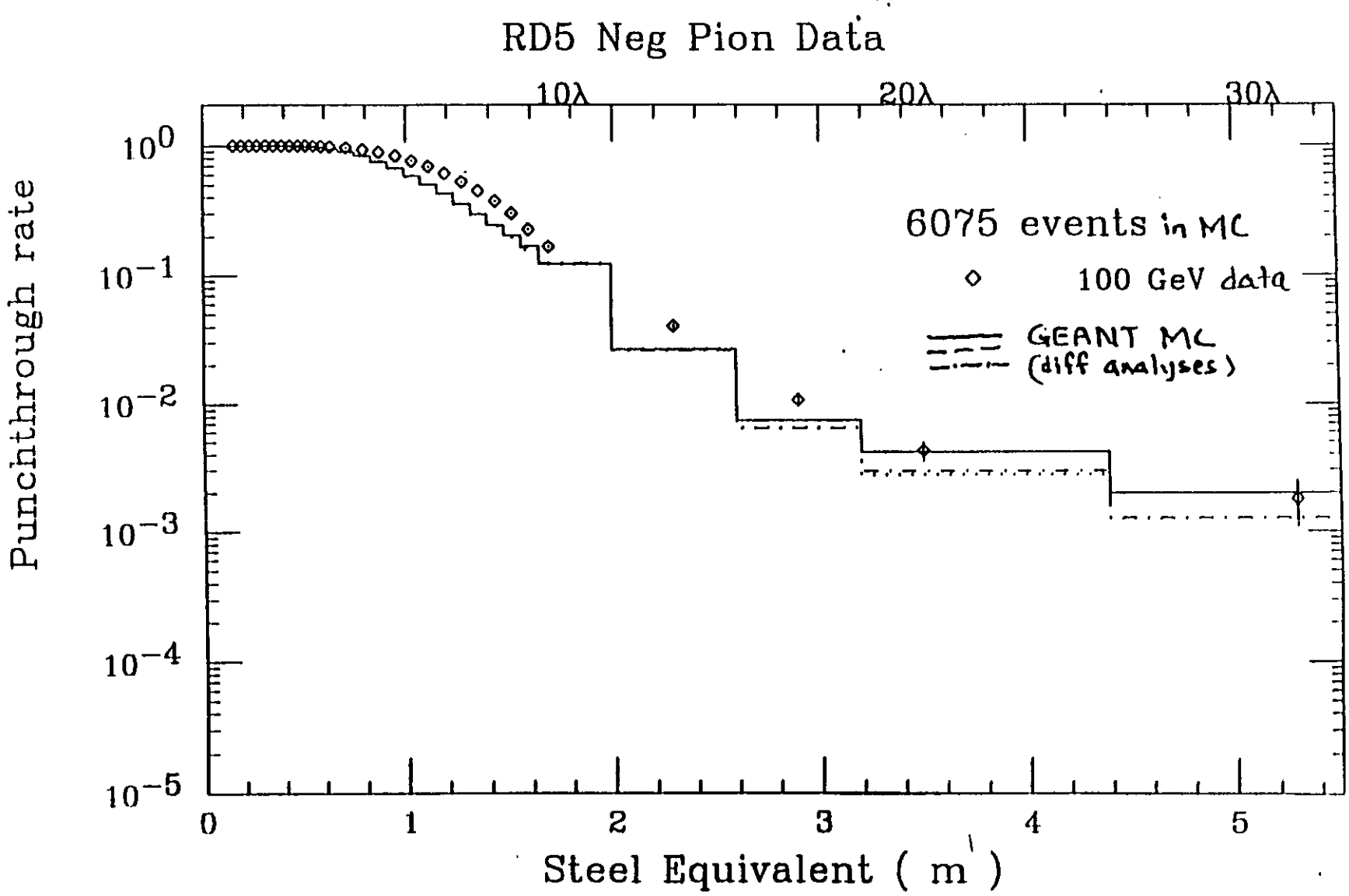

GEANT Cutoffs all 1MeV in Absorber

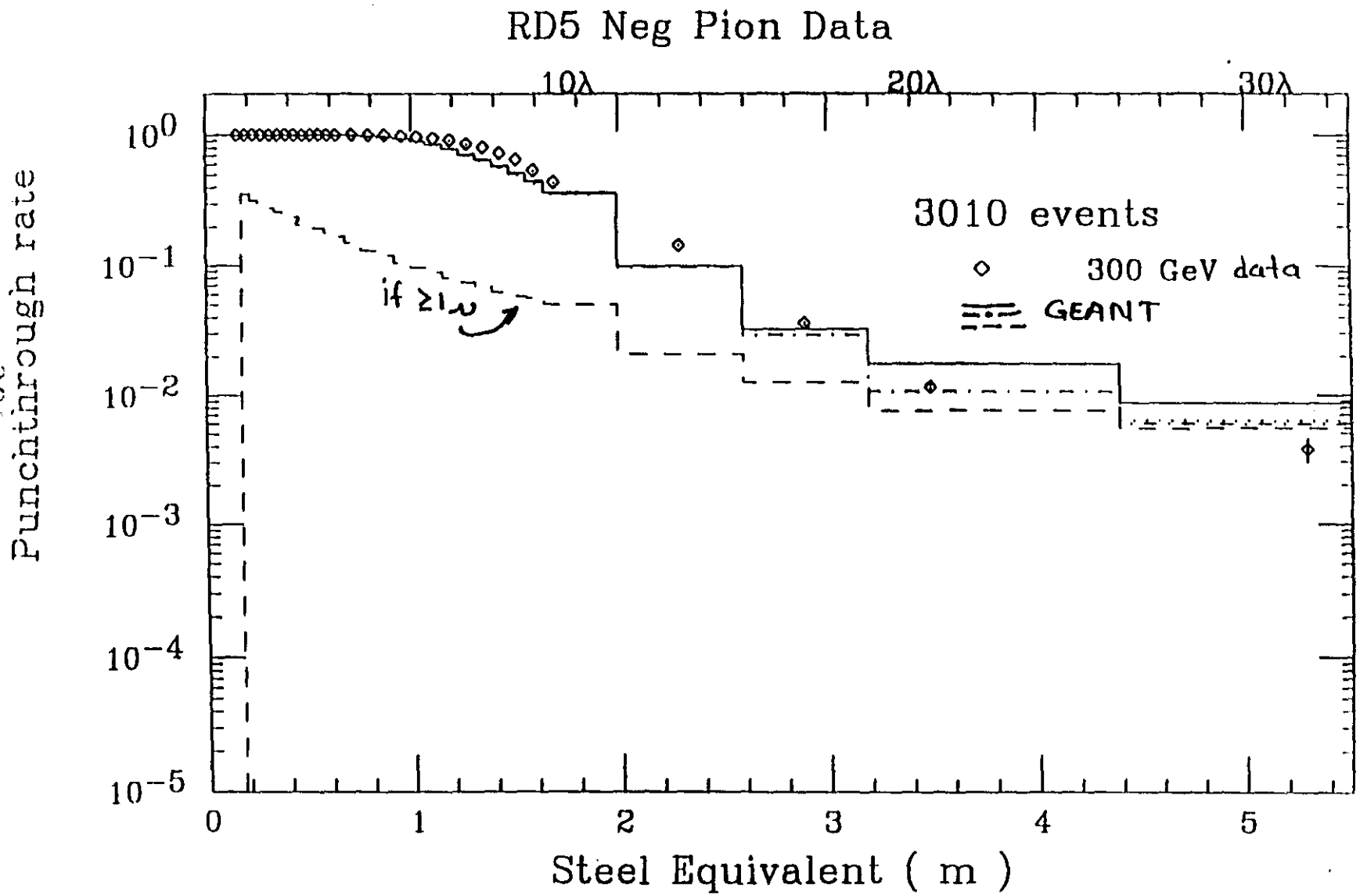

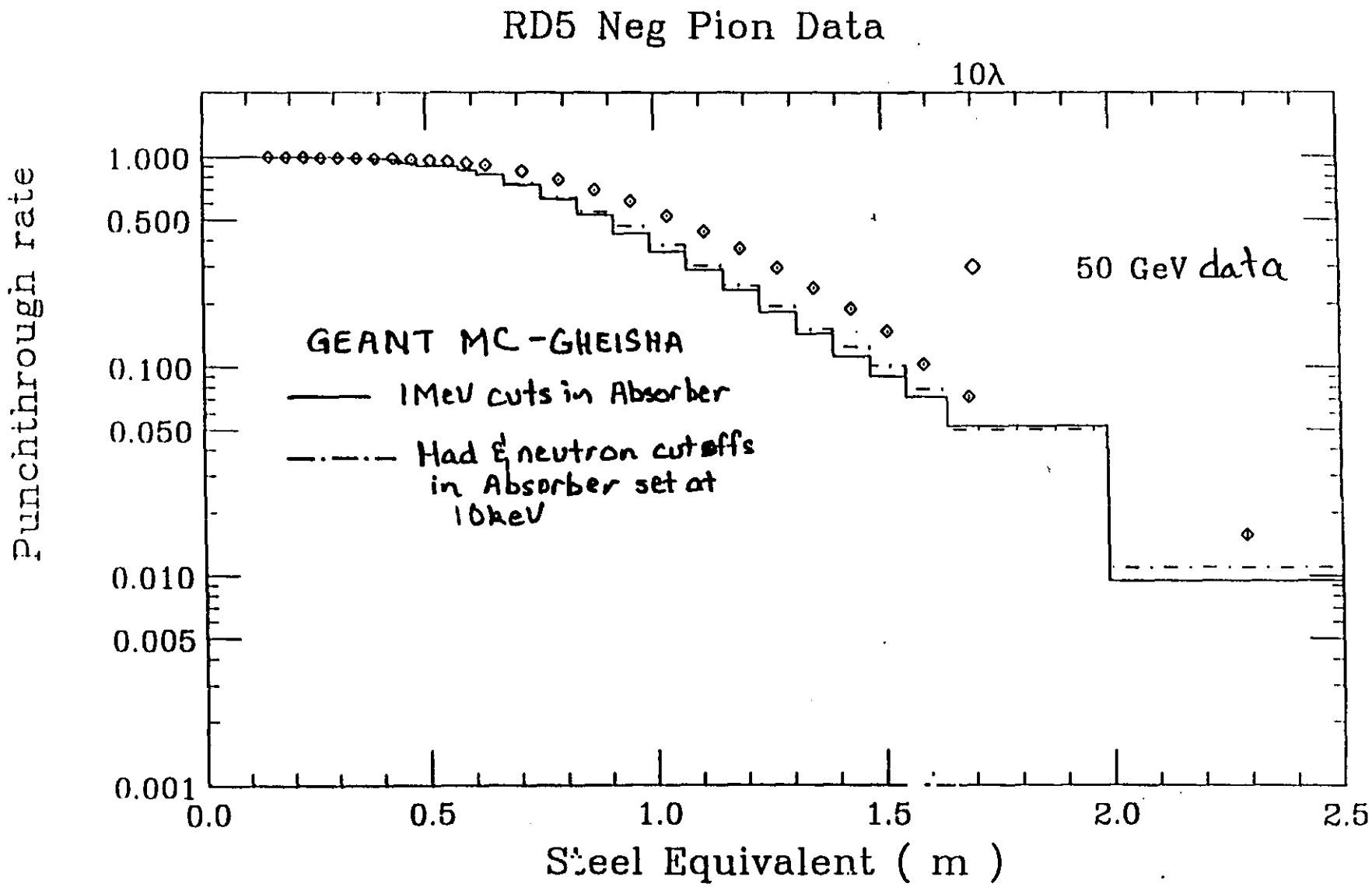
RD5 Neg Pion Data
10λ
Punchthrough rate
1.000
0.500
0.100
0.050
0.010
0.005
0.001
0.0
0.5
1.0
1.5
2.0
2.5
Steel Equivalent (m)
50 GeV data
GEANT MC-GHEISHA
1MeV cuts in Absorber
Had & neutron cutoffs in Absorber set at 10keV

Convert to CSC 4-strip occupancy

at $10^{34}\ s^{-1}\ cm^{-2}$

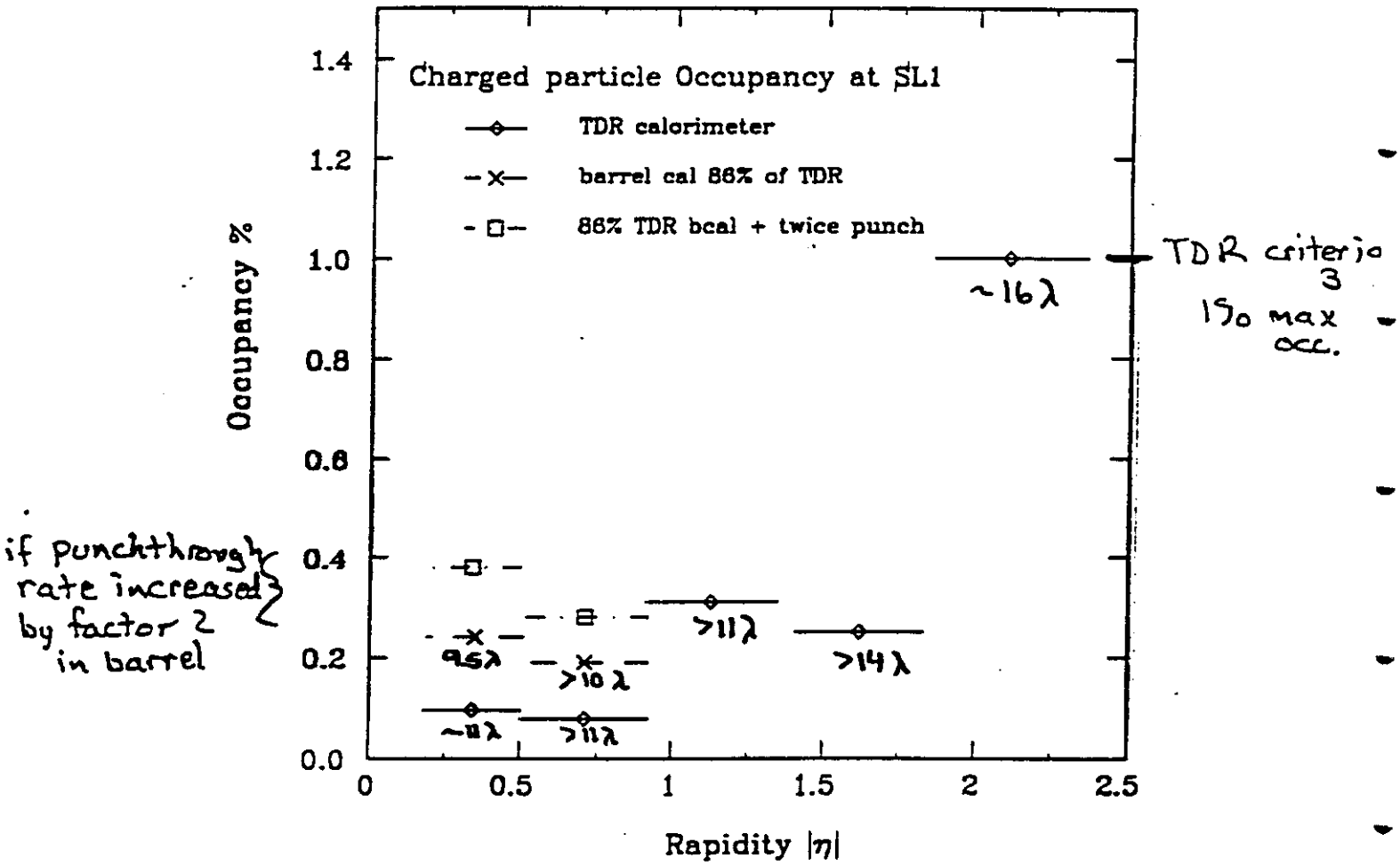

Even with punchthrough rate increased by factor 2, and barrel calorimeter thickness reduced by 14% criterion 3 satisfied.

We will satisfy criterion 3 for the cal depth of $\gtrsim 9\lambda$ at 90°

Transverse momentum spectrum in barrel region $0<\eta<0.5$

Increase in particle rate from reduction of cal depth to 9.5λ comes mainly at low P_T.

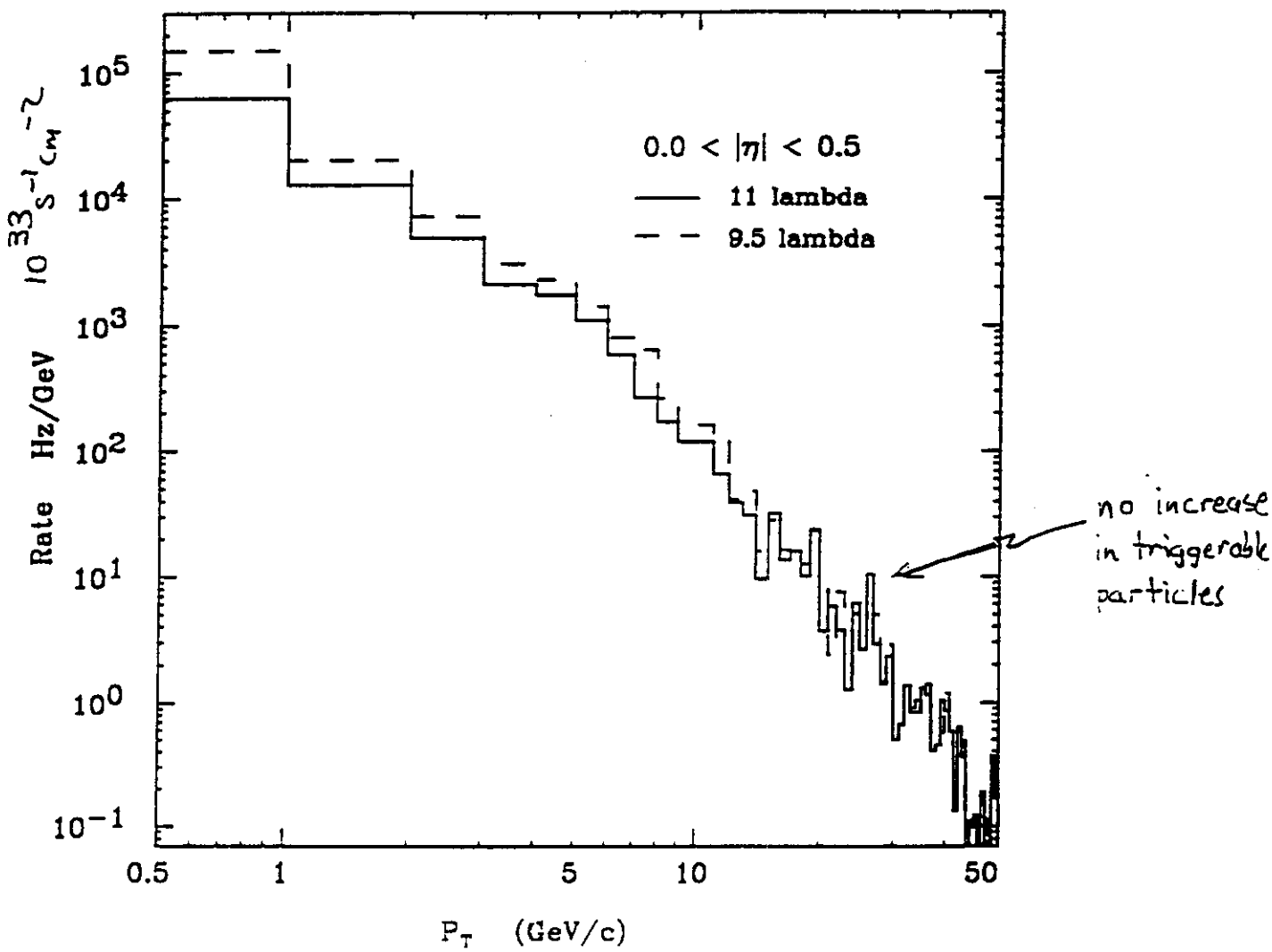

Convert to CSC 4-strip occupancy

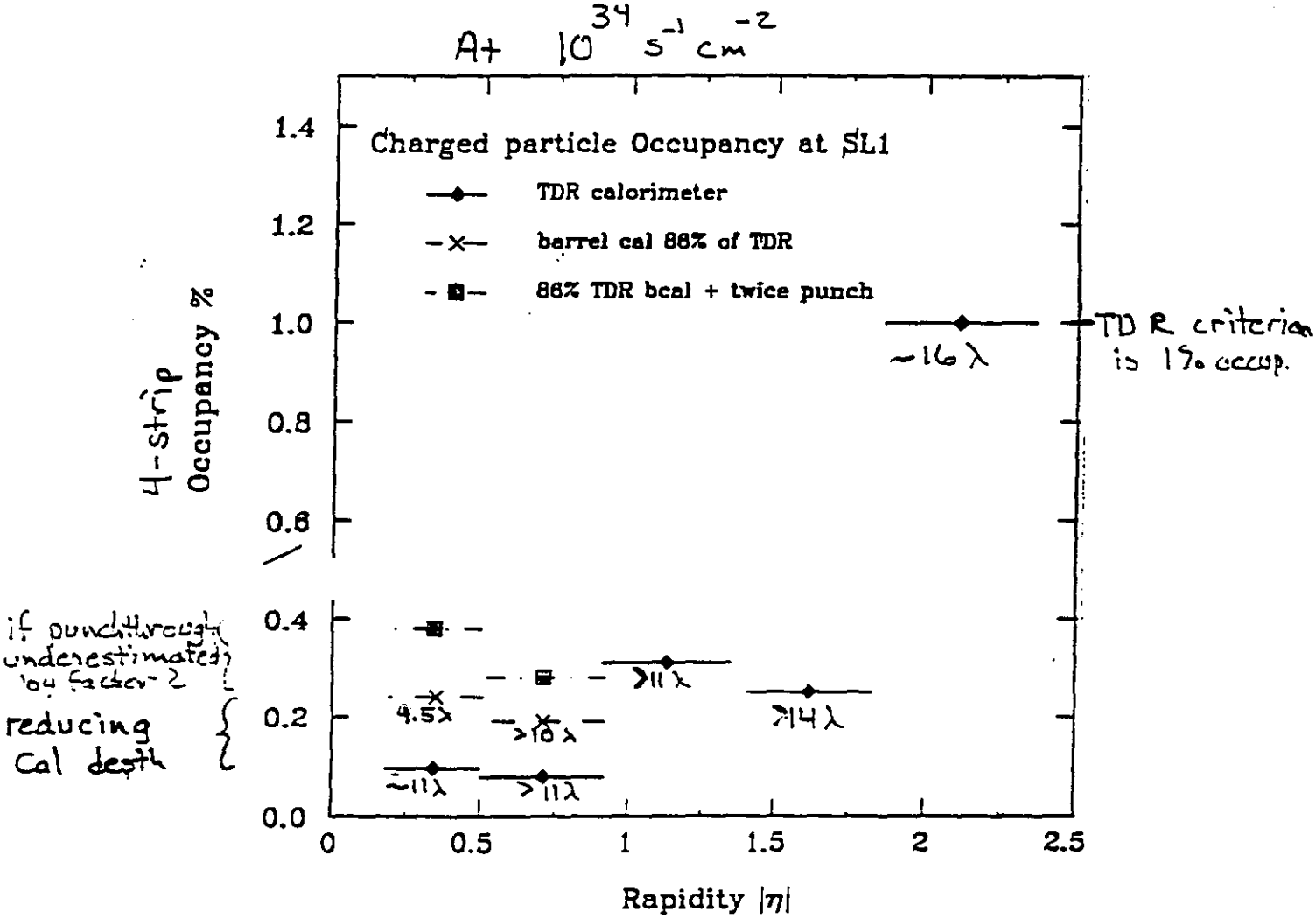

Even with factor 2 increase in punchthrough and barrel calorimeter reduced to 9.5 λ at 90° CSC 4-strip occupancy still below 1% at 10^{34} lum.

Conclusions

By using only criterion 3 in the barrel, the calorimeter depth can be further reduced

- In the range $0<|\eta|<0.5$, 9.5λ will be adequate calorimeter thickness to satisfy criterion 3, where $11-12\lambda$ was used in the GEM Calorimeter TDR design.

- In the range $0.5<|\eta|<1.0$, the calorimeter depth can be reduced further by $\sim 15\%$ and still satisfy criterion 3.

What would we gain?

- more lever arm – better resolution
- higher fraction of high resol. calorimetry – ν Eless
- less costly calorimeter

Making this thickness reduction puts greater reliance on details of hadron punchthrough simulation. Further validation of codes (RDS) needed.